DOE/MC/30098 -- 5320
(DE97002068)
Distribution Category UC-109

Pilot Plant Assessment of Blend Properties

Topical Report

October 1996

Work Performed Under Contract No.: DE-FC21-93MC30098

For
U.S. Department of Energy
Office of Fossil Energy
Morgantown Energy Technology Center
P.O. Box 880
Morgantown, West Virginia 26507-0880

By
University of North Dakota
Energy & Enviromental Research Center
15 North 23rd Street
P. O. Box 9018
Grand Forks, North Dakota 58202-9018

Disclaimer

DISCLAIMER

This report was prepared as an account of work sponsored by an agency of the United States Government. Neither the United States Government, nor any agency thereof, nor any of their employees makes any warranty, express or implied, or assumes any legal liability or responsibility for the accuracy, completeness, or usefulness of any information, apparatus, product, or process disclosed or represents that its use would not infringe privately owned rights. Reference herein to any specific commercial product, process, or service by trade name, trademark, manufacturer, or otherwise does not necessarily constitute or imply its endorsement, recommendation, or favoring by the United States Government or any agency thereof. The views and opinions of authors expressed herein do not necessarily state or reflect those of the United States Government or any agency thereof.

ACKNOWLEDGMENT

This final report was prepared with the support of the U.S. Department of Energy (DOE), Morgantown Energy Technology Center, Cooperative Agreement No. DE-FC21-86MC10637. However, any opinions, findings, conclusions, or recommendations expressed herein are those of the author(s) and do not necessarily reflect the views of the DOE.

EERC DISCLAIMER

LEGAL NOTICE This research report was prepared by the Energy & Environmental Research Center (EERC), an agency of the University of North Dakota, as an account of work sponsored by U.S. Department of Energy Pittsburgh Energy Technology Center, Consolidation Coal Company, Empire State Electric Energy Research Corporation, Electric Power Research Institute, and Zeigler Coal Company. Because of the research nature of the work performed, neither the EERC nor any of its employees makes any warranty, express or implied, or assumes any legal liability or responsibility for the accuracy, completeness, or usefulness of any information, apparatus, product, or process disclosed, or represents that its use would not infringe privately owned rights. Reference herein to any specific commercial product, process, or service by trade name, trademark, manufacturer, or otherwise does not necessarily constitute or imply its endorsement or recommendation by the EERC.

TABLE OF CONTENTS

LIST OF FIGURES iii

LIST OF TABLES vii

EXECUTIVE SUMMARY ix

1.0 BACKGROUND AND INTRODUCTION 1

2.0 GOALS AND OBJECTIVES 2

3.0 WORK PLAN 3
- 3.1 Task 1 - Coal Selection 3
- 3.2 Task 2 - Mill Performance 3
- 3.3 Task 3 - Flame Stability 4
- 3.4 Task 4 - High-Temperature Fouling 4
- 3.5 Task 5 - Low-Temperature Fouling 4
- 3.6 Task 6 - ESP Performance 4

4.0 RESULTS AND DISCUSSION 6
- 4.1 Parent Coal Analyses 7
  - 4.1.1 Chemical Fractionation Analyses 8
  - 4.1.2 Computer-Controlled Scanning Electron Microscopy (CCSEM) Analyses . . 9
- 4.2 Mill Performance 11
  - 4.2.1 Blend Ratios Tested 15
  - 4.2.2 Test Format 15
  - 4.2.3 Measured Parameters 15
  - 4.2.4 Discussion of Results 18
  - 4.2.5 Summary Observations 26
- 4.3 High-Temperature Fouling 38
  - 4.3.1 Combustion Test Sample Handling and Preparation 38
  - 4.3.2 Combustion Test Fuel Properties 38
  - 4.3.3 Combustor Operating Parameters 43
  - 4.3.4 High-Temperature Ash-Fouling Test Results 44
  - 4.3.5 Slag Probe Test Results 59
  - 4.3.6 System Ash Characterization 60
- 4.4 Low-Temperature Ash Deposition and Testing Program 60
  - 4.4.1 Experimental Procedures 60
  - 4.4.2 Testing of Low-Temperature Ash Deposits 65
  - 4.4.3 Upstream Deposits of Black Thunder and Antelope 68
  - 4.4.4 Strength Testing 73

Continued . . .

TABLE OF CONTENTS (continued)

4.5 Flame Stability Tests 82
4.6 Stack Emissions and ESP Performance 84

5.0 SUMMARY AND CONCLUSIONS 96

6.0 REFERENCES 98

DESCRIPTION OF TEST FACILITIES AND PROCEDURES . . . . . Appendix A

PLOTS OF ADDITIONAL DATA . . . . . Appendix B

LIST OF FIGURES

1 CONSOL pulverizer pilot plant 19

2 Moisture content of the pulverized test fuels at various mill operating conditions 26

3 Quantities of water removed during pulverization of the test fuels at various mill operating conditions 27

4 Mill feed and air-dried fuel moisture contents of the test fuels 27

5 Maximum mill mass throughput of the test fuels at the various mill operating conditions 28

6 Maximum mill thermal throughput of the test fuels at the various mill operating conditions 29

7 Results of product fuel particle-size analyses from the various mill operating conditions . 30

8 Mill thermal throughput reductions due to the test fuels relative to 100% Illinois No. 6 at equivalent pulverizer conditions 31

9 Mill thermal throughput reductions due to the test fuels relative to 100% Illinois No. 6 at baseline operating conditions 32

10 Differences in mill inlet temperature due to fuel type at the various mill operating conditions 33

11 Estimated mill inlet temperatures of indirect- versus direct-fired pulverizers for selected test fuels 34

12 Estimated mill outlet temperatures of indirect- versus direct-fired pulverizers for selected coals 36

13 Pulverizer heat requirements per MMBtu of test fuel processed for the various mill operating conditions investigated 37

14 System heat requirements as a percentage of the baseline test condition (Illinois No. 6 coal at low mill air rate/high mill outlet temperature) for the test fuels at various mill operating conditions 39

15 Photograph of sinter deposit at 2200°F, 100% Black Thunder 48

16 Photograph of sinter deposit at 2000°F, 100% Black Thunder 49

Continued . . .

LIST OF FIGURES (continued)

17 Photograph of sinter deposit at 2200°F, 100% Bailey 49

18 Photograph of sinter deposit at 2000°F, 100% Bailey 50

19 Photograph of sinter deposit at 2200°F, 35/65 Bailey/Black Thunder 50

20 Photograph of sinter deposit at 2000°F, 35/65 Bailey/Black Thunder 51

21 Photograph of sinter deposit at 2200°F, 65/35 Bailey/Black Thunder 51

22 Photograph of sinter deposit at 2000°F, 65/35 Bailey/Black Thunder 52

23 Photograph of sinter deposit at 2200°F, 100% Antelope 52

24 Photograph of sinter deposit at 2000°F, 100% Antelope 53

25 Photograph of sinter deposit at 2200°F, 35/65 Bailey/Antelope 53

26 Photograph of sinter deposit at 2000°F, 35/65 Bailey/Antelope 54

27 Photograph of sinter deposit at 2200°F, 65/35 Bailey/Antelope 54

28 Photograph of sinter deposit at 2000°F, 65/35 Bailey/Antelope 55

29 Oblique schematic of low-temperature ash-fouling bank used for testing 63

30 End view of one column set of low-temperature ash-fouling probes 64

31 Concentrations of major elemental oxides versus area of deposition for upstream Antelope low-temperature fouling deposits 70

32 Particle-size distribution of sample of upstream Antelope low-temperature fouling deposit 71

33 Porosity of upstream Antelope deposit sample 72

34 Concentrations of major elemental oxides versus area of deposition for upstream Black Thunder low-temperature fouling deposits 72

35 Particle-size distribution of sample of upstream Black Thunder low-temperature fouling deposit 73

Continued . . .

LIST OF FIGURES (continued)

36 Porosity of upstream Black Thunder deposit sample 74

37 Results of compressive strength testing versus sintering time for ESP ash pellets sintered at 1850°F 75

38 Shedding index of selected ash samples versus time for both upstream and downstream low-temperature fouling deposits 76

39 Results of compressive strength testing versus sintering time for ESP ash pellets sintered at 1560°F 77

40 Results of XRF analyses performed on ash pellets sintered for 24 hr at 1560°F 79

41 SEMPC analyses of fractured pellet pieces after compressive strength testing – 100% Antelope 80

42 SEMPC analyses of fractured pellet pieces after compressive strength testing – 35%/65% Bailey/Antelope 80

43 SEMPC analyses of fractured pellet pieces after compressive strength testing – 65%/35% Bailey/Antelope 81

44 SEMPC analyses performed on a circular cross section of sintered pellet from 100% Antelope ash 81

45 SEMPC analyses performed on a circular cross section of sintered pellet from 100% Antelope ash 82

46 Burner swirl versus % carbon in ash for each parent fuel at full-load and turndown conditions 86

47 Burner swirl versus % carbon in ash for the Bailey/Black Thunder fuel blends at full-load conditions 86

48 Burner swirl versus % carbon in ash for the Bailey/Antelope fuel blends at full-load conditions 87

49 Flue gas emissions of sulfur dioxide and nitrogen oxides, Bailey/Black Thunder system, 2200°F FEGT 89

Continued . . .

LIST OF FIGURES (continued)

50 Flue gas emissions of sulfur dioxide and nitrogen oxides, Bailey/Antelope system, 2200°F FEGT 89

51 Schematic depicting the equipment utilized for fly ash resistivity testing 91

52 Predicted fly ash resistivities of the parent fuels by the Bickelhaupt model 92

53 Laboratory resistivity results for EERC pilot plant ESP hopper ash for the three parent fuels 92

54 Predicted fly ash resistivities of the parent fuels by the Bickelhaupt model without SO_3 present for the Bailey fly ash 93

55 Predicted fly ash resistivities of the Bailey/Black Thunder blend system by the Bickelhaupt model 94

56 Laboratory resistivity results for EERC pilot plant ESP hopper ash for the Bailey/Black Thunder fuel blend system 94

57 Predicted fly ash resistivities of the Bailey/Antelope blend system by the Bickelhaupt model 95

58 Laboratory resistivity results for EERC pilot-scale ESP hopper ash for the Bailey/Antelope fuel blend system 95

LIST OF TABLES

1 Identification of Tested Fuels 6

2 Comparison of Parent Coal Properties 7

3 Comparison of Parent Coal Ash Properties 8

4 Chemical Fractionation Results 10

5 CCSEM Analysis of Bailey Bituminous Coal 12

6 CCSEM Analysis of Black Thunder Subbituminous Coal 13

7 CCSEM Analysis of Antelope Subbituminous Coal 14

8 Input SO_2 Levels for the Parent Coals and Blends 16

9 Mill Feed Coal Analyses 17

10 Pulverizer Air Rate and Outlet Temperature Differential Test Strategy 18

11 Pulverizer Pilot Plant Summary Results 20

12 Mill Product Coal Analyses 22

13 Moisture Content of Test Fuels 25

14 Maximum Bituminous Coal Sulfur Concentrations in a PRB Blend to Satisfy Compliance Requirements 25

15 Properties of Parent and Blend Fuel Test Samples – High-Temperature Fouling 40

16 Ash Properties of Parent and Blend Test Samples – Standard Ash-Fouling Tests 42

17 Run Average Combustor Operating Parameters – Standard Ash-Fouling Tests 45

18 Summary of High FEGT (2200°F) Ash-Fouling Probe Test Results 46

19 Summary of Low FEGT (2000°F) Ash-Fouling Probe Test Results 47

20 Probe Bank Sinter Layer SEMPC Results, Standard Ash-Fouling Tests 56

21 Probe Bank Inner and Sinter Layer XRD Results, Standard Ash-Fouling Tests 58

Continued . . .

LIST OF TABLES (continued)

22 System Ash Mass Balance, Standard Ash-Fouling Tests 61

23 Fly Ash Sample Analyses, Standard Ash-Fouling Tests 62

24 Combustions Runs for Low-Temperature Ash Deposition and Testing Program 63

25 Multicyclone Samples Retrieved During Low-Temperature Ash-Fouling Combustion Tests 65

26 Calculated Rates of Low-Temperature Ash-Fouling Deposition 66

27 Results of XRD Analyses of Selected Low-Temperature Ash-Fouling Deposits 67

28 Results of X-Ray Diffraction Analyses of Multicyclone-Separated Samples 69

29 Changes in Ash Pellet Color During Strength Testing 75

30 Results of X-Ray Diffraction Analyses of Ash Specimens Sintered for 24 hr at 850°C . . 78

31 Properties of Parent and Blend Fuel Test Samples – Flame Stability Testing 83

32 Summary of Flame Stability Test Results at Simulated Full Load 85

33 Gaseous and Particulate Emissions 88

34 ESP Performance Testing 90

PILOT PLANT ASSESSMENT OF BLEND PROPERTIES AND THEIR IMPACT ON CRITICAL POWER PLANT COMPONENTS

EXECUTIVE SUMMARY

A series of tests were performed to determine the effects of blending eastern bituminous coals with western subbituminous coals on utility boiler operation. Mill performance tests were performed by CONSOL, Inc., at its facility in Library, PA, while all other testing was performed at the Energy & Environmental Research Center (EERC) in Grand Forks, ND.

Mill performance tests indicated that at design pulverizer conditions (relative to pulverization of bituminous coal), the decreased thermal input of the subbituminous coals resulted in derates on the mill of up to 55% of the maximum thermal input of the bituminous coals. One Pittsburgh seam bituminous coal, one Illinois No. 6 seam bituminous coal, and two Powder River Basin (PRB) subbituminous coals were tested. By raising the mill outlet temperature between 5° and 25°F, thermal throughput for the subbituminous coals could be increased by 10% to 20%. Increasing the air/fuel ratio also tended to increase thermal throughput, but at the expense of a coarser product. At the maximum thermal throughput for the subbituminous coals and at the highest air/fuel ratio, product fineness (less than 200 mesh) decreased by up to 15 percentage points. Interestingly, the lowest heat content subbituminous coal exhibited the lowest thermal derate of the two PRB coals tested, but required much higher mill energy input.

Testing at the EERC investigated the effects of blending one Pittsburgh seam bituminous coal with two PRB subbituminous coals. The tests were performed to determine the propensity for fouling of high-temperature heat exchange surfaces exposed to high flue gas temperatures (both 2000° and 2200°F), the propensity for fouling of low-temperature heat exchange surfaces exposed to moderate flue gas temperatures (1500° to 1600°F), flame stability characteristics, and gaseous and particulate emission characteristics. High-temperature fouling tests indicated comparable fouling rates for each of the parent coals, with the blends exhibiting a lower ash-fouling rate. The lower fouling rate of the blends was attributed to interactions between the two ash types. However, in each case, the strength of the deposit increased irrespectively of the fouling rate as the percentage of subbituminous coal in the blend was increased. The highest sodium content subbituminous coal produced consistently stronger deposits than its lower sodium counterpart.

Low-temperature fouling tests indicated that similar deposition rates could be expected for each of the fuels tested, with a slight increase in rate noted as the percentage of subbituminous coal in the blend was increased. It was expected that as the percentage of subbituminous coal in the test fuels increased, with corresponding increases in fuel ash calcium concentrations, the resulting low-temperature deposits would develop increasingly greater strengths because of the effect of ash calcium content on deposit sintering behavior. Results were inconclusive to support this theory, as the parent coals exhibited much lower strength than any of the blends tested. There would appear to be some interaction between ash types to create the stronger deposits, although the mechanism was not easily discernible from the data generated.

Flame stability testing indicated that each of the parent coals and coal blends would exhibit excellent fuel ignitability and flame stability characteristics over a wide range of burner settings.

There was a general trend toward lower carbon-in-ash values as the percentage of subbituminous coal in blend with the bituminous coal was increased. Based on the results obtained here, the use of subbituminous coal in blend with the bituminous coal should increase overall carbon conversion and provide adequate or improved flame stability, which could offset some of the limits to grinding efficiency noted above in the mill performance tests performed by CONSOL.

Flue gas emissions of SO_2 were dramatically reduced as the percentage of subbituminous coal was increased in blend with the bituminous coal tested here. In general, the emission reductions corresponded with decreases in the input sulfur concentrations. However, there was evidence of increased sulfur capture in the ash as the percentage of subbituminous coal in the blends increased. This trend was even more pronounced for those tests performed at the lowest furnace exit gas temperature, indicating a temperature dependence on the level of sulfur capture in ash. Emissions of nitrogen oxides (NO_x) also decreased as the percentage of subbituminous coal in the blends increased. Levels noted during testing of the parent subbituminous coals were roughly one-half that of the parent bituminous coal. Particulate emission testing indicated similar results for all fuels tested under similar conditions. There was no apparent trend toward decreased collection efficiency via electrostatic precipitation for either of the bituminous/subbituminous coal blend sets, although one of the blend sets indicated a slight reduction in collection efficiency as the percentage of subbituminous coal in the blend increased.

Relative to the baseline bituminous coal, the testing reported here indicated that there were significant impacts to boiler performance due to the blending of the eastern and western coals. Results indicated that fuel blending can be used to adequately control flue gas emissions of both SO_2 and NO_x at the expense of reduced milling efficiency, increased sootblowing in the high-temperature and low-temperature regions of the boiler and, to a lesser extent, decreased collection efficiency for an electrostatic precipitator. The higher reactivity of the subbituminous coal increased the overall combustion efficiency, which may tend to decrease the impact of milling efficiency losses. The extent of these impacts was directly related to the percentage of subbituminous coal in the blends. At the lowest blend ratios of subbituminous coal, the impacts were greatly reduced.

PILOT PLANT ASSESSMENT OF BLEND PROPERTIES AND THEIR IMPACT ON CRITICAL POWER PLANT COMPONENTS

1.0 BACKGROUND AND INTRODUCTION

Many eastern and midwestern utilities are considering coal switching or blending as a means to reduce sulfur emissions in order to gain compliance with the 1990 amendments to the Clean Air Act (CAA). The majority of these units were designed for high-sulfur bituminous coals. The amendments placed caps on SO_2 emissions from utilities in two phases. The Phase I emission limit was set at 2.5 lb SO_2/MMBtu, while the Phase II limit is 1.2 lb SO_2/MMBtu. Utilities must now look toward utilizing low-sulfur bituminous coals or western subbituminous coals to meet the new standard, with either choice having potential impacts on unit capacity and performance.

Low-sulfur western subbituminous coals can be economically mined and are readily available to many eastern and midwestern utilities. Therefore, they are primary candidates for fuel switching to meet lower sulfur emissions requirements. The primary disadvantage of as-mined subbituminous coals is that they contain much higher moisture contents than bituminous coals, resulting in significantly lower heat contents. A utility may be required to fire up to 50% more coal tonnage in a unit to maintain the same thermal input. The higher tonnage, in turn, will impact transportation costs, coal storage and handling facilities, pulverizer capacity, and boiler efficiency for units considering such a fuel switch. In addition, western coals typically have an alkaline ash that is very different from that of bituminous coals, with potential impacts on boiler tube ash fouling, furnace wall slagging, and electrostatic precipitator (ESP) performance. All of these factors potentially have a capital and operating cost impact on the utility boiler.

These impacts were confirmed during a previous project entitled Technology Assessment for Blending Western and Eastern Coals for SO_2 Compliance and sponsored by the U.S. Department of Energy (DOE) and the Electric Power Research Institute (EPRI) (1). During this project, researchers documented the blending experience at 12 utility stations. Results indicated a wide range of experience at each site, with further study required to more adequately address system response to the blended fuel. As a follow-up to that project, this pilot-scale study was initiated by the Energy & Environmental Research Center (EERC) to quantify the impacts of the blend on mill performance, flame stability, convective pass fouling, and ESP performance.

2.0 GOALS AND OBJECTIVES

To determine the impact of blends containing western subbituminous coal and eastern bituminous coal on system performance in boilers designed to fire bituminous coal, the University of North Dakota EERC formed a consortium of interested parties to support a pilot-scale research effort. A series of pilot-scale combustion tests were designed to evaluate and compare the combustion characteristics of two PRB subbituminous coals and one Pittsburgh seam bituminous coal individually and together at two distinct blend ratios. Among the areas evaluated were boiler tube ash-fouling potential in the high- and low-temperature regions typical of the convective pass of a bituminous-design boiler, furnace wall slagging, carbon conversion, flame stability, ESP performance, and SO_2, NO_x, and particulate emissions. The EERC facilities have been used for many years to study the combustion characteristics of pulverized solid fuels (2). Another aspect of this program was to evaluate some of the major and minor pulverizer differences (fuel and equipment) which occur as a result of a fuel switch, in this case, blending high-sulfur bituminous coal with low-sulfur Powder River Basin (PRB) subbituminous coal.

3.0 WORK PLAN

To accomplish project goals and objectives, several specific tasks were developed. These are summarized below.

3.1 Task 1 – Coal Selection

Because of the wide variation in coal properties between and among coal types, it was essential that coals be selected that provided as wide a range of properties as possible. In addition, the test coals needed to represent those coals that were readily available for use in a blending scenario. Selection criterion for the bituminous coals included location, heat content, and ash composition (mainly iron content). Since funding allowed for only two bituminous coals, a high-iron content Illinois No. 6 coal (Rend Lake) and a high-heat-content, lower-iron-content Pittsburgh seam coal (Bailey) were chosen to represent the bituminous coals. Subbituminous coals were chosen to represent the range of properties existing in the PRB. One higher-heat-content (Antelope) and one lower-heat-content (Caballo Rojo) PRB coal were chosen for the mill performance tests. Because of the mine strike of 1993, only the Bailey bituminous coal was available to the EERC for use in pilot-scale testing. Selection criterion for the PRB coals fired in the pilot tests performed by the EERC included sodium content and low-temperature fouling tendencies (calcium-based deposition of back-end surfaces). The Antelope coal was chosen to represent the higher-sodium-content PRB coal, while Black Thunder subbituminous PRB coal represented the lower-sodium-content coal. Sodium content plays a major role in determining the strength of high-temperature fouling deposits and also provides the conditioning agent for adequate collection of particulates by ESP. A low-temperature fouling index developed by the EERC also indicated a difference between these two fuels in terms of the potential to form significant deposits in the reheater/primary superheater section of a utility boiler.

3.2 Task 2 – Mill Performance

One of the first areas impacted by a blend containing subbituminous coal at a utility designed to fire bituminous coals is the pulverizer (1). Higher-moisture-content subbituminous coal tends to lower the mill outlet temperature below design limits. Attempts to maintain this temperature result in boiler derate as the tempering air dampers close. Pilot testing was designed to determine the limits to mill throughput resulting from a switch to subbituminous coal or a blend containing subbituminous coal.

The Rend Lake Illinois No. 6 bituminous coal, Bailey Pittsburgh seam bituminous coal, and two PRB coals (Antelope and Caballo Rojo) were tested in the pilot mill at CONSOL's Research and Development Facility in Library, PA. To determine baseline conditions, the bituminous coals were milled to determine the maximum throughput for each coal under normal operating conditions. Once established, the maximum throughput for each of the subbituminous coals and two blends containing subbituminous coal was determined. Changes to pulverizer operating parameters were then investigated to determine the effect of varying primary air flow and mill outlet temperature on throughput for the blends and the parent subbituminous coals.

3.3 Task 3 - Flame Stability

Lower mill exit temperatures resulting from the use of blends containing high-moisture-content subbituminous coal may affect flame stability and carbon carryover when fired in boilers designed for bituminous coals. Flame stability for the parent coals and coal blends was determined using an International Flame Research Foundation (IFRF)-type secondary air swirl generator, with supporting measurements of the combustion environment and carbon carryover. The swirl generator provides adjustments to swirl number between 0 (no swirl) and 1.9. Swirl number is defined as the ratio of tangential momentum to axial momentum of the secondary air stream. Furnace exit gas temperature (FEGT), flame temperature, furnace wall heat flux, and flue gas emissions were measured, and fly ash samples were taken at each swirl setting. Testing determined flame stability at full load and at 75% of full load.

3.4 Task 4 - High-Temperature Fouling

Because of the wide variation in ash properties between and among coal types, boiler tube ash fouling is a concern for utilities firing blends of eastern bituminous and western subbituminous coal. In general, the higher alkaline content subbituminous coals will form lower melting point ash deposits, requiring increased sootblowing of convective pass heat-transfer surfaces (1). Pilot testing addressed this concern by firing each of the parent coals and blends at a rate sufficient to achieve FEGTs of 2200°F, a temperature similar to that of many utilities firing bituminous coals. To determine the effect of temperature on deposit formation and strength development, deposits were also collected at a FEGT of 2000°F. Deposits were analyzed for bulk chemical composition using x-ray fluorescence (XRF), crystalline composition using x-ray diffraction (XRD), and advanced scanning electron microscope analyses (scanning electron microscope point count, SEMPC) to determine the phases responsible for deposit growth and strength development. In addition, a laboratory technique developed at the EERC was used to evaluate deposit strength for each deposit collected.

3.5 Task 5 - Low-Temperature Fouling

Studies have indicated that fouling of low-temperature superheater and reheater surfaces of utility boilers is increased when high-calcium-content coals are fired (3). Because bituminous design boilers have relatively close tube spacings in the back end and few sootblowers in this region, it was anticipated that low-temperature deposition could be troublesome for those utilities firing blends containing subbituminous coal. To assess low-temperature deposition, fouling deposits were collected on simulated reheater/primary superheater surfaces and analyzed for composition and strength development. Gas temperatures entering this region were controlled to approximately 1550°F. These tests were conducted firing 100% Antelope subbituminous coal, 100% Bailey bituminous coal, and two blends of these fuels. Bulk chemical analysis by XRF, crystalline composition by XRD, SEMPC, and laboratory sintering tests were performed to characterize the deposits collected.

3.6 Task 6 - ESP Performance

For eastern bituminous design boilers, the ESP is sized relative to the sulfur content of the bituminous coal that will be fired. Sulfur trioxide (SO_3) is the naturally occuring conditioning

agent available to achieve adequate collection of the fly ash in these installations. In general, the less sulfur present in the feed coal, the larger the ESP must be to remove an equal amount of fly ash from the flue gas. Attempts to lower SO_2 emissions by blending low-sulfur PRB coals with higher-sulfur bituminous supplies decrease the level of SO_3 in the flue gas. SO_3 is usually present at approximately 1% to 2% of the SO_2 concentration. In addition, the high alkaline content of the PRB coal ash will combine with sulfur oxides to form sulfate salts, further decreasing the available SO_3 for conditioning. A tubular ESP was used to collect the fly ash, and EPA Method 5 sampling was performed to determine the collection efficiency across the pilot ESP. Laboratory evaluation of fly ash resistivity was also performed to determine the effect of blending on this critical fly ash property.

This report details the results of the pilot-scale combustion and pulverizer tests conducted during the fall of 1993 and spring of 1994. A description of test facilities and analytical procedures is presented in Appendix A. Supporting information is included in Appendix B.

4.0 RESULTS AND DISCUSSION

Samples of subbituminous coal from the Antelope and Black Thunder mines in Wyoming and bituminous coal from the Bailey mine operating in the Pittsburgh seam were shipped to the EERC for use in pilot-scale combustion tests. The combustion test run numbers and the fuels tested are listed in Table 1. Mill performance testing was performed by CONSOL at its research and development facility in Library, PA. Milling tests utilized the Bailey and Antelope coals mentioned above, an Illinois No. 6 bituminous coal (Rend Lake), and Caballo Rojo subbituminous coal. The purpose of the blend program was to evaluate the relative milling and combustion characteristics for each of the 100% subbituminous coal, 100% bituminous coal, and combinations of each.

TABLE 1

Identification of Tested Fuels

		As-Burned Fuel		
Run Number	Fuel Description	Moisture, %	HHV, Btu/lb	Input Sulfur, lb SO_2/MMBtu
AF-CTS-699	Black Thunder (BT)–Wyoming PRB	26.0	9,015	0.84
AF-CTS-700	BT–Wyoming PRB	23.9	9,102	0.81
AF-CTS-701	Bailey–Pittsburgh Seam	2.2	13,713	2.51
AF-CTS-702	Blend: 35/65 Bailey–BT	11.8	11,325	1.54
AF-CTS-703	Blend: 65/35 Bailey–BT	9.7	12,057	2.07
AF-CTS-706	Antelope–Wyoming PRB	24.7	8,994	0.75
AF-CTS-707	Blend: 35/65 Bailey–Antelope	16.8	10,642	1.54
AF-CTS-708	Blend: 65/35 Bailey–Antelope	9.6	12,069	2.10

Each run number listed in Table 1 actually represents four separate tests, with the exception of Run Nos. AF-CTS-699 and AF-CTS-700. Each run consisted of a flame stability test, a 2200°F FEGT high-temperature ash-fouling test, a 2000°F FEGT high-temperature ash-fouling test, and a low-temperature ash-fouling test. Run No. AF-CTS-699 was a 100% Black Thunder flame stability test only, while the remainder of the 100% Black Thunder high- and low-temperature ash-fouling tests were performed under Run No. AF-CTS-700.

The report has been formatted into six distinct sections: 1) Fuel Analyses, 2) Mill Performance, 3) High-Temperature Fouling, 4) Low-Temperature Fouling, 5) Flame Stability, and 6) Particulate and Gaseous Emissions. Test results for each of these areas follow.

4.1 Parent Coal Analyses

The as-received samples of bituminous and subbituminous coals used during the pilot-scale combustion tests were analyzed for their proximate, ultimate, heating value, and bulk mineral contents. Analytical results are provided in Tables 2 and 3.

The Bailey bituminous coal contains high heat content (13,560 Btu/lb), low moisture content (3.2%), and moderate ash content (6.6%). The major drawback of the bituminous coal as a boiler fuel, relative to today's emission standards, is its high as-received sulfur content of 1.76% (2.6 lb SO_2/MMBtu). The mineral matter of the bituminous coal sample was found to be dominated by SiO_2, Al_2O_3, and Fe_2O_3, as shown in Table 3.

TABLE 2

Comparison of Parent Coal Properties

Fuel Description:	Black Thunder Subbituminous		Bailey Bituminous		Antelope Subbituminous	
Sample Number:	93-0946		93-0947		93-1177	
	As-Received	H_2O-Free	As-Received	H_2O-Free	As-Received	H_2O-Free
Proximate Analysis, wt%						
Moisture	26.30	—	3.20	—	27.80	—
Volatile Matter	35.62	48.34	37.78	39.03	32.78	45.38
Fixed Carbon	34.10	46.27	52.43	54.16	34.82	48.25
Ash	3.97	5.39	6.59	6.81	4.60	6.37
Ultimate Analysis, wt%						
Hydrogen	6.92	5.42	5.09	4.89	6.54	4.79
Carbon	52.47	71.19	76.80	79.34	50.05	69.30
Nitrogen	0.69	0.94	1.45	1.50	0.92	1.28
Sulfur	0.33	0.45	1.76	1.82	0.32	0.44
Oxygen	35.63	16.61	8.31	5.64	37.56	17.83
Ash	3.97	5.39	6.59	6.81	4.60	6.37
Moisture	26.30	—	3.20	—	27.80	—
Heating Value, Btu/lb	8879	12,048	13,563	14,013	8685	12,024
Input Sulfur, lb SO_2/MMBtu	0.74		2.59		0.74	
Input Ash, lb/MMBtu	4.47		4.86		5.30	
Sulfur Forms, wt%[1]						
Sulfatic	0.04	0.05	0.14	0.14	0.05	0.07
Pyritic	0.02	0.02	0.74	0.77	0.02	0.02
Organic	0.38	0.52	1.19	1.22	0.24	0.32
Hardgrove Index[1]	44		49		39	
Sample moisture content, wt%	25.42		2.82		24.39	

[1] Analyses performed by an independent laboratory.

TABLE 3

Comparison of Parent Coal Ash Properties

Fuel Description:	Black Thunder Subbituminous		Bailey Bituminous		Antelope Subbituminous	
Sample Number:	93-0946		93-0947		93-1177	
Ash Analysis, wt%		SO_3-Free		SO_3-Free		SO_3-Free
SiO_2	22.43	25.57	48.17	49.60	32.02	35.39
Al_2O_3	17.75	20.23	26.20	26.98	15.50	17.13
Fe_2O_3	5.43	6.19	15.18	15.63	4.03	4.45
TiO_2	1.69	1.93	0.82	0.85	0.86	0.95
P_2O_5	1.80	2.06	0.32	0.33	1.63	1.80
CaO	27.81	31.70	2.86	2.94	28.35	31.33
MgO	9.77	11.13	1.64	1.69	6.64	7.34
Na_2O	0.65	0.74	0.87	0.89	1.02	1.13
K_2O	0.39	0.45	1.05	1.08	0.44	0.49
SO_3	12.28	—	2.90	—	9.53	—
Total	100.00	100.00	100.01	99.99	100.02	100.01

The samples of subbituminous coal used for these tests were similar to many of the PRB coals found in Wyoming, with relatively high moisture (26.3% and 27.8%) and low ash (4.0% and 4.6%) contents. The heating values of 8879 and 8685 Btu/lb reported in Table 2 for the two subbituminous coals are typical of the heat content for PRB coals from the southern portion of the basin. The mineral matter, also typical of PRB coals, is dominated by CaO, SiO_2, and Al_2O_3 (Table 3). These PRB coals were chosen for use during the combustion tests to accentuate the differences in boiler tube ash fouling and ESP performance based on sodium content. The Black Thunder coal contained sodium at 0.65%, while the Antelope contained sodium at the 1.02% level.

The results of sulfur forms analysis reported in Table 2 indicated that about 57% of the sulfur in the bituminous coal was present in an organic form and about 36% was pyrite. The analysis of the subbituminous coal indicated that 77% and 86% of the sulfur was organic in nature, and only about 5% to 6% of the sulfur in each was pyritic.

Hardgrove grindability indices (HGI) were determined for each of the parent coals and ranged from 39 to 49 at the noted moisture contents, with the bituminous coal exhibiting the highest index.

4.1.1 Chemical Fractionation Analyses

Chemical fractionation (described in detail in Appendix C) uses successive extractions by three different solutions as a means to quantitatively assess the mode of occurrence and relative availability of critical ash-forming inorganics in the as-received coal. The coal is first exposed to water to extract both water-soluble and organically associated species that are easily ion-exchanged from the coal matrix. Next, a split of the first sample is exposed to ammonium acetate. A portion

of the residue remaining is then analyzed, and the remaining portion of the residue is leached with HCl to extract carbonate minerals and minerals associated with organic coordination complexes. This technique was applied to each of the parent coals, and results are provided in Table 4.

Typical of many bituminous coals, analysis of the Bailey coal indicated the majority of all ash-forming species are either tied up with aluminosilicates or present as quartz or pyrite. Of the alkaline species in the bituminous coal, only sodium and calcium appeared to have a significant portion of organically associated species (those extracted during the leaching process). Organically associated alkaline species are vaporized during combustion and are available to react with silica and clay mineral species to lower their melting point, forming strong, silicate-based deposits on heat-transfer surfaces in a utility boiler. Since sodium and calcium species are present in the bituminous coal at very low levels, it would be expected that the abundant, higher melting point quartz and clays would dominate deposit formation and that those deposits would be weakly bonded to boiler surfaces.

By contrast, analysis of the chemical fractionation results for the subbituminous coals indicates a very high percentage of organically associated alkaline species, with calcium present as a significant percentage of the total ash composition. In addition, a high proportion of organically bound ash-forming constituents in the original coal tends to indicate a high potential for the formation of finer fly ash particles.

A comparison of ash sodium levels and relative availability between the three parent test coals indicates that the ash from the subbituminous coals would be expected to form more troublesome deposits than the Bailey coal ash. The chemical fractionation data indicate a large proportion of iron is extracted during the leaching process, especially from the subbituminous coals. Iron that is leached during this procedure with water and ammonium acetate is considered to be organically associated and may be available to contribute to deposit formation. The higher percentage of this available iron in the Antelope coal in combination with the higher percentage of iron in the ash would also indicate the potential to form more troublesome deposits than the Black Thunder coal analyzed here.

4.1.2 Computer-Controlled Scanning Electron Microscopy (CCSEM) Analyses

CCSEM is an advanced analytical procedure used by the EERC to determine the composition and size distribution of inorganic components in coal. A quantitative estimate of in-place mineral forms is accomplished by analyzing inorganic particles for relative proportions of elements in each sized particle. The mineral species present are inferred from elemental compositions. During combustion, the liberated minerals undergo transformations that may significantly alter the characteristics of the fly ash. In addition, the new mineral forms tend to segregate in the boiler based on size. For example, fine particulate is more likely to be deposited as an initial layer on heat-transfer surfaces or be carried by the flue gas to the particulate collection device. Conversely, relatively few of the very large mineral grains (>46 μm) in the coal will escape the furnace proper. When used in conjunction with chemical fractionation data and scanning electron microscopy point count (SEMPC, performed on deposits and fly ash) data, the CCSEM analysis can provide insight into the mineral transformations occurring during the combustion process.

TABLE 4

Chemical Fractionation Results

Bailey Bituminous		Portion of Initial Component Removed, %			
Ash Component	Starting Sample, wt%	Removed by H_2O	Removed by NH_4OAc	Removed by HCl	Remaining[1]
SiO_2	49.71	0	0	0	100
Al_2O_3	26.15	0	0	0	100
Fe_2O_3	16.07	0	0	29	71
TiO_2	0.89	0	0	0	100
P_2O_5	0.53	14	4	43	39
CaO	3.11	34	32	12	22
MgO	1.37	6	8	15	71
Na_2O	0.79	36	7	16	41
K_2O	1.38	0	0	4	96
Black Thunder Subbituminous		Portion of Initial Component Removed, %			
Ash Component	Starting Sample, wt%	Removed by H_2O	Removed by NH_4OAc	Removed by HCl	Remaining
SiO_2	37.16	0	0	0	100
Al_2O_3	19.63	0	0	52	48
Fe_2O_3	6.82	5	0	95	0
TiO_2	1.56	0	0	61	39
P_2O_5	1.52	3	0	97	0
CaO	26.44	0	43	54	3
MgO	5.65	3	51	41	5
Na_2O	1.06	38	53	8	1
K_2O	0.17	15	0	0	85
Antelope Subbituminous		Portion of Initial Component Removed, %			
Ash Component	Starting Sample, wt%	Removed by H_2O	Removed by NH_4OAc	Removed by HCl	Remaining
SiO_2	32.25	0	0	0	100
Al_2O_3	16.99	0	0	58	42
Fe_2O_3	10.67	10	0	90	0
TiO_2	1.06	0	0	23	77
P_2O_5	1.46	0	0	100	0
CaO	29.81	2	42	54	2
MgO	5.97	3	50	42	5
Na_2O	1.64	24	72	3	1
K_2O	0.15	0	0	0	100

[1] Results normalized to zero percent silicon loss.

CCSEM analyses of the parent coals are shown in Tables 5–7. The ash-forming minerals from all of the coals are dominated by quartz (SiO_2), various aluminosilicates (particularly kaolinite), and pyrite. Additionally, there is a significant contribution from a calcium aluminophosphate species in the subbituminous coal ashes. The minerals present in the parent coals are relatively fine, with 60.7% to 68.7% of the measured size distributions less than 10 μm and 79.0% to 88.2% less than 22 μm for the three samples analyzed.

In terms of the subbituminous coal samples, the most dominant mineral forms, quartz and kaolinite, are fairly evenly distributed in all size ranges less than 46 μm. The other dominant mineral form in the subbituminous coals, the calcium aluminophosphate, is concentrated in the <10-μm size range. The relatively fine size distribution of these mineral species, which represent about 70%–80% of all mineral forms identified in the subbituminous coals, indicate the potential for formation of fine particulate.

The bituminous coal ash is made up predominantly of the aluminosilicate mineral species (45%), followed by pyrite (27.7%), and to a lesser extent quartz (9.8%). Between 77% and 90% of the aluminosilicate minerals, as well as the quartz, in the bituminous coal ash are concentrated in the <10-μm size range. There appears to be an equal split of pyrite between the >10-μm size range and the <10-μm size range.

Fouling of heat-transfer surfaces is initiated by the very fine particulate (usually less than 1 or 2 μm) migrating to the surface by thermophoretic forces. This layer should be established rather quickly during combustion of any of the three coals selected for the blend program based on CCSEM analysis (15.6% to 22.7% of all minerals were in the 1.0- to 2.2-μm size range) and chemical fractionation analysis (the majority of the Ca, Mg, and Na were ion-exchangeable). The mass of the deposit (sintered layer) is then established by the impaction of larger particulate. The larger particulate from the Antelope sample is dominated by quartz, while that from the Bailey sample is dominated by pyrite. The larger particulate from the Black Thunder subbituminous coal is dominated equally by quartz and aluminosilicate minerals, especially kaolinite. The strength of the deposit will be determined by the availability of fluxing agents, mainly sodium, and its interaction with the surface of the impacting ash particles. The presence of a large proportion of pure SiO_2 (quartz) in the subbituminous parent coals indicates its availability to react with these fluxing agents to lower its melting temperature. The results of the CCSEM and chemical fractionation analyses indicate that the quartz and organically bound sodium present in the subbituminous coals have the potential to significantly contribute to ash-fouling deposit rate and strength development in the blends of the subbituminous coals with the bituminous coal.

4.2 Mill Performance

As mentioned previously, the pulverizer is usually the first area impacted by the switch to a blended fuel containing subbituminous coal. The high moisture content of the subbituminous coal contributes to a decreased mill outlet temperature (below the design limit) as the moisture evaporates in the mill. Attempts to maintain the design outlet temperature by closing tempering air dampers results in a limitation to achieving rated load as the proportion of subbituminous coal in the blend increases. Allowing the mill exit temperature to decrease provides some room to achieve rated load at higher blend ratios. However, some minimum temperature exists that is required to maintain adequate velocity for coal pipe transport. When this limit has been reached, attempts to

TABLE 5

CCSEM Analysis of Bailey Bituminous Coal

Size Distribution of Minerals	Size Distribution Range, μm 1.0–2.2	2.2–4.6	4.6–10	10–22	22–46	46–100	Totals
All Minerals	19.8	28.0	20.9	19.5	9.0	2.8	100.0
Quartz, SiO_2	19.4	32.7	33.7	12.2	2.0	0.0	100.0
Iron Oxide, Fe_2O_3	19.0	9.5	4.8	28.6	9.5	28.6	100.0
Rutile, TiO_2	0.0	0.0	100.0	0.0	0.0	0.0	100.0
Alumina, Al_2O_3	0.0	100.0	0.0	0.0	0.0	0.0	100.0
Calcite, $CaCO_3$	0.0	0.0	16.0	44.0	16.0	24.0	100.0
Dolomite, $(Ca,Mg)CO_3$	0.0	0.0	0.0	66.7	33.3	0.0	100.0
Kaolinite, $Al_4Si_4O_{10}(OH)_8$	22.8	35.0	19.5	16.7	4.9	1.2	100.0
Montmorillonite, $(0.5Ca,Na)_{0.7}(Al,Fe)_4(Si,Al)_8O_{20}(OH)_4$	42.5	30.0	7.5	10.0	10.0	0.0	100.0
K Al-Silicate	28.3	42.5	19.7	7.1	2.4	0.0	100.0
Fe Al-Silicate	21.4	64.3	14.3	0.0	0.0	0.0	100.0
Ca Al-Silicate	50.0	0.0	50.0	0.0	0.0	0.0	100.0
Aluminosilicate	17.6	47.1	17.6	17.6	0.0	0.0	100.0
Mixed Al-Silicate	50.0	50.0	0.0	0.0	0.0	0.0	100.0
Pyrite, FeS_2	10.5	15.6	24.3	33.0	16.7	0.0	100.0
Pyrrhotite, FeS	71.4	0.0	14.3	14.3	0.0	0.0	100.0
Gypsum, $CaSO_4 \cdot 2H_2O$	4.8	11.9	16.7	21.4	23.8	21.4	100.0
Apatite, $Ca_5F(PO_4)_3$	0.0	50.0	50.0	0.0	0.0	0.0	100.0
Si-Rich	14.3	28.6	14.3	7.1	21.4	14.3	100.0
Ca-Rich	25.0	50.0	25.0	0.0	0.0	0.0	100.0
Ca–Si-Rich	0.0	0.0	0.0	0.0	100.0	0.0	100.0
Unknown	35.3	33.3	15.7	7.8	3.9	3.9	100.0

Mineral Distribution Within Each Size Range	All Minerals	Size Distribution Range, μm 1.0–2.2	2.2–4.6	4.6–10	10–22	22–46	46–100
Quartz	9.8	9.6	11.5	15.9	6.2	2.2	0.0
Iron Oxide	2.1	2.0	0.7	0.5	3.1	2.2	21.4
Rutile	0.1	0.0	0.0	0.5	0.0	0.0	0.0
Alumina	0.3	0.0	1.1	0.0	0.0	0.0	0.0
Calcite	2.5	0.0	0.0	1.9	5.7	4.4	21.4
Dolomite	0.3	0.0	0.0	0.0	1.0	1.1	0.0
Kaolinite	24.7	28.4	30.8	23.1	21.1	13.3	10.7
Montmorillonite, $(0.5Ca,Na)_{0.7}(Al,Fe)_4(Si,Al)_8O_{20}(OH)_4$	4.0	8.6	4.3	1.4	2.1	4.4	0.0
K Al-Silicate	12.8	18.3	19.4	12.0	4.6	3.3	0.0
Fe Al-Silicate	1.4	1.5	3.2	1.0	0.0	0.0	0.0
Ca Al-Silicate	0.2	0.5	0.0	0.5	0.0	0.0	0.0
Aluminosilicate	1.7	1.5	2.9	1.4	1.5	0.0	0.0
Mixed Al-Silicate	0.2	0.5	0.4	0.0	0.0	0.0	0.0
Pyrite	27.7	14.7	15.4	32.2	46.9	51.1	0.0
Pyrrhotite	0.7	2.5	0.0	0.5	0.5	0.0	0.0
Gypsum	4.2	1.0	1.8	3.4	4.6	11.1	32.1
Apatite	0.2	0.0	0.4	0.5	0.0	0.0	0.0
Si-Rich	1.4	1.0	1.4	1.0	0.5	3.3	7.1
Ca-Rich	0.4	0.5	0.7	0.5	0.0	0.0	0.0
Ca–Si-Rich	0.1	0.0	0.0	0.0	0.0	1.1	0.0
Unknown	5.1	9.1	6.1	3.8	2.1	2.2	7.1
Totals	100.0	100.0	100.0	100.0	100.0	100.0	100.0

TABLE 6

CCSEM Analysis of Black Thunder Subbituminous Coal

Size Distribution of Minerals	Size Distribution Range, μm 1.0–2.2	2.2–4.6	4.6–10	10–22	22–46	46–100	Totals
All Minerals	15.6	22.3	22.8	18.3	13.7	7.3	100.0
Quartz, SiO_2	17.8	15.4	28.2	14.5	20.7	3.3	100.0
Iron Oxide, Fe_2O_3	8.7	13.0	30.4	19.6	28.3	0.0	100.0
Rutile, TiO_2	20.0	0.0	0.0	80.0	0.0	0.0	100.0
Alumina, Al_2O_3	0.0	0.0	100.0	0.0	0.0	0.0	100.0
Calcite, $CaCO_3$	0.0	12.5	12.5	0.0	25.0	50.0	100.0
Dolomite, $(Ca,Mg)CO_3$	0.0	0.0	0.0	0.0	0.0	100.0	100.0
Kaolinite, $Al_4Si_4O_{10}(OH)_8$	13.4	29.0	21.4	16.6	13.1	6.6	100.0
Montmorillonite, $(0.5Ca,Na)_{0.7}(Al,Fe)_4(Si,Al)_8O_{20}(OH)_4$	5.6	28.2	9.9	29.6	15.5	11.3	100.0
K Al-Silicate	28.6	57.1	14.3	0.0	0.0	0.0	100.0
Fe Al-Silicate	0.0	75.0	25.0	0.0	0.0	0.0	100.0
Ca Al-Silicate	14.3	57.1	14.3	0.0	14.3	0.0	100.0
Aluminosilicate	4.3	19.1	10.6	53.2	2.1	10.6	100.0
Mixed Al-Silicate	20.0	20.0	60.0	0.0	0.0	0.0	100.0
Pyrite, FeS_2	10.4	0.0	2.1	45.8	12.5	29.2	100.0
Pyrrhotite, FeS	100.0	0.0	0.0	0.0	0.0	0.0	100.0
Oxidized Pyrrhotite	33.3	0.0	0.0	0.0	66.7	0.0	100.0
Gypsum, $CaSO_4 \cdot 2H_2O$	0.0	100.0	0.0	0.0	0.0	0.0	100.0
Barite, $BaSO_4$	14.3	28.6	57.1	0.0	0.0	0.0	100.0
Ca Al-P	16.3	31.6	40.8	9.2	2.0	0.0	100.0
Gypsum/Barite	100.0	0.0	0.0	0.0	0.0	0.0	100.0
Si-Rich	14.3	33.3	23.8	0.0	9.5	19.0	100.0
Ca-Rich	0.0	0.0	0.0	0.0	100.0	0.0	100.0
Ca-Si-Rich	0.0	100.0	0.0	0.0	0.0	0.0	100.0
Unknown	42.9	14.3	17.1	7.1	11.4	7.1	100.0

Mineral Distribution Within Each Size Range	All Minerals	Size Distribution Range, μm 1.0–2.2	2.2–4.6	4.6–10	10–22	22–46	46–100
Quartz	24.2	27.6	16.7	30.0	19.2	36.5	11.0
Iron Oxide	4.6	2.6	2.7	6.2	4.9	9.5	0.0
Rutile	1.0	1.3	0.0	0.0	4.4	0.0	0.0
Alumina	0.2	0.0	0.0	0.9	0.0	0.0	0.0
Calcite	0.8	0.0	0.5	0.4	0.0	1.5	5.5
Dolomite	0.6	0.0	0.0	0.0	0.0	0.0	8.2
Kaolinite	29.1	25.0	37.8	27.3	26.4	27.7	26.0
Montmorillonite, $(0.5Ca,Na)_{0.7}(Al,Fe)_4(Si,Al)_8O_{20}(OH)_4$	7.1	2.6	9.0	3.1	11.5	8.0	11.0
K Al-Silicate	0.7	1.3	1.8	0.4	0.0	0.0	0.0
Fe Al-Silicate	0.4	0.0	1.4	0.4	0.0	0.0	0.0
Ca Al-Silicate	0.7	0.6	1.8	0.4	0.0	0.7	0.0
Aluminosilicate	4.7	1.3	4.1	2.2	13.7	0.7	6.8
Mixed Al-Silicate	0.5	0.6	0.5	1.3	0.0	0.0	0.0
Fe Silicate	0.0	0.0	0.0	0.0	0.0	0.0	0.0
Pyrite	4.8	3.2	0.0	0.4	12.1	4.4	19.2
Pyrrhotite	0.1	0.6	0.0	0.0	0.0	0.0	0.0
Oxidized Pyrrhotite	0.3	0.6	0.0	0.0	0.0	1.5	0.0
Gypsum	0.2	0.0	0.9	0.0	0.0	0.0	0.0
Barite	0.7	0.6	0.9	1.8	0.0	0.0	0.0
Ca Al-P	9.8	10.3	14.0	17.6	4.9	1.5	0.0
Gypsum/Barite	0.1	0.6	0.0	0.0	0.0	0.0	0.0
Gypsum/Al-Silicate	0.0	0.0	0.0	0.0	0.0	0.0	0.0
Si-Rich	2.1	1.9	3.2	2.2	0.0	1.5	5.5
Ca-Rich	0.1	0.0	0.0	0.0	0.0	0.7	0.0
Ca-Si-Rich	0.1	0.0	0.5	0.0	0.0	0.0	0.0
Unknown	7.0	19.2	4.5	5.3	2.7	5.8	6.8
Totals	100.0	100.0	100.0	100.0	100.0	100.0	100.0

TABLE 7

CCSEM Analysis of Antelope Subbituminous Coal

Size Distribution of Minerals	Size Distribution Range, μm 1.0–2.2	2.2–4.6	4.6–10	10–22	22–46	46–100	Totals
All Minerals	22.7	24.0	15.4	18.3	12.8	6.9	100.0
Quartz, SiO_2	20.7	20.3	13.4	21.0	16.9	7.6	100.0
Iron Oxide, Fe_2O_3	6.3	6.3	15.6	30.2	19.8	21.9	100.0
Rutile, TiO_2	14.3	0.0	0.0	85.7	0.0	0.0	100.0
Calcite, $CaCO_3$	30.0	70.0	0.0	0.0	0.0	0.0	100.0
Dolomite, $(Ca,Mg)CO_3$	33.3	66.7	0.0	0.0	0.0	0.0	100.0
Kaolinite, $Al_4Si_4O_{10}(OH)_8$	18.2	21.6	21.0	18.8	13.6	6.8	100.0
Montmorillonite, $(0.5Ca,Na)_{0.7}(Al,Fe)_4(Si,Al)_8O_{20}(OH)_4$	46.9	22.4	14.3	10.2	6.1	0.0	100.0
K Al-Silicate	35.0	15.0	5.0	10.0	20.0	15.0	100.0
Fe Al-Silicate	0.0	0.0	0.0	100.0	0.0	0.0	100.0
Ca Al-Silicate	46.2	53.8	0.0	0.0	0.0	0.0	100.0
Aluminosilicate	55.6	44.4	0.0	0.0	0.0	0.0	100.0
Mixed Al-Silicate	100.0	0.0	0.0	0.0	0.0	0.0	100.0
Fe Silicate	100.0	0.0	0.0	0.0	0.0	0.0	100.0
Pyrite, FeS_2	36.8	0.0	26.3	0.0	36.8	0.0	100.0
Oxidized Pyrrhotite	0.0	26.7	6.7	0.0	66.7	0.0	100.0
Gypsum, $CaSO_4 \cdot 2H_2O$	23.5	35.3	17.6	11.8	11.8	0.0	100.0
Barite, $BaSO_4$	25.0	50.0	25.0	0.0	0.0	0.0	100.0
Apatite, $Ca_5F(PO_4)_3$	100.0	0.0	0.0	0.0	0.0	0.0	100.0
Ca Al-P	14.9	42.1	28.9	13.2	0.8	0.0	100.0
Gypsum/Barite	100.0	0.0	0.0	0.0	0.0	0.0	100.0
Gypsum/Al-Silicate	50.0	50.0	0.0	0.0	0.0	0.0	100.0
Si-Rich	38.5	30.8	7.7	23.1	0.0	0.0	100.0
Ca-Rich	33.3	66.7	0.0	0.0	0.0	0.0	100.0
Unknown	34.1	22.0	9.9	11.0	11.0	12.1	100.0

Mineral Distribution Within Each Size Range	All Minerals	Size Distribution Range, μm 1.0–2.2	2.2–4.6	4.6–10	10–22	22–46	46–100
Quartz	28.8	26.3	24.5	25.2	33.2	38.0	31.9
Iron Oxide	9.5	2.6	2.5	9.7	15.8	14.7	30.4
Rutile	1.4	0.9	0.0	0.0	6.5	0.0	0.0
Calcite	2.0	2.6	5.8	0.0	0.0	0.0	0.0
Dolomite	0.3	0.4	0.8	0.0	0.0	0.0	0.0
Kaolinite	17.5	14.0	15.8	23.9	17.9	18.6	17.4
Montmorillonite, $(0.5Ca,Na)_{0.7}(Al,Fe)_4(Si,Al)_8O_{20}(OH)_4$	4.9	10.1	4.6	4.5	2.7	2.3	0.0
K Al-Silicate	2.0	3.1	1.2	0.6	1.1	3.1	4.3
Fe Al-Silicate	0.8	0.0	0.0	0.0	4.3	0.0	0.0
Ca Al-Silicate	1.3	2.6	2.9	0.0	0.0	0.0	0.0
Aluminosilicate	0.9	2.2	1.7	0.0	0.0	0.0	0.0
Mixed Al-Silicate	0.2	0.9	0.0	0.0	0.0	0.0	0.0
Fe Silicate	0.1	0.4	0.0	0.0	0.0	0.0	0.0
Pyrite	1.9	3.1	0.0	3.2	0.0	5.4	0.0
Oxidized Pyrrhotite	1.5	0.0	1.7	0.6	0.0	7.8	0.0
Gypsum	1.7	1.8	2.5	1.9	1.1	1.6	0.0
Barite	0.4	0.4	0.8	0.6	0.0	0.0	0.0
Apatite	0.1	0.4	0.0	0.0	0.0	0.0	0.0
Ca Al-P	12.0	7.9	21.2	22.6	8.7	0.8	0.0
Gypsum/Barite	0.1	0.4	0.0	0.0	0.0	0.0	0.0
Gypsum/Al-Silicate	0.4	0.9	0.8	0.0	0.0	0.0	0.0
Si-Rich	2.6	4.4	3.3	1.3	3.3	0.0	0.0
Ca-Rich	0.6	0.9	1.7	0.0	0.0	0.0	0.0
Unknown	9.0	13.6	8.3	5.8	5.4	7.8	15.9
Totals	100.0	100.0	100.0	100.0	100.0	100.0	100.0

achieve higher blend ratios of subbituminous coal result in boiler derate (1). Pilot mill testing was designed to address the limits to achieving rated mill capacity when bituminous/subbituminous blends are fired.

4.2.1 Blend Ratios Tested

This portion of the test program evaluated two PRB fuels, two bituminous coals, and five blends. The overall objective was to evaluate the influence of increasing concentrations of the PRB fuels in the blend. Four of the blends consisted of 70 wt% PRB and 30 wt% bituminous coal, and one blend contained 30 wt% PRB and 70 wt% bituminous coal. Many high-sulfur bituminous coals require a minimum blend of 70 wt% PRB fuel in order to comply with CAA Phase I sulfur limits (2.5 lb SO_2/MMBtu). Including 30 wt% PRB in a bituminous coal blend could bring medium-sulfur bituminous coals into Phase I compliance and low-sulfur bituminous coal into Phase II compliance (1.2 lb SO_2/MMBtu). The parent coals and blends tested are listed in Table 8 with further analyses summarized in Table 9. These data show that with the bituminous coals used, the concentration of PRB fuels would have to be increased slightly above the 70 wt% level in order to achieve the Phase II emission limit.

4.2.2 Test Format

Four pulverizer tests were completed on each of the nine fuel categories listed in Table 8, producing 36 sets of results. A high and low mill air flow rate and a high and low mill outlet temperature differential constituted the four tests per fuel category as shown in Table 10. Test 1 conditions represent typical bituminous coal baseline operating settings. Low Mill Air Rate refers to the manufacturer-recommended air/fuel ratio, with the High Mill Outlet Temperature Differential corresponding to a gas temperature about 30°F above the dew point temperature. The other settings listed represent conditions which may occur as a consequence of switching to PRB fuels or including high-moisture PRB coals in a blend.

4.2.3 Measured Parameters

The following list covers the measurements recorded during the pulverizer tests or obtained later following analysis. Pilot plant operating and performance data were automatically logged at 30-second intervals. Mill feed and product samples were collected throughout the test period and submitted to the analytical lab. Mill reject material was insignificant for all fuels and conditions.

Moisture Levels. Moisture levels were determined for each test on both the mill feed and pulverized product. Air-dried moisture concentrations are also reported.

Mill Air (inerted) Flow Rate. The flow rate of inerted air flowing out of the mill was monitored by an in situ mass flowmeter.

Mill Throughput Rates. A Merrick controller and weigh belt fed crushed coal to an airlock feeder and the mill. As-fed (wet, lb/hr) and thermal throughput rates (MMBtu/hr) are discussed. Throughput reductions, relative to various test conditions, are reported. The mill was operated at or near maximum capacity for all tests. Therefore, throughput data results refer to changes relative to the maximum throughput.

TABLE 8

Input SO_2 Levels for the Parent Coals and Blends

	Wet-Blend Ratio	Dry-Blend Ratio	Avg. lb SO_2/ MMBtu
Bituminous Coal			
Pittsburgh Seam, Bailey Steam Coal (Pitts.)	—	—	2.06
Illinois No. 6 Seam, Rend Lake Steam Coal (Ill.)	—	—	2.18
PRB Coal			
Antelope (Ant.)	—	—	0.77
Caballo Rojo (Cab. Rojo)	—	—	0.87
Blends			
70/30 Ant./Pitts.	69/31	64/36	1.31
70/30 Ant./Ill.	70/30	64/36	1.33
70/30 Cab. Rojo/Pitts.	69/31	63/37	1.34
70/30 Cab. Rojo/Ill.	67/33	60/40	1.39
30/70 Ant./Pitts.	29/71	24/76	1.71

Water Removed (drying). Water removed (lb H_2O/MMBtu) is discussed for all test conditions.

Product Fineness. Complete size analyses (all), as well as incremental size analysis (selected products), are reported.

Preferential Pulverization. Refers to constituent coals of a blend preferentially pulverizing into specific size fractions at a ratio different than that of the composite blend.

Power Requirements. Mill power draw (kW) was continuously recorded (30-second intervals) and later normalized by the corresponding thermal throughput (MMBtu/hr), yielding kWh/MMBtu results.

Mill Inlet/Outlet Temperatures. As previously described, recorded at 30-second intervals.

Gas Dew Point. A continuous relative humidity meter and thermocouple yielded corresponding wet-bulb and dew point temperature values used in selecting mill outlet temperatures for each individual pulverizer test.

Heat Requirements. A transmitting natural gas flowmeter monitored the firing rate of the heating/inerting gas-fired furnace. This furnace is the only significant source of external heat. The firing rate of the furnace is controlled by the mill outlet temperature set point value.

TABLE 9

Mill Feed Coal Analyses

Fuel:	Pittsburgh Seam (PGH) Steam Coal				Illinois No. 6 Seam (ILL) Steam Coal				Antelope (ANT) Powder River Basin				Caballo Rojo (CR) Powder River Basin				70/30 ANT/ILL Blend				70/30 CR/ILL Blend				70/30 ANT/PGH Blend				70/30 CR/PGH Blend				30/70 CR/PGH Blend			
Test Number:	1	2	3	4	5	6	7	8	9	10	11	12	13	14	15	16	17	18	19	20	21	22	23	24	25	26	27	28	29	30	31	32	33	34	35	36
Total Moisture, %	8.75	8.90	9.43	8.81	10.74	11.47	12.86	12.09	30.91	30.48	30.63	30.27	33.07	32.64	31.31	32.13	24.59	25.37	24.99	24.12	24.86	25.07	24.49	24.55	24.31	24.63	24.33	22.12	25.41	25.30	24.74	25.00	14.17	13.89	15.39	14.61
Proximate Analysis, wt% (dry)																																				
Ash	6.69	6.30	6.48	6.51	11.07	12.31	12.19	12.29	6.06	5.94	5.96	5.92	6.60	6.60	6.43	6.41	9.37	9.39	9.24	9.23	9.92	9.78	9.80	9.75	7.13	6.96	7.36	7.21	7.08	7.26	7.41	7.47	7.07	7.03	7.07	6.92
Vol. Matter	36.42	36.48	36.63	36.99	35.24	35.39	35.14	34.87	47.34	47.12	47.22	47.43	47.52	47.36	46.67	47.07	42.03	42.19	42.44	42.60	42.16	42.34	42.38	41.64	42.73	42.98	42.80	42.60								
Fixed Carbon	56.89	57.22	56.89	56.50	53.69	52.30	52.67	52.84	46.60	46.94	46.82	46.65	45.88	46.03	46.90	46.52	48.60	48.43	48.32	48.17	47.92	47.88	47.81	48.61	50.15	50.06	49.84	50 19	49.73	49.12	49.32	49.65	53.84	53.07	52.52	53.24
Ultimate Analysis, wt% (dry)																																				
Carbon	79.46	79.31	79.21	79.37	74.56	72.41	72.39	72.40	69.12	69.34	69.47	69.47	69.34	69.16	68.97	68.99	70.16	69.98	70.11	70.13	70.57	70.65	70.90	70.24	72.73	72.15	71.76	72.79	72.34	72.44	72.79	73.24	76.53	76.59	75.94	76.56
Hydrogen	5.01	5.00	5.02	5.02	4.73	4.66	4.67	4.70	4.75	4.79	4.74	4.75	4.77	4.78	4.77	4.76	4.73	4.71	4.70	4.72	4.73	4.70	4.72	4.74	4.88	4.85	4.82	4.87	4.87	4.90	4.85	4.85	5.01	5.01	5.02	5.04
Nitrogen	1.75	1.76	1.55	1.61	1.80	1.91	1.72	1.87	1.32	1.16	1.31	1.18	1.23	1.38	1.40	1.32	1.45	1.73	1.56	1.50	1.48	1.41	1.41	1.33	1.47	1.38	1.38	1.28	1.23	1.33	1.33	1.41	1.49	1.54	1.54	1.58
Sulfur	1.50	1.46	1.42	1.44	1.44	1.39	1.43	1.46	0.43	0.41	0.42	0.44	0.50	0.55	0.53	0.53	0.92	0.93	0.91	0.88	0.92	0.92	0.91	0.92	0.91	0.81	0.85	0.91	0.87	0.84	0.88	0.88	1.19	1.12	1.09	1.17
Ash	6.69	6.30	6.48	6.51	11.07	12.31	12.19	12.29	6.06	5.94	5.96	5.92	6.60	6.60	6.43	6.41	9.37	9.39	9.24	9.23	9.92	9.78	9.80	9.75	7.13	6.96	7.36	7.21	7.08	7.26	7.41	7.47	7.07	7.03	7.07	6.92
Oxygen	5.59	6.17	6.33	6.05	6.40	7.32	7.60	7.28	18.31	18.36	18.10	18.24	17.56	17.53	17.89	17.99	13.37	13.26	13.47	13.54	12.39	12.55	12.25	13.01	12.89	13.86	13.82	12.93	13.60	13.22	12.74	12.14	8.71	8.71	9.35	8.72
Btu/lb, dry	14,050	---	---	14,081	13,105	---	---	12,764	11,665	---	---	11,725	11,743	---	---	11,686	12,042	---	---	12,180	12,180	---	---	12,134	12,534	---	---	12,646	12,541	---	---	12,606	13,507	---	---	13,470
Btu/lb, as-milled	12,821	---	---	12,841	11,697	---	---	11,221	8059	---	---	8176	7860	---	---	7932	9081	---	---	9242	9152	---	---	9155	9487	---	---	9849	9355	---	---	9454	11,593	---	---	11,502
lb SO_2/MMBtu	2.14	---	---	2.05	2.20	---	---	2.29	0.74	---	---	0.76	0.86	---	---	0.90	1.52	---	---	1.44	1.50	---	---	1.52	1.44	---	---	1.44	1.39	---	---	1.39	1.76	---	---	1.74
HCl	56	---	---	57	54	---	---	54	52	---	---	50	61	---	---	57	49	---	---	46	53	---	---	52	49	---	---	49	0	---	---	58	0	---	---	0
@ % Moisture	2.47	---	---	2.62	6.01	---	---	4.27	14.71	---	---	15.59	13.61	---	---	12.42	8.27	---	---	11.61	10.50	---	---	12.53	7.73	---	---	8 04	8.18	---	---	9.50	3.92	---	---	5.40
Mill Feed Size																																				
½ in.	0	---	---	0	0	---	---	0	0	---	---	0	0	---	---	0	0	---	---	0	0.8	---	---	0	0	---	---	0	0	---	---	0	0	---	---	0.7
¼ in.	1.4	---	---	0.7	0.7	---	---	2.5	0	---	---	0.4	1.7	---	---	1.1	0.5	---	---	1.9	1.2	---	---	1.6	0.3	---	---	0.5	2.8	---	---	0.9	0.9	---	---	0.1
8 mesh	15.8	---	---	13.6	13.6	---	---	21.9	3.1	---	---	8	23.7	---	---	21	8.6	---	---	19.9	14	---	---	22.1	7.1	---	---	14.2	31.4	---	---	13.7	21.2	---	---	9.8
28 mesh	45.3	---	---	47	47	---	---	40.2	54.1	---	---	57.8	49	---	---	55.4	57.9	---	---	50.7	51.2	---	---	48.1	52.6	---	---	52 7	44.1	---	---	51.2	46.2	---	---	50.5
-28 mesh	37.5	---	---	38.7	38.7	---	---	35.4	42.8	---	---	33.8	25.6	---	---	22.5	33	---	---	27.5	32.8	---	---	28.2	40	---	---	32.6	21.7	---	---	34.2	31.7	---	---	38.9

TABLE 10

Pulverizer Air Rate and Outlet Temperature Differential Test Strategy

	Mill Air Rate	Mill Outlet Temperature Differential
Test 1	Low	High
Test 2	High	High
Test 3	High	Low
Test 4	Low	Low

Inerted Gas Analysis. Two in situ Hagen probes monitored the oxygen levels at the discharge of the fabric filter baghouse and at the exit of the heating/inerting furnace. Ambient air was admitted automatically to maintain the system oxygen concentration at 8.0 vol% O_2 for all tests.

4.2.4 Discussion of Results

The objective of the pulverization program was to evaluate typical bituminous-to-subbituminous coal switching conditions. Two situations commonly encountered are reduced mill outlet temperatures and varying air/fuel (lb/lb) ratios. Mill outlet temperature, air/fuel ratio, and fuel properties were the independently controlled variables in this program. The mill was operated at near the maximum throughput capacity with identical classifier settings for all tests. A simplified schematic of the CONSOL pulverizer pilot plant is shown in Figure 1.

Four pulverizer tests were completed with each of the nine fuel groups. Pulverizer summary operating results from the 36 tests are listed in Table 11. Product fuel analyses are listed in Table 12.

Mill Outlet Temperature. The CONSOL pulverizer pilot plant is an indirect pulverization system which recycles most of the circulating gases. The design and safe operation of this pilot plant require that the oxygen concentrations remain below 10 vol% and that circulating gases remain above the dew point temperature. Dew point condensation cannot be tolerated in the fabric filter baghouse. Also, wet metal surfaces and sticky fine coal may ultimately lead to fires and explosions.

To avoid condensation within the pulverizer pilot plant, gas temperatures were maintained at either 5°–10°F or 20°–30°F above the wet-bulb temperature of the gas. These control points were achieved by continuously monitoring both the relative humidity and the gas temperature.

Throughout this text, low and high mill outlet temperatures refer to low and high differences between the dry-bulb (actual gas) temperature and the wet-bulb temperature measurement (calculated from dry gas temperature and relative humidity). It is worth noting that at the operating temperatures and relative humidities within the CONSOL pulverizer pilot plant, dew point and wet-bulb gas temperature values are nearly identical.

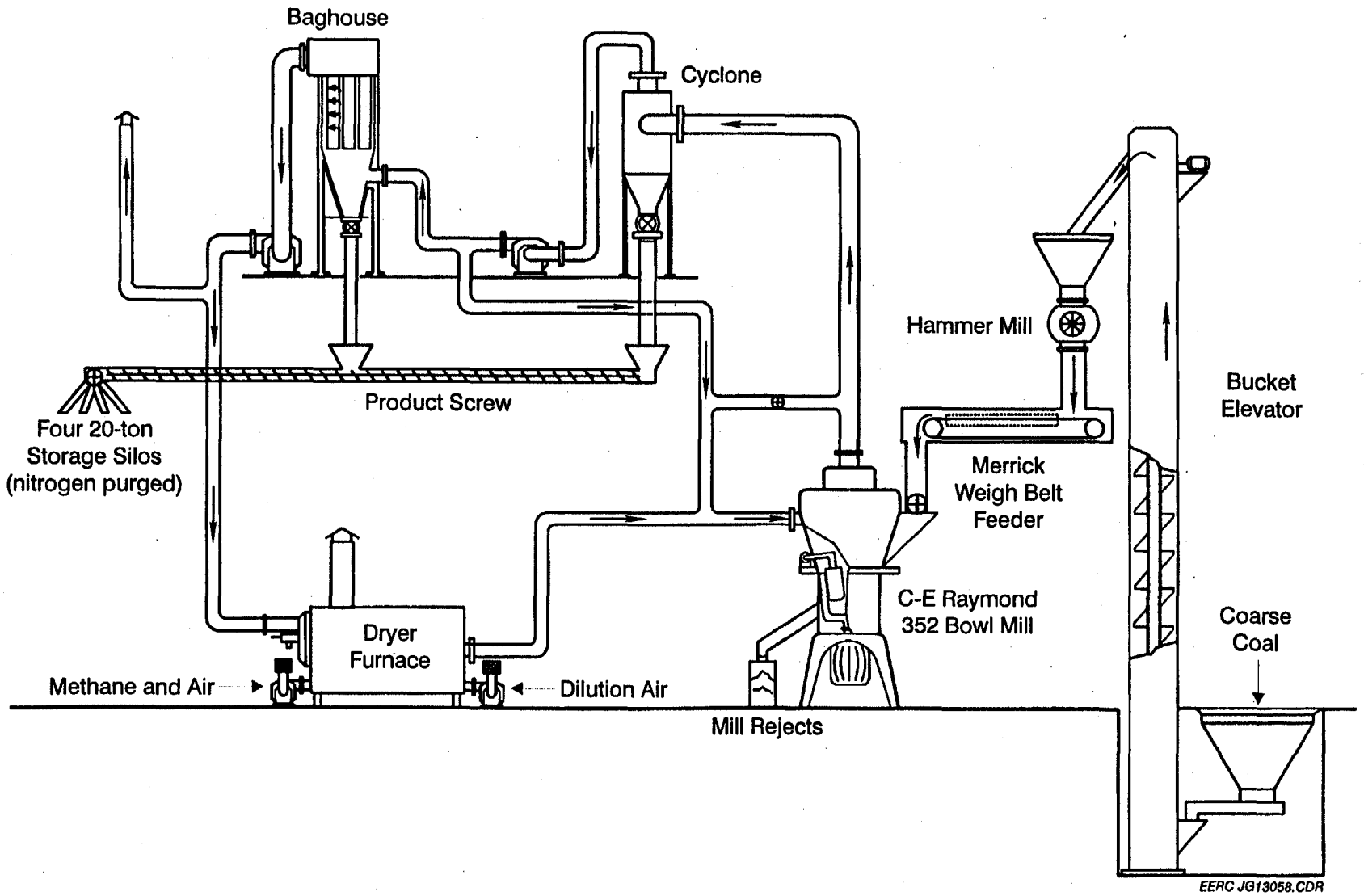

Figure 1. CONSOL pulverizer pilot plant.

TABLE 11

Pulverizer Pilot Plant Summary Results

Fuel:	Pittsburgh Seam (PGH) Steam Coal				Illinois No. 6 Seam (ILL) Steam Coal				Antelope (ANT) Powder River Basin			Caballo Rojo (CR) Powder River Basin				
Test Number:	Test 1	Test 2	Test 3	Test 4	Test 5	Test 6	Test 7	Test 8	Test 9	Test 10	Test 11	Test 12	Test 13	Test 14	Test 15	Test 16
Moisture, wt%																
Mill Feed	8.75	8.9	9.43	8.81	10.74	11.47	12.86	12.09	30.91	30.48	30.63	30.27	33.07	32.64	31.31	32.13
Mill Product	2.33	2.34	1.80	1.85	3.52	4.65	6.87	5.90	18.93	21.99	14.38	11.30	10.46	15.65	20.83	17.18
Mill Settings																
Mill, scfm	1730	2197	2197	1712	1706	2226	2183	1926	1768	2202	2206	1833	1898	2226	2175	1924
T-Twb, °F	2.3	7.2	29.4	29.8	30.6	28.1	7.1	8.9	3.3	2.0	21.3	20.0	19.9	12.1	8.3	6.0
Mill Results																
Mill, lb/h	2349	2642	2935	2875	2711	3191	2432	2425	1528	1741	2584	2439	2329	2805	1907	1913
Outlet Wet Gas/Coal, lb/lb	3.4	3.8	3.5	2.7	2.9	3.2	4.1	3.7	5.3	5.8	3.9	3.5	3.8	3.7	5.3	4.7
Inlet Wet Gas/Coal, lb/lb	3.3	3.8	3.4	2.7	2.9	3.1	4.1	3.6	5.2	5.7	3.8	3.3	3.5	3.5	5.1	4.5
Inlet Dry Gas/Coal, lb/lb	2.6	2.9	2.7	2.1	2.3	2.5	3.3	3.0	3.9	4.2	2.7	2.4	2.6	2.5	3.8	3.3
Mill In. T, °F	299	270	340	408	410	413	286	320	366	310	585	653	706	601	403	470
Mill Out. T, °F	163	168	189	188	190	189	164	164	168	167	190	187	187	181	174	174
Twb @ Mill, °F	161	161	159	158	160	161	157	155	164	165	168	167	167	169	166	168
Tdp @ Mill, °F	160	160	158	157	158	159	155	154	164	165	168	166	166	169	165	167
Product Fineness, wt%																
+50 mesh	0.2	1.3	1.2	0.1	0.2	0.4	0.4	0.0	0.2	1.1	0.5	0.1	0.1	0.1	0.6	0.1
-200 mesh	77.1	62.9	65.4	78.7	75.9	75.3	72.9	82.7	84.6	70.3	70.1	84.4	86.2	84.2	76.6	86.8
Properties, Btu/lb																
Mill Feed	12,776	12,755	12,681	12,768	11,465	11,371	11,192	11,291	8,088	8,139	8,121	8,163	7,852	7,902	8,058	7,962
Mill Product	13,675	13,674	13,750	13,743	12,392	12,247	11,962	12,086	9,491	9,133	10,024	10,385	10,504	9,895	9,287	9,716
Mill Power																
Mill-kW	15.32	12.04	13.15	17.41	14.14	15.47	12.54	15.31	12.58	11.51	12.90	15.79	13.12	14.50	10.68	12.25
kW/*ton*	13.0	9.1	9.0	12.1	10.4	9.7	10.3	12.6	16.5	13.2	10.0	13.0	11.3	10.3	11.2	12.8
kWh/MMBtu	0.51	0.36	0.35	0.47	0.46	0.43	0.46	0.56	1.02	0.81	0.61	0.79	0.72	0.65	0.69	0.80
Actual Rates																
Mill Feed, lb/h	2349	2642	2935	2875	2711	3191	2432	2425	1528	1741	2584	2439	2329	2805	1907	1913
Mill Product, lb/h	2195	2465	2707	2671	2508	2963	2276	2265	1302	1552	2094	1917	1741	2240	1654	1568
MMBtu/h	30.0	33.7	37.2	36.7	31.1	36.3	27.2	27.4	12.4	14.2	21.0	19.9	18.3	22.2	15.4	15.2
Est. Rates @ 17 kW																
tph - Mill Feed	1.3	1.9	1.9	1.4	1.6	1.8	1.6	1.3	1.0	1.3	1.7	1.3	1.5	1.6	1.5	1.3
MMBtu/h	35.3	50.4	50.9	38.0	39.6	42.2	39.1	32.2	17.7	22.2	29.3	22.7	25.1	27.5	25.9	22.4
Water Evaporated																
lb/h	154	177	228	204	203	228	156	160	226	190	490	522	588	565	252	345
lb/ton Mill Feed	131	134	155	142	150	143	129	132	296	218	380	428	505	403	265	361
lb/MMBtu	5.1	5.3	6.1	5.6	6.5	6.3	5.7	5.8	18.3	13.4	23.4	26.2	32.2	25.5	16.4	22.7
Mill Humidity																
H(in), lb/lb	0.296	0.295	0.265	0.253	0.265	0.281	0.247	0.230	0.330	0.349	0.367	0.335	0.328	0.380	0.348	0.366
H(out), lb/lb	0.309	0.307	0.282	0.273	0.284	0.297	0.259	0.244	0.349	0.361	0.399	0.379	0.376	0.417	0.365	0.391
Hs(out), lb/lb	0.345	0.410	0.843	0.828	0.890	0.846	0.347	0.350	0.400	0.394	0.874	0.794	0.785	0.652	0.499	0.491
Hwb(out)	0.318	0.317	0.297	0.289	0.300	0.313	0.270	0.255	0.356	0.368	0.411	0.391	0.388	0.424	0.373	0.398
RH(out), %	89	83	55	54	54	57	82	79	88	90	67	68	68	78	82	85

Continued . . .

TABLE 11 (continued)

Fuel:	70/30 ANT/ILL Blend				70/30 CR/ILL Blend				70/30 ANT/PGH Blend				70/30 CR/PGH Blend				30/70 ANT/PGH Blend			
Test Number:	Test 17	Test 18	Test 19	Test 20	Test 21	Test 22	Test 23	Test 24	Test 25	Test 26	Test 27	Test 28	Test 29	Test 30	Test 31	Test 32	Test 33	Test 34	Test 35	Test 36
Moisture, wt%																				
Mill Feed	24.59	25.37	24.99	24.12	24.86	25.07	24.49	24.55	24.31	24.63	24.33	22.12	25.41	25.3	24.74	25	14.17	13.89	15.39	14.61
Mill Product	13.89	16.30	10.85	8.57	11.93	15.35	9.47	7.01	7.19	10.10	14.87	12.06	14.43	15.20	8.75	7.51	6.37	6.27	5.35	4.58
Mill Settings																				
Mill, scfm	1798	2211	2204	1827	1988	2202	2216	1914	1721	2213	2230	1835	1975	2212	2197	1898	1898	2200	2212	1927
T-Twb, °F	8	3	23	25	8	7	23	26	29	24	1	8	3	2	23	25	7	4	25	26
Mill Results																				
Mill, lb/h	1769	1915	2480	2269	2001	2128	2451	2267	1477	2154	2028	1612	1752	1954	2274	2058	1729	2108	2360	2042
Outlet Wet Gas/Coal, lb/lb	4.7	5.3	4.1	3.7	4.6	4.8	4.2	3.9	5.4	4.8	5.1	5.3	5.2	5.2	4.5	4.3	5.1	4.8	4.3	4.4
Inlet Wet Gas/Coal, lb/lb	4.6	5.2	3.9	3.5	4.4	4.7	4.0	3.7	5.2	4.6	5.0	5.1	5.1	5.1	4.3	4.1	5.0	4.7	4.2	4.3
Inlet Dry Gas/Coal, lb/lb	3.5	3.8	2.9	2.7	3.3	3.4	3.0	2.9	4.1	3.5	3.6	3.9	3.7	3.7	3.2	3.1	3.8	3.5	3.2	3.3
Mill In. T, °F	395	333	511	557	426	376	524	587	462	456	336	341	355	352	548	604	311	301	429	460
Mill Out. T, °F	171	169	190	188	173	173	189	189	189	188	168	170	170	170	189	189	169	168	188	188
Twb @ Mill, °F	163	166	166	164	165	166	166	163	160	164	167	163	167	167	166	164	161	164	163	162
Tdp @ Mill, °F	162	166	165	162	164	166	165	162	158	163	167	162	166	167	165	163	160	164	162	161
Product Fineness, wt%																				
+50 mesh	0.2	0.3	0.6	0.1	0.1	0.6	1.1	0.1	0.0	0.5	0.2	0.3	0.2	0.4	0.4	0.1	0.2	0.3	0.3	0.1
-200 mesh	84.2	77.8	69.4	84.3	84.0	73.1	71.3	81.7	78.9	72.0	81.8	80.6	81.1	74.9	73.9	82.2	80.8	75.5	82.3	83.3
Properties, Btu/lb																				
Mill Feed	9,110	9,016	9,062	9,167	9,164	9,138	9,209	9,202	9,494	9,454	9,492	9,769	9,380	9,394	9,464	9,432	11,577	11,615	11,412	11,517
Mill Product	10,403	10,112	10,771	11,046	10,741	10,324	11,041	11,341	11,642	11,277	10,679	11,031	10,761	10,664	11,476	11,631	12,629	12,642	12,766	12,871
Mill Power																				
Mill-kW	13.60	12.46	12.58	15.05	12.47	11.58	11.86	12.66	10.91	12.01	15.58	11.61	11.69	12.04	11.89	12.54	13.13	13.70	13.30	13.45
kW/ton	15.4	13.0	10.1	13.3	12.5	10.9	9.7	11.2	14.8	11.2	15.4	14.4	13.3	12.3	10.5	12.2	15.2	13.0	11.3	13.2
kWh/MMBtu	0.84	0.72	0.56	0.72	0.68	0.60	0.53	0.61	0.78	0.59	0.81	0.74	0.71	0.66	0.55	0.65	0.66	0.56	0.49	0.57
Actual Rates																				
Mill Feed, lb/h	1769	1915	2480	2269	2001	2128	2451	2267	1477	2154	2028	1612	1752	1954	2274	2058	1729	2108	2360	2042
Mill Product, lb/h	1549	1707	2086	1883	1708	1883	2044	1840	1205	1806	1803	1427	1527	1721	1875	1669	1585	1936	2110	1827
MMBtu/h	16.1	17.3	22.5	20.8	18.3	19.4	22.6	20.9	14.0	20.4	19.3	15.7	16.4	18.4	21.5	19.4	20.0	24.5	26.9	23.5
Est. Rates @ 17 kW																				
tph - Mill Feed	1.1	1.3	1.7	1.3	1.4	1.6	1.8	1.5	1.2	1.5	1.1	1.2	1.3	1.4	1.6	1.4	1.1	1.3	1.5	1.3
MMBtu/h	21.3	24.9	32.1	24.9	26.5	30.2	34.3	29.7	23.1	30.5	22.2	24.4	25.3	27.4	32.6	27.9	27.5	32.2	36.4	31.5
Water Evaporated																				
lb/h	220	207	393	386	294	244	407	428	272	348	225	184	225	233	399	389	144	171	250	215
lb/ton Mill Feed	249	217	317	340	294	230	332	377	369	323	222	229	257	238	351	378	167	163	212	210
lb/MMBtu	13.6	12.0	17.5	18.6	16.0	12.6	18.0	20.5	19.4	17.1	11.7	11.7	13.7	12.7	18.5	20.1	7.2	7.0	9.3	9.1
Mill Humidity																				
H(in), lb/lb	0.312	0.358	0.340	0.298	0.327	0.357	0.330	0.286	0.258	0.318	0.372	0.312	0.361	0.377	0.343	0.305	0.297	0.338	0.307	0.298
H(out), lb/lb	0.331	0.371	0.366	0.332	0.349	0.373	0.358	0.322	0.285	0.342	0.386	0.327	0.377	0.392	0.370	0.337	0.309	0.349	0.324	0.316
Hs(out), lb/lb	0.444	0.419	0.872	0.826	0.482	0.482	0.847	0.851	0.841	0.826	0.401	0.440	0.434	0.431	0.867	0.843	0.413	0.410	0.833	0.824
Hwb(out)	0.340	0.378	0.379	0.346	0.358	0.381	0.371	0.337	0.300	0.356	0.391	0.337	0.384	0.397	0.383	0.351	0.318	0.357	0.339	0.330
RH(out), %	83	89	64	62	82	84	64	60	55	63	92	82	88	90	64	62	82	87	61	60

TABLE 12

Mill Product Coal Analyses

Fuel:	Pittsburgh Seam (PGH) Steam Coal				Illinois No. 6 Seam (ILL) Steam Coal				Antelope (ANT) Powder River Basin				Caballo Rojo (CR) Powder River Basin			
Test Number:	1	2	3	4	5	6	7	8	9	10	11	12	13	14	15	16
Product Moisture, %	2.33	2.34	1.80	1.85	3.52	4.65	6.87	5.90	18.93	21.99	14.38	11.30	10.46	15.65	20.83	17.18
Product Fineness, wt%																
+50 mesh	0.2	1.3	1.2	0.1	0.2	0.4	0.4	0.0	0.2	1.1	0.5	0.1	0.1	0.1	0.6	0.1
-200 mesh	77.1	62.9	65.4	78.7	75.9	75.3	72.9	82.7	84.6	70.3	70.1	84.4	86.2	84.2	76.6	86.8
Proximate, dry%																
Ash	6.57	6.36	6.49	6.73	11.36	12.05	11.73	12.13	6.27	6.08	6.02	5.94	6.71	6.58	6.67	6.86
Vol. Matter	36.25	35.77	36.31	36.44	34.89	34.84	34.44	34.94	47.81	48.00	46.88	47.20	47.26	47.64	48.02	48.17
Fixed Carbon	57.18	57.87	57.20	56.83	53.75	53.11	53.83	52.93	45.92	45.92	47.10	46.86	46.03	45.78	45.31	44.97
Ultimate, dry%																
Carbon	79.04	78.93	79.11	78.92	73.65	71.83	72.52	72.35	69.26	69.39	69.68	69.61	69.61	69.37	69.47	69.36
Hydrogen	5.28	5.29	5.32	5.19	4.84	5.12	5.25	5.20	6.59	7.20	6.02	4.84	4.76	6.25	7.02	6.38
Nitrogen	1.75	1.76	1.55	1.61	1.80	1.91	1.72	1.87	1.32	1.16	1.31	1.18	1.23	1.38	1.40	1.32
Sulfur	1.52	1.48	1.39	1.36	1.43	1.37	1.43	1.38	0.45	0.46	0.46	0.45	0.51	0.51	0.53	0.51
Ash	6.57	6.36	6.49	6.73	11.36	12.05	11.73	12.13	6.27	6.08	6.02	5.94	6.71	6.58	6.67	6.86
Oxygen	5.84	6.18	6.14	6.18	6.93	7.72	7.35	7.07	16.11	15.71	16.51	17.99	17.19	15.91	14.91	15.57
Btu/lb, dry	14,003	---	---	14,002	12,942	---	---	12,750	11,654	---	---	11,760	11,763	---	---	11,698
Btu/lb, as-fired	13,677	---	---	13,743	12,486	---	---	11,998	9448	---	---	10,432	10,533	---	---	9,688
lb SO_2/MMBtu	2.17	---	---	1.94	2.20	---	---	2.16	0.77	---	---	0.76	0.87	---	---	0.87
Ash Fusion, °F																
Reducing																
Initial	---	---	---	2475	2496	---	---	---	---	---	---	2320	2165	---	---	---
Softening	---	---	---	2518	2540	---	---	---	---	---	---	2345	2198	---	---	---
Hemispherical	---	---	---	2549	2578	---	---	---	---	---	---	2399	2220	---	---	---
Fluid	---	---	---	2603	2637	---	---	---	---	---	---	2420	2245	---	---	---
Oxidizing																
Initial	---	---	---	2620	2609	---	---	---	---	---	---	2375	2181	---	---	---
Softening	---	---	---	2661	2657	---	---	---	---	---	---	2419	2214	---	---	---
Hemispherical	---	---	---	2691	2691	---	---	---	---	---	---	2431	2242	---	---	---
Fluid	---	---	---	2714	2720	---	---	---	---	---	---	2449	2290	---	---	---
Ash Elements, wt%																
SiO_2	---	---	---	50.29	54.04	---	---	---	---	---	---	22.78	29.46	---	---	---
Al_2O_3	---	---	---	24.74	24.09	---	---	---	---	---	---	13.30	16.69	---	---	---
TiO_2	---	---	---	1.03	1.11	---	---	---	---	---	---	0.98	1.34	---	---	---
Fe_2O_3	---	---	---	13.28	10.97	---	---	---	---	---	---	6.70	5.40	---	---	---
CaO	---	---	---	2.71	1.69	---	---	---	---	---	---	28.00	24.17	---	---	---
MgO	---	---	---	0.84	1.05	---	---	---	---	---	---	4.99	4.38	---	---	---
Na_2O	---	---	---	0.50	0.93	---	---	---	---	---	---	1.76	1.32	---	---	---
K_2O	---	---	---	1.79	2.50	---	---	---	---	---	---	0.20	0.46	---	---	---
P_2O_5	---	---	---	0.53	0.16	---	---	---	---	---	---	2.03	1.17	---	---	---
SO_3	---	---	---	2.07	1.29	---	---	---	---	---	---	16.92	16.53	---	---	---
Undetermined	---	---	---	2.22	2.17	---	---	---	---	---	---	2.34	-0.92	---	---	---

Continued . . .

Table 12 (continued)

Fuel:	70/30 ANT/ILL Blend				70/30 CR/ILL Blend			70/30 ANT/PGH Blend					70/30 CR/PGH Blend				30/70 ANT/PGH Blend			
Test Number:	17	18	19	20	21	22	23	24	25	26	27	28	29	30	31	32	33	34	35	36
Product Moisture, %	13.89	16.30	10.85	8.57	11.93	15.35	9.47	7.01	7.19	10.10	14.87	12.06	14.43	15.20	8.75	7.51	6.37	6.27	5.35	4.58
Product Fineness, wt%																				
+50 mesh	0.2	0.3	0.6	0.1	0.1	0.6	1.1	0.1	0.0	0.5	0.2	0.3	0.2	0.4	0.4	0.1	0.2	0.3	0.3	0.1
-200 mesh	84.2	77.8	69.4	84.3	84.0	73.1	71.3	81.7	78.9	72.0	81.8	80.6	81.1	74.9	73.9	82.2	80.8	75.5	82.3	83.3
Proximate, dry%																				
Ash	9.39	8.88	8.77	9.38	9.75	9.34	9.68	9.80	7.19	6.77	7.22	7.24	7.13	7.27	7.70	7.58	6.84	6.90	7.01	6.84
Vol. Matter	43.74	42.80	42.52	43.53	42.79	42.40	42.44	43.45	42.88	44.29	44.03	42.21	42.86	44.00	42.14	43.00	38.85	39.33	39.84	39.76
Fixed Carbon	46.87	48.32	48.72	47.09	47.46	48.26	47.88	46.75	49.94	48.94	48.75	50.55	50.01	48.73	50.16	49.41	54.31	53.77	53.15	53.39
Ultimate, dry%																				
Carbon	70.45	70.56	70.64	70.50	71.49	70.63	70.50	70.60	72.77	72.99	72.85	73.85	73.39	73.85	72.84	72.82	76.67	77.48	76.49	76.85
Hydrogen	5.86	6.20	4.72	4.74	5.63	4.91	4.78	4.83	4.92	4.88	4.83	5.95	6.12	4.80	4.81	4.95	5.52	4.93	4.95	5.09
Nitrogen	1.45	1.73	1.56	1.50	1.48	1.41	1.41	1.33	1.47	1.38	1.38	1.28	1.23	1.33	1.33	1.41	1.49	1.54	1.54	1.58
Sulfur	0.82	0.84	0.79	0.79	0.86	0.89	0.87	0.83	0.82	0.77	0.80	0.85	0.82	0.85	0.90	0.84	1.16	1.20	1.13	1.15
Ash	9.39	8.88	8.77	9.38	9.75	9.34	9.68	9.80	7.19	6.77	7.22	7.24	7.13	7.27	7.70	7.58	6.84	6.90	7.01	6.84
Oxygen	12.03	11.79	15.08	13.10	10.79	14.24	14.17	12.60	12.83	14.58	14.30	10.83	11.31	13.23	13.75	12.40	8.32	9.49	10.43	8.48
Btu/lb, dry	12,070	---	---	12,092	12,228	---	---	12,164	12,544	---	---	---	---	---	---	12,575	---	---	---	13,488
Btu/lb, as-fired	10,393	---	---	11,056	10,769	---	---	11,311	11,642	---	---	---	---	---	---	11,631	---	---	---	12,871
lb SO_2/MMBtu	1.36	---	---	1.30	1.41	---	---	1.36	1.31	---	---	---	---	---	---	1.34	---	---	---	1.71
Ash Fusion, °F																				
Reducing																				
Initial	---	---	---	2140	---	---	---	2229	2053	---	---	---	---	---	---	2196	---	---	---	2211
Softening	---	---	---	2188	---	---	---	2274	2109	---	---	---	---	---	---	2240	---	---	---	2249
Hemispherical	---	---	---	2263	---	---	---	2328	2165	---	---	---	---	---	---	2298	---	---	---	2304
Fluid	---	---	---	2331	---	---	---	2400	2237	---	---	---	---	---	---	2416	---	---	---	2388
Oxidizing																				
Initial	---	---	---	2266	---	---	---	2321	2198	---	---	---	---	---	---	2280	---	---	---	2345
Softening	---	---	---	2289	---	---	---	2341	2227	---	---	---	---	---	---	2315	---	---	---	2360
Hemispherical	---	---	---	2351	---	---	---	2394	2267	---	---	---	---	---	---	2390	---	---	---	2419
Fluid	---	---	---	2409	---	---	---	2447	2317	---	---	---	---	---	---	2461	---	---	---	2478
Ash Elements, wt%																				
SiO_2	---	---	---	38.34	---	---	---	39.97	30.57	---	---	---	---	---	---	33.05	---	---	---	42.61
Al_2O_3	---	---	---	18.69	---	---	---	20.43	16.02	---	---	---	---	---	---	18.66	---	---	---	20.81
TiO_2	---	---	---	1.06	---	---	---	1.17	0.95	---	---	---	---	---	---	1.09	---	---	---	1.00
Fe_2O_3	---	---	---	8.03	---	---	---	7.45	9.08	---	---	---	---	---	---	7.64	---	---	---	11.59
CaO	---	---	---	12.58	---	---	---	11.87	16.49	---	---	---	---	---	---	14.83	---	---	---	8.44
MgO	---	---	---	2.85	---	---	---	2.95	3.10	---	---	---	---	---	---	2.75	---	---	---	1.72
Na_2O	---	---	---	1.33	---	---	---	1.08	1.33	---	---	---	---	---	---	1.00	---	---	---	0.87
K_2O	---	---	---	1.57	---	---	---	1.62	0.84	---	---	---	---	---	---	0.89	---	---	---	1.41
P_2O_5	---	---	---	1.00	---	---	---	0.56	1.23	---	---	---	---	---	---	0.80	---	---	---	0.82
SO_3	---	---	---	15.28	---	---	---	14.00	19.81	---	---	---	---	---	---	17.56	---	---	---	9.32
Undetermined	---	---	---	0.73	---	---	---	0.70	0.58	---	---	---	---	---	---	1.73	---	---	---	1.41

These temperature ranges were chosen to provide two scenarios: 1) a pulverizer exhausting bituminous coal and air at about 140°F, i.e., about 30°F above the dew point temperature of the gas and 2) the lower-temperature range representing the lowest safe operating temperature of the pilot plant system and presumably direct-fired utility mills as well.

Air/Fuel Ratio (lb/lb). Many mills are air-flow adjusted so that coal pipe velocities always exceed minimum values, typically 60 feet/second (fps), but remain under maximum suggested velocities of 85 to 90 fps. These velocities prevent particle drop-out and drifting in nonvertical coal pipe runs while minimizing erosion. Similarly, minimum air flow rates are required in vertical spindle mills to provide adequate air velocity in the throat area between the bowl and the mill; excessive coal spillage will result otherwise.

As described above, the air flow requirements of a given mill fall within a fairly narrow range. This air requirement range is independent of fuel changes, unless major system upgrades precede the fuel switch. The net result is that air/fuel ratios (lb air into mill/lb of wet coal fed) increase if the mass throughput of the mill cannot be maintained. It is conceivable that the air/fuel ratio could decline if the thermal throughput could be maintained and thus increase the mass throughput. This was not the case in any of the pilot plant tests.

The C-E Raymond 352 bowl mill in the CONSOL pulverizer pilot plant is designed to operate with air/fuel (lb/lb) ratios of 2.3–3.0. These ratios are based on Pittsburgh seam coals with a HGI value of 55. These air/fuel ratios decline as the mill size increases. During this test program, the resulting dry air/fuel ratios ranged from 2.1–3.3 lb/lb for the bituminous coals and 2.4–4.2 lb/lb for the subbituminous coals tested. With all of the pulverizer tests, only two air flow rates were used: 1) the system minimum, limited by the valve positioner and 2) an air rate 20%–30% higher than the minimum setting. The resulting range of air/fuel mass ratio values occurred as a result of maximum coal mass throughput changes due to fuel quality differences, while the mass rate of gas through the mill remained relatively constant.

Fuel Quality. The most significant quality difference, regarding milling, was the moisture content of the coals and blends. All coals were relatively clean (rock- and trash-free) and top-sized with a hammer mill prior to pulverization. The average moisture levels of the fuels tested are listed in Table 13 with complete analyses listed in Table 9.

The two bituminous coals, the Pittsburgh and Illinois No. 6 seam coals, are washed fuels. The Pittsburgh seam coal was lower in moisture and ash and had an as-milled heat content of about 12,800 Btu/lb. The Illinois No. 6 seam coal was higher in moisture and ash and had an as-delivered thermal content of 11,300 Btu/lb. Both coals had similar HGI values. The main difference in the bituminous coals was the lower thermal and higher moisture levels associated with the Illinois seam coal.

The two bituminous coals, the Pittsburgh and Illinois No. 6 seam coals, are washed fuels. The Pittsburgh seam coal was lower in moisture and ash and had an as-milled heat content of about 12,800 Btu/lb. The Illinois No. 6 seam coal was higher in moisture and ash and had an as-delivered thermal content of 11,300 Btu/lb. Both coals had similar HGI values. The main difference in the bituminous coals was the lower thermal and higher moisture levels associated with the Illinois seam coal.

TABLE 13

Moisture Content of Test Fuels

Fuels	wt% H_2O
Bituminous Coal	
Pittsburgh Seam (Pitts.)	9.0
Illinois No. 6 Seam (Ill.)	11.8
PRB Coal	
Antelope (Ant.)	30.6
Caballo Rojo (Cab. Rojo)	32.3
Blends	
70/30 Ant./Pitts.	23.9
70/30 Ant./Ill.	24.8
70/30 Cab. Rojo/Pitts.	25.1
70/30 Cab. Rojo/Ill.	24.7
30/70 Ant./Pitts.	14.5

The two PRB coals represent moisture differences between various regions of the PRB. The main area of interest for the testing reported here was to compare changes in pulverizer characteristics attributable to the higher moisture content of the Caballo Rojo coal relative to the Antelope coal. However, as described above, the moisture content and the heating values differed only slightly. The as-received heating value of the Antelope coal was about 8150 Btu/lb, whereas the Caballo Rojo delivered about 7900 Btu/lb. The heating value of the PRB coals was slightly lower than what is typically reported for these fuels. This occurred due to additional moisture absorption during storage. The Caballo Rojo coal, and blends containing Caballo Rojo, consistently produced higher (softer) HGI values as compared to the Antelope coal and blends. However, associating HGI values with subbituminous coal grinding performance has been inconsistent and often incorrect.

The blend ratios of 70/30 and 30/70 PRB/bituminous were chosen to represent fuel ratios to satisfy either Phase I or Phase II SO_2 compliance levels. The required blend ratio depends on the sulfur and heat content of the constituent coals. Table 14 shows maximum bituminous coal sulfur concentrations on a dry weight basis to satisfy compliance requirements at the two blend ratios tested.

TABLE 14

Maximum Bituminous Coal Sulfur Concentrations[1] in a PRB Blend to Satisfy Compliance Requirements[2]

Compliance	70/30 PRB/Bituminous	30/70 PRB/Bituminous
Phase I	3.8%	1.9%
Phase II	1.3%	0.8%

[1] Dry weight % basis.

[2] PRB at 0.8 lb SO_2/MMBtu and approximately 0.5 wt% sulfur, bituminous coal at 12,000 Btu/lb (dry basis).

4.2.5 Summary Observations

The following sections briefly describe the major findings from this fuel pulverization program. In the following analyses, the Illinois No. 6 seam coal with Low Mill Air Rate/High Mill Outlet Temperature is referred to as the baseline test case against which other results are compared.

Product and Feed Coal Moisture Levels. Product moisture results are shown in Figure 2. Generally, high mill outlet temperature differentials produced lower product moisture levels than the lower mill outlet temperatures. Also, moisture levels always increased with higher air flows, regardless of the temperature.

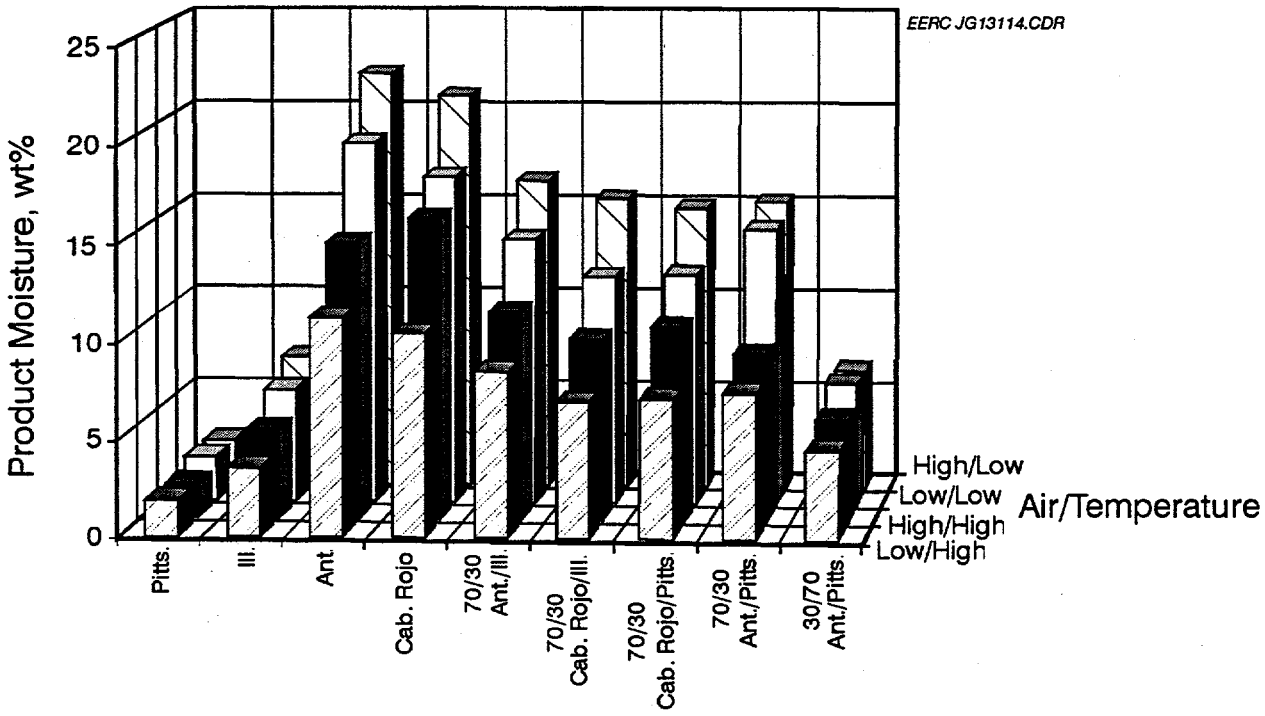

Figure 2. Moisture content of the pulverized test fuels at various mill operating conditions.

The quantities of water removed during the pulverization process have an enormous impact on the pulverization rate. In order to achieve the product moistures shown in Figure 2, three to six times as much water was removed (lb/MMBtu) in pulverizing the PRB coals as compared to the bituminous coals. Figure 3 displays these data. Both Figures 2 and 3 indicate that varying the air flow rate and/or operating temperatures for the bituminous coals and the 30/70 PRB/bituminous blend had little effect on product moisture values or moisture removal, relative to the high moisture fuels. In all cases, higher air flow rates decreased water removal, regardless of temperature, and higher temperatures increased water removal (lb/MMBtu), regardless of air flow rates.

Mill feed and air-dried moisture values are shown in Figure 4. The air-dried moisture content of the mill feed coal is not an ASTM (American Society for Testing and Materials) procedure, but does indicate the relative amounts of easily removed water. Most of the mill

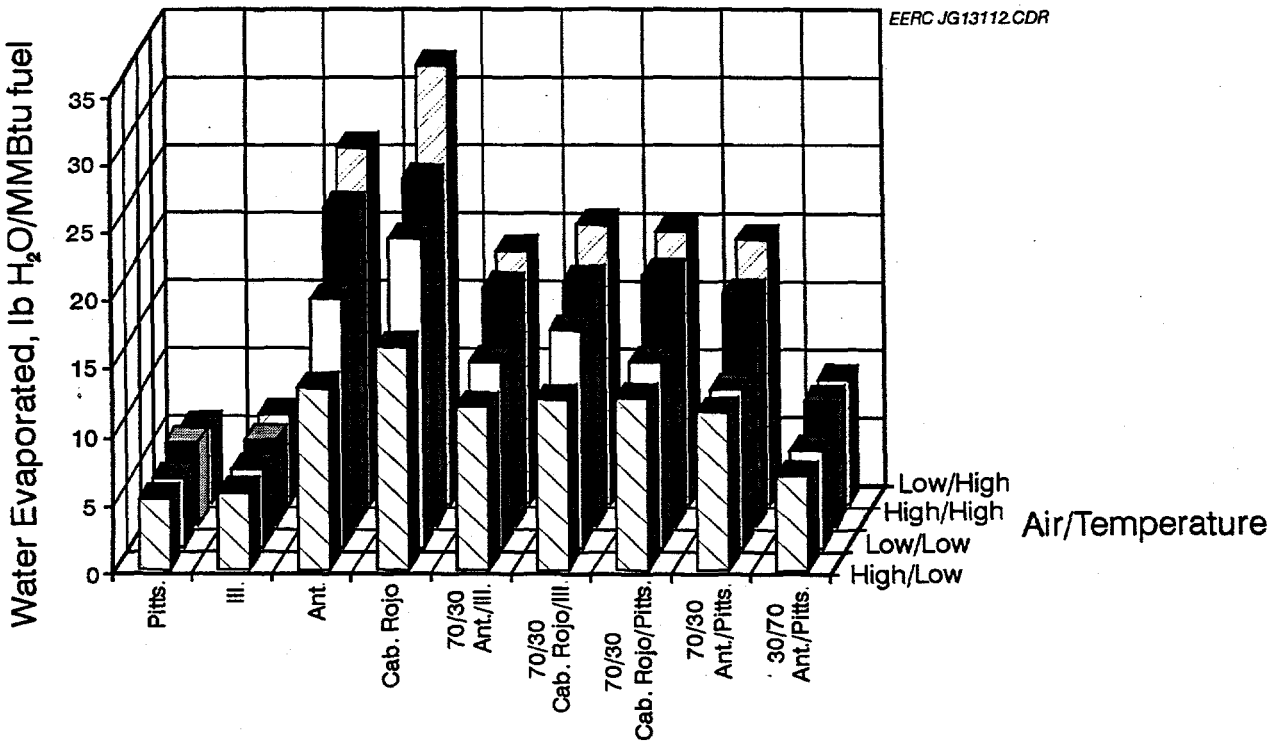

Figure 3. Quantities of water removed during pulverization of the test fuels at various mill operating conditions.

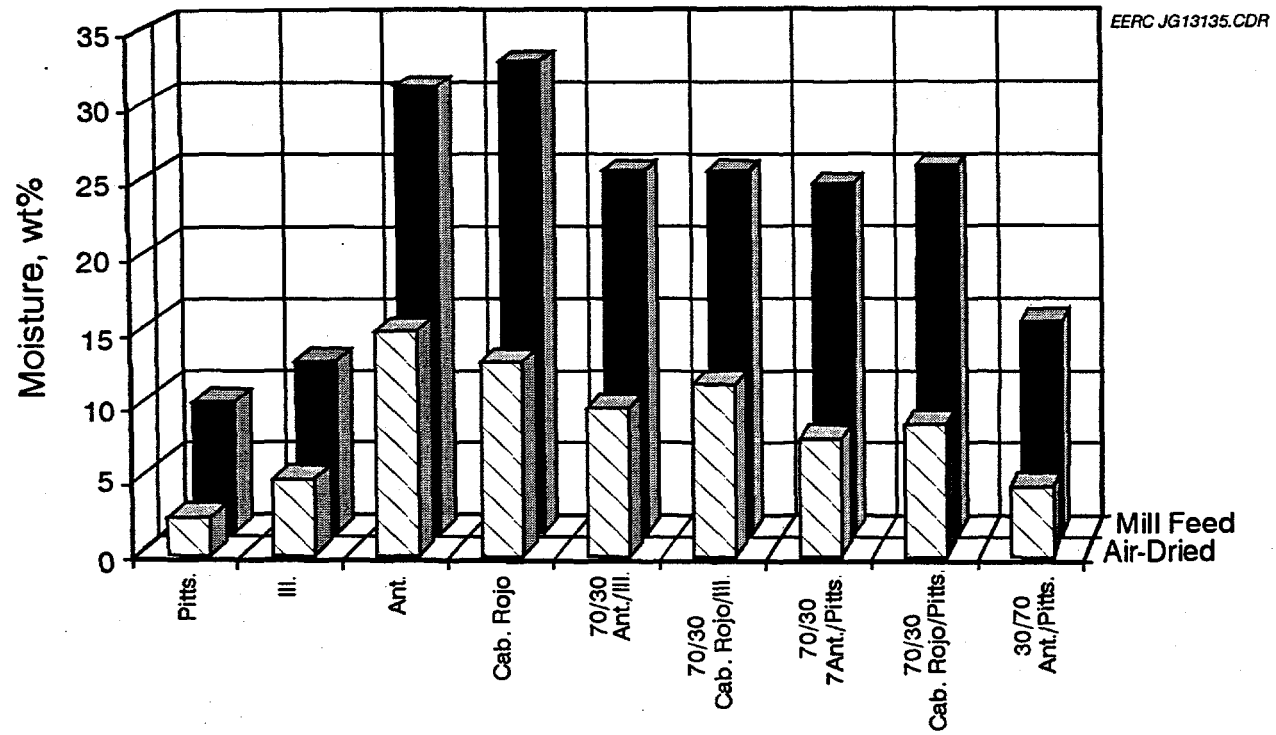

Figure 4. Mill feed and air-dried fuel moisture contents of the test fuels.

products depicted in Figure 2 and listed in Table 11 have moisture contents higher than the air-dried values shown in Figure 4. Product moisture values obtained from Low Mill Air Rate/High Mill Outlet Temperature tests had moisture contents at or slightly below the air-dried values. This suggests that for these tests the particle surface temperature was elevated above the wet-bulb temperature of the gas.

Mill Throughput (wet lb/hr). As shown in Figure 5, the PRB coals and 70/30 PRB/bituminous blends pulverized at 5%–20% lower mass throughput rates as compared to the maximum throughput rate of the bituminous coals. By increasing mill air flow rates, PRB coals and blends can be pulverized at mass rates comparable to bituminous coal. Increased mill outlet temperatures also facilitated higher mass throughput rates.

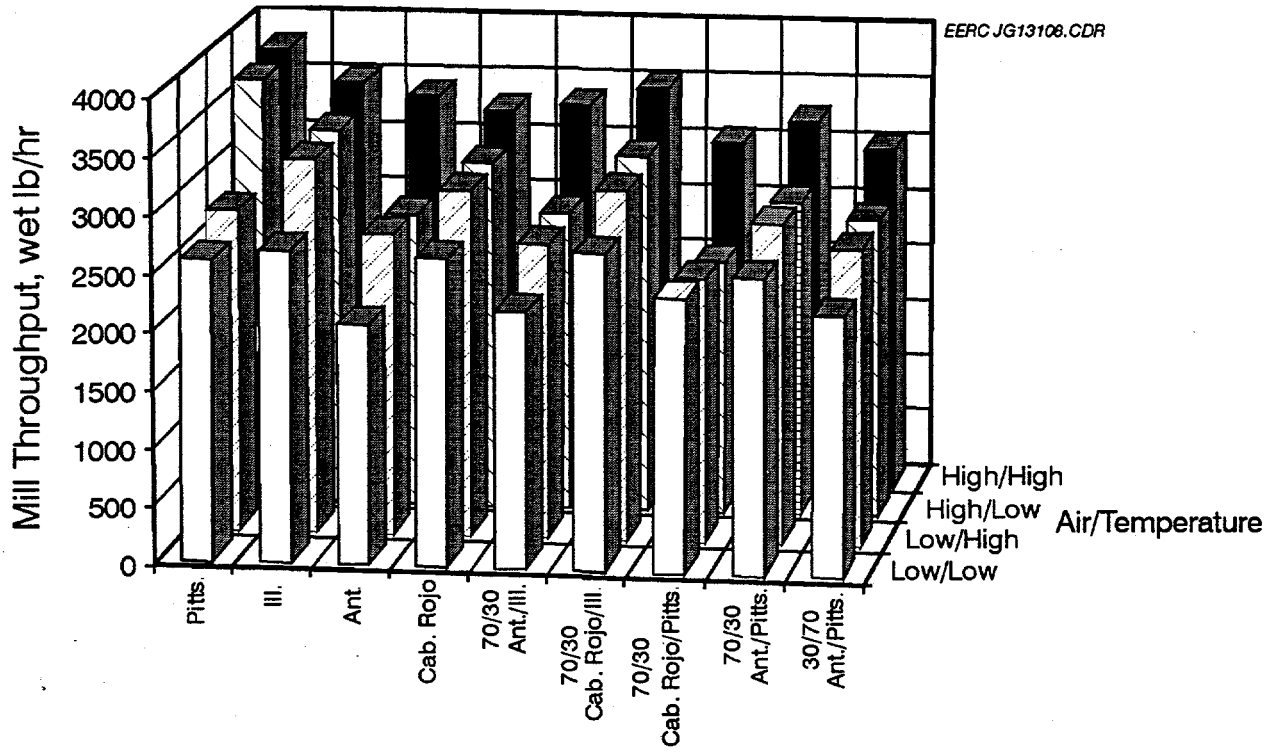

Figure 5. Maximum mill mass throughput of the test fuels at the various mill operating conditions.

The Caballo Rojo coal pulverized at a noticeably higher mass throughput rate as compared to the lower-moisture Antelope coal. This trend continued with the blends as displayed in Figure 5. The higher mass throughput more than compensated for its lower heat content, and thus the Caballo Rojo and blends also produced higher thermal throughput rates. The Caballo Rojo has an HGI value of 59 (@13.0% H_2O), as compared to 51 (@15.2% H_2O) for the Antelope coal. The Caballo Rojo coal also had a lower air-dried moisture value (Figure 4) in spite of a higher feed moisture content. A factor not shown with this increased rate observation is the considerably higher mill inlet temperatures required for the Caballo Rojo coal compared to the Antelope coal, as discussed below.

Mill Throughput (MMBtu/hr). The impact of only slightly lower maximum mass throughput rates is significantly magnified when both the moisture content and lower thermal values associated with PRB coals are examined. Including these factors into the maximum mass throughput results shown in Figure 5 produces the distinctively different maximum thermal throughput rate results, displayed in Figure 6. These data show that the maximum thermal throughput rate of the mill declined as much as 45%–55% for the PRB coals relative to the Illinois No. 6 baseline test (Low Mill Air Rate/High Mill Outlet Temperature).

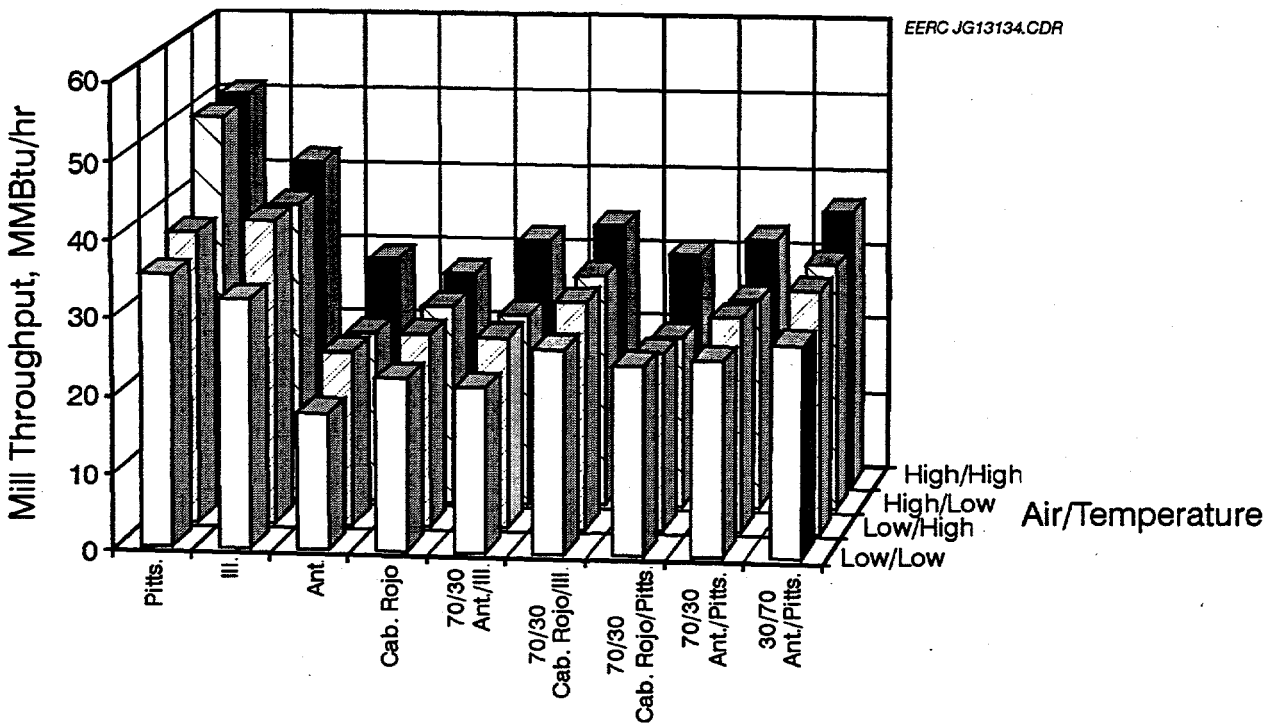

Figure 6. Maximum mill thermal throughput of the test fuels at the various mill operating conditions.

Raising the mill outlet temperature differential from about 5°F to about 25°F increased thermal throughput rates by only 10%–20%, although air heater demands rose by 50%–100%. Increasing the air/fuel ratio also increased the mill throughput. This gain in maximum thermal throughput capacity was magnified when both mill air rates and temperature differentials increased simultaneously. However, higher mill air rates increase throughput rates at the expense of coarser and higher-moisture products.

Product Fineness. With few exceptions, the Low Mill Air Rate conditions produced finer pulverized products. This difference was as much as 15 percentage points (passing 200 mesh). At a given air flow rate, the mill outlet temperature differential did not have a consistent effect on product fineness values. Overall, the PRB coals and blends pulverized finer than the bituminous coals alone under the same conditions. This corresponds to longer residence times for the PRB parent coals and blends in the mill. These data are graphically presented in Figure 7.

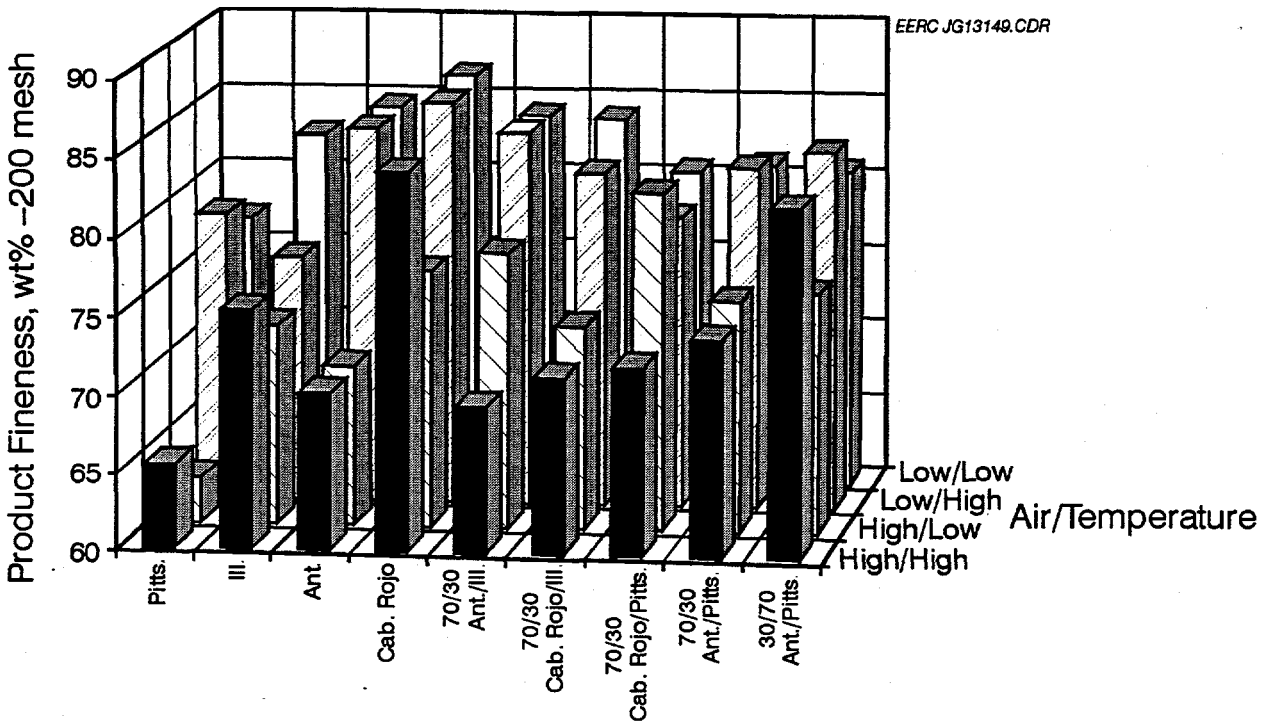

Figure 7. Results of product fuel particle-size analyses from the various mill operating conditions.

Mill (thermal) Derate. The maximum thermal throughput capacity of the mill declined for every test which included the high-moisture PRB component. A derate value is derived from a defined baseline value. For evaluation purposes, the thermal reductions in throughput capacity are discussed below using two different reference conditions:

1. Reductions relative to the Illinois No. 6 seam coal pulverized at the same test conditions.

2. Reductions relative to the Illinois No. 6 pulverized at the Low Mill Air Rate/High Mill Outlet Temperature condition.

Reductions Relative to the Illinois No. 6 Seam Coal Pulverized at the Same Test Conditions. Thermal throughput rate reductions referenced in this manner are shown in Figure 8. The data bars in this chart depict the rate changes relative to the Illinois coal pulverized under the same test conditions. This comparison could also be considered as maintaining the same operating conditions and simply switching fuels. Thus, compared to the Illinois coal tests, thermal throughput rates declined 30%–45% for the parent PRB coals, and the 70/30 PRB/Illinois blends declined by 18%–35%.

Compared to Illinois No. 6, the Pittsburgh seam coal pulverized at a somewhat higher rate in most cases. The 70/30 PRB/Pittsburgh blends were similar to, but showed slightly more thermal rate reductions than, the PRB/Illinois blends. The 30/70 PRB/Pittsburgh blends showed 15%–20% rate reductions.

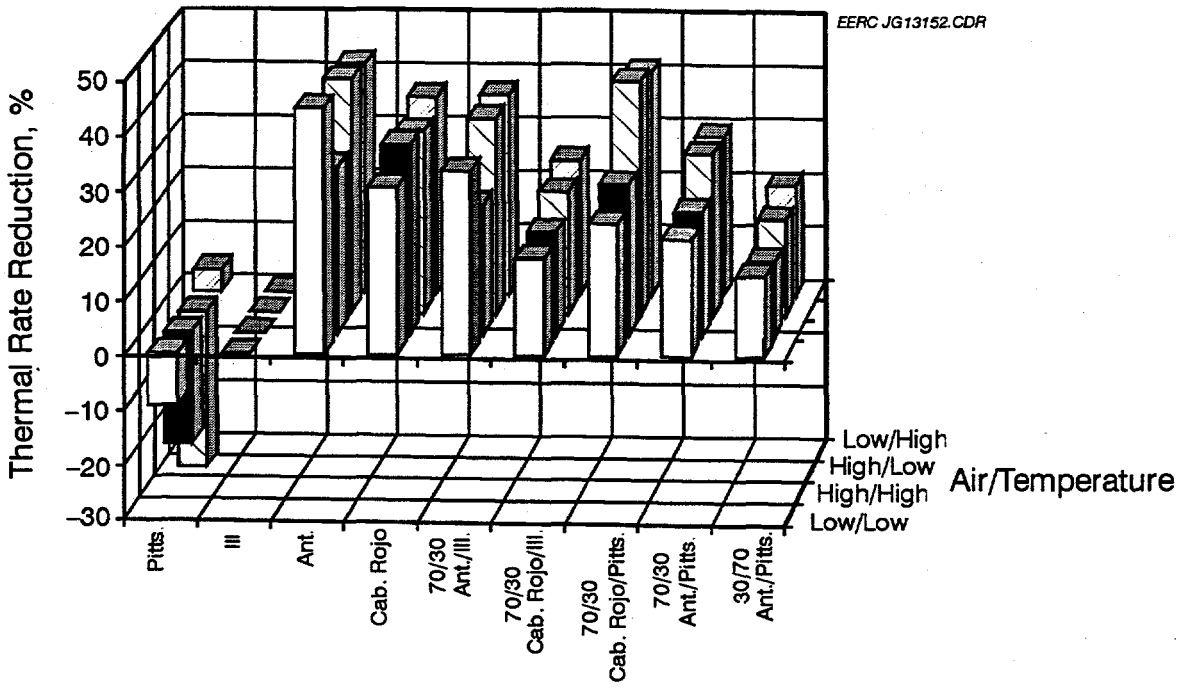

Figure 8. Mill thermal throughput reductions due to the test fuels relative to 100% Illinois No. 6 at equivalent pulverizer conditions.

The derate was less with the Caballo Rojo coal and blends as compared to the Antelope coal and blends, in spite of the higher moisture and lower heat content of the Caballo Rojo fuel. As previously mentioned, pulverizing the Caballo Rojo required considerably more air heater energy to operate at similar test conditions.

Reductions Relative to the Illinois No. 6 Seam Coal Pulverized at Low Air Rate/High Mill Outlet Temperature Baseline Conditions. Thermal throughput rate reductions referenced in this manner are shown in Figure 9. The data bars in this chart depict the rate changes relative to the Ill. No. 6 pulverized at normal baseline conditions (Low Mill Air Rate/High Mill Outlet Temperature). These comparisons would represent changes resulting from a fuel change and not maintaining similar operating conditions, e.g., lower mill outlet temperature or increasing air flow rates. Relative changes in throughput reference only the Ill. No. 6 baseline condition of Low Mill Air Rate/High Mill Outlet Temperature.

Relative to the Ill. No. 6 results, thermal derates for the Antelope and Caballo Rojo parent coals were 55% and 45%, respectively, at mill outlet temperatures about 5°F above the wet-bulb temperature. Increasing the mill air flow rate reduced this reduction by about 10 percentage points for each of the PRB parent coals.

High Mill Air Rate/High Mill Outlet Temperature conditions limited thermal throughput reductions to about 30% for the PRB fuels and 15%–20% for the 70/30 PRB/bituminous blends. These conditions were energy-intensive and produced coarser and higher-moisture-containing products.

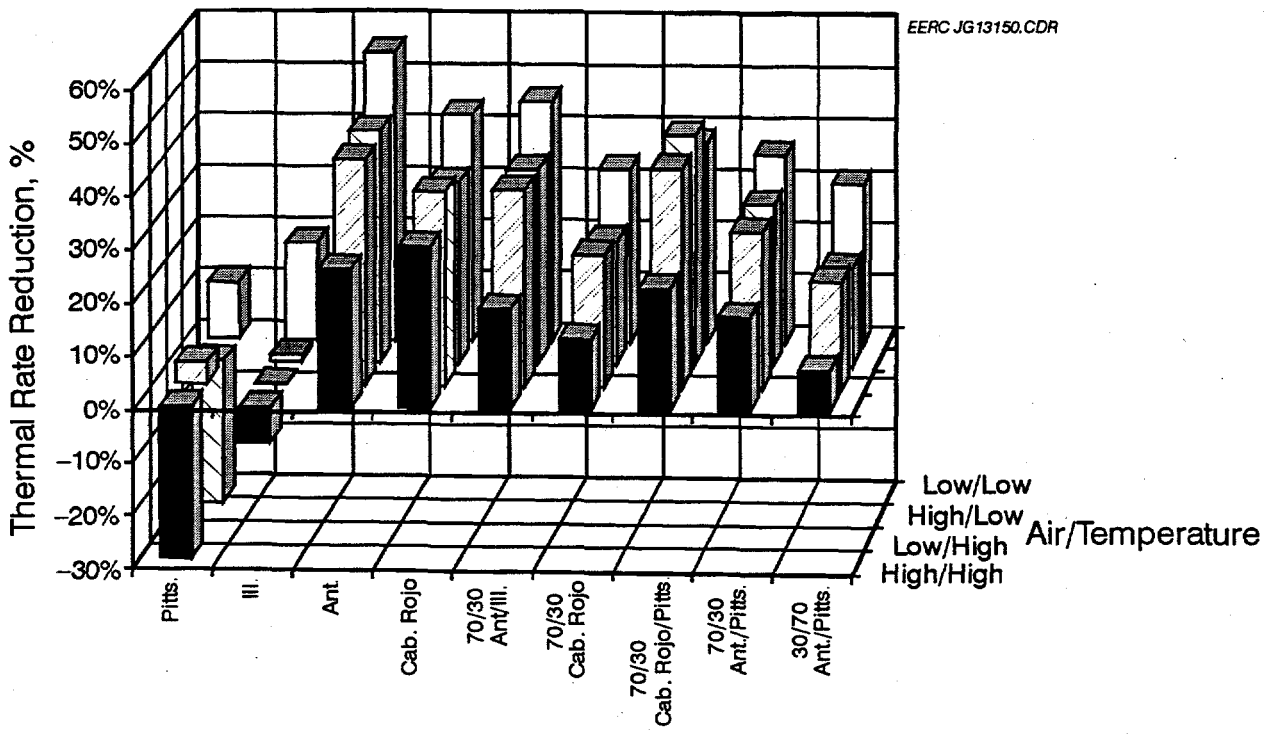

Figure 9. Mill thermal throughput reductions due to the test fuels relative to 100% Illinois No. 6 at baseline operating conditions (low air rate, high temperature).

Generally, the 30/70 PRB/bituminous blend had about 10%–20% less thermal throughput rate reduction in all condition categories, as compared to the corresponding 70/30 PRB/bituminous blend.

Preferential Pulverization. The PRB coals consistently preferentially pulverized into the finer (–325 mesh) size fraction, whereas the bituminous coal concentrated into the coarser size fractions.

Mill Inlet Temperatures. Maintaining bituminous baseline (Low Mill Air Rate/High Mill Outlet Temperature) pulverizer conditions for the PRB coals required increasing mill inlet temperatures from about 400°F (bituminous) to 650°–700°F for the PRB fuels. For the same conditions, the 70/30 PRB/bituminous blends required mill inlet temperatures of 550°–600°F. The 30/70 PRB/bituminous blend had a mill inlet temperature of 450°F for baseline pulverizer conditions. These data are shown in Figure 10.

Mill inlet temperatures for the PRB and PRB/bituminous blends dropped to the 300°–450°F range when the mill outlet temperature was reduced to near dew point temperatures.

The Caballo Rojo coal and blends, as compared to the Antelope coal and blends, consistently required higher (25°–100°F) mill inlet temperatures to attain specified pulverizer conditions. These higher temperatures correspond to increased energy demands on the air heater required to attain the test conditions.

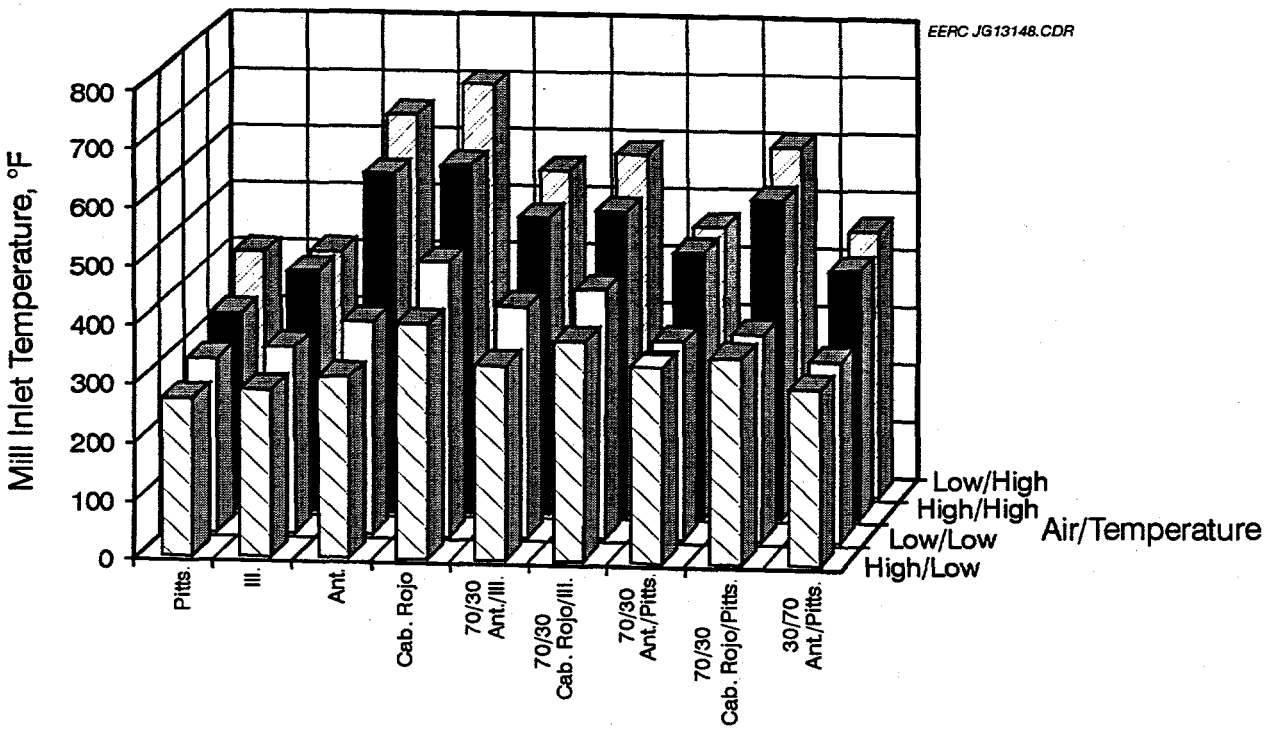

Figure 10. Differences in mill inlet temperature due to fuel type at the various mill operating conditions.

Mill inlet temperatures could be reduced 50°–100°F, while maintaining high mill outlet temperature differentials, when the mill air flow rate was increased. However, higher air rates through the mill increased the product coarseness and moisture content.

Direct-Fired Mill Inlet Temperature Estimates. Estimation of mill inlet temperature requirements for the direct-firing of the same mill can be made using the following assumptions:

- Maintaining the same mill inlet temperature differential produces the same drying rate, i.e., the same product moistures.
- Maintaining the same mill inlet temperature differential produces the same throughput rate.
- Heat losses are the same for both mill types.

The high humidity levels associated with indirect recycle mills must also be addressed when estimating direct-fired mill inlet and outlet temperatures. There are two extremes: 1) subtract the humidity (equivalent dry gas mass rate) component from the direct-fired estimations or 2) treat the humidity component as if it were air (equivalent total gas mass rate). The resulting temperature estimates using these assumptions are shown in Figure 11. Item No. 1 would maintain the same dry air/fuel ratio but with lower velocities through the mill. This could influence product moisture, rates, and fineness. Also, lower gas mass velocities will result in an increase in the gas temperature in order to maintain the same heating requirements. Item No. 2 would increase the dry air/fuel ratio

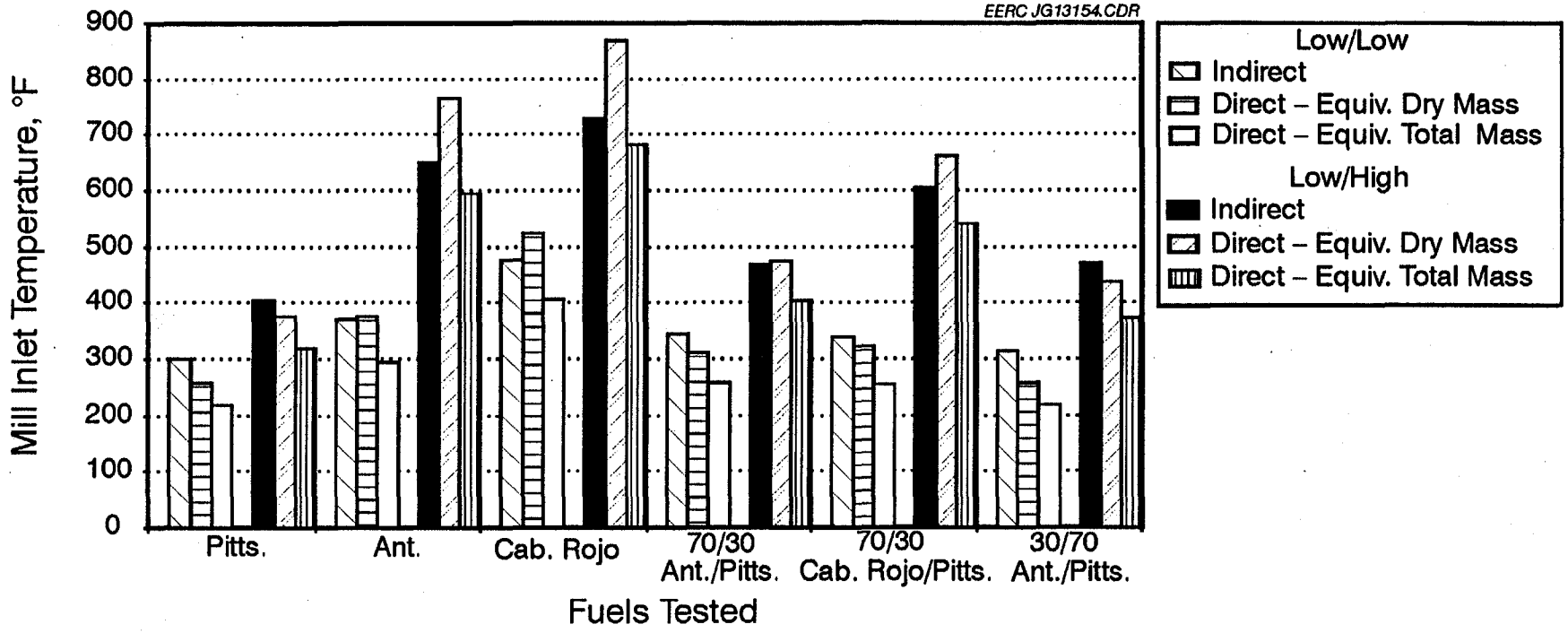

Figure 11. Estimated mill inlet temperatures of indirect- versus direct-fired pulverizers for selected test fuels.

but maintain similar gas velocities through the mill. This item tends to push dry air/fuel ratios rather high. The temperature estimation differences resulting from these two items increase as the moisture in the feed coal increases. As depicted in Figure 11, the differences between these two assumptions is about 50°F for both bituminous coals, increasing to about a 150°F difference for the PRB coals.

Mill Outlet Temperatures. Mill outlet temperatures for this indirect pulverizer system are about 40°F higher than a direct-fired mill, although the temperature difference between the dry gas and wet-bulb temperatures are the same. This results from humidity differences between the two mill types. The mill outlet temperatures were adjusted for individual tests to obtain high- and low-temperature differences between the dry-gas and wet-bulb temperatures. For most of the fuels and blends tested, the low-temperature differentials required outlet temperatures in the 160°–170°F range. The high-outlet-temperature differentials required 185°–190°F gas temperatures.

Direct-Fired Mill Outlet Temperature Estimates. Estimation of mill outlet temperature requirements for the direct-firing of the same mill can be made using the same assumptions for the mill inlet temperature:

- Maintaining the same mill outlet temperature differential produces the same drying rate, i.e., the same product moistures.
- Maintaining the same mill outlet temperature differential produces the same throughput rate.
- Heat losses are the same for both mill types.

The high humidity levels associated with indirect recycle mills must also be addressed when estimating direct-fired mill inlet and outlet temperatures. There are two extremes: 1) subtract the humidity (equivalent dry gas mass rate) component from the direct fired estimations or 2) treat the humidity component as if it were air (equivalent total gas mass rate). The resulting temperature estimates using these assumptions are shown in Figure 12. Item No. 1 would maintain the same dry air/fuel ratio but with lower velocities through the mill. This could influence product moisture, rates and fineness. Also, lower gas mass velocities increase the mill outlet temperature in order to maintain the same elevation above the dew point because the same mass of water is residing in less gas (higher humidity). Item No. 2 would increase the dry air/fuel ratio but maintain similar gas velocities through the mill. This item tends to push the dry air/fuel ratio rather high and lowers the mill outlet temperature because the same moisture is diluted with more gas (lower humidity). The temperature estimation differences resulting from these two items is about 10°F for most cases, as depicted in Figure 12.

System Heat Requirements. Obtaining desired mill outlet temperature differentials and the corresponding mill inlet temperatures for the wide variation in tested fuels required vastly different system heat requirements. Air heating requirement data are presented in two formats:

- Heat required per MMBtu processed. These data reflect both air heater duty and thermal throughput rates.

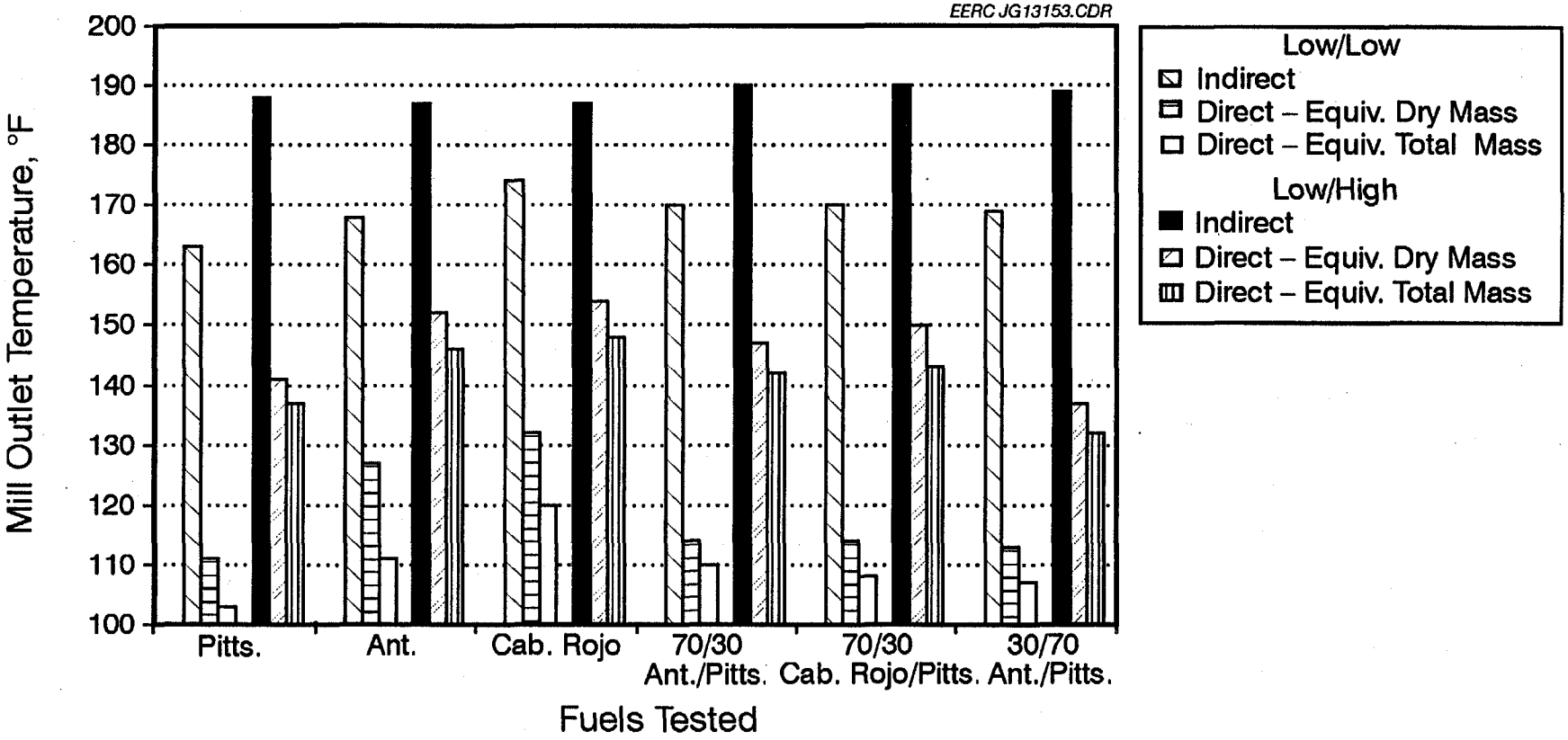

Figure 12. Estimated mill outlet temperatures of indirect- versus direct-fired pulverizers for selected coals.

- System heat requirement changes. These results examine air heater demand without regard to rates through the mill.

Heat Requirements per MMBtu. These data are plotted in Figure 13 and represent the quotient of air heater duties (Btu) and the thermal throughput rate (MMBtu). Pulverizing PRB coals and 70/30 PRB/bituminous blends at bituminous baseline conditions (Low Mill Air Rate/High Mill Outlet Temperature) had three times the heat requirement as compared to the bituminous coals. The 30/70 PRB/bituminous blend required about a 50% increase in heat input.

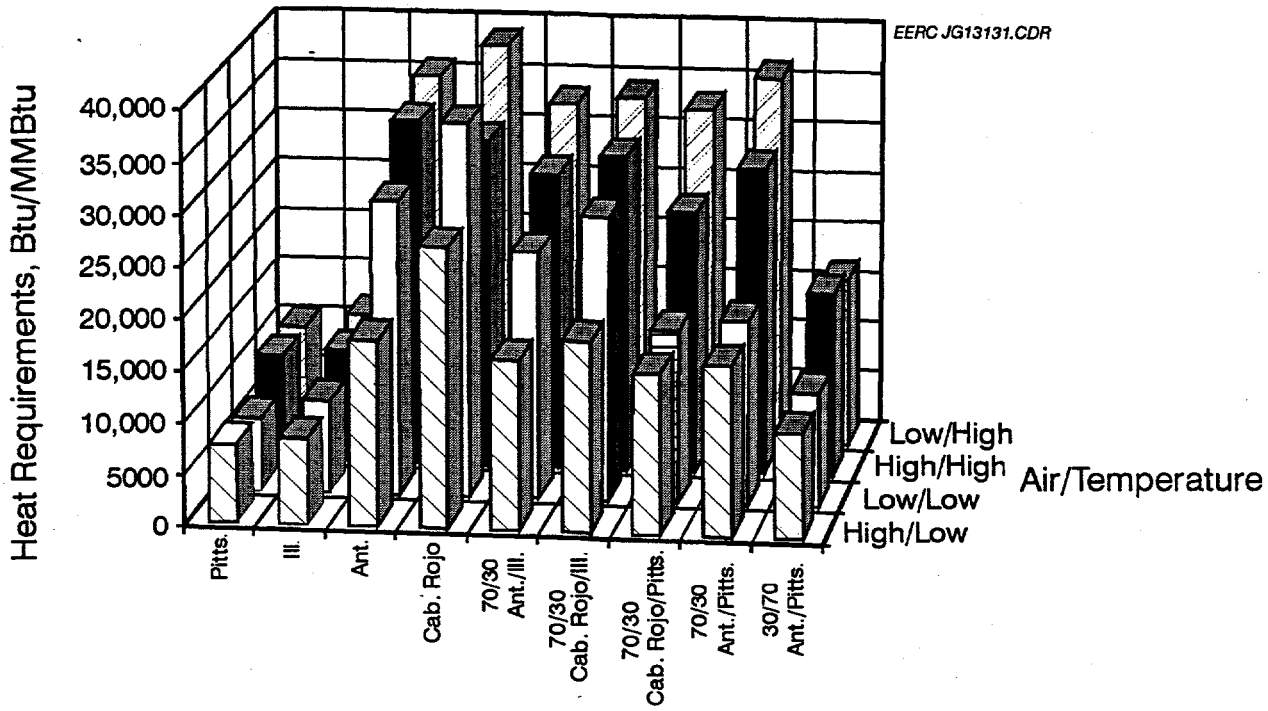

Figure 13. Pulverizer heat requirements per MMBtu of test fuel processed for the various mill operating conditions investigated.

High Mill Air Rate/Low Mill Outlet Temperature conditions consistently halved (to 1.5 times baseline) PRB and 70/30 PRB/bituminous blend heating requirements. Low Mill Air Rate/Low Mill Outlet Temperature conditions also reduced heat requirements somewhat but was offset by significantly lower mill throughput rates.

Heating requirements presented in this manner show the large increases demanded by high-moisture coals. Figure 13 also shows the advantages in blending lower-moisture, higher-thermal-content coals with PRB fuels, most notably at lower mill outlet temperature differentials.

The impact that the higher-moisture Caballo Rojo coal has on energy requirements can be observed in Figure 13. Considerably more thermal energy was required in order to maintain the same mill operating conditions as the Antelope coal. As previously discussed, the higher throughput rates observed with the Caballo Rojo coal, as compared to the Antelope coal, occurred at a considerable energy cost.

System Heat Input Changes Relative to Ill. No. 6 Baseline. In this data analysis, only the demand on the air heater is examined and compared to the baseline case, the Ill. No. 6 coal at Low Mill Air Rate/High Mill Outlet Temperature conditions. These results are shown in Figure 14. The bars in Figure 14 reflect the firing rate of the air heater relative to the Ill. No. 6 baseline results. Most PRB coals and blends, pulverizing at Low Mill Outlet Temperature conditions, actually required less heat than the baseline case, at a considerable derate from the maximum throughput however. If the derated throughput is sufficient to fire the boiler, then any of these fuels requiring less than or equal amounts of heat energy could replace the baseline coal and not exceed the capacity of the air-heating system.

Figure 14 also shows the considerable demand increases caused by raising the mill outlet temperature from 5° to about 25°F above the wet-bulb temperature of the gas.

4.3 High-Temperature Fouling

4.3.1 Combustion Test Sample Handling and Preparation

Bulk samples of the three parent coals to be used for the pilot-scale combustion tests (Bailey bituminous, Black Thunder subbituminous, and Antelope subbituminous) were received at the EERC at the 2-in. topsize normally supplied to utility boiler customers. Each of the parent fuels was crushed to minus ¼ in., split into four equal portions, and mixed thoroughly prior to blending. The Bailey/Black Thunder and Bailey/Antelope blends were prepared to achieve bituminous coal proportions of 65% and 35% by weight. The blended fuels were then split and mixed prior to pulverization to ensure sample homogeneity. The pulverization equipment, consisting of a hammer-mill pulverizer and associated aerodynamic classifier, was adjusted to achieve a combustion test grind consisting of approximately 70% <200 mesh (75 μm). The pulverized samples were charged to transport hoppers for use in the combustion tests.

4.3.2 Combustion Test Fuel Properties

Fuel samples were taken directly from the feeder during combustion testing at intervals of approximately 30 minutes to produce a one-quart composite for each run. Each composite fuel sample was then submitted for proximate, ultimate, higher heating value (HHV), coal ash composition, ash fusibility, and sieve analyses.

Proximate, Ultimate, Heating Value, and Sieve Analyses. The results of the analyses listed here are presented in Table 15. Each of the subbituminous coals were blended with the Bailey bituminous coal at ratios of 35% and 65% by weight. The blend ratio of 35% PRB to 65% Bailey was selected based on past blend experience from utilities designed to burn high-sulfur eastern bituminous coal. Utility experience has shown that blending up to approximately 35% PRB coal with the design bituminous coal does not significantly affect system operations such as mill performance, fouling of boiler tube surfaces, and fly ash collectability. The 65% PRB blend level was selected arbitrarily as an intermediate point between the 35% and 100% PRB blend levels.

Since moisture levels vary from the as-received samples (due to moisture losses in handling and grinding), it is best to compare the moisture-free values of the various components when evaluating the effects of the blend on fuel properties. The moisture-free analyses reported in

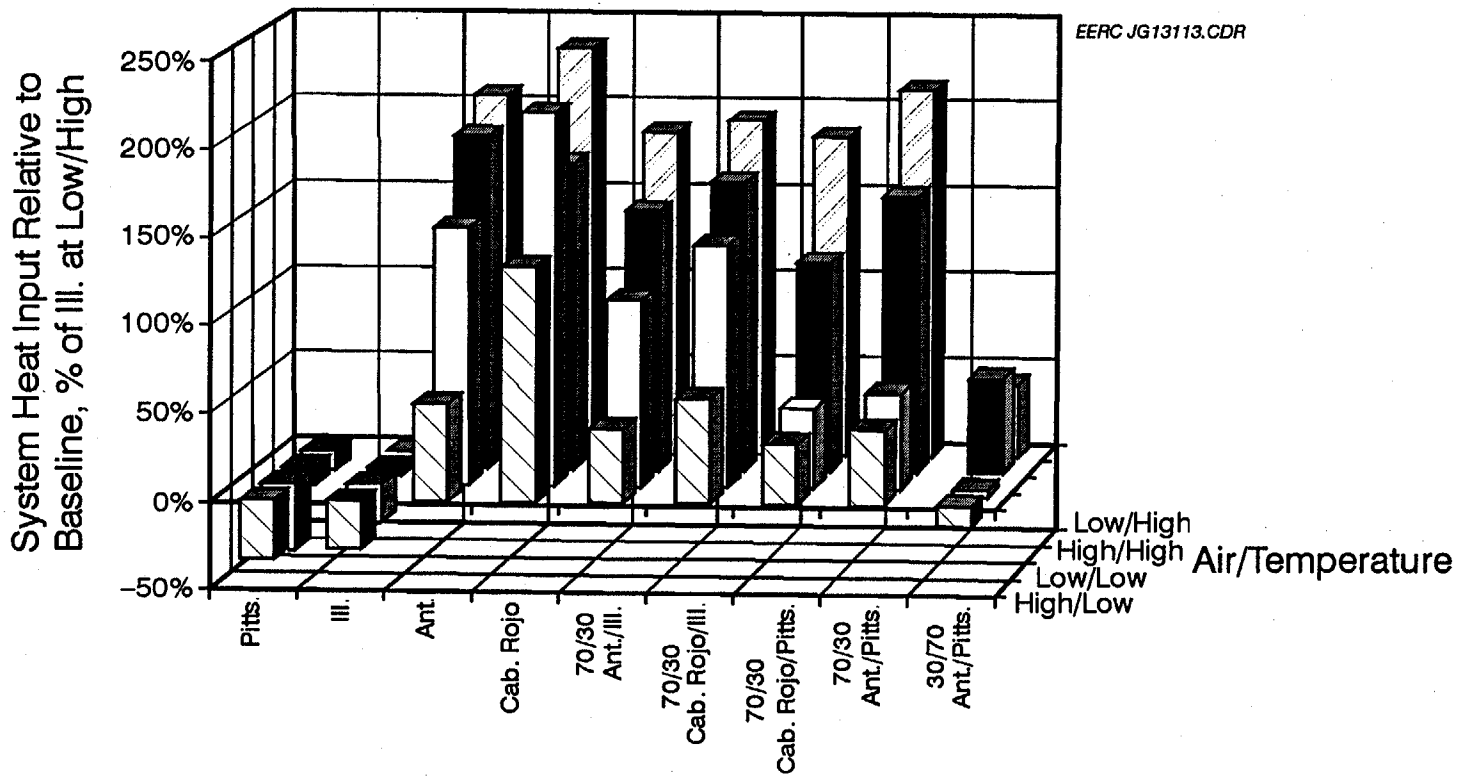

Figure 14. System heat requirements as a percentage of the baseline test condition (Illinois No. 6 coal at low mill air rate/high mill outlet temperature) for the test fuels at various mill operating conditions.

TABLE 15

Properties of Parent and Blend Fuel Test Samples – High-Temperature Fouling

Fuel Description:	Black Thunder		Bailey		Bailey/ Black Thunder[1]		Bailey/ Black Thunder[1]		Antelope		Bailey/ Antelope		Bailey/ Antelope	
Blend Ratio, wt%	100		100		35/65		65/35		100		35/65		65/35	
Run Number	AF-CTS-700		AF-CTS-701		AF-CTS-702		AF-CTS-703		AF-CTS-706		AF-CTS-707		AF-CTS-708	
Sample Number(s)	93-1092		93-1103		93-1028, 1034		93-1040, 1046		94-0491		94-0004		94-0034	
Proximate Analysis, wt%	As-Fired	H_2O-Free	As-Fired	H_2O-Free	As-Fired	H_2O-Free	As-Fired	H_2O-Free	As-Fired	H_2O-Free	As-Fired	H_2O-Free	As-Fired	H_2O-Free
Moisture	24.90	---	2.50	---	15.90	---	9.85	---	24.60	---	17.00	---	10.10	---
Volatile Matter	34.87	46.43	37.21	38.16	36.33	43.20	36.65	40.65	34.36	45.57	35.29	42.52	36.09	40.14
Fixed Carbon	35.74	47.59	53.99	55.37	41.75	49.64	47.14	52.29	36.35	48.21	41.57	50.08	47.31	52.63
Ash	4.49	5.98	6.30	6.46	6.02	7.16	6.36	7.05	4.69	6.22	6.14	7.40	6.50	7.23
Ultimate Analysis, wt%														
Hydrogen	3.53	4.70	5.33	5.47	4.55	5.41	4.39	4.87	3.61	4.79	4.12	4.96	4.52	5.03
Carbon	52.42	69.80	75.88	77.83	62.34	74.13	68.34	75.81	52.17	69.19	60.15	72.47	67.84	75.46
Nitrogen	0.68	0.91	1.42	1.46	0.99	1.18	1.16	1.29	0.86	1.14	1.06	1.28	1.22	1.36
Sulfur	0.36	0.48	1.73	1.77	0.82	0.98	1.26	1.39	0.33	0.44	0.79	0.95	1.19	1.32
Oxygen	13.62	18.14	6.84	7.02	9.38	11.15	8.64	9.58	13.74	18.22	10.74	12.94	8.63	9.60
Ash	4.49	5.98	6.30	6.46	6.02	7.16	6.36	7.05	4.69	6.22	6.14	7.40	6.50	7.23
Moisture	24.90	---	2.50	---	15.90	---	9.85	---	24.60	---	17.00	---	10.10	---
Heating Value														
Btu/lb	9050	12,051	13,746	14,098	10,776	12,813	12,056	13,373	9011	11,951	10,725	12,922	12,019	13,369
mmmf[2]	9475		14,670		11,466		12,875		9454		11,427		12,855	
Sulfur Input, lb/MMBtu	0.80		2.52		1.52		2.09		0.73		1.47		1.98	
Ash Input, lb/MMBtu	4.96		4.58		5.59		5.28		5.20		5.72		5.41	
Sulfur Forms, as-received[3]														
Sulfatic	0.04		0.14		0.08		0.11		0.05		0.08		0.11	
Pyritic	0.02		0.77		0.28		0.51		0.02		0.28		0.51	
Organic	0.24		1.22		0.58		0.88		0.24		0.58		0.88	
Fixed Carbon/Volatile Matter	1.02		1.45		1.15		1.29		1.06		1.18		1.31	
Sieve Analysis,														
% < 200 mesh	63.76		76.82		71.17		75.52		67.77		72.11		74.58	

[1] Average analysis of high temperature (2200°F) and low temperature (2000°F) coal samples.
[2] Mineral matter-, moisture-free.
[3] Analyses performed by an independent laboratory. Percentages reported for blends are calculated from parent coal analyses.

Table 15 indicate that blending of the PRB coals with the bituminous coal resulted in decreased sulfur content, carbon content, and heating value, while moisture and volatile matter were increased. The net result when firing the blended fuel should be lower flame temperature, increased heat capacity of the flue gas, and lower emissions of SO_2, relative to the bituminous coal. The increase in volatile matter resulting from the blend may tend to improve flame stability and carbon conversion when compared to firing the bituminous coal. Although the volatile content of the bituminous coal (38.16%) is similar to that of the subbituminous coals (46.43% for the Black Thunder and 45.57% for the Antelope), it is believed that the higher fixed-carbon content of the bituminous coal would lead to higher levels of carbon in ash.

Blending of the PRB coals with the bituminous coal resulted in a sulfur input reduction from 2.52 lb SO_2/MMBtu for the bituminous coal to roughly 2.0 lb SO_2/MMBtu at the lowest PRB blend ratio and 1.5 lb SO_2/MMBtu at the highest PRB blend ratio. However, the moisture-free heating value was also reduced from roughly 14,100 Btu/lb to roughly 13,370 Btu/lb and 12,900 Btu/lb for the 35% PRB and 65% PRB blends, respectively. In terms of ash input levels (lb/MMBtu), the fuel blends all showed significant increases over the levels in the parent coals, with the 35/65 ratio of bituminous/subbituminous coal blends producing the largest levels of ash input at 5.59 and 5.72 lb/MMBtu for the Bailey/Black Thunder and Bailey/Antelope fuel blends, respectively. This is due, in part, to the contribution of increased sulfur from the bituminous coal and increased alkali (calcium and sodium) from the subbituminous coals which tend to form more sulfate species during the ASTM ashing procedure, leading to increased levels of ash reported. Also, carbonates may form during the ashing procedure that tend to increase the weight of the residue remaining from the ashing procedure. Because of this phenomenon and because the sulfur capture in ash during the ashing procedure is not representative of actual sulfur capture during combustion, the SO_3-free ash analysis has been calculated for each sample (see Table 16).

Sieve analyses of each fuel are also shown in Table 15. Results indicate size distributions between 71.17% and 76.82% passing a 200-mesh (75-μm) screen for the parent bituminous coal and the bituminous/subbituminous blends. The parent subbituminous coals indicated 63.76% and 67.77% passing 200 mesh for the Black Thunder and Antelope coals, respectively. A normal utility grind is generally in the range of 70% passing 200 mesh. Although the larger size of the Black Thunder coal caused concern for increased carbon-in-ash levels, analysis of ESP ash samples obtained during testing indicated no detrimental impacts in relation to carbon content based on the size of the feed.

Ash Analyses. The results of chemical analyses, determined by XRF of the ASTM ash, are reported in Table 16 for each of the fuels tested. As expected, the bituminous coal is dominated by SiO_2, Al_2O_3, and Fe_2O_3, with alkaline species present in small amounts. While the subbituminous coals also contain similar major ash-forming species, they also contain a high percentage of calcium that is mainly organically associated (see chemical fractionation data). These calcium species will be available to react with SiO_2 and sulfur species in the flue gas. The result is usually lower-melting-temperature ash deposits and higher concentrations of sulfur retained in the ash.

Ash Fusion Analyses. Each of the parent coals and coal blends were submitted for ash fusion analyses under oxiding and reducing conditions. Results (reported in Table 16) indicate lower fusion temperatures under both oxidizing and reducing conditions for the subbituminous coals and coal blends when compared to the fusion temperatures of the Bailey bituminous coal. Comparing the ash fusion temperatures of the parent subbituminous coals reveals that the Black Thunder is the lowest fusion temperature coal. The fusion temperatures of the blends are not

TABLE 16

Ash Properties of Parent and Blend Test Samples – Standard Ash-Fouling Tests

Fuel Description:	Black Thunder		Bailey		Bailey Black Thunder[1]		Bailey/ Black Thunder[1]		Antelope		Bailey/ Antelope		Bailey/ Antelope	
Blend Ratio, wt%	100		100		35/65		65/35		100		35/65		65/35	
Run Number	AF-CTS-700		AF-CTS-701		AF-CTS-702		AF-CTS-703		AF-CTS-706		AF-CTS-707		AF-CTS-708	
Sample Number(s)	93-1092		93-1103		93-1028, 1034		93-1040, 1046		94-0015, 0491		94-0004		94-0034	
Coal Ash Analysis, wt%		SO_3-Free		SO_3-Free		SO_3-Free		SO_3-Free		SO_3-Free		SO_3-Free		SO_3-Free
SiO_2	30.47	34.55	47.49	48.33	35.05	41.55	39.50	43.51	24.89	32.25	34.56	41.67	40.47	44.78
Al_2O_3	17.93	20.33	26.24	26.70	19.47	23.08	21.74	23.94	13.11	16.99	16.23	19.57	19.56	21.64
Fe_2O_3	6.09	6.91	17.11	17.41	8.85	10.49	14.07	15.50	8.23	10.66	9.29	11.20	13.72	15.18
TiO_2	1.23	1.39	0.95	0.97	0.92	1.09	0.78	0.86	0.82	1.06	0.85	1.02	1.06	1.17
P_2O_5	1.17	1.33	0.47	0.48	1.22	1.45	1.18	1.30	1.13	1.46	1.25	1.51	0.78	0.86
CaO	24.81	28.13	2.28	2.32	12.44	14.75	8.55	9.42	23.01	29.82	15.06	18.16	9.67	10.70
MgO	5.49	6.23	1.51	1.54	4.64	5.51	3.23	3.56	4.61	5.97	3.88	4.68	3.05	3.37
Na_2O	0.85	0.96	0.81	0.82	1.00	1.19	0.93	1.02	1.26	1.63	1.11	1.34	0.98	1.08
K_2O	0.15	0.17	1.40	1.42	0.76	0.90	0.81	0.89	0.11	0.14	0.71	0.86	1.09	1.21
SO_3	11.80	---	1.75	---	15.65	---	9.21	---	22.82	---	17.06	---	9.65	---
Total	99.99	100.00	100.01	100.00	100.00	100.00	100.00	100.00	99.99	100.00	100.00	100.00	100.03	100.00
Ash Fusion Temp., °F	Oxidize[2]	Reduce[3]	Oxidize	Reduce	Oxidize	Reduce	Oxidize	Reduce	Oxidize	Reduce	Oxidize	Reduce	Oxidize	Reduce
Initial Deformation	2182	2147	2548	2031	2287	2183	2329	2194	2258	2253	2258	2030	2332	2127
Softening	2207	2163	2583	2235	2351	2264	2395	2316	2282	2293	2282	2165	2402	2302
Hemisphere	2221	2180	2617	2353	2395	2298	2439	2381	2300	2331	2300	2208	2430	2352
Fluid	2354	2225	2659	2439	2452	2372	2461	2402	2404	2349	2404	2295	2480	2382
Base/Acid	0.753		0.309		0.499		0.445		0.959		0.582		0.467	
Dolomite Ratio	0.810		0.164		0.617		0.427		0.742		0.630		0.446	
SiO_2/Al_2O_3	1.699		1.810		1.800		1.817		1.899		2.129		2.069	
$Fe_2O_3/(CaO+MgO)$	0.201		4.515		0.518		1.194		0.298		0.491		1.079	

[1] Average analysis of high-temperature (2200°F) and low-temperature (2000°F) coal ash samples.
[2] Oxidizing atmosphere.
[3] Reducing atmosphere.

directly related, however, as the table indicates higher fusion temperatures for the 35/65 Bailey/Black Thunder blend than the corresponding Bailey/Antelope blend.

4.3.3 Combustor Operating Parameters

In general, the blend program was designed to compare the ash fouling, slagging, and fly ash collection properties of each of the blends with those of the parent coals. Specifically, the test program consisted of one standard 5.25-hr fouling/slagging/ESP performance test at a FEGT of 2200°F, one standard 5.25-hr test at a FEGT of 2000°F, and one nonstandard 12.0-hr low-temperature fouling test at a FEGT of 2200°F generating deposits in the low-temperature (1500°F–1600°F) region of the pilot-scale system for each fuel. Excess air was controlled to near 20% for each of the tests.

The two standard 5.25-hr combustion tests were designed to investigate ash fouling tendencies on high temperature heat exchange surfaces. A set of three side-by-side steam-cooled Type 304 stainless steel deposition probes was inserted into the combustion chamber exit duct to collect ash fouling deposits under conditions similar to those occurring on high-temperature steam tubes located at the furnace exit in a utility boiler. Tube metal temperatures were controlled to near 1000°F during each test, using steam as the cooling medium.

The nonstandard 12.0-hr combustion tests were designed to investigate ash-fouling tendencies on low-temperature heat exchange surfaces. A separate set of four 2-in. diameter steam-cooled deposition probes was inserted into the flue gas duct just upstream of the first water-cooled flue gas heat exchanger to collect ash-fouling deposits. These low-temperature fouling probes were designed to simulate conditions similar to those occurring on steam tubes located in the reheat/economizer section of a utility boiler. The probe bank consisted of two side-by-side probes with two additional probes positioned directly downstream. Tube metal temperatures were controlled with steam to a surface metal temperature near 850°F.

The design of the low-temperature fouling probes required special attention due to the projected nature of the ash-fouling deposits. It was assumed that the deposits would be soft, friable, and easily disturbed with handling. Therefore, the flue gas ducting in the area of the low-temperature fouling probes was designed and constructed in a vertical orientation so that the probes could be maintained in a horizontal plane at all times. Also, special attention was paid to the design and materials of construction for the probes themselves. Each low-temperature fouling probe was constructed with a body of Monel 400 and a welded end cap of Type 304 stainless steel. Removable sleeves, fashioned from 1.25% chromium, 0.5% molybdenum alloy seamless tubing, were designed with close tolerances to just fit over the probe bodies. The probe bodies were fabricated from Monel 400 due to the excellent thermal conductivity which Monel alloys provide, and the 1.25 Cr–0.5 Mo alloy used for the probe sleeves is the type used for utility boiler tubes.

The characteristics of gaseous and particulate emissions from each fuel were also evaluated during the test burns as well as the relative collectibility of the fly ash from each in a pilot-scale ESP. To allow for direct comparison of results, the operational objectives for each combustion test were to maintain a given FEGT, excess air level near 20%, and ash deposition probe metal surface temperatures of 1000°F for the high-temperature deposition probes and 850°F for the low-temperature deposition probes. The temperature entering the ESP was maintained between 300°

and 350°F for each test. The voltage across the ESP was controlled to the maximum attainable without sparkover, usually 60 kV. However, lower voltages were noted during testing of the Bailey and Black Thunder parent coals, which may have affected the collection efficiency observed during these tests.

A summary of the run average operating parameters over the course of each of the tests is provided in Table 17. The concentrations of O_2, CO_2, CO, SO_2, and NO_x reported were continuously monitored at a port located in the duct downstream from the high-temperature ash-fouling probe bank. The combustor operating parameters indicate very comparable conditions for each of the test burns within a particular type of test.

4.3.4 High-Temperature Ash-Fouling Test Results

It is unclear to what extent the ash-forming species in a subbituminous coal will interact with those from a bituminous coal to form deposits in a utility boiler. Experience has suggested that these interactions are not readily applicable to all fuel blends; therefore, no hard and fast estimate of fouling tendencies may be provided by simply proportioning the results of ASTM ash analyses at the desired blend ratios. For this reason, a single bituminous coal was blended with two subbituminous coals to determine their fouling tendencies at two load levels. To represent the high-load condition, the fuels were fired at a rate sufficient to achieve a FEGT of 2200°F, that typical of many utility boilers designed to fire bituminous coal. The low-load condition utilized a firing rate sufficient to achieve 2000°F at the furnace exit. The ash-fouling deposits accumulated during each test burn were removed, weighed, and analyzed at the completion of each test to determine their characteristics in terms of deposition rate and strength of deposit.

Summary of Test Results. A summary of the critical deposit properties, operating conditions, and amount of deposits for each test burn is provided in Tables 18 and 19. The reported run averages of FEGT and excess air levels indicate good reproducibility of these parameters during the various test burns. The average probe metal temperatures for the high FEGT ash-fouling tests showed some significant deviation from the desired setpoint of 1000°F. Three of the test burns in the series had deviations in probe metal temperature ranging from about 3% (1032°F) to 9% (1096°F) above the desired temperature. All of the other test burns in both the high FEGT and low FEGT test series were within a 1.5% difference from the set point. However, the relatively narrow range of operating parameters in general should allow a good basis for comparing ash-fouling tendencies for the fuels tested here.

The weight of ash deposited on the probe bank during a standard 5.25-hour test is used to rank each fuel for its relative ash-fouling potential. The deposit weights reported in Tables 18 and 19 generally indicate that the 2200°F FEGT tests had a much higher potential for ash fouling than the 2000°F FEGT tests. The ash-fouling deposit weights from the high FEGT test series ranged from 57.7 to 577.8 g, while the deposit weights from the low FEGT test series ranged from 21.3 to 220.0 g. These same tables indicate that the 100% subbituminous coal fuels had the greatest potential for ash fouling at both the 2200° and 2000°F FEGTs, with the Antelope producing deposits weighing approximately twice as much as those produced from combustion of the Black Thunder coal. Interestingly, the weight of the deposits produced from the combustion

TABLE 17

Run Average Combustor Operating Parameters – Standard Ash-Fouling Tests

Run Number:	AF-CTS-700		AF-CTS-701		AF-CTS-702		AF-CTS-703		AF-CTS-706		AF-CTS-707		AF-CTS-708	
Test Designation:	A	B	A	B	A	B	A	B	A	B	A	B	A	B
Fuel:	Black Thunder		Bailey		Bailey/Black Thunder		Bailey/Black Thunder		Antelope		Bailey/Antelope		Bailey/Antelope	
Blend Ratio, wt. %:	100		100		35/65		65/35		100		35/65		65/35	
Date	11/09/93		11/11/93		11/15/93		11/17/93		12/16/93		12/20/93		12/22/93	
Start Time	0541	1239	0542	1137	0616	1213	0608	1248	0514	1058	0549	1146	0530	1108
End Time	1056	1754	1057	1633	1131	1728	1209	1803	1029	1613	1118	1701	1045	1623
Test Duration, hr	5.25	5.25	5.25	4.92	5.25	5.25	5.25	5.25	5.25	5.25	5.25	5.25	5.25	5.25
Total Fuel Fed, lb	389.93	286.53	239.72	164.28	324.27	218.78	274.31	191.09	405.74	296.56	338.15	231.1	288.75	205.79
Fuel Rate, lb/hr	74.27	54.58	45.66	33.39	61.77	41.67	52.25	36.4	77.28	56.49	64.41	44.02	55	39.2
Heat Input, Btu/hr	672,165	493,923	627,655	458,982	665,587	449,062	627,047	440,817	696,404	509,010	690,792	472,104	661,045	471,122
FEGT, °F	2209	2015	2214	2007	2215	2017	2216	2013	2192	2006	2190	2009	2204	2004
Probe Metal Temperature,[1] °F	1002	997	1007	993	1032	985	1016	1001	1009	1006	1048	1012	1096	1006
Flue Gas Analysis														
O_2, dry %	3.51	3.97	3.53	3.61	3.71	3.65	3.92	3.76	3.45	3.7	3.53	3.74	3.61	3.76
CO_2, dry %	16.48	15.05	15.36	15.43	15.43	15.83	14.97	14.58	15.4	NA[2]	13.81	15	14.83	14.44
CO, dry ppm	NA	NA	NA	NA	NA	NA	NA	NA	10.29	NA	28.4	63.86	NA	39.5
SO_2, dry ppm	315	254	1123	1193	743	700	915	973	329	201	714	632	981	931
Calc. @ 3.55% O_2	314	260	1121	1198	750	704	939	985	327	NA	713	639	984	942
NO_x, dry ppm	110	101	248	126	199	193	218	155	125	155	174	192	235	129
Calc. @ 3.55% O_2	109	104	248	127	200	194	222	156	125	NA	173	194	236	130
Excess Air, %	19.85	23.06	19.76	20.3	21.03	20.61	22.59	21.41	19.43	21.14	19.88	21.32	20.38	21.41
System Temperatures, °F														
Primary Air	402	311	318	449	587	546	576	541	557	527	530	445	516	492
Secondary Air	675	660	671	620	674	639	673	639	701	686	707	679	714	692
Tertiary Air	692	674	688	653	688	660	688	663	737	742	738	712	737	711
Probe Bank Outlet	1952	1760	1926	1743	1920	1741	1875	1718	1998	1805	1890	1686	1837	1674
ESP Inlet	NA	NA	NA	NA	NA	NA	NA	NA	307	345	306	317	319	315
ESP Outlet	293	291	272	285	296	299	307	286	277	306	271	284	282	284
ID Fan Inlet	254	238	256	224	248	227	261	217	243	229	241	216	236	220
System Pressures, in. H_2O														
FD Fan Out, Static	77.52	88.77	79.79	87.57	78.31	87.66	79.74	87.79	81.65	85	80	86.7	80.38	87.34
Combustor Static	-0.25	-0.24	-0.19	-0.24	-0.22	-0.3	-0.34	-0.19	-0.2	-0.29	-0.22	-0.29	-0.19	-0.16
ESP Inlet Static	-6.16	-4.02	-4.5	-3.86	-5.3	-3.04	-5.25	-2.95	-5.78	-4.08	-5.8	-3.17	-5	-2.86
ESP Outlet Static	-7.1	-5.23	-5.03	-4.6	-5.93	-3.8	-5.88	-3.43	-6.46	-4.76	-6.3	-3.53	-5.63	-3.5
ID Fan Inlet Static	-14.04	-11.59	-12.64	-12.04	-13.37	-11.89	-12.64	-11.9	-14.12	-7.46	-13.39	-11.72	-13.01	-9.86

[1] High-temperature ash-fouling probes.
[2] Not available.

TABLE 18

Summary of High FEGT (2200°F) Ash-Fouling Probe Test Results

Test Number:	AF-CTS-700A		AF-CTS-701A		AF-CTS-702A		AF-CTS-703A		AF-CTS-706A		AF-CTS-707A		AF-CTS-708A	
Fuel:	Black Thunder		Bailey		Bailey/Black Thunder		Bailey/Black Thunder		Antelope		Bailey/Antelope		Bailey/Antelope	
Blend Ratio, wt%:	100		100		35/65		65/35		100		35/65		65/35	
Operating Conditions														
FEGT, °F	2209		2214		2215		2216		2192		2190		2204	
Probe Metal Temperature, °F	1002		1007		1032		1016		1009		1048		1096	
Excess Air, %	19.85		19.76		21.03		22.59		19.43		19.88		20.38	
Ash Fouling Probe wt, g														
Inner Layer	11.6		6.6		6.2		7.9		13.8		10		8.2	
Sinter Layer	325.5		233.7		106.8		49.8		564		230		77.8	
Total	337.1		240.3		113		57.7		577.8		240		86	
Ash Specific Deposit Rate, g/kg-input ash	42.45		35.08		12.76		7.25		66.94		25.48		10.1	
Deposit Strength	371		95		345		117		443		370		225	
Deposit Composition, wt%														
Inner Layer														
Sample Number	93-1095		93-1106		93-1030		93-1042		94-0017		94-0006		94-0036	
		SO_3-free		SO_3-free		SO_3-free		SO_3-free		SO_3-free		SO_3-free		SO_3-free
SiO_2	42.44	46.48	45.83	46.42	46.15	48.49	41.91	43.37	32.56	38.56	39.53	43.18	43.45	45.37
Al_2O_3	14.19	15.54	24.12	24.43	18.99	19.95	21.53	22.28	10.01	11.85	15.81	17.27	19.99	20.88
Fe_2O_3	6.07	6.65	21.89	22.17	12.53	13.17	18.35	18.99	6.12	7.25	12.4	13.55	16.64	17.38
TiO_2	1.07	1.17	0.72	0.73	0.89	0.93	1.04	1.08	0.89	0.94	1.04	1.08	0.94	0.98
P_2O_5	1.08	1.18	0.48	0.49	0.69	0.73	0.53	0.55	1.64	1.94	0.97	1.06	0.59	0.62
CaO	21.6	23.66	2.37	2.4	12.26	12.88	8.8	9.11	25.52	30.22	16.37	17.88	8.89	9.28
MgO	2.78	3.04	1.39	1.41	1.67	1.75	2.42	2.5	3.46	4.1	2.6	2.84	2.25	2.35
Na_2O	1.87	2.05	0.83	0.84	1.59	1.67	0.96	0.99	3.29	3.9	1.76	1.92	1.5	1.57
K_2O	0.21	0.23	1.1	1.11	0.4	0.42	1.09	1.13	0.93	1.1	1.28	1.4	1.51	1.58
SO_3	8.68	---	1.27	---	4.83	---	3.36	---	15.55	---	8.45	---	4.25	---
Total	99.99	100	100	100	100	100	99.99	100	100	100	99.99	100	100.01	100
SiO_2/Al_2O_3	2.99		1.90		2.43		1.95		3.25		2.50		2.17	
Base/Acid	0.56		0.39		0.43		0.49		0.90		0.61		0.48	
Dolomite Ratio	0.75		0.14		0.49		0.36		0.74		0.55		0.36	
$Fe_2O_3/(CaO+MgO)$	0.25		5.82		0.90		1.64		0.21		0.65		1.49	
Sinter Layer														
Sample Number	93-1097		93-1107		93-1029		93-1041		94-0016		94-0005		94-0035	
		SO_3-free		SO_3-free		SO_3-free		SO_3-free		SO_3-free		SO_3-free		SO_3-free
SiO_2	43.56	44.31	47.26	47.33	43.14	43.36	46.09	46.11	33.64	33.8	39.44	39.72	44.91	45.12
Al_2O_3	15.26	15.52	24.32	24.35	19.13	19.23	21.83	21.84	13.27	13.33	17.4	17.52	21.62	21.72
Fe_2O_3	6.28	6.39	22.11	22.14	11.82	11.88	14.62	14.63	8.93	8.97	13.11	13.2	15.93	16
TiO_2	1.65	1.68	1.09	1.09	1.43	1.44	1.23	1.23	1.47	1.48	1.1	1.11	0.92	0.92
P_2O_5	0.67	0.68	0.27	0.27	0.55	0.55	0.39	0.39	0.96	0.96	0.6	0.6	0.32	0.32
CaO	26.12	26.57	2	2	18.08	18.17	11.44	11.45	33.17	33.33	22.14	22.3	11.52	11.57
MgO	3.9	3.97	0.96	0.96	4.05	4.07	2.83	2.83	6.98	7.01	4.23	4.26	2.63	2.64
Na_2O	0.75	0.76	0.59	0.59	0.62	0.62	0.64	0.64	0.84	0.84	0.65	0.65	0.73	0.73
K_2O	0.12	0.12	1.26	1.26	0.68	0.68	0.88	0.88	0.27	0.27	0.63	0.63	0.96	0.96
SO_3	1.71	---	0.14	---	0.52	---	0.05	---	0.46	---	0.7	---	0.46	---
Total	100.02	100	100	100	100.02	100	100	100	99.99	100	100	100	100	100
SiO_2/Al_2O_3	2.86		1.94		2.26		2.11		2.54		2.27		2.08	
Base/Acid	0.62		0.37		0.55		0.44		1.04		0.70		0.47	
Dolomite Ratio	0.81		0.11		0.63		0.47		0.80		0.65		0.45	
$Fe_2O_3/(CaO+MgO)$	0.21		7.47		0.53		1.03		0.22		0.50		1.13	

TABLE 19

Summary of Low FEGT (2000°F) Ash-Fouling Probe Test Results

Test Number:	AF-CTS-700B		AF-CTS-701B		AF-CTS-702B		AF-CTS-703B		AF-CTS-706B		AF-CTS-707B		AF-CTS-708B	
Fuel:	Black Thunder		Bailey		Bailey/Black Thunder		Bailey/Black Thunder		Antelope		Bailey/Antelope		Bailey/Antelope	
Blend Ratio, wt%:	100		100		35/65		65/35		100		35/65		65/35	
Operating Conditions														
FEGT, °F	2015		2007		2017		2013		2006		2009		2004	
Probe Metal Temperature, °F	997		993		985		1001		1014		1012		1006	
Excess Air, %	23.06		20.3		21.6		21.41		NA		21.32		21.41	
Ash Fouling Probe wt, g														
Inner Layer	7.4		5.3		5.2		5.4		8.9		10		6.1	
Sinter Layer	75.8		16		23		35.7		211.1		30		19.3	
Total	83.2		21.3		28.2		41.1		220		40		25.4	
Ash Specific Deposit Rate, g/kg-input ash	14.26		4.54		4.72		7.5		34.87		6.21		4.19	
Deposit Strength	142		ND[1]		47		ND		183		66		ND	
Deposit Composition, wt%														
Inner Layer														
Sample Number	93-1100		93-1110		93-1036		93-1048		94-0022		94-0011		94-0041	
		SO_3-free		SO_3-free		SO_3-free		SO_3-free		SO_3-free		SO_3-free		SO_3-free
SiO_2	41.18	44.32	45.78	47.18	39.69	42.08	44.66	45.99	34.27	37.49	39.86	43.34	43.72	45.55
Al_2O_3	16.19	17.43	24.56	25.31	20.19	21.41	23.38	24.08	12.04	13.17	17.51	19.04	21.3	22.19
Fe_2O_3	5.93	6.38	20.08	20.69	13.70	14.52	16.04	16.52	6.71	7.34	11.7	12.72	15.73	16.39
TiO_2	1.25	1.35	0.88	0.91	1.12	1.19	1.01	1.04	0.78	0.85	0.9	0.98	0.96	1
P_2O_5	1.24	1.33	0.41	0.42	1.05	1.11	0.51	0.53	1.8	1.97	1.22	1.33	0.57	0.59
CaO	21.67	23.32	2.07	2.13	13.35	14.15	7.29	7.51	28.27	30.92	14.96	16.27	8.61	8.97
MgO	3.23	3.48	1.4	1.44	3.19	3.38	2.2	2.27	4.18	4.57	2.71	2.95	2.24	2.33
Na_2O	2.01	2.16	0.8	0.82	1.11	1.18	0.86	0.89	2.72	2.98	1.92	2.09	1.45	1.51
K_2O	0.21	0.23	1.06	1.09	0.92	0.97	1.15	1.18	0.65	0.71	1.19	1.29	1.41	1.47
SO_3	7.1	---	2.94	---	5.68	---	2.89	---	8.59	---	8.04	---	4	---
Total	100.01	100	99.98	100	100	99.99	99.99	100	100.01	100	100.01	100	99.99	100
SiO_2/Al_2O_3	2.54		1.86		1.96		1.91		2.85		2.28		2.05	
Base/Acid	0.56		0.36		0.53		0.40		0.90		0.56		0.45	
Dolomite Ratio	0.75		0.14		0.51		0.35		0.76		0.54		0.37	
$Fe_2O_3/(CaO+MgO)$	0.24		5.79		0.83		1.69		0.21		0.66		1.45	
Sinter Layer														
Sample Number	93-1102		93-1111		93-1035		93-1047		94-0021		94-0010		94-0040	
		SO_3-free		SO_3-free		SO_3-free		SO_3-free		SO_3-free		SO_3-free		SO_3-free
SiO_2	49.21	52.38	46.68	47.44	47.17	48.84	43.54	46.43	38.23	40.06	44.16	46.36	45.46	46.61
Al_2O_3	14.48	15.41	24.27	24.66	20.83	21.57	21.34	22.76	13.01	13.63	17.79	18.68	21.06	21.59
Fe_2O_3	5.35	5.7	21.67	22.02	10.10	11.29	15.93	16.99	8.38	8.78	11.1	11.65	15.41	15.8
TiO_2	1.53	1.63	0.59	0.6	0.98	1.02	0.74	0.79	1.08	1.13	1.01	1.06	0.91	0.93
P_2O_5	0.76	0.81	0.43	0.44	0.61	0.63	0.57	0.61	0.82	0.86	0.67	0.7	0.47	0.48
CaO	19.29	20.53	2.07	2.1	12.07	12.5	8.23	8.78	27.46	28.77	16.33	17.14	10.06	10.31
MgO	2.41	2.57	1.25	1.27	2.33	2.41	1.91	2.04	5.18	5.43	2.5	2.62	2.21	2.27
Na_2O	0.78	0.83	0.5	0.51	0.80	0.83	0.68	0.73	0.96	1.01	0.76	0.8	0.79	0.81
K_2O	0.13	0.14	0.94	0.96	0.88	0.93	0.83	0.89	0.32	0.34	0.94	0.99	1.16	1.19
SO_3	6.05	---	1.59	---	3.42	---	6.22	---	4.55	---	4.75	---	2.48	---
Total	99.99	100	99.99	100	99.99	100.02	99.99	100	99.99	100	100.01	100	100.01	100
SiO_2/Al_2O_3	3.40		1.92		2.26		2.04		2.94		2.48		2.16	
Base/Acid	0.43		0.37		0.39		0.42		0.81		0.50		0.44	
Dolomite Ratio	0.78		0.13		0.53		0.37		0.77		0.60		0.41	
$Fe_2O_3/(CaO+MgO)$	0.25		6.53		0.76		1.57		0.26		0.06		1.26	

[1] Not determined. No deposit strength determination was possible because of the friability of the deposit sample.

of the bituminous/subbituminous coal blends was equal to, or less than, those of the parent coals in all cases for the 2200°F FEGT tests. The deposits collected and measured from the 2000°F FEGT tests showed the following trend from largest to smallest: 100% subbituminous, 35%/65% bituminous/subbituminous blend, 65%/35% blend, 100% bituminous. However, even though the deposit formed from 100% Antelope at 2000°F was more than twice that produced from 100% Black Thunder (220 vs. 83.2 g), the deposit formed from a 65/35 Bailey/Antelope blend was significantly less than the deposit formed from a 65/35 Bailey/Black Thunder blend (41.1 vs. 25.4 g). In all cases for both FEGT test series, the rate of deposition from the coal blends increased as the portion of subbituminous coal increased from 35% to 65%. Another criterion developed to assess boiler tube ash-fouling potential from results of combustion test facility (CTF) pilot-scale testing is the ash specific deposit weight. This calculated value of grams of deposit per kilogram of input ash represents a measure of the relative efficiency of ash deposition for each fuel. For the fuels tested here, the relative differences in ash-specific deposit weights reported in Tables 18 and 19 essentially follow the same order as the probe deposit weights.

Deposit strength evaluations were also made for each of the deposits formed. For the most part, the strength of each deposit reflected the deposit weight for each sample. For the bituminous coal and the lowest percentage of subbituminous coal in blend, the deposits were sloughed from the tube as the weight of the deposit exceeded some threshold level, indicating very low deposit strength for these samples. Photographs of the deposits and the probe bank surface at the completion of each test tend to indicate this phenomenon. Photographs for each of the deposits can be found in Figures 15–28.

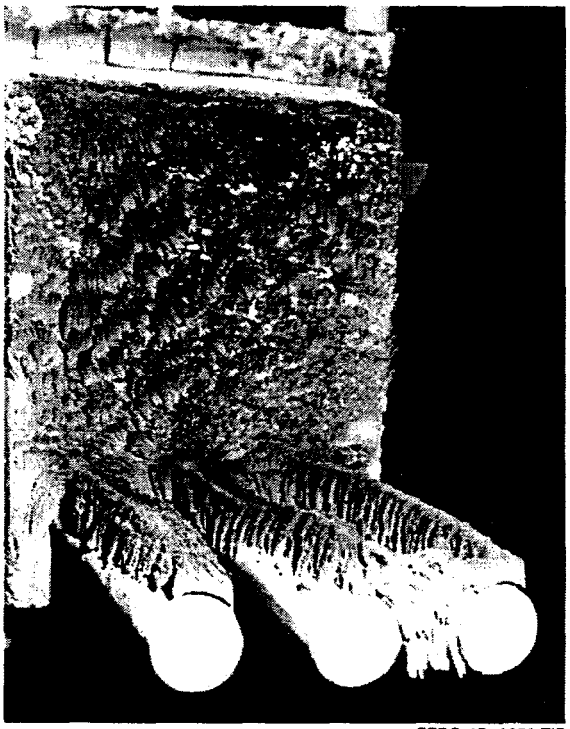

EERC JG13070.TIF

Figure 15. Photograph of sinter deposit at 2200°F, 100% Black Thunder.

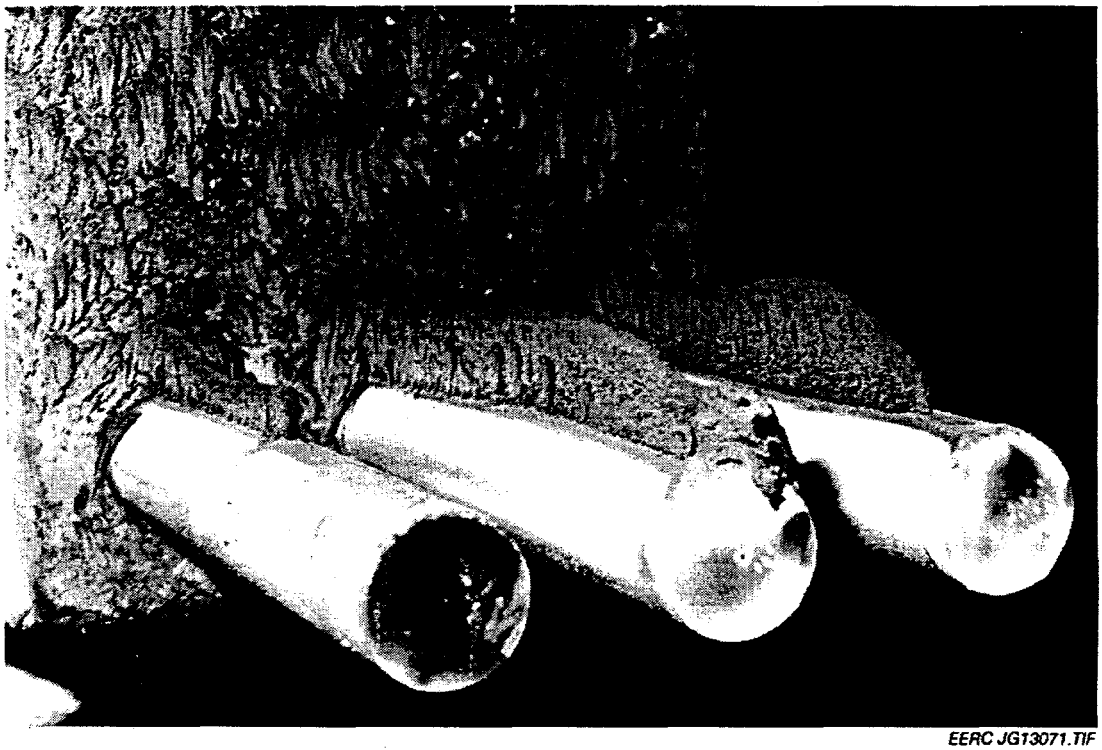

EERC JG13071.TIF

Figure 16. Photograph of sinter deposit at 2000°F, 100% Black Thunder.

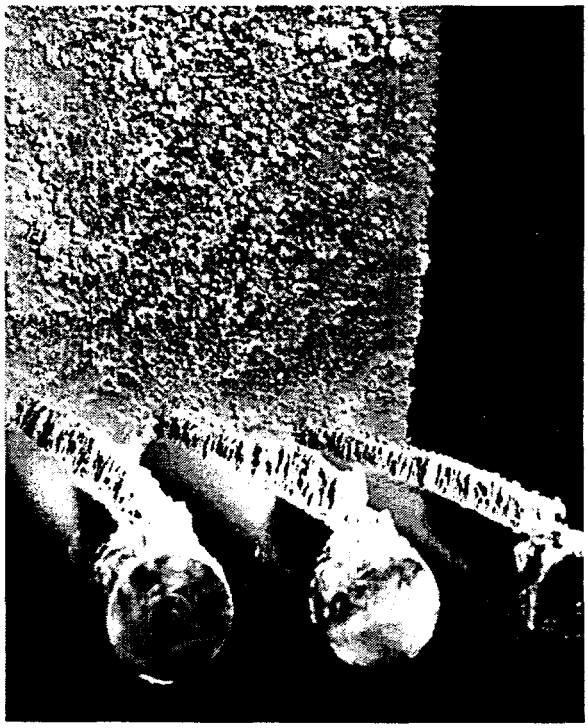

EERC JG13072.TIF

Figure 17. Photograph of sinter deposit at 2200°F, 100% Bailey.

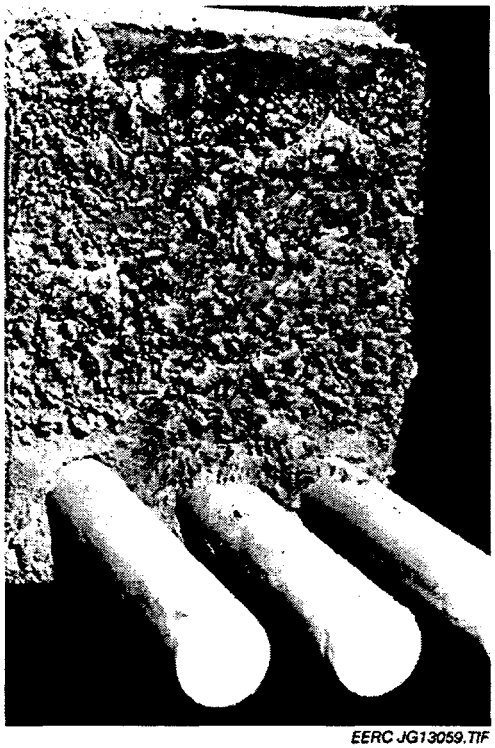

Figure 18. Photograph of sinter deposit at 2000°F, 100% Bailey.

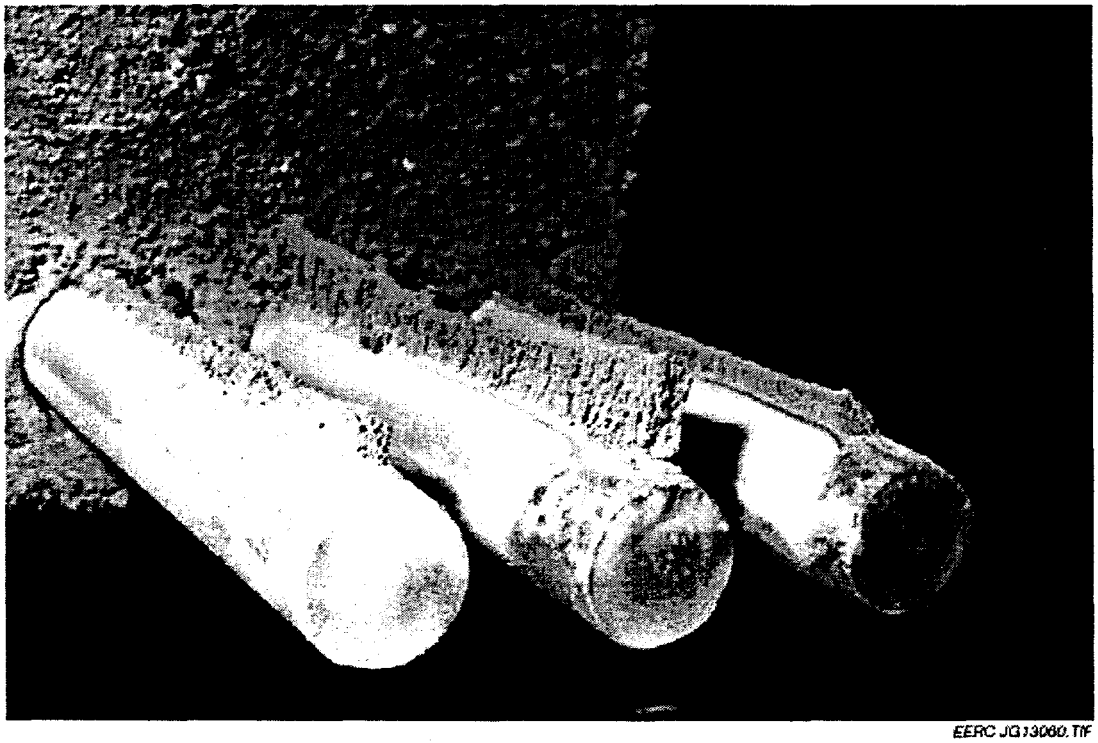

Figure 19. Photograph of sinter deposit at 2200°F, 35/65 Bailey/Black Thunder.

Figure 20. Photograph of sinter deposit at 2000°F, 35/65 Bailey/Black Thunder.

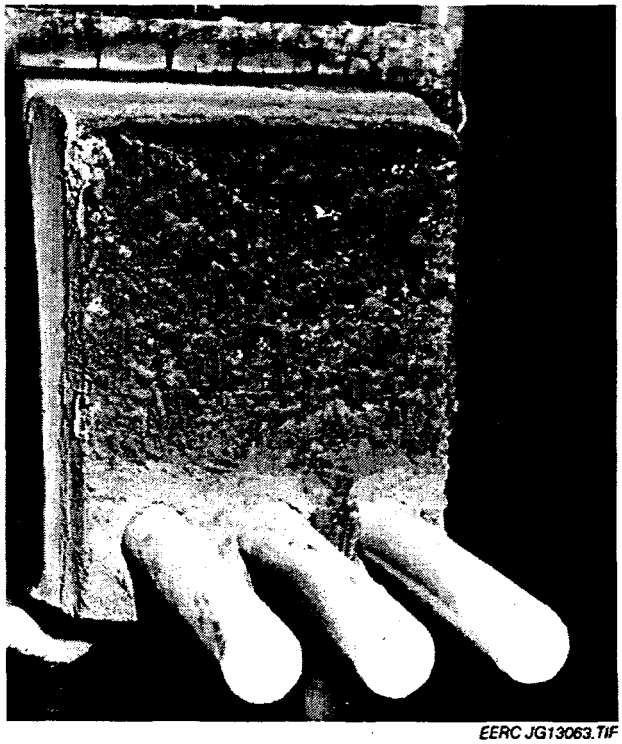

Figure 21. Photograph of sinter deposit at 2200°F, 65/35 Bailey/Black Thunder.

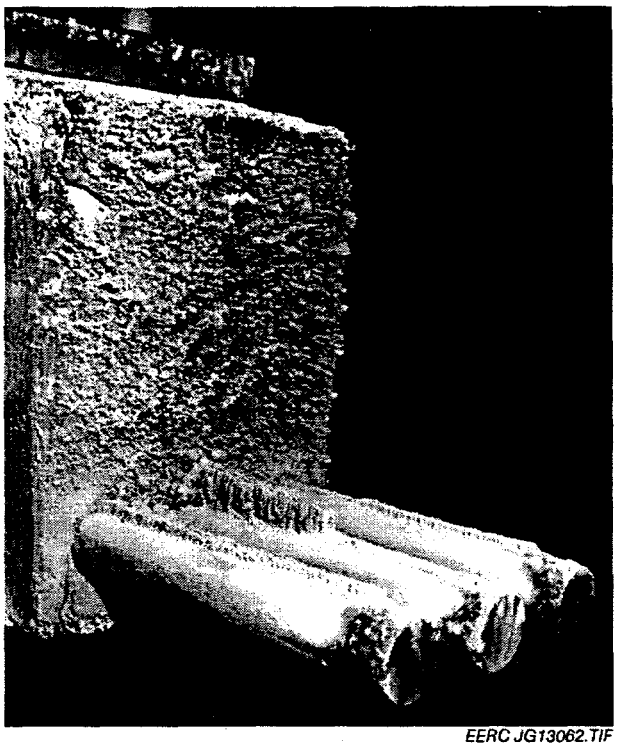

Figure 22. Photograph of sinter deposit at 2000°F, 65/35 Bailey/Black Thunder.

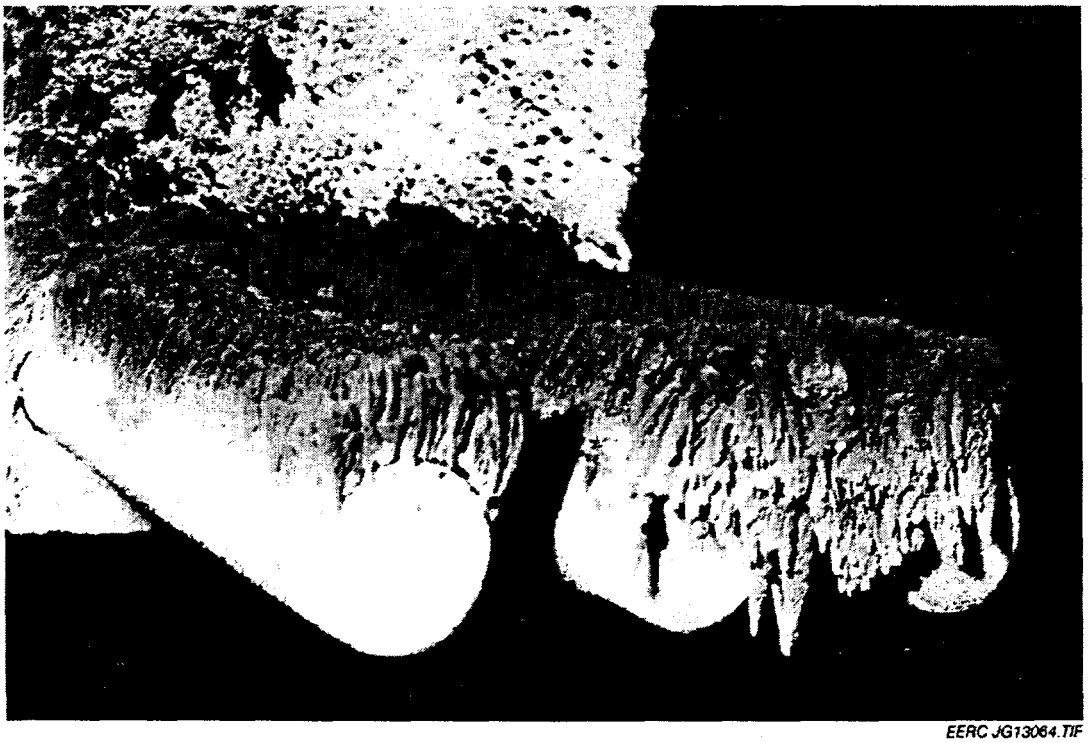

Figure 23. Photograph of sinter deposit at 2200°F, 100% Antelope.

Figure 24. Photograph of sinter deposit at 2000°F, 100% Antelope.

Figure 25. Photograph of sinter deposit at 2200°F, 35/65 Bailey/Antelope.

EERC JG13069.TIF

Figure 26. Photograph of sinter deposit at 2000°F, 35/65 Bailey/Antelope.

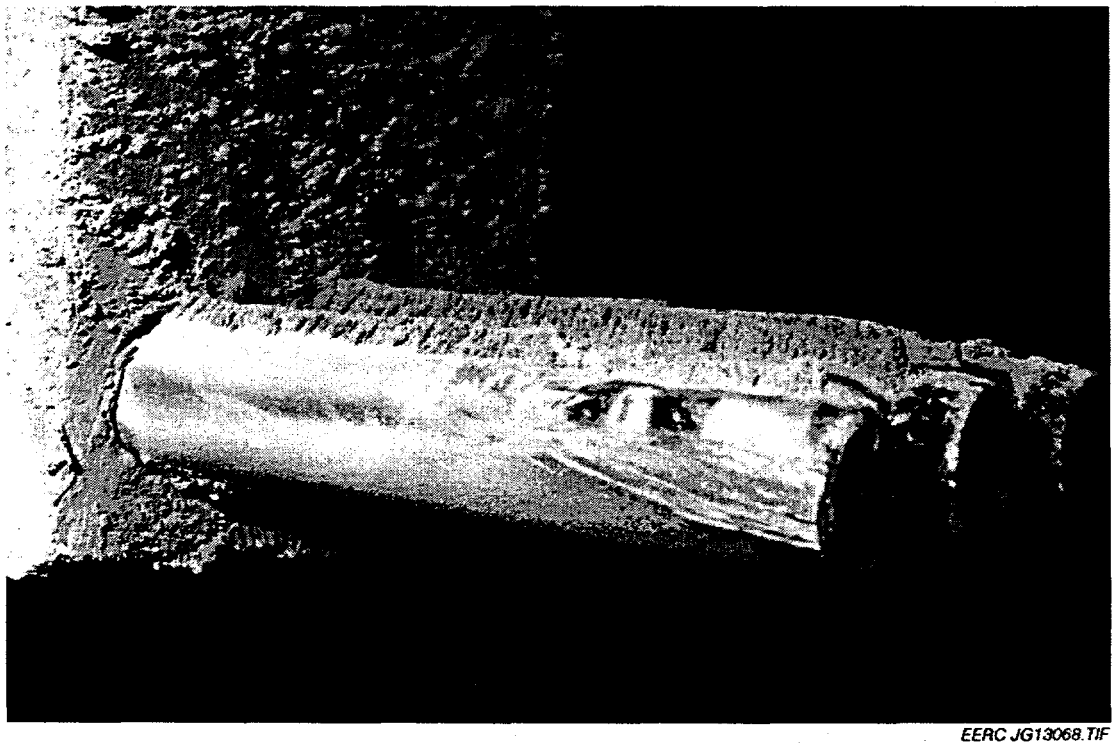

EERC JG13068.TIF

Figure 27. Photograph of sinter deposit at 2200°F, 65/35 Bailey/Antelope.

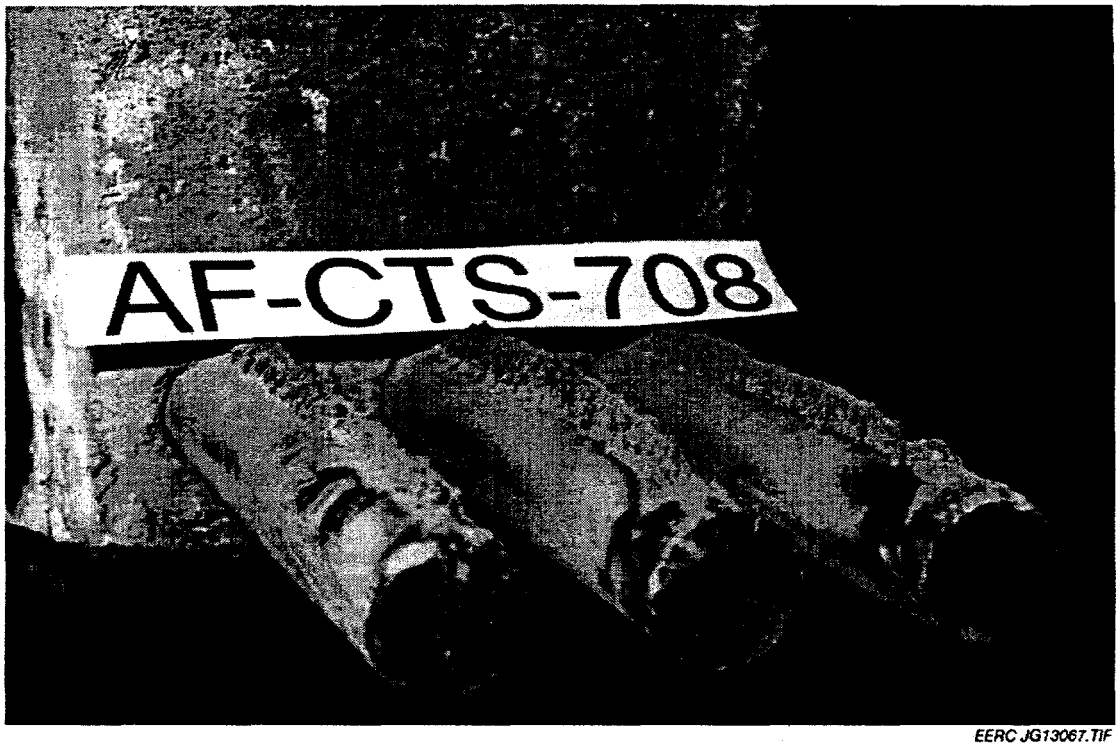

Figure 28. Photograph of sinter deposit at 2000°F, 65/35 Bailey/Antelope.

Each of the deposits was submitted for SEMPC analysis to determine the phase transformations that occurred during combustion leading to the deposition phenomena noted.

Probe Deposit Characterization. The deposits produced from the combustion of the parent coals and coal blends were examined using XRF, SEMPC analysis, and XRD. The results of the XRF analyses are given in Tables 18 and 19, while the results of the SEMPC and XRD analyses are presented in Tables 20 and 21, respectively.

Before discussing the chemistry and mineralogy of the probe deposits, we summarize pertinent data from the coal analyses and combustion test:

- The Bailey coal is an eastern bituminous coal with a mineral content high in silica, alumina, and iron with low amounts of calcium.

- By contrast, both the western subbituminous Black Thunder and Antelope coals are lower in silica with low amounts of iron and with high calcium content. The alumina content is comparable to the Bailey coal.

- Both the Black Thunder and Antelope coals have significantly more sodium content than the Bailey, with approximately 50% of the Black Thunder and all of the Antelope sodium being organically bound.

TABLE 20

Probe Bank Sinter Layer SEMPC Results, Standard Ash-Fouling Tests

Run Number:	AF-CTS-700		AF-CTS-701		AF-CTS-702		AF-CTS-703		AF-CTS-706		AF-CTS-707		AF-CTS-708	
Fuel:	Black Thunder		Bailey		Bailey/Black Thunder		Bailey/Black Thunder		Antelope		Bailey/Antelope		Bailey/Antelope	
Blend Ratio, wt%:	100		100		35/65		65/35		100		35/65		65/35	
Test Number:	A	B	A	B	A	B	A	B	A	B	A	B	A	B
Target FEGT, °F:	2200	2000	2200	2000	2200	2000	2200	2000	2200	2000	2200	2000	2200	2000
Sample Number	6184	6187	6189	6191	6160	6164	6168	6172	6350	6347	6351	6348	6352	6349b
Number of Points Analyzed	250	249	255	250	374	253	250	353	250	250	254	250	250	260
Frequency Percent														
Oxide-Rich														
Aluminum Oxide	0	0	0	0	0	0	0	0.6	0	0	0	0.4	0	0
Calcium Oxide	0.4	0	0	0	0	0	0	0.3	0	0.4	0	0	0	0
Iron Oxide	0	0.4	5.5	2	1.6	2.4	1.6	2.3	0	1.6	1.2	1.6	3.2	3.8
Mixed-Oxide-Rich	0.4	0.4	0.8	0.8	0	0.4	0.4	1.4	0.8	0.4	0.4	0	0	0
Total for Group	0.8	0.8	6.3	2.8	1.6	2.8	2	4.6	0.8	2.4	1.6	2	3.2	3.8
Sulfur-Rich														
Pyrite	0.4	0.8	0	0	0	0.4	0	0.3	0	0.8	0	1.2	0	0.8
Calcium Sulfate	3.6	6	0	0.4	0	2.8	0	0.3	1.6	2.8	0	2.8	0	0.8
Barite	0	0.4	0	0	0	0	0	0	0	0	0	0	0	0
Mixed-Sulfur-Rich	1.6	14.5	0	0.4	0	6.3	0	2.3	0.8	4.4	0.8	6.4	0	3.5
Total for Group	5.6	21.7	0	0.8	0	9.5	0	2.9	2.4	8	0.8	10.4	0	5.1
Phosphorus-Rich														
Apatite	0	0.4	0	0	0	0	0	0	0.4	0	0	0	0	0
Mixed-Phosphorus-Rich	2	2.8	0	0.4	0.5	0.8	0	0.6	1.2	0	0.8	1.6	1.2	0.4
Total for Group	2	3.2	0	0.4	0.5	0.8	0	0.6	1.6	0	0.8	1.6	1.2	0.4
Carbon-Rich														
Calcite	0	1.2	0	0	0	0	0	0	0	2.8	0	0	0	0
Dolomite	0	0.4	0	0	0	0	0	0	0	0	0	0	0	0
Mixed-Carbon-Rich	1.2	0.4	0.4	3.6	0	0	0	0	0.8	0	0.4	1.2	0.4	2.3
Total for Group	1.2	2	0.4	3.6	0	0	0	0	0.8	2.8	0.4	1.2	0.4	2.3
Metal-Rich														
Iron	0	0	0	0.4	0	0	0	0	0	0	0	0.4	0	0.8
Mixed-Metal-Rich	0	1.2	0	0	0	0	0.4	0.3	0.4	0.4	0.4	0	0.8	6.9
Total for Group	0	1.2	0	0.4	0	0	0.4	0.3	0.4	0.4	0.4	0.4	0.8	7.7

Continued . . .

TABLE 20 (continued)

Run Number:	AF-CTS-700		AF-CTS-701		AF-CTS-702		AF-CTS-703		AF-CTS-706		AF-CTS-707		AF-CTS-708	
Fuel:	Black Thunder		Bailey		Bailey/Black Thunder		Bailey/Black Thunder		Antelope		Bailey/Antelope		Bailey/Antelope	
Blend Ratio, wt%:	100		100		35/65		65/35		100		35/65		65/35	
Test Number:	A	B	A	B	A	B	A	B	A	B	A	B	A	B
Target FEGT, °F:	2200	2000	2200	2000	2200	2000	2200	2000	2200	2000	2200	2000	2200	2000
Silicon-Rich														
Quartz	6	16.1	11.4	6.4	4	16.6	6.8	17	2.4	16	0.8	15.2	5.2	8.1
Albite	0	0	0	0.4	0	0	0	0.3	0	0.4	0	0	0	0
Anorthite	11.6	6.8	0.8	1.2	44.4	7.5	33.6	9.3	9.2	8.8	39	12.4	29.2	11.9
Kaolinite	0.8	3.6	6.3	12.8	0.5	5.1	0.8	7.1	0	2.4	0	0.8	0	2.3
Altered Kaolinite	0	2.8	4.7	5.2	1.1	5.1	2.4	1.1	0	1.6	0.8	2.8	4.8	4.2
Illite	1.2	2.4	9.4	16.8	1.6	6.7	4	11.9	0	3.6	0.8	10	10.4	8.5
Montmorillonite	3.2	2.4	12.5	2.4	11	6.7	20.8	11.6	1.2	7.6	11.4	10	14	11.9
Pyroxene	1.2	0.4	0	0	1.3	0.4	0.4	0	3.6	2	1.2	1.6	0.4	0.4
Wollastonite	5.2	3.2	0	0	7.2	5.5	3.6	1.7	8.8	5.2	6.3	4.4	4.8	0
Calcium Silicate	1.2	2	0	0	0	0.4	0	0.8	2	1.6	0	0.4	0	0.4
Gehlenite	0.4	0	0	0	0	0	0	0	0.4	0	0	0	0	0
Akermanite	1.6	0.4	0	0	0	0.4	0	0	0	0.4	0	0	0	0
Spurrite	0	0.4	0	0	0	0	0	0	0	0.4	0	0	0	0
Mixed-Silicon-Rich	41.6	20.5	48.2	46.8	25.7	23.3	24	28.6	58	20.4	33.9	20	23.6	28.5
Total for Group	74	61	93.3	92	96.8	77.9	96.4	89.5	85.6	70.4	94.1	77.6	92.4	76.2
Other	16.4	10	0	0	1.1	9.1	1.2	2.3	8.4	16	2	6.8	2	4.6
Bulk Composition, wt%														
SiO_2	32.6	37.4	54.2	52	45.7	47.2	48.8	54	33.4	41.1	39.2	44.1	48.2	43.1
Al_2O_3	17.3	15.5	24.6	28.3	21.1	19.6	21.5	21.3	14.3	15	18.9	18.4	21.3	19.2
Fe_2O_3	5.4	4.5	12.8	10.2	7.4	6.6	9.5	6.5	7.9	6.3	9.6	7.3	10.6	11.3
TiO_2	1.7	1.3	0.7	0.9	1.3	1	1.4	1	1	1.3	1.2	1.3	1.1	1.1
P_2O_5	1.5	1.3	0.3	0.4	0.6	0.6	0.4	0.5	1.3	0.7	0.8	0.9	0.8	0.8
CaO	29.7	23.3	2.2	1.7	18.4	15.2	13.8	10.3	32.2	24.3	23.4	16.9	12.7	12.8
MgO	6.3	4.5	0.9	0.6	3.4	3.7	2.6	1.9	5.9	5	4.1	3.5	2.6	2.2
Na_2O	0.6	0.6	0.6	0.5	0.6	0.5	0.6	0.5	1.2	1.3	0.8	0.8	0.8	0.6
K_2O	0.4	0.4	1.5	1.8	0.7	0.8	0.8	1	0.3	0.4	0.7	0.9	1.3	1.1
SO_3	3.5	9.5	0.4	0.7	0.2	4.1	0.1	1.4	1.7	3.8	0.5	4.7	0.1	2.2
Total	99	98.3	98.2	97.1	99.4	99.3	99.5	98.4	99.2	99.2	99.2	98.8	99.5	94.4
Base/Acid	0.82	0.61	0.23	0.18	0.45	0.4	0.38	0.27	0.975	0.65	0.65	0.46	0.4	0.442
Dolomite Ratio	0.85	0.84	0.17	0.16	0.72	0.71	0.6	0.6	0.8	0.79	0.71	0.69	0.55	0.54
SiO_2/Al_2O_3	1.88	2.41	2.2	1.84	2.17	2.41	2.27	2.54	2.336	2.74	2.07	2.4	2.26	2.245
$Fe_2O_3/(CaO+MgO)$	0.15	0.16	4.13	4.44	0.34	0.35	0.58	0.53	0.207	0.22	0.35	0.36	0.69	0.75

TABLE 21

Probe Bank Inner and Sinter Layer XRD Results, Standard Ash-Fouling Tests

Run Number:	AF-CTS-700		AF-CTS-701		AF-CTS-702		AF-CTS-703		AF-CTS-706		AF-CTS-707		AF-CTS-708	
Fuel:	Black Thunder		CONSOL		CONSOL/Black Thunder		CONSOL/Black Thunder		Antelope		CONSOL/Antelope		CONSOL/Antelope	
Blend Ratio, wt%:	100		100		35/65		65/35		100		65/35		65/35	
Test Designation:	A	B	A	B	A	B	A	B	A	B	A	B	A	B
Target FEGT, °F:	2200	2000	2200	2000	2200	2000	2200	2000	2200	2000	2200	2000	2200	2000
Inner Layer														
Sample Number	6182	6185	6188	6190	6161	6165	6169	6173	6359	6361	6354	6356	6368	6370
Quartz, SiO_2	Major	Major	Major	Major	Major	Major	Major	Major	Major	Major	Major	Major	Major	Major
Anhydrite, $CaSO_4$	Major	Minor	Minor	Minor	Major	Major	Minor	Minor	Major	Major	Major	Major	Major	Major
Mullite, $Al_6Si_2O_{13}$	---	---	Major	Minor	Minor	Minor	Minor	Minor	---	---	Minor	Minor	Minor	Minor
Hematite, Fe_2O_3	Minor	Minor	Major	Minor	---	Minor	Minor	Minor	Minor	Minor	Minor	Minor	Minor	Minor
Lime, CaO	Minor	Minor	---	---	---	---	---	---	Minor	Minor	---	---	---	Minor
Periclase, MgO	---	Minor	---	---	---	---	---	---	---	---	---	---	---	---
Merwinite, $Ca_3Mg(SiO_4)_2$	Minor	Minor	---	---	---	---	---	Possible (Minor)	Minor	Minor	Minor	Minor	---	---
Plagioclase, $(Ca,Na)(Al,Si)_4O_8$	---	---	---	---	---	---	---	---	---	---	Possible (Minor)	---	---	---
Ferrite Spinel, $(Mg,Fe)(Fe,Al)_2O_4$	---	---	---	---	Minor	---	---	---	---	---	---	---	---	---
Akermanite, $Ca_2MgSi_2O_7$	---	---	---	---	---	---	---	---	---	---	---	---	Minor	---
Sinter Layer														
Sample Number	6184	6187	6189	6191	6160	6164	6168	6172	6350	6347	6351	6348	6352	6349
Quartz, SiO_2	Minor	Major	Major	Major	Major	Major	Major	Major	Minor	Major	Minor	Major	Major	Major
Anhydrite, $CaSO_4$	---	Minor	---	Minor	Minor	Minor	---	Minor	Minor	Minor	Minor	Minor	Major	Minor
Gehlenite, $Ca_2Al_2SiO_7$	Major	---	---	---	---	---	Minor	---	---	---	Minor	---	---	---
Mullite, $Al_6Si_2O_{13}$	---	---	Major	Minor	---	Minor	Minor	Minor	---	---	---	Possible (Minor)	Minor	Minor
Hematite, Fe_2O_3	Possible (Minor)	Minor	Major	Minor	Minor	Minor	Minor	Minor	---	Minor	Minor	Minor	Minor	Minor
Lime, CaO	---	Minor	---	---	---	---	---	---	Minor	---	---	---	---	---
Periclase, MgO	---	Minor	Minor	---	---	---	---	---	---	---	---	---	---	---
Merwinite, $Ca_3Mg(SiO_4)_2$	---	Minor	---	---	---	---	---	---	Minor	Minor	---	Minor	---	---
Plagioclase, $(Ca,Na)(Al,Si)_4O_8$	Minor	Minor	---	---	Major	Minor	Major	Minor	---	Minor	Major	Minor	Minor	Minor
Clinopyroxene, $Ca(Fe,Mg,Al)Si_2O_6$	---	---	---	---	Minor	---	Minor	---	Minor	Minor	---	Minor	Minor	Minor
Akermanite, $Ca_2MgSi_2O_7$	---	---	---	---	---	---	---	---	Major	---	---	---	---	---
Calcium Silicate, $CaSiO_4$	---	---	---	---	---	---	---	---	Minor	---	---	---	---	---
Maghemite, Fe_2O_3	---	---	---	---	---	---	---	---	Minor	---	---	---	---	---
Augite, $Ca(Fe,Mg)Si_2O_6$	---	---	---	---	---	---	---	---	---	---	Major	---	---	---

- The deposits produced under high FEGT conditions showed a roughly linear decrease in strength from the pure subbituminous through the blends to the Bailey bituminous deposits. However, the deposition rates of the blends were substantially less than that of either the pure subbituminous or bituminous deposits.

- The deposits produced under low FEGT conditions showed deposition rates from both blend ratios nearly equal to that of the pure Bailey deposit. Further, the strengths and deposition rates of all of the low FEGT deposits were significantly less than those of the corresponding high FEGT deposits.

The most striking feature of the SEMPC analyses of the deposit sinter layers under high FEGT is the presence of significant anorthite ($CaAl_2Si_2O_8$) in the blends. The anorthite is inferred from chemical composition in the SEMPC technique and is probably amorphous (noncrystalline), since it is not detected as a major phase from the XRD analysis of the blends. This is seen for both sets of blends, with the amount of anorthite in the Bailey/Black Thunder blends being slightly higher than that of the Bailey/Antelope blends. Along with this is an apparent depletion of quartz in the blends and an approximately linear increase in the amounts of clays (kaolinite, altered kaolinite, illite, and montmorillonite) from the subbituminous to the bituminous deposits.

Deposits formed under low FEGT conditions, by contrast, show no enhanced presence of anorthite for the blends, as well as less total anorthite present. No depletion of quartz is seen, and the clays, while still increasing linearly from subbituminous through the blends to the bituminous deposit, are more prevalent. It is evident that the rather small 200°F change in FEGT is responsible for quite profound changes in the deposit mineralogy and physical properties.

The differences in deposit strengths and deposition rates for the two subbituminous coals can be explained by the higher quartz and kaolinite content of the Antelope coal as compared to Black Thunder. On reaction with calcium to form calcium aluminosilicate species, the Antelope ash deposit forms a more pure silicate phase, resulting in a lower viscosity melt and increased deposition. On cooling, this produces a stronger deposit. The larger amount of organically bound sodium in the Antelope coal also provides a fluxing agent enhancing this effect.

The Bailey coal ash, by contrast, introduces significant silica, alumina, and iron species into the blends. With little calcium present, the pure Bailey coal forms deposits of mixed aluminosilicate species with moderate strength and deposition rates. Under high FEGT conditions, the admixture of calcium and sodium from the subbituminous coals in the blends provides the elements needed for the formation of the relatively high-viscosity anorthite phase present, reducing the "stickiness" of the blend deposits and reducing the deposition rates. Under low FEGT conditions, the temperature is too low for substantial anorthite formation, and the bituminous ash quartz and clays remain essentially unaltered while diluting the calcium aluminosilicate matrix arising from the subbituminous coal ash, producing a low deposition rate and quite weak blend deposits.

4.3.5 Slag Probe Test Results

Deposits were collected on water-cooled slag probes inserted through the wall of the test furnace during the course of each test, with probe metal surface temperatures maintained near

850°F. For each of the fuels tested, there was no significant buildup of furnace wall slag deposits. The deposits were present as a dusty layer that was lightly attached to the probe metal surface. Deposits of this nature should be easily removed by wall blowers in a conventional combustion system. The lack of significant deposit and the observed lack of physical strength for all deposits indicated no significant interactions between fuel ash types to form troublesome wall deposits. For this reason, these deposits were not submitted for the rigorous examination of physical and chemical characteristics as were each of the high- and low-temperature fouling deposits.

4.3.6 System Ash Characterization

Ash samples were collected from various regions of the combustion system. Results of the mass balance performed after completion of each test burn are presented in Table 22. Input ash levels are calculated based on ASTM ash levels reported in Table 2. Samples collected represent between 58.6% and 82.6% of the total ash input. A significant portion of the unaccounted for ash was likely retained on refractory surfaces in the test furnace. A small portion of the unaccounted ash exited the system via the stack. The chemical composition of samples taken from the ESP hopper catch are reported in Table 23.

4.4 Low-Temperature Ash Deposition and Testing Program

4.4.1 Experimental Procedures

Ash Deposition Sampling Procedure. Low-temperature ash-fouling deposits were obtained from the seven combustion test runs listed in Table 24. As described in Section 4.3.3, a total of four steam-cooled probes were inserted into the flue gas duct just upstream of the water-cooled heat exchangers to collect ash-fouling deposits. The probe bank was designed to be located in a section of the flue gas ducting in which the flue gas temperature was approximately 1550°F to simulate reheat/economizer boiler tubes.

The probe bank consisted of two sets of two probes fitted with removable sleeves that were maintained in a horizontal orientation and perpendicular to the direction of flow. As shown in Figure 29, two of the probes were designed to be in-line and directly downstream of the other two probes. For purposes of ash-fouling analyses and the following discussion, the probes were separated into two column sets, each set consisting of an upstream probe and the probe positioned directly downstream. The column arrangement of one set of probes, shown from an end view, is given in Figure 30 which illustrates the sampling zones into which each probe was divided. From one column of upstream and downstream probes, loose ash deposits were removed for XRD analyses. Additionally, these materials were quantified to determine deposition rates for each of the sampling zones.

Samples were obtained from each of the indicated zones. On the upstream probe, the upstream deposit (noted as Zone 2) consisted of a single deposit ridge running along the center of the zone area. This type of deposit is representative of only the first tube in each row. The deposit on the upstream side of the downstream probe is composed of small crests or humps that form on either side of the center line of the tube, leaving the center line clear. This mode of ash deposition would be considered typical for the majority of the tubes in a series of rows and columns. For the downstream probe, sample collection was performed on the deposits from Zones 2 and 3.

TABLE 22

System Ash Mass Balance, Standard Ash-Fouling Tests

Run Number:	AF-CTS-700	AF-CTS-701	AF-CTS-702	AF-CTS-703	AF-CTS-706	AF-CTS-707	AF-CTS-708
Date:	11/09/93	11/11/93	11/15/93	11/17/93	12/16/93	12/20/93	12/22/93
Fuel:	Black Thunder	Bailey	Bailey/Black Thunder	Bailey/Black Thunder	Antelope	Bailey/Antelope	Bailey/Antelope
Blend Ratio:	100	100	35/65	65/35	100	35/65	65/35
Test Duration, hr	10.5	10.17	10.5	10.5	10.5	10.5	10.5
Total Coal Fed, lb	676.46	404	543.05	470.4	702.29	569.24	494.54
Ash Input Rate, lb/MMBtu	4.96	4.58	5.59	5.28	5.2	5.72	5.41
Total Ash Input, lb	30.37	25.45	32.69	29.95	32.94	34.95	32.15
Total Ash Input, g	13,777	11,545	14,829	13,586	14,941	15,854	14,581
Ash Balance							
Furnace, g							
Bottom and Walls	1138	1540	2029.8	1375.5	1106.8	1100	2082.7
Wall Slag Probe	---	---	---	---	---	15	5
Horiz. Slag Probe	---	---	---	---	---	10	6.9
Total	1138	1540	2029.8	1375.5	1106.8	1125	2094.6
% of Input Ash	8.26	13.34	13.69	10.12	7.41	7.1	14.37
Probe Area, g							
Probe Bank - Test A							
Inner Layer	11.6	6.6	6.2	7.9	13.8	10	8.2
Sinter Layer	325.5	233.7	106.8	49.8	564	230	77.8
Probe Bank - Test B							
Inner Layer	7.4	5.3	5.2	5.4	8.9	10	6.1
Sinter Layer	75.8	16	23	35.7	211.1	30	19.3
Duct Ash							
Preprobe	---	---	1200.1	---	1433.3	1725	559.5
Postprobe	3082.6	4155	939.2	3050.8	1950.4	200	2285.4
Total	3502.9	4416.6	2280.5	3149.6	4181.5	2205	2956.3
% of Input Ash	25.43	38.26	15.38	23.18	27.99	13.91	20.28
Heat Exchangers, g							
HX No. 1	108	254.6	306.8	74.4	553.4	108.9	682.2
HX No. 2	95.6	180.7	155.6	176.2	145	139	217.8
HX No. 3	36.2	207.1	144	131.5	62	141.1	193.6
HX No. 4	316.7	176.8	233.5	175.4	128	287.1	319.3
HX No. 5	14	89.3	274	232.6	241	385.8	26.4
HX No. 6	53.9	15.9	2.5	1.8	178	182.4	95.8
HX No. 7	33.9	199.6	228.1	0	289	84.3	80.6
HX No. 8	369.5	390.6	329.8	411.9	295	794.2	69.6
Total	1027.8	1514.6	1674.3	1203.8	1891.4	2122.8	1685.3
% of Input Ash	7.46	13.12	11.29	8.86	12.66	13.39	11.56
Pilot-Scale ESP, g							
After Test A	1171.4	NA[1]	1258.4	1093.5	1233.8	1084.1	NA
After Test B	1652.4	1237.7	1423.1	1686	1475	1602.7	1990
Bypass Cyclone, g	915.5	578.3	190	1319	990	1095.2	305
Sampling Cyclone, g	223	151.9	212.1	234.9	---	---	---
Ductwork, g	50.3	92.6	89.6	97.5	120	54.8	45
Total	4012.6	2060.5	3173.2	4430.9	3818.8	3836.8	2340
% of Input Ash	29.13	17.85	21.4	32.61	25.56	24.2	16.05
Unaccounted For, g	4095.7	2013.3	5671.2	3426.2	3942.5	6564.4	5504.8
% of Input Ash	29.73	17.44	38.24	25.22	26.39	41.41	37.75

[1] Not available.

TABLE 23

Fly Ash Sample Analyses, Standard Ash-Fouling Tests

Run Number:	AF-CTS-700		AF-CTS-701		AF-CTS-702		AF-CTS-703			AF-CTS-706		AF-CTS-707		AF-CTS-708	
Fuel:	Black Thunder		Bailey		Bailey/Black Thunder		Bailey/Black Thunder			Antelope		Bailey/Antelope		Bailey/Antelope	
Blend Ratio, wt%:	100		100		35/65		65/35			100		35/65		65/35	
Test Designation:	A	B	A	B	A	B	A	B	B	A	B	A	B	A	B
Target FEGT, °F:	2200	2000	2200	2000	2200	2000	2200	2000	2000	2200	2000	2200	2000	2200	2000
ESP Hopper Ash															
Time	1056	1754	NA[1]	EOT	1138	1840	1230	NA	EOT	1040	EOT	1119	EOT	1046	EOT
Sample Number	93-1096	93-1101	NA	93-1112	93-1033	93-1039	93-1045	93-1051	93-1050	94-0020	94-0025	94-0009	94-0014	94-0038	94-0044
Carbon in Ash, %	0.1	0.22	NA	14.12	1.78	4.12	1.87	5.98	NA	0.23	0.18	2.4	3.18	2.24	5.62
Ash Analysis, wt%															
SiO_2	45.37	40.58	NA	46.93	42.73	41.19	45.5	45.08	45.67	35.47	33.72	39.18	37.98	44.58	41.55
Al_2O_3	17.95	16.83	NA	24.71	21.54	21.98	22.39	22.72	22.48	13.45	12.92	19.92	20.18	21.65	21.63
Fe_2O_3	5.25	6.12	NA	19.54	9.75	11.4	14.37	13.58	13.57	6.03	6	12.33	12.05	13.96	14.57
TiO_2	1.21	1.25	NA	1.14	1.06	1.17	1.18	1.14	1.29	0.87	0.8	0.97	1.15	0.99	1.14
P_2O_5	0.95	0.9	NA	0.19	0.87	0.75	0.53	0.68	0.47	1.37	1.39	0.68	0.9	0.53	0.64
CaO	22.69	25.3	NA	2.65	15.58	15.26	9.5	8.94	8.83	30.96	31.41	18.46	17.91	10.74	10.76
MgO	2.84	3.93	NA	1.49	3.74	3.43	2.38	2.33	2.37	4.8	4.8	3.97	3.56	2.53	2.9
Na_2O	1.19	1.68	NA	0.62	1.37	1.11	1	1.18	1.17	2.53	2.53	1.45	1.48	1.36	1.04
K_2O	0.15	0.16	NA	1.08	1.07	0.82	1.43	1.45	1.46	0.51	0.49	0.73	0.75	1.4	0.83
SO_3	2.41	3.24	NA	1.66	2.29	2.9	1.72	2.9	2.69	4.01	5.94	2.31	4.05	2.26	4.93
Total	100.01	99.99	NA	100.01	100	100.01	100	100	100	100	100	100	100.01	100	99.99
SO_3-Free, wt%															
SiO_2	46.49	41.94	NA	47.72	43.73	42.42	46.3	46.43	46.93	36.95	35.85	40.11	39.58	45.61	43.71
Al_2O_3	18.39	17.4	NA	25.12	22.04	22.63	22.78	23.4	23.1	14.01	13.74	20.39	21.03	22.15	22.75
Fe_2O_3	5.38	6.33	NA	19.87	9.98	11.74	14.62	13.99	13.95	6.28	6.38	12.62	12.56	14.28	15.33
TiO_2	1.24	1.29	NA	1.16	1.08	1.2	1.2	1.17	1.33	0.91	0.85	0.99	1.2	1.01	1.2
P_2O_5	0.97	0.93	NA	0.19	0.89	0.77	0.54	0.7	0.48	1.43	1.48	0.7	0.94	0.54	0.67
CaO	23.25	26.15	NA	2.69	15.95	15.71	9.67	9.21	9.07	32.25	33.39	18.9	18.66	10.99	11.32
MgO	2.91	4.06	NA	1.51	3.83	3.53	2.42	2.4	2.44	5	5.1	4.06	3.71	2.59	3.05
Na_2O	1.22	1.74	NA	0.63	1.4	1.14	1.02	1.22	1.2	2.64	2.69	1.48	1.54	1.39	1.09
K_2O	0.15	0.17	NA	1.1	1.1	0.84	1.46	1.49	1.5	0.53	0.52	0.75	0.78	1.43	0.87
Total	100	100	NA	100	100	100	100	100	100	100	100	100	100	100	100
SiO_2/Al_2O_3	2.528	2.411	NA	1.899	1.984	1.874	2.032	1.984	2.032	2.637	2.61	1.967	1.882	2.059	1.921
Base/Acid	0.498	0.634	NA	0.349	0.482	0.498	0.415	0.399	0.395	0.9	0.953	0.615	0.603	0.446	0.468
Dolomite Ratio	0.795	0.786	NA	0.163	0.613	0.584	0.414	0.41	0.409	0.798	0.801	0.607	0.601	0.442	0.454
$Fe_2O_3/(CaO+MgO)$	0.206	0.209	NA	4.72	0.505	0.61	1.21	1.205	1.212	0.169	0.166	0.55	0.561	1.052	1.067
Sampling Cyclone															
Sample No. 1															
Time	855		825		820		NA[1]			750		905		750	
Sample Number	93-1093		93-1104		93-1031		93-1043			94-0018		94-0007		94-0037	
Carbon in Ash, %	0.01		5.05		3.09		3.28			0.22		2.92		2.62	
Sample No. 2															
Time	950		1005		1020		1055			1025		1115		1022	
Sample Number	93-1094		93-1105		93-1032		93-1044			94-0019		94-0008		94-0039	
Carbon in Ash, %	0.13		5.04		1.38		1.52			0.24		3.52		1.97	
Sample No. 3															
Time		1500		1345		1455		1450			1325		1445		1355
Sample Number		93-1098		93-1108		93-1037		93-1049			94-0023		94-0012		94-0042
Carbon in Ash, %		0.35		15.01		3.43		6.24			0.2		2.92		7.44
Sample No. 4															
Time		1650		1535		1640			1630		1600		1655		1625
Sample Number		93-1099		93-1109		93-1038			93-1050		94-0024		94-0013		94-0043
Carbon in Ash, %		0.36		10.66		3.64			5.88		0.18		4.86		9.93

[1] Not available.

TABLE 24

Combustions Runs for Low-Temperature Ash Deposition and Testing Program

Run No.	Fuel Source	Date of Run
AF-CTS-700L	100% Black Thunder	11/29/93
AF-CTS-702L	35%/65% Bailey/Black Thunder	12/01/93
AF-CTS-703L	65%/35% Bailey/Black Thunder	12/03/93
AF-CTS-701L	100% Bailey	12/07/93
AF-CTS-706L	100% Antelope	12/28/93
AF-CTS-707L	35%/65% Bailey/Antelope	12/30/93
AF-CTS-708L	65%/35% Bailey/Antelope	1/19/94

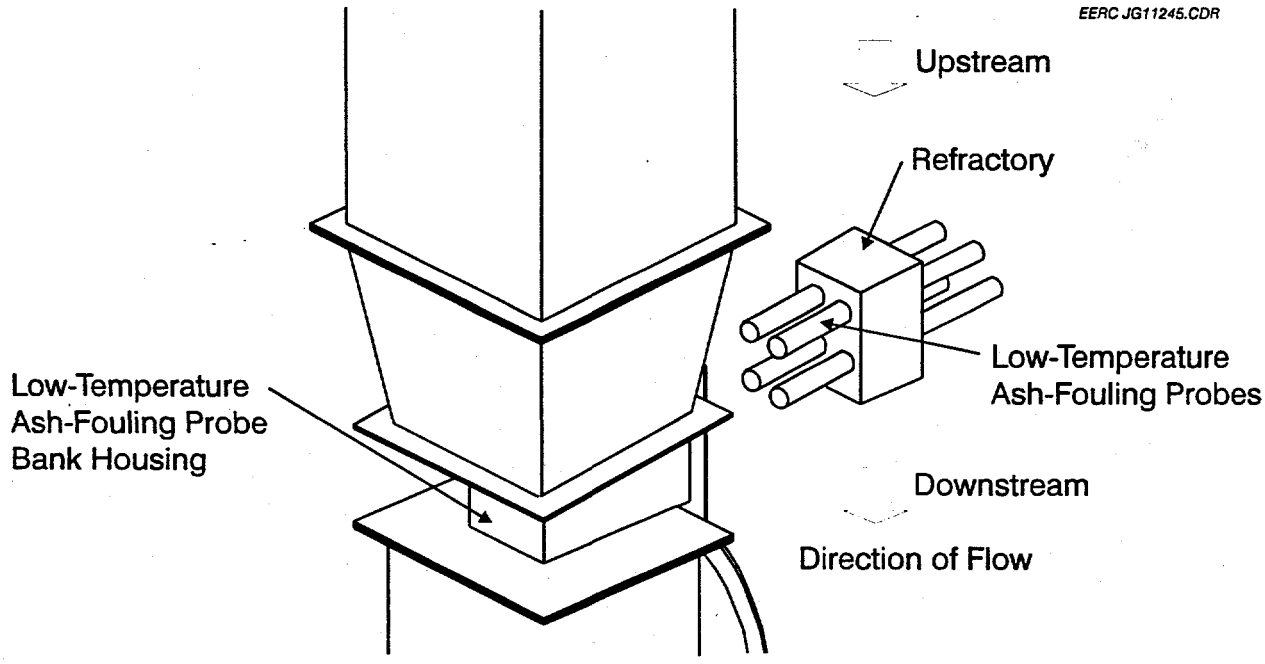

Figure 29. Oblique schematic of low-temperature ash-fouling bank used for testing.

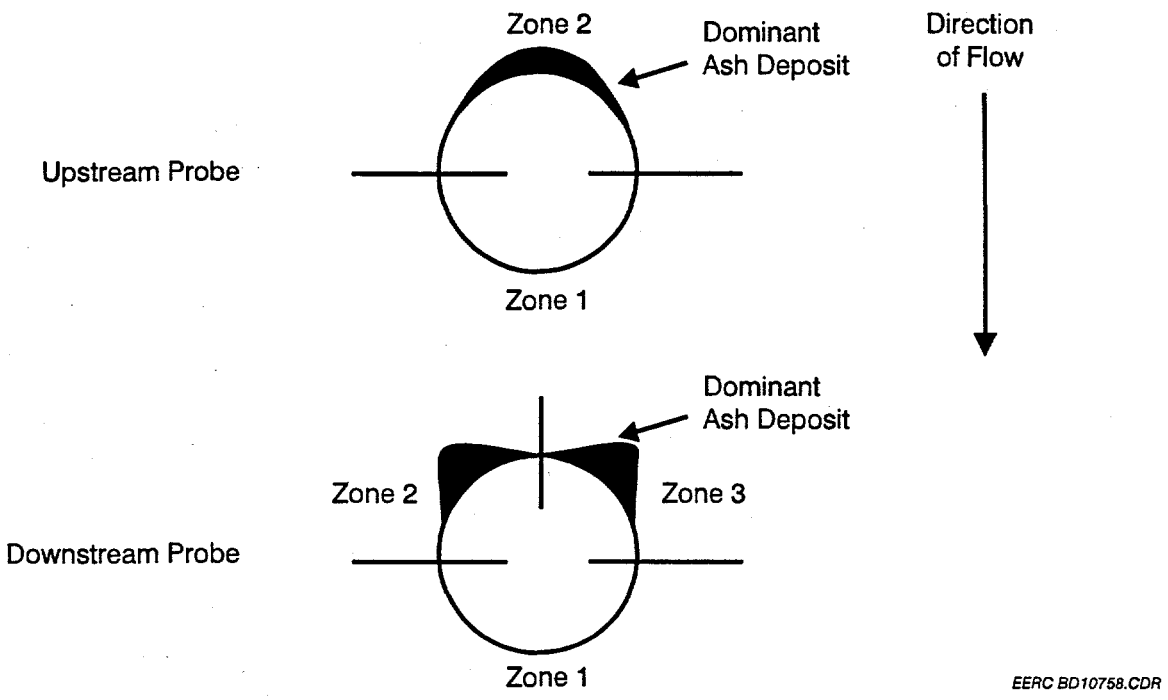

Figure 30. End view of one column set of low-temperature ash-fouling probes.

The other column set, along with the deposits which had formed, was dealt with in a different manner. A dilute epoxy compound was gently sprayed onto the deposit to bind the loose ash to the sleeve. In some instances, the deposit was extremely loose, which resulted in a slight loss of material while removing the probe sleeves, as well as when applying the dilute epoxy solution. After the dilute epoxy solution hardened, the sleeves were submerged into a full-strength epoxy mixture. The epoxy-treated sleeves were subsequently cut into 1-in.-long sections and submitted for SEMPC determination and morphology.

The flue gas flowing past the low-temperature ash-fouling probe bank was sampled via multicyclone for five of the seven fuels. Various multicyclone cuts were submitted for point count determination and XRD analyses. The established method for characterizing the crystalline phases present is by XRD. Even in complex materials, the crystalline phases present can be identified by their characteristic peaks in x-ray diffractograms. These peaks can be identified by comparing them to a database of minerals and other inorganic phases. Even mineral grains that are too small to be detected by optical or SEM can be identified by XRD methods. SEMPC provides quantitative chemical analysis of phases present for point analyses down to 1 square micron in area. The cut point (D_{50}) for each stage of the multicyclone, along with the quantity of ash collected, is shown in Table 25. The multicyclone samples that were selected for detailed analysis are shown in bold type.

Strength-Testing Procedures. Strength testing was performed on ESP ash collected from the combustion of the five fuels listed in Table 25. In preparation for the strength-testing procedure, the ESP ash samples were physically classified to remove fractions greater

TABLE 25

Multicyclone Samples Retrieved During Low-Temperature Ash-Fouling Combustion Tests

	D_{50} Cut Size, μm/Sample Collected, g[1]					
Fuel Source	Stage 1	Stage 2	Stage 3	Stage 4	Stage 5	Backup Filter
100% Black Thunder	**5.4/3.60**	4.9/3.84	2.4/1.38	**1.3/0.54**	0.9/0.10	0.3/0.20
100% Bailey	**9.4/5.10**	5.6/2.68	**2.9/0.80**	1.5/0.29	1.1/0.08	0.4/0.51
100% Antelope	**6.2/2.50**	4.8/1.31	2.3/0.87	**1.2/0.32**	0.9/0.07	0.3/0.04
35%/65% Bailey/Antelope	**14.0/3.70**	4.6/3.42	**2.2/1.00**	1.2/0.27	0.8/0.05	0.3/0.10
65%/35% Bailey/Antelope	**10.0/3.20**	6.3/1.95	3.3/0.90	**1.7/0.47**	1.2/0.12	0.5/0.07

[1] Bold numbers indicate samples analyzed for point counts and XRD.

than 10 μm. Use of the -10-μm fraction was to simulate size fractions most likely to interact with downstream deposits. The classified samples were subsequently evaluated for size gradation using a Malvern 2600 laser diffraction particle sizer. The results of the particle sizing are enclosed in Appendix B. The sintering atmosphere consisted of 0.5% SO_2, 3% O_2, 15% H_2O, and the balance nitrogen. The first series of strength development tests was sintered at 1010°C (1850°F). A second series of strength development tests was performed under the same atmospheric condition but at 850°C (1560°F). Sintering times at the high-temperature condition were 8, 24, and 48 hr, while those for the low-temperature condition were 8, 24, and 96 hr.

4.4.2 Testing of Low-Temperature Ash Deposits

Testing of Ash Deposits. Calculated deposition rates for the low-temperature ash-fouling deposits are shown in Table 26. Because of budget constraints, the ash samples from Runs 702L and 703L were not analyzed extensively. Samples were taken from a 3-in. band near the center of the deposition probes for each 12-hr run. The deposits formed on the upstream probe were relatively light, with an average formation rate of 0.064 g/in.^{2}-hr for all tests, and were essentially equally distributed between Zones 1 and 2. There was no discernible order of deposition, in terms of any one fuel blend causing significantly more or less fouling than any other fuel blend tested.

The downstream probe showed much more significant deposits in Zones 2 and 3 than those formed in Zone 1. The Zone 2 and 3 deposits on the downstream probe are due to the double-ridge deposit as described above. On average, the downstream probe held at least 4½ times the quantity of deposit as the upstream probe. Combustion of the parent bituminous coal as well as the four fuel blends resulted in roughly equivalent downstream probe deposit quantities. The average

TABLE 26

Calculated Rates of Low-Temperature Ash-Fouling Deposition (g/in.^{2}-hr)[1]

Fuel	Run Number	Upstream Zone 1	Upstream Zone 2	Downstream Zone 1	Downstream Zone 2	Downstream Zone 3
100% Black Thunder	700L	0.033	0.042	0.089	0.128	0.156
35%/65% Bailey/Black Thunder	702L[2]	0.024	0.028	0.085	0.097	0.107
65%/35% Bailey/Black Thunder	703L[2]	0.030	0.036	0.085	0.079	0.091
100% Bailey	701L	0.030	0.046	0.084	0.107	0.096
100% Antelope	706L	0.024	0.014	0.078	0.059	0.220
35%/65% Bailey/Antelope	707L	0.030	0.028	0.069	0.091	0.088
65%/35 Bailey/Antelope	708L	0.022	0.063	0.066	0.116	0.116

[1] All calculations based on deposition over a 3-in. length of the projected area of the 2-in.-diameter probe for a 12-hr run.

[2] Samples not submitted for XRD, SEMPC analyses, or strength development.

deposit weight of the five test cases mentioned here was 0.275 g/in.^{2}-hr, with each of the deposit weights falling within $\pm 10\%$ of the average. However, combustion of the parent subbituminous coals produced significantly more downstream probe deposits. The measured deposit weights for the Black Thunder and Antelope tests were 35% and 72% greater, respectively, than the average deposit weight from the other five fuels tested.

Powder samples submitted for XRD analyses were retrieved from Zone 1 of the upstream probe and Zone 2 of the downstream probe. These locations are considered to be the most representative of ash deposits that would occur in a matrix of boiler tubes. Mineral phases identified from the XRD are listed in Table 27.

The low-temperature fouling deposits, cemented to the removable sleeves with epoxy, were evaluated via SEMPC. The deposit zones isolated for viewing were Zone 1 of the upstream probe sleeve and Zones 2 and 3 of the downstream probe sleeve. As stated previously, the Zone 1 deposit of the upstream probe tended to be extremely light and adhered closely to the coupon surface. When cross-sectioned, the deposit was so close to the coupon surface that point count analysis was not possible. Thus, for determining the bulk composition of the upstream probe Zone 1 deposit, the powdered samples originally submitted for XRD were analyzed by SEMPC as well.

Comparisons between the upstream and downstream probe deposits showed that there was no significant difference in bulk compositions, with the exception of the deposits from the 100% Antelope run and the 35%/65% Bailey/Antelope blend run. Analysis of these deposits showed a

TABLE 27

Results of XRD Analyses of Selected Low-Temperature Ash-Fouling Deposits

Run Number	AF-CTS-700L		AF-CTS-701L		AF-CTS-706L		AF-CTS-707L		AF-CTS-708L	
Fuel	Black Thunder		Bailey		Antelope		Bailey/Antelope		Bailey/Antelope	
Blend	100		100		100		35/65		65/35	
Sample Location	Zone 1	Zone 2	Zone 1	Zone 2	Zone 1	Zone 2	Zone 1	Zone 2	Zone 1	Zone 2
Mineral Phases										
Quartz, SiO_2	Minor	Minor	Major	Minor	Minor	Minor	Minor	Minor	Minor	Minor
Anhydrite, $CaSO_4$	Minor	Minor	Minor	Minor	Minor	Minor	Major	Major	Minor	Minor
Periclase, MgO	Minor	Minor	---	---	Minor	Minor	Minor	Minor	---	Minor
Merwinite, $Ca_3Mg(SiO_4)_2$	Minor	Minor	---	---	Minor	Minor	Minor	Minor	Minor	Minor
Lime, CaO	Minor	Minor	---	---	Minor	Minor	Minor	Minor	Minor	---
Hematite, Fe_2O_3	Minor	---	Minor	Minor	---	---	---	---	Minor	Minor
Mullite, $Al_6Si_2O_{13}$	Minor	Minor	Major	Major	---	---	Minor	Minor	Minor	Major
Maghemite, Fe_2O_3	---	---	Minor	---	Minor	Minor	Minor	Minor	Minor	Minor
Gehlenite, $Ca_2Al_2SiO_7$	---	---	---	---	Minor	---	---	---	---	---
Amorphous	Major	Major	Minor	Minor	Major	Major	Minor	Minor	Minor	Minor

significantly greater contribution of silicate component in the upstream probe deposit as opposed to that on the downstream probe (approximately 31% versus 18% for the straight Antelope run and 40% versus 31% for the fuel blend). Plots of the data from each of the runs listed in Table 26, with the exception of Runs 702L and 703L, can be found in Appendix B.

Visual Examination. The Bailey bituminous coal produced more deposition on the first row of probes in both the upstream and downstream zones than the other fuels tested. However, the deposits on both rows of probes were very loose and easy to dislodge during handling. These deposits were noticeably weaker and less dense than the deposits from any of the other fuels. Removal of the probe sleeves for initial application of the dilute epoxy solution was difficult without disturbing the deposits.

For the 100% Black Thunder run, the ash deposited on the first row of probes was extremely light in comparison to the downstream tubes. As the particulate moved past the first row of probes, the aerodynamic flow pattern affected the rate of deposition. A peaked deposit formed along the edges of the upstream zones of the downstream probe, as described in Section 4.4.1 above. As the ratio of Black Thunder coal in the Bailey/Black Thunder blend decreased, the total amount of ash deposition decreased but there were still significant differences between the quantities of upstream and downstream probe deposits.

The 100% Antelope combustion run produced minimal deposits in both zones of the upstream probes, but resulted in relatively thick deposits in all three zones of the downstream probes. In comparison to the deposit trends noted for the Bailey/Black Thunder blend series, the decrease in the quantity of deposition was not as significant with the Bailey/Antelope blend series as the ratio of Antelope in the fuel blends decreased.

Multicyclone Samples. Ash samples were aerodynamically separated into six distinct size fractions using a multicyclone sampling apparatus. The cut sizes (D_{50}) and corresponding amounts collected from each multicyclone stage are listed in Table 25. The two particulate fractions from each multicyclone sample presented in bold on Table 25 were submitted for SEMPC and XRD analyses. Table 28 summarizes the mineral phases identified for the multicyclone samples submitted for XRD analyses.

The compositions of the selected multicyclone samples shown in Table 28 were determined by SEMPC. The SEMPC analyses did not reveal any significant particle-size fraction-related differences within any particular sample set. Plots of the results of these analyses can be found in Appendix B.

4.4.3 Upstream Deposits of Black Thunder and Antelope

Upstream deposits from the 100% Black Thunder and 100% Antelope test runs were epoxied to the corresponding removable sleeve and prepared for examination by SEM. Area analyses were performed on five areas of each deposit, beginning next to the metal surface and progressing outward to the surface of the deposit. Each area was analyzed for bulk composition, particle-size distribution, and porosity or void space. In each area, three side-by-side columns were analyzed. Results were averaged for the three columns for graphical presentation.

TABLE 28

Results of X-Ray Diffraction Analyses of Multicyclone-Separated Samples

Run Number	AF-CTS-700L		AF-CTS-701L		AF-CTS-706L		AF-CTS-707L		AF-CTS-708L	
Fuel	Black Thunder		Bailey		Antelope		Bailey/Antelope		Bailey/Antelope	
Blend	100		100		100		35/65		65/35	
D_{50}, μm	5.4	1.3	9.4	2.9	6.2	1.2	14.0	2.2	10.0	1.7
Mineral Phases										
Quartz, SiO_2	Minor	Minor	Minor	Minor	Minor	Minor	Minor	Minor	Minor	Minor
Anhydrite, $CaSO_4$	Minor	Minor	Minor	---	Minor	Minor	Minor	Minor	Minor	Minor
Periclase, MgO	Minor	Minor	---	---	Minor	Minor	Minor	Minor	Minor	---
Merwinite, $Ca_3Mg(SiO_4)_2$	---	Minor	---	---	---	---	---	---	Minor	---
Lime, CaO	---	Minor	---	---	Minor	---	---	---	Minor	---
Hematite, Fe_2O_3	Minor	Minor	---	Minor	Minor	Minor	---	---	Minor	Minor
Mullite, $Al_6Si_2O_{13}$	---	Minor	Major	Minor	---	---	Minor	Minor	Major	Minor
Maghemite, Fe_2O_3	---	---	Minor	Minor	---	---	---	Minor	Minor	Minor
Gehlinite, $Ca_2Al_2SiO_7$	---	---	---	---	Minor	---	---	---	---	---
Calcite, $CaCO_3$	---	---	---	---	Minor	---	---	---	---	---
Gypsum, $CaSO_4 \cdot 2H_2O$	---	---	---	---	---	---	Minor	---	---	---
Ettringite, $Ca_6Al_2(SO_4)_3(OH)_{12} \cdot 26H_2O$	---	---	---	---	---	---	Minor	---	---	---
Amorphous	Major	Major	Minor	Minor	Major	Major	Minor	Major	Minor	---

Antelope. Normalized bulk composition for the oxides of the major elements is given in Figure 31. Compositional changes from the inside of the deposit out were moderately noticeable with a decrease in CaO and an increase in SO_3 as the area analysis progressed away from the sleeve metal surface, implying an increase in particle-size distribution.

Results of particle-size distribution analysis (Figure 32) indicated that nearly all of the particles making up the ash deposit consisted of cross-sectional diameters of less than 10 μm. There is a significant difference between definitions of cross-sectional, caliper, and aerodynamic diameter. Instruments can be used, such as a laser particle analyzer, to measure and quantify caliper diameter sizes by measuring a silhouette diameter. When we determine cross-sectional diameters using SEM methods, the deposit matrix is cut with an arbitrary plane, leaving a cross-section of the spherical ash particles present. However, since the matrix is made up of various sizes of randomly packed particles, the plane does not reveal the true caliper diameters of all the particles. Thus cross-section diameters will tend to be smaller than true caliper diameters. Previous efforts at the EERC used a computer program to determine the cross-sectional diameter of a sphere having a caliper diameter equal to 1.0. Through 100,000 iterations, i.e., the sphere was arbitrarily sliced and measured 100,000 times, the average cross-sectioned diameter was determined to be 78.6% of the caliper diameter (4).

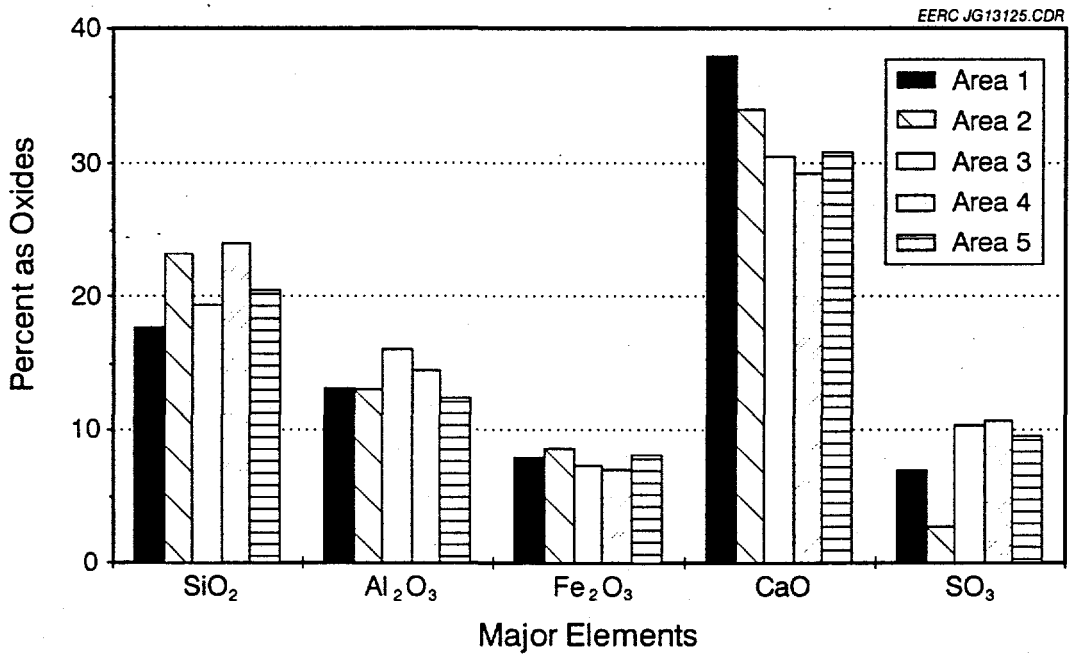

Figure 31. Concentrations of major elemental oxides versus area of deposition for upstream Antelope low-temperature fouling deposits.

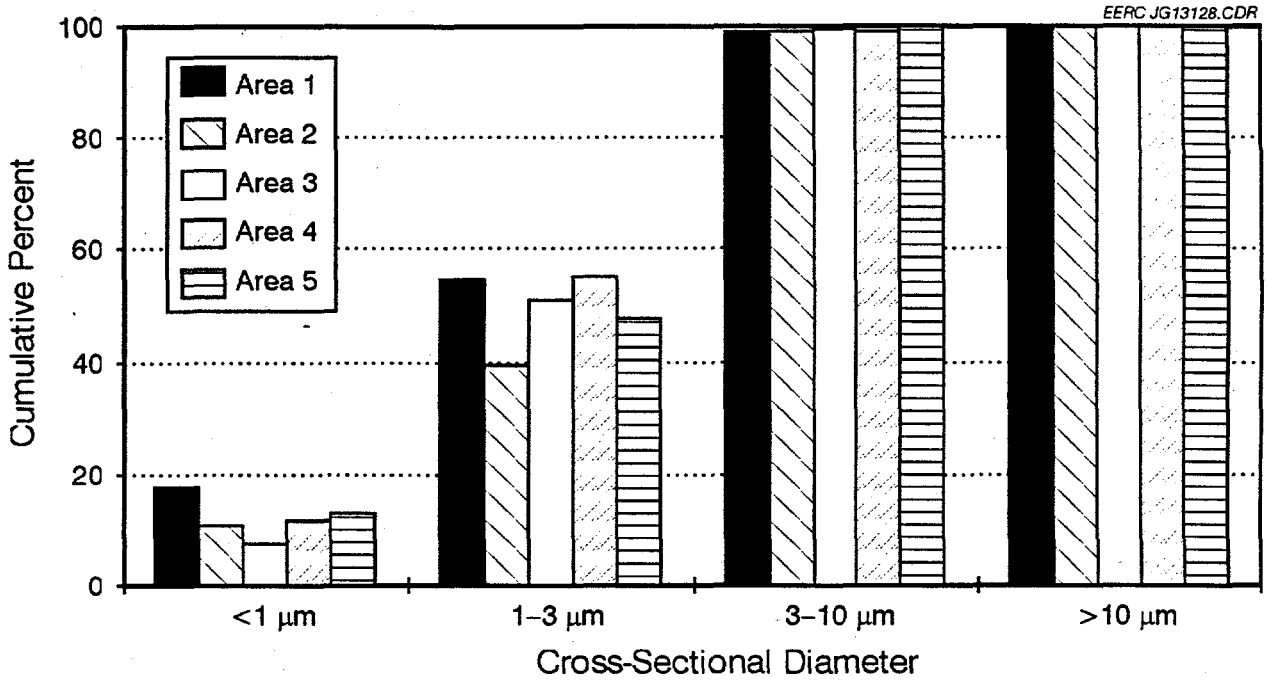

Figure 32. Particle-size distribution of sample of upstream Antelope low-temperature fouling deposit.

Aerodynamic diameters are those of particles that are separated from the combustion gas stream through a means of a physical separation such as a cyclone separator. When particles are separated based on an aerodynamical diameter, three main variables are important: particle size, shape, and density. The larger the particle is and the higher the particle density, the less likely the particle will stay entrained in the gas stream. Thus the separation of a particle on the basis of its aerodynamic diameter is a function of its physical characteristics.

Porosity of the epoxied samples was measured using a binary image analyzer. The porosity of the Antelope deposit was very high (80%–90%) for all five of the designated areas (Figure 33). During the epoxy application procedure, it is possible for air bubbles to form in the mixture. It is also possible for some particles to be removed during the polishing step of the sample preparation procedure which could increase porosity. However, the areas closest to the metal surface would be anticipated to be less porous because the deposit would have more time to pack together from subsequent deposition.

Black Thunder. The normalized bulk compositions of the low-temperature ash-fouling deposits from the 100% Black Thunder combustion test are given in Figure 34. The most noticeable trends were the increase in SiO_2 and decrease in CaO as the deposit progressed away from the metal surface. Distribution of the cross-sectional diameters were very similar for both sources of ash (100% Antelope and 100% Black Thunder, Figure 35). Approximately 50% of the ash particles were less than 3 μm in size. The average cross-sectional diameter of all five areas analyzed for both ash deposits was between 3 and 4 μm.

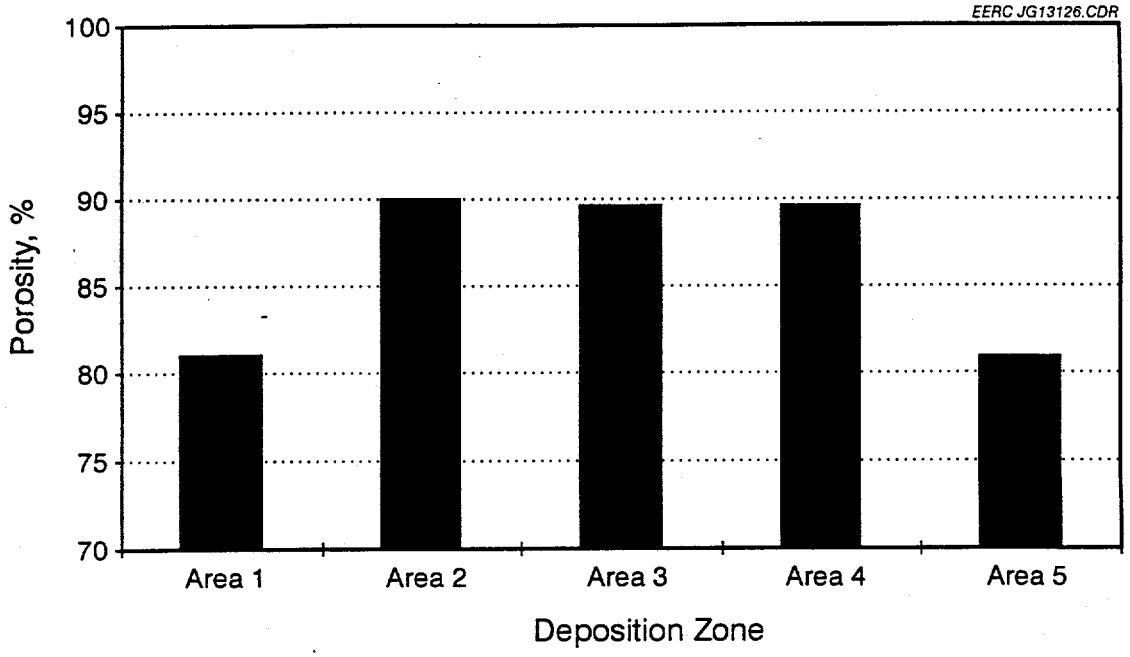

Figure 33. Porosity of upstream Antelope deposit sample.

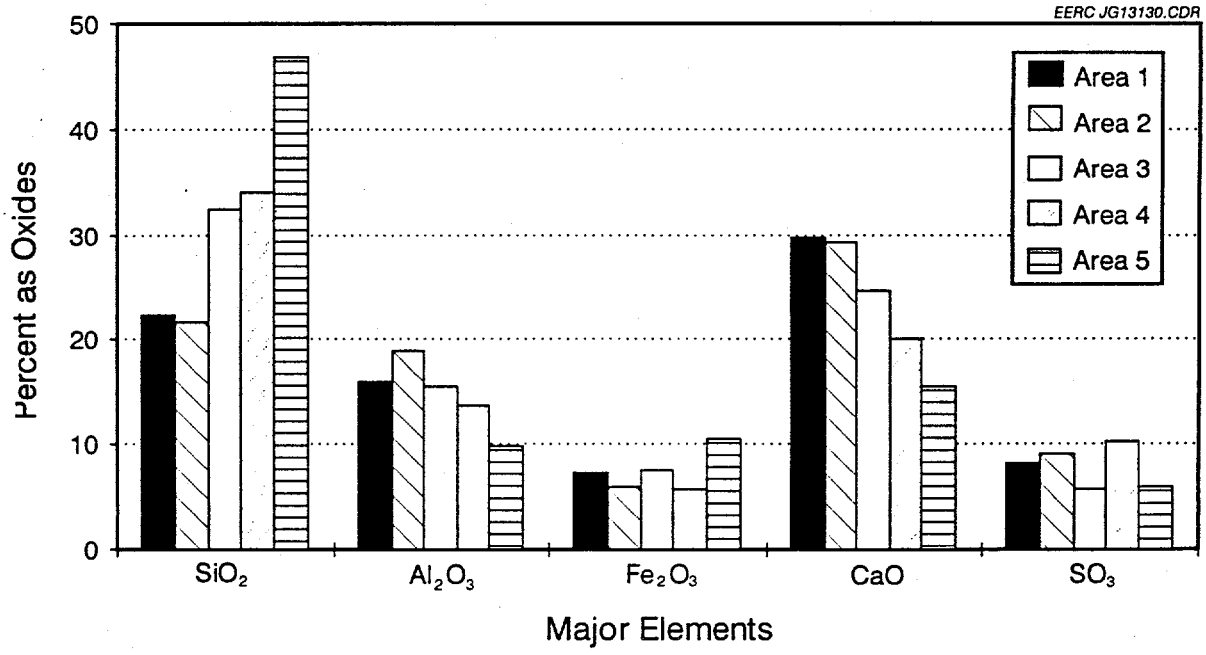

Figure 34. Concentrations of major elemental oxides versus area of deposition for upstream Black Thunder low-temperature fouling deposits.

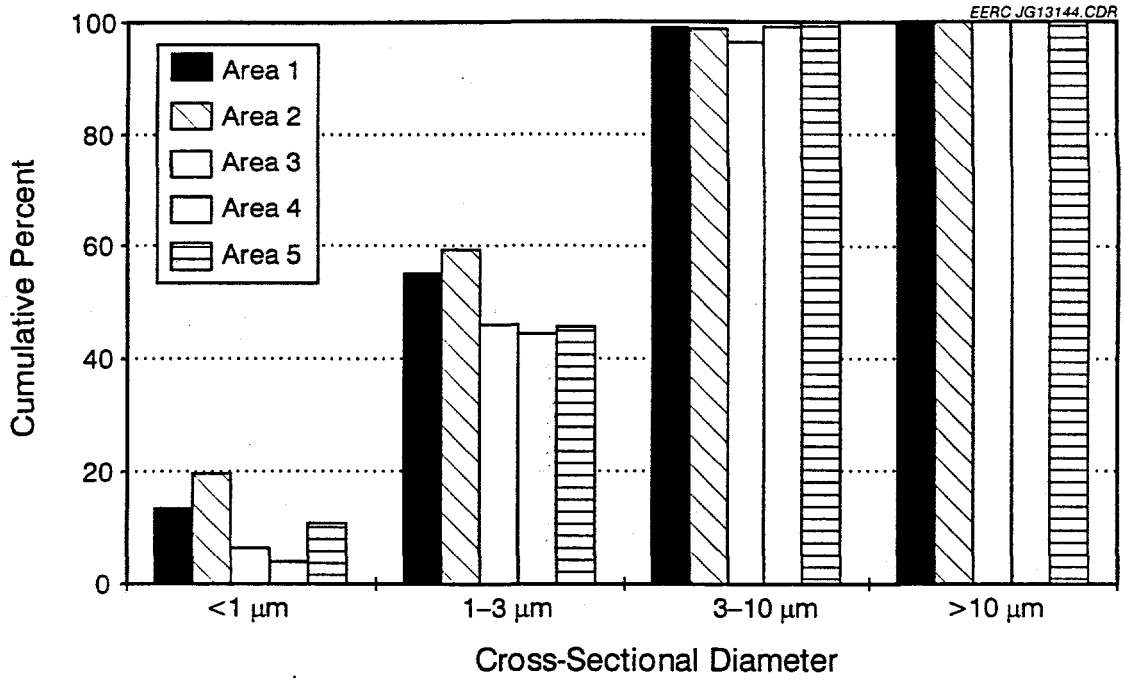

Figure 35. Particle-size distribution of sample of upstream Black Thunder low-temperature fouling deposit.

The porosities of the Black Thunder ash deposit (Figure 36) were similar to the Antelope deposit at areas closest to and farthest away from the coupon surface (80%–85%). However, in the regions between these areas, the porosities of the Black Thunder deposit were less, indicating a higher level of compaction.

4.4.4 Strength Testing

ESP ash produced from the five combustion runs identified in Table 25 was used to evaluate the propensity for strength development. Because most low-temperature deposits are composed of smaller ash particles, the ESP ash was aerodynamically classified to remove larger particles, although much of the smaller ash particles were also lost. Therefore, the ash used for strength determinations fell in the aerodynamic diameter range of approximately 2–15 μm. However, in general, 50% of the aerodynamically classified ash samples fell into the size range of 1–6 μm, thereby reducing the effects of particle-size distributions on the development of strength and emphasizing the composition effects.

Ash pellets were prepared by hand for the strength development tests using a punch and die. The diameter of the die was ½ in., and pellets approximately 0.6–0.7 in. in length were prepared. Methanol was used as a binder due to preparation difficulties encountered with the as-received ash. Each prepared pellet was pressed with an applied force of 21–22 pounds, and six pellets from each ESP ash sample were prepared for each sintering condition. After the pellets had been subjected to the sintering atmosphere for a given period of time, the compressive strength of each was

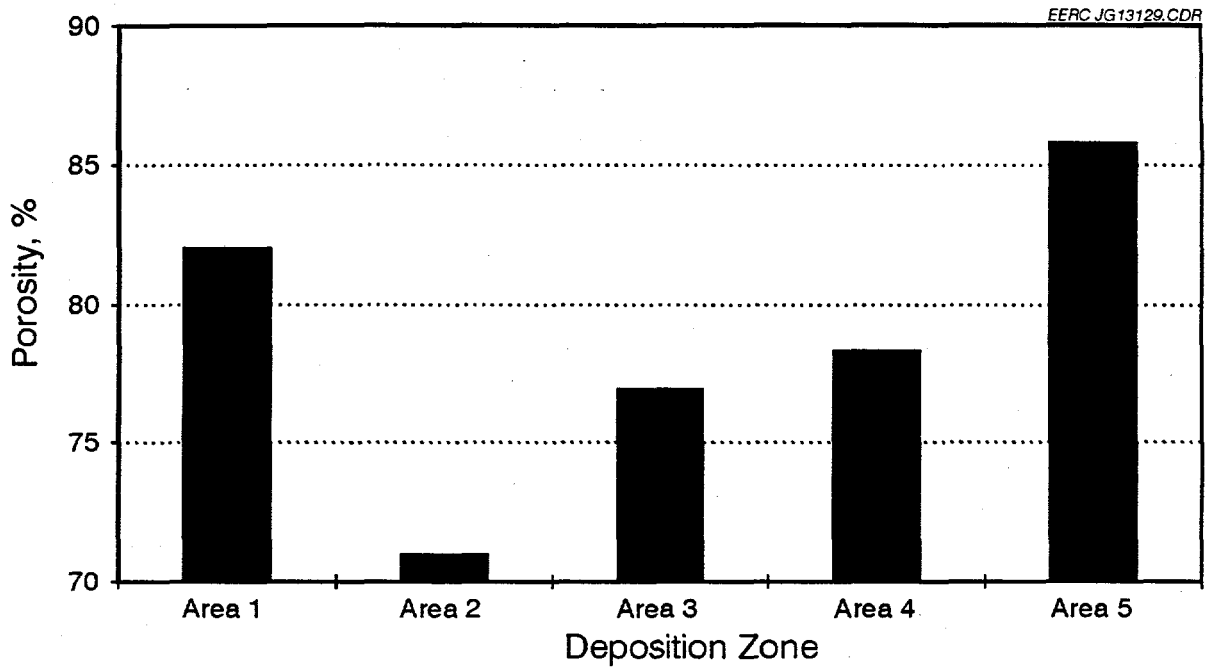

Figure 36. Porosity of upstream Black Thunder deposit sample.

determined using a hydraulic compression tester fitted with an electronic load cell and digital read out. All pellets were crushed at a ramp-loading rate of 0.02 in. per minute at room temperature.

Sintering Conditions. A simulated flue gas was formulated to serve as the sintering atmosphere for the strength development tests which consisted of 0.5% SO_2 (5000 ppm), 3% oxygen, 10%–15% H_2O, and the balance nitrogen. In earlier experiments performed at the EERC, it was determined that CO_2 was not a necessary component for laboratory sintering. Thermodynamic calculations and determinations of carbon dioxide fixation indicated that the fixation did not occur in the presence of SO_2. A gas flow rate of 1 liter/minute was used for all sintering conditions.

Strength Testing Results. Series of ash pellets were subjected to the simulated flue gas at 1850°F (1010°C) for durations of 8, 24, and 48 hours. Over the course of the strength development tests, the color of the ash pellets changed as described in Table 29. The color changes are most likely due to the oxidation of iron from the Fe^{2+} state which causes ash to appear black to the Fe^{3+} state which makes it appear more reddish.

Results of the compressive strength tests versus sintering time are given in Figure 37. The bar graph shows the average compressive strengths of from three to six ESP ash pellet samples for each of the five combustion runs. The average compressive strengths of the two Bailey/Antelope blends were the highest for all sintering times. The pellets derived from the parent coals developed

TABLE 29

Changes in Ash Pellet Color During Strength Testing

Run Number	AF-CTS-700L	AF-CTS-701L	AF-CTS-706L	AF-CTS-707L	AF-CTS-708L
Fuel	Black Thunder	Bailey	Antelope	Bailey/Antelope	Bailey/Antelope
Blend	100	100	100	35/65	65/35
Sintering Period, hr					
0	Tan	Yellow	Dark Gray	Tan	Light Gray
8	Light Tan	Light Brown	Brown	Tan	Light Brown
24	Light Tan	Light Brown	Rusty Brown	Rust	Dark Brown
48	Light Tan	Light Brown	Rusty Brown	Rust	Dark Brown

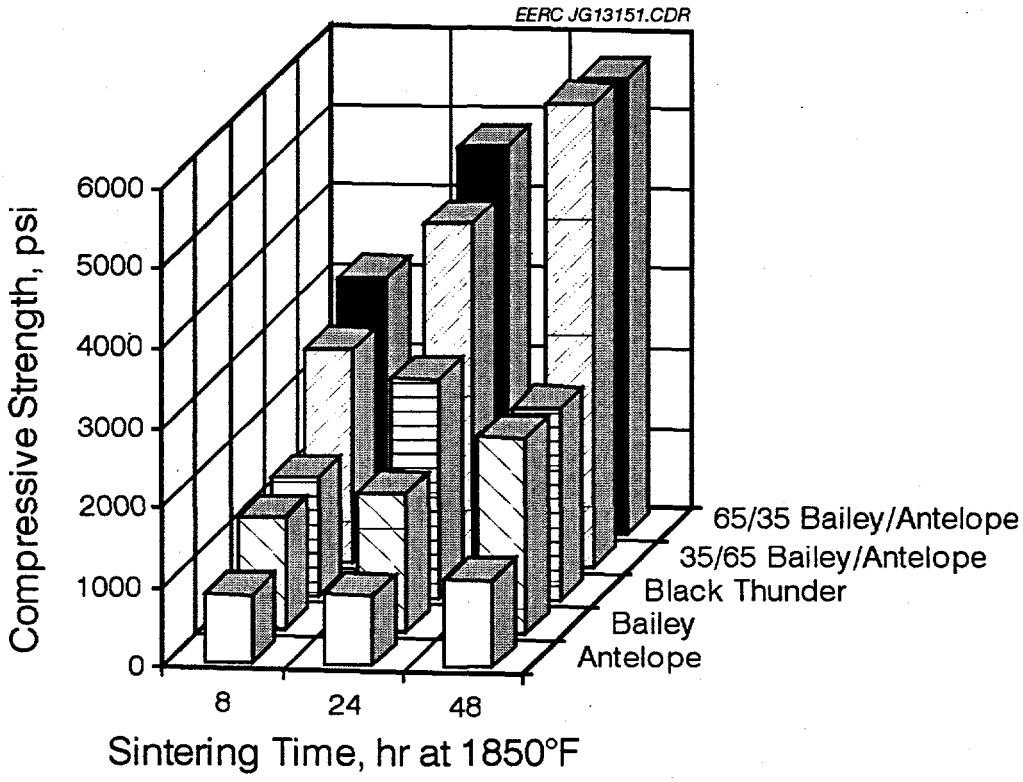

Figure 37. Results of compressive strength testing versus sintering time for ESP ash pellets sintered at 1850°F.

significantly less strength than those from the fuel blends. The lowest level of strength development was with the 100% Antelope ash. An earlier study produced similar results with the Antelope ash at the same sintering temperature with simulated flue gas containing 1000 ppm SO_2 (5). Black Thunder ash was also evaluated in the same study but instead produced compressive strengths less than those for Antelope.

Shedding index is an important parameter when determining the potential for an ash deposit to be removed from a fouled surface under its own weight or by some other means such as sootblowing. The shedding index is the ratio of the rate of deposition compared to the rate of strength development. Deposits which build more slowly tend to develop higher strengths. A high shedding index implies deposits will form quickly, but may shed under their own weight. A low shedding index implies that deposits will form slowly and develop more strength and, therefore, will be less likely to shed under their own weight. Figure 38 shows the shedding indexes at the 8-, 24-, and 48-hr strength development periods for upstream and downstream deposits from the 100% Bailey, 100% Antelope, and blends of the two coal sources. These figures generally show that blending Antelope subbituminous coal with Bailey bituminous coal up to the 65%/35% blend ratio does not appear to significantly affect the shedding index of either upstream or downstream deposits. The shedding index only increased significantly with the ash from combustion of the 100% Antelope fuel.

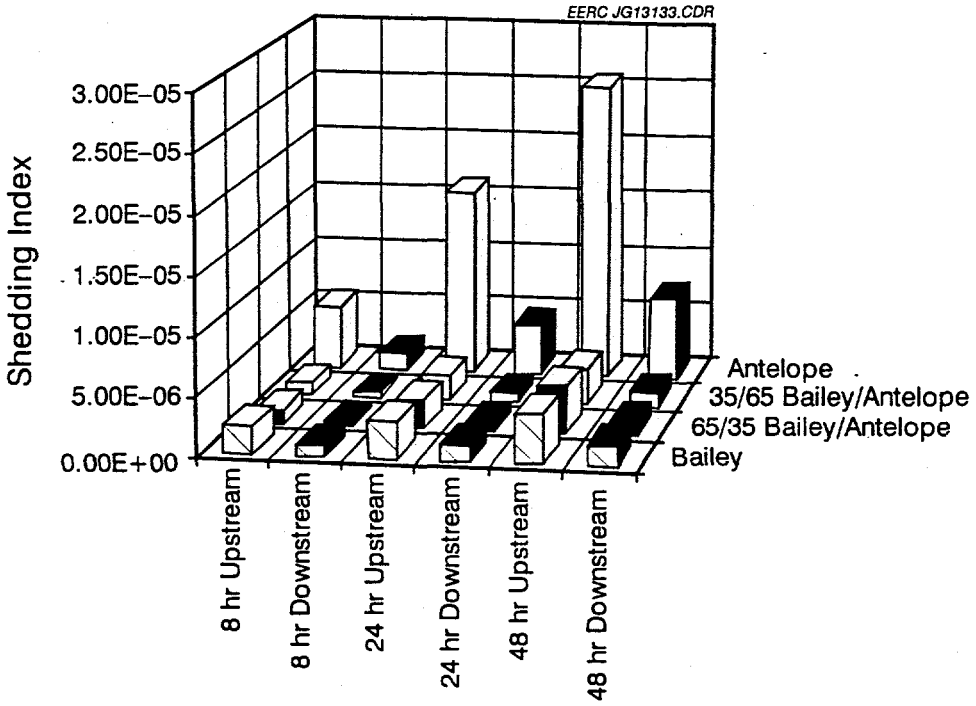

Figure 38. Shedding index of selected ash samples versus time for both upstream and downstream low-temperature fouling deposits.

Another series of strength development tests were also performed under the same sintering atmosphere as described above, but at a temperature of 1560°F (850°C). In addition, sintering times were set at 8, 24, and 96 hr. Generally, there was less strength development at the lower sintering temperature as shown in Figure 39. The ash samples from the Bailey/Antelope fuel blends still exhibited substantially higher strengths than the ash derived from the combustion of 100% Antelope. Shedding index results from the lower sintering temperature tests showed the same general trends as those from the high sintering temperature tests; i.e., there was no significant increases in shedding index with increasing ratios of Antelope in the fuel blends.

Chemical/Mineralogical Testing. Samples of three of the low-temperature sintering specimens mentioned above (100% Antelope and the two Bailey/Antelope blends) were further examined to identify the mineralogical associations between the particles. An XRD analysis was performed on a specimen from the strength development tests operated at the 24-hr sintering time frame. Results of the XRD analyses are summarized in Table 30.

The results do not indicate any substantial difference between the three test samples analyzed. Samples from the 100% Antelope ash exhibited severe cracking around the circumference of the pellet after sintering. Fractured portions of an Antelope pellet were further examined under XRD analysis. Fracture pieces were retrieved from outside and inside portions of the pellet. The significant difference between the two portions was the lack of the anhydrite as a major phase in the inside portion. The XRF analyses of the sintered pellets are presented in Figure 40. This figure shows that the trends are as expected based on analyses of the test fuels; i.e., as the ratio of Antelope increased, there was a corresponding decrease in SiO_2, Al_2O_3, and Fe_2O_3 and increasing contributions from CaO and SO_3.

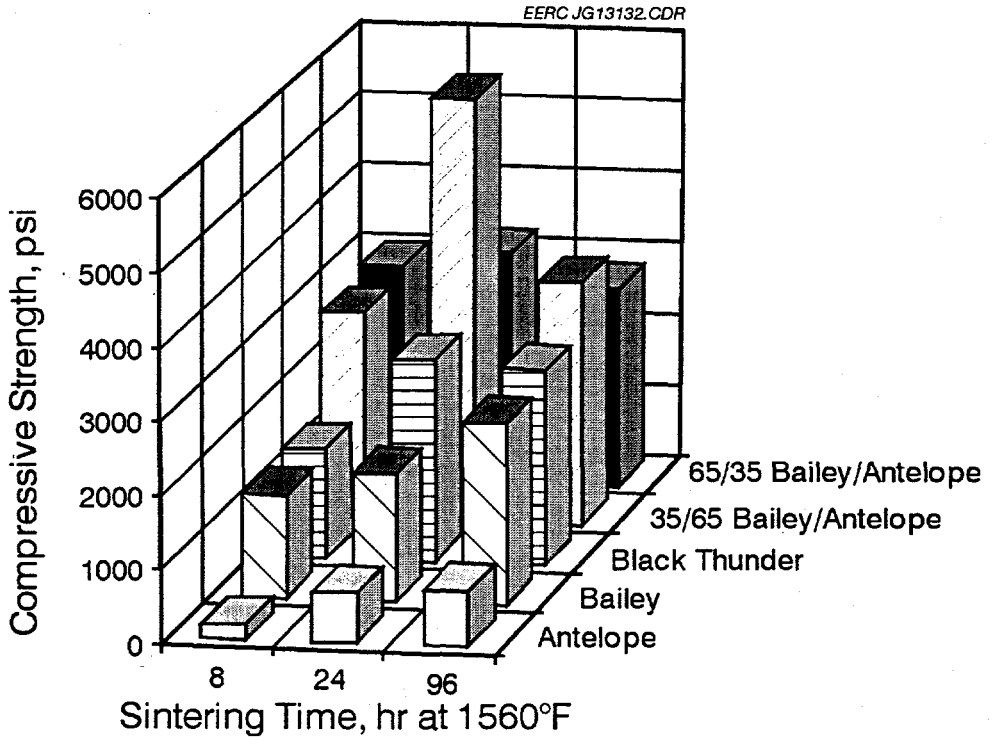

Figure 39. Results of compressive strength testing versus sintering time for ESP ash pellets sintered at 1560°F.

TABLE 30

Results of X-Ray Diffraction Analyses of Ash Specimens Sintered for 24 hr at 850°C

Run Number	AF-CTS-706L	AF-CTS-707L	AF-CTS-708L	AF-CTS-706L	
Fuel	Antelope	Bailey/Antelope	Bailey/Antelope	Antelope	
Blend	100	35/65	65/35	100	
Portion of Fractured Sample	---	---	---	Outside	Inside
Mineral Phases					
Quartz, SiO_2	---	Minor	---	Minor	---
Anhydrite, $CaSO_4$	Major	Major	Major	Major	Minor
Merwinite, $Ca_3Mg(SiO_4)_2$	---	---	---	Minor	Major
Hematite, Fe_2O_3	Minor	Minor	Minor	---	---
Maghemite, Fe_2O_3	----	---	---	Minor	Minor
Sodalite, $Na_2Al_3Si_3O_{12}Cl$	Minor	Minor	Minor	Minor	Minor
Clinopyroxene, $Ca(Fe,Mg,Al)Si_2O_6$	Minor	Minor	Minor	Minor	---
Plagioclase, $(Ca,Na)(Al,Si)_4O_8$	---	Minor	---	---	---
Melilite, $(Na,Ca)_2(Mg,Al)(Si,Al)_2O_7$	---	---	---	Major	Major

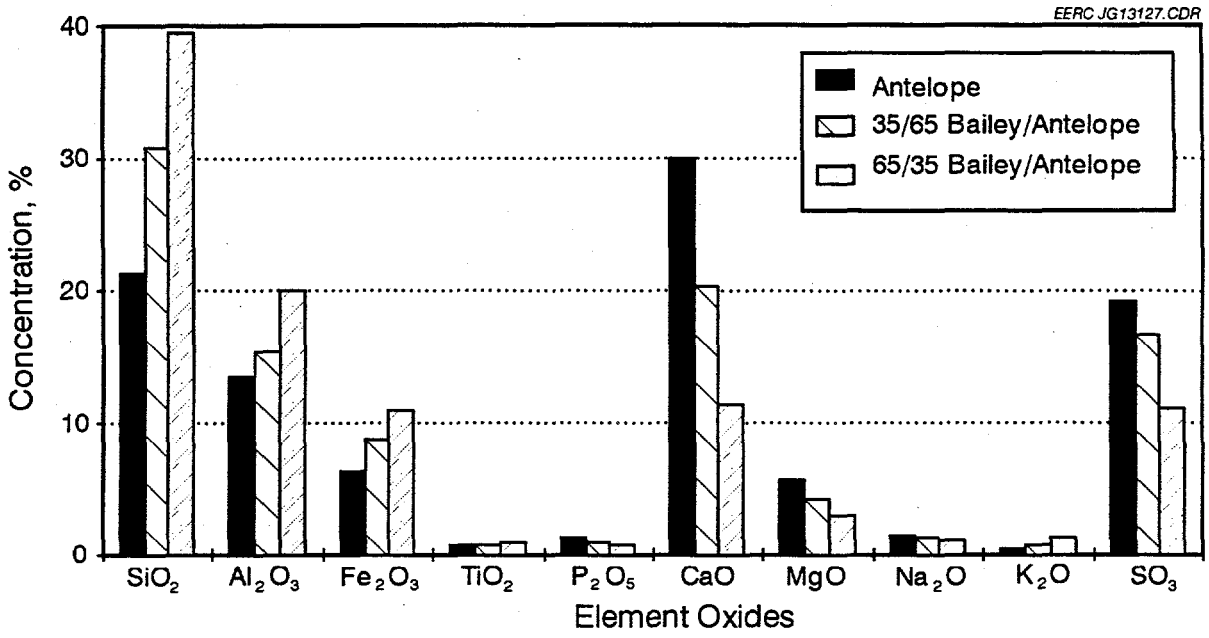

Figure 40. Results of XRF analyses performed on ash pellets sintered for 24 hr at 1560°F.

The cylindrically shaped pellets were placed upright in a rectangular crucible during sintering. After compressive testing, fractured pieces were evaluated by SEMPC to better assess the sintering process of the preformed samples. Comparative SEMPC analyses are given in Figures 41–45.

The sintering mechanism employed here is not the same as would be encountered inside an actual combustion system. In a combustion process, the ash particles would be sintering while being deposited. In the laboratory, the ash pellets are sintering from the outside inward. In general, areas of increased sintering are slightly enriched in calcium and highly enriched in sulfur as compared to the rest of the pellet. The calcium enrichment may be due to migration of calcium ions from the interior of local ash particles to the exterior of the particles where they sulfate or, more likely, migration of calcium ions from particle to particle until they are trapped in the sulfated areas. This would be indicated by a higher level of calcium in the outside areas of a sintered pellet.

Figures 41–45 indicate a slight contradiction to the general concepts stated above. However, it should be pointed out that all numerical representations were normalized with the SO_3 contribution included. An adjustment for the presence of SO_3 would produce trends more in line with the concept of calcium migration towards the outside portions of the sintered pellets. This is shown more clearly in the results of an SEMPC analysis of a circular cross section of the Antelope pellet (Figures 44 and 45). The presence of SO_3 increased significantly as the analysis progressed outward from the center of the sintered pellet.

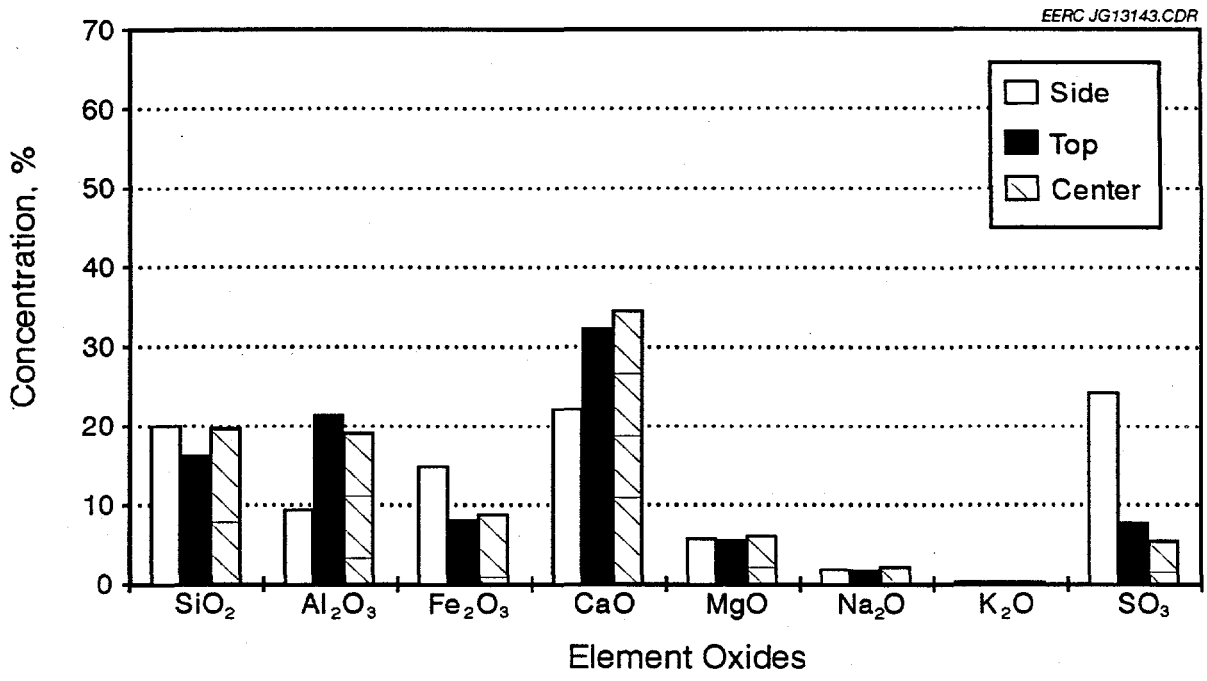

Figure 41. SEMPC analyses of fractured pellet pieces after compressive strength testing – 100% Antelope.

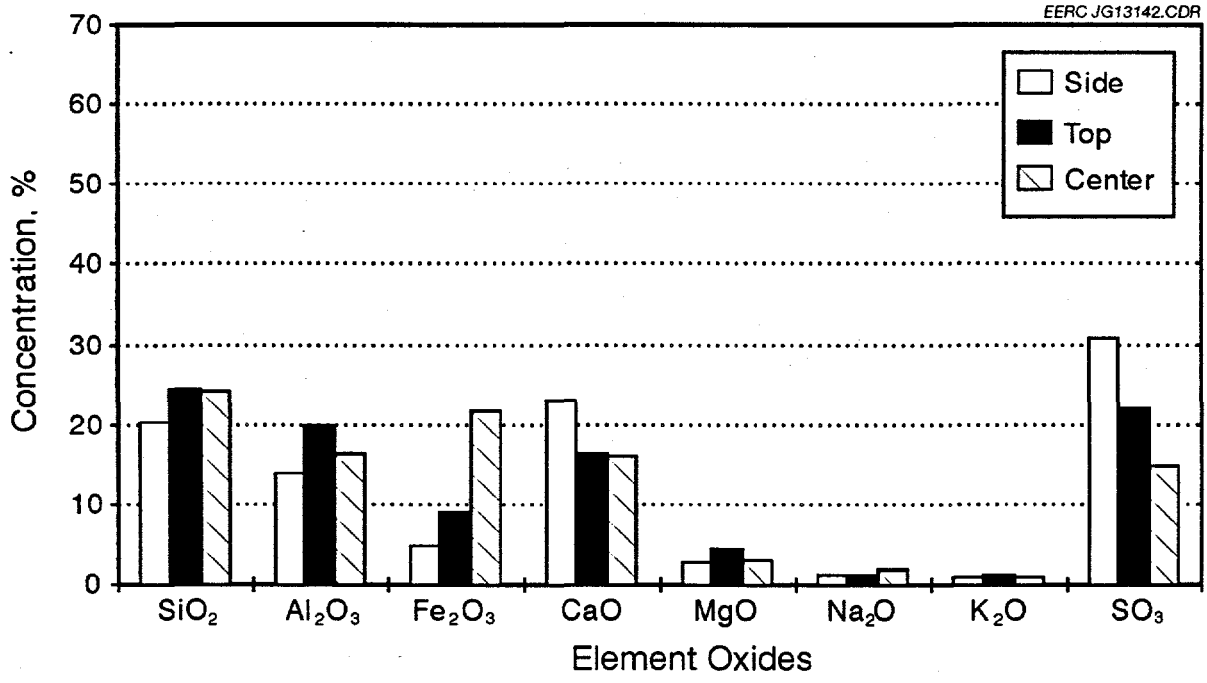

Figure 42. SEMPC analyses of fractured pellet pieces after compressive strength testing – 35%/65% Bailey/Antelope.

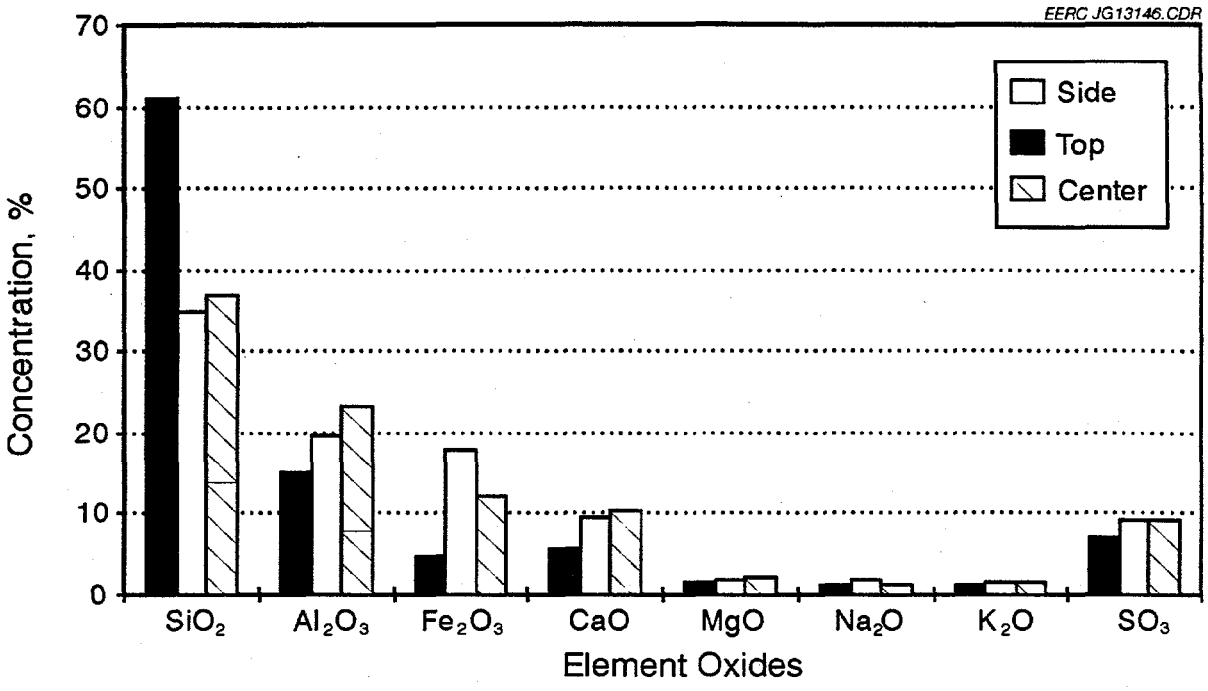

Figure 43. SEMPC analyses of fractured pellet pieces after compressive strength testing – 65%/35% Bailey/Antelope.

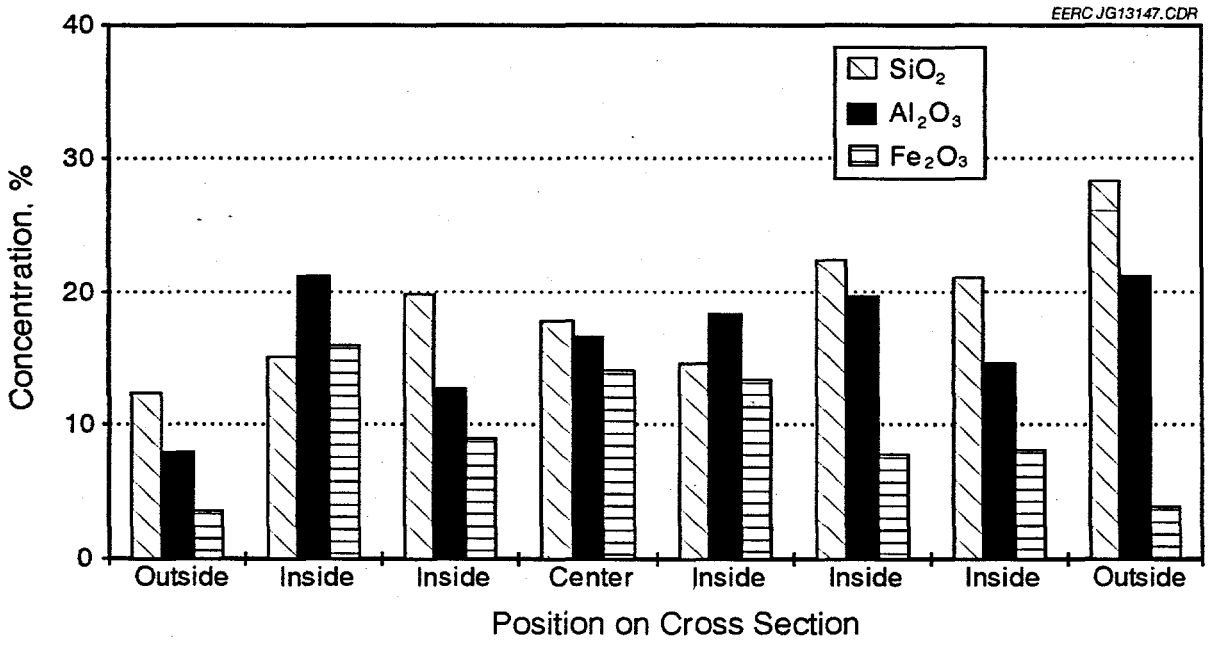

Figure 44. SEMPC analyses performed on a circular cross section of sintered pellet from 100% Antelope ash.

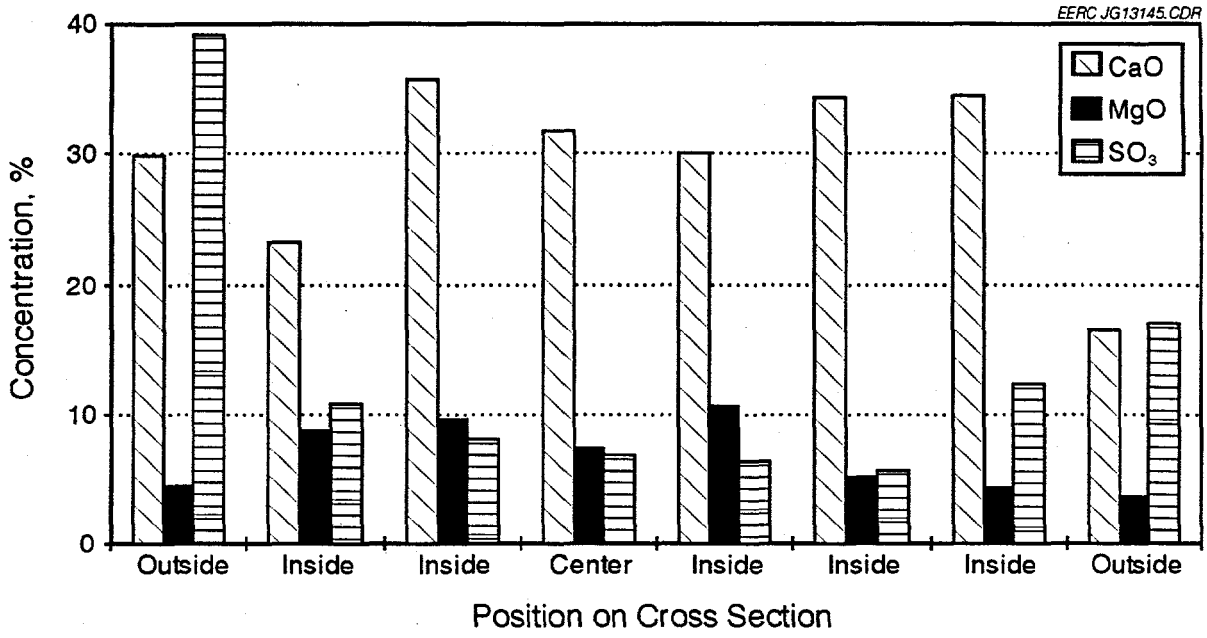

Figure 45. SEMPC analyses performed on a circular cross section of sintered pellet from 100% Antelope ash.

4.5 Flame Stability Tests

The EERC utilizes an adjustable swirl burner constructed to IFRF specifications in special combustion tests on the CTF to establish the relative flame stability characteristics of test fuels. The applicable theory, test equipment, and operating conditions are described in Appendix A. Flame stability tests were run independently of the tests described in earlier discussions.

During the present test program, flame stability tests were run on each of the fuels in two operating modes: simulated full load at approximately 600,000 Btu/hr and turndown conditions at 2/3 of full load or 400,000 Btu/hr. The tests were run at the following three secondary air swirl levels under each load condition: 1) repeatable swirl levels of 0.60 at full load and 0.75 at turndown, 2) the swirl representing the onset of flame separation from the burner quarl at each load level, and 3) the optimum swirl condition at each load. Performance of each fuel is evaluated in terms of the visual appearance of the flame, carbon burnout, furnace temperatures, and heat flux at each swirl condition.

Fuel properties for each of the flame stability test samples are summarized in Table 31. Comparisons of flame stability between fuels in a given boiler can be related to coal fineness and the relative levels of carbon and volatile matter (fixed carbon/volatile matter ratio, FC/VM) present in each fuel. Size analysis via dry sieve indicated a relatively narrow range of coal fineness between the fuels tested at 62.1% to 76.4% <200 mesh. As expected, the FC/VM ratio decreased

TABLE 31

Properties of Parent and Blend Fuel Test Samples – Flame Stability Testing

Fuel Description	Black Thunder		Bailey		Bailey/Black Thunder		Bailey/Black Thunder		Antelope		Bailey/Antelope		Bailey/Antelope	
Blend Ratio, wt%	100		100		35/65		65/35		100		35/65		35/65	
Test Designation	AF-CTS-700		AF-CTS-701		AF-CTS-702		AF-CTS-703		AF-CTS-706		AF-CTS-707		AF-CTS-708	
Sample Number(s)	93-1092		93-1103		93-1028, 1034		93-1040, 1046		94-0491		94-0004		94-0034	
Proximate Analysis, wt%	As-Fired	H_2O-Free	As-Fired	H_2O-Free	As-Fired	H_2O-Free	As-Fired	H_2O-Free	As-Fired	H_2O-Free	As-Fired	H_2O-Free	As-Fired	H_2O-Free
Moisture	24.90	---	2.50	---	15.90	---	9.85	---	24.60	---	17.00	---	10.10	---
Volatile Matter	34.87	46.43	37.21	38.16	36.33	43.20	36.65	40.65	34.36	45.57	35.29	42.52	36.09	40.14
Fixed Carbon	35.74	47.59	53.99	55.37	41.75	49.64	47.14	52.29	36.35	48.21	41.57	50.08	47.31	52.63
Ash	4.49	5.98	6.30	6.46	6.02	7.16	6.36	7.05	4.69	6.22	6.14	7.40	6.50	7.23
Ultimate Analysis, wt%														
Hydrogen	3.53	4.70	5.33	5.47	4.55	5.41	4.39	4.87	3.61	4.79	4.12	4.96	4.52	5.03
Carbon	52.42	69.80	75.88	77.83	62.34	74.13	68.34	75.81	52.17	69.19	60.15	72.47	67.84	75.46
Nitrogen	0.68	0.91	1.42	1.46	0.99	1.18	1.16	1.29	0.86	1.14	1.06	1.28	1.22	1.36
Sulfur	0.36	0.48	1.73	1.77	0.82	0.98	1.26	1.39	0.33	0.44	0.79	0.95	1.19	1.32
Oxygen	13.62	18.14	6.84	7.02	9.38	11.15	8.64	9.58	13.74	18.22	10.74	12.94	8.63	9.60
Ash	4.49	5.98	6.30	6.46	6.02	7.16	6.36	7.05	4.69	6.22	6.14	7.40	6.50	7.23
Moisture	24.90	---	2.50	---	15.90	---	9.85	---	24.60	---	17.00	---	10.10	---
Heating Value														
Btu/lb	9050	12,051	13,746	14,098	10,776	12,813	12,056	13,373	9011	11,951	10,725	12,922	12,019	13,369
mmmf	9475		14,670		11,466		12,875		9454		11,427		12,855	
Sulfur Input, lb/MMBtu	0.80		2.52		1.52		2.09		0.73		1.47		1.98	
Fixed Carbon/Volatile Matter	1.02		1.45		1.15		1.29		1.06		1.18		1.31	
Sieve Analysis, % < 200 mesh	63.76		76.82		71.17		75.52		67.77		72.11		74.58	

as the ratio of bituminous coal in the blends decreased, indicating the potential for better fuel ignitability, carbon conversion, and flame stability.

Flame stability test results for the parent fuels and test blends are given in Table 32. Swirl number is plotted versus carbon content of the fly ash for each of the parent fuels tested under full-load and turndown conditions in Figure 46. The data indicate that the subbituminous coals exhibit excellent carbon burnout at both full-load and turndown conditions over the entire range of swirl settings tested. Figure 46 also indicates that increasing swirl setting increases carbon burnout of the bituminous coal due to increased particle residence time in the furnace. Similar plots of the Bailey/Black Thunder blends and Bailey/Antelope blends at full-load conditions, along with the results of tests conducted with the parent coals are given in Figures 47 and 48, respectively. These graphs generally indicate that carbon burnout increases with increasing swirl setting and increasing percentage of subbituminous coal in the fuel blend. More specifically, comparing Figures 47 and 48 suggests that blending a bituminous coal, such as the Bailey, with the Black Thunder would produce better carbon conversion than with a similar Bailey/Antelope blend.

Overall, flame stability test results indicated that, relative to the Bailey bituminous coal, the blends of Bailey with the subbituminous coals studied here would not dramatically impact the ignitability and stability of the combustion flame. Each of the fuels tested provided stable combustion flames over a wide range of secondary air swirl. Carbon in ash evaluation indicated a trend toward lower ash carbon levels as the proportion of subbituminous coal in the blend was increased.

4.6 Stack Emissions and ESP Performance

Flue gas emissions of O_2, CO_2, and SO_2 were continuously monitored at the exit of the combustion system, while emissions of NO_x were measured at the furnace exit. The run-average concentration of these flue gas constituents are compared in Table 33. In general, SO_2 emissions reflect the input sulfur content of each fuel; however, there is a trend toward higher sulfur retention in ash with increased proportions of subbituminous coal. Emissions of SO_2 and NO_x for each of the parent coals and coal blends are also compared in Figures 49 (Bailey/Black Thunder) and 50 (Bailey/Antelope).

Of particular interest were the flue gas emissions of NO_x. For each blend system, NO_x levels decreased with increasing proportion of subbituminous coal in blends with the bituminous coal. Because the pilot plant burner and furnace geometry do not reflect typical geometries of full-scale design, the absolute values of the reported NO_x emissions for all fuels tested are most likely low in comparison to full-scale NO_x emissions. However, the relative differences between gas samples obtained in this furnace tend to reflect the effect of fuel properties and operating conditions on NO_x. Nitrogen oxide emissions were reduced from 248 ppm (0.348 lb/MMBtu) for the parent bituminous coal to 109 ppm (0.152 lb/MMBtu) and 125 ppm (0.174 lb/MMBtu) for the parent subbituminous coals.

A tubular-design pilot-scale ESP was used to collect particulate during each of the combustion tests. A summary of the performance data collected is provided in Table 34. No performance data were collected during testing of the 65/35 Bailey/Black Thunder test designated

TABLE 32

Summary of Flame Stability Test Results at Simulated Full Load

Test Number	AF-CTS-699 FS					AF-CTS-701 FS			AF-CTS-702 FS			AF-CTS-703 FS			AF-CTS-706 FS			AF-CTS-707 FS			AF-CTS-708 FS		
Date	11/05/93					01/25/94			11/19/93			11/19/93			01/27/94			01/24/94			01/27/94		
Fuel	Black Thunder					Bailey			Bailey/Black Thunder			Bailey/Black Thunder			Antelope			Bailey/Antelope			Bailey/Antelope		
Blend Ratio, %	100					100			35/65			65/35			100			35/65			65/35		
Visual Appearance of Flame	Onset of Separation		Optimum			Onset of Separation		Optimum	Onset of Separation		Optimum	Onset of Separation		Optimum	Onset of Separation		Optimum	Onset of Separation		Optimum	Onset of Separation		Optimum
Full Load																							
Time	840	1004	1035	1450	1535	955	1037	1107	1126	1159	1227	602	646	716	1443	1508	1536	912	950	1021	919	956	1028
Swirl Setting	0.6	0.22	0.855	0.5	0.5	0.6	0.29	0.39	0.6	0.21	0.46	0.6	0	0.54	0.6	0.23	0.5	0.6	0.25	0.63	0.6	0.21	0.39
Sample Number	93-1068	93-1069	93-1070	93-1076	93-1077	94-0191	94-0192	94-0193	93-1086	93-1087	93-1088	93-1079	93-1080	93-1081	94-0202	94-0203	94-0204	94-0184	94-0185	94-0186	94-0209	94-0210	94-0211
Carbon in Ash, %	0.25	0.15	0.09	0.16	0.06	1.96	7.48	4.48	0.75	1.93	1.33	2.33	2.16	2.14	0.6	0.46	0.21	0.56	2.54	0.78	1.63	5.22	3.92
Fuel Feed Rate, lb/hr	75	75	75	75	75	48.86	49	48.31	62.8	62.8	62.8	55.3	55.3	55.3	77.28	77.09	76.87	63.72	63.44	63.33	7.06	56.1	56.08
Heat Input, Btu/hr	676,125	676,125	676,125	676,125	676,125	668,893	670,810	661,364	748,702	748,702	748,702	669,683	669,683	669,683	693,820	692,114	690,139	677,344	674,367	673,198	685,861	675,430	674,082
FEGT, °F	2182	2224	2197	2062	2135	2169	2195	2192	2124	2186	2149	2174	2214	2184	2148	2190	2175	2172	2221	2202	2159	2190	2174
Furnace HVT Temp., °F	2265	n.a.	2390	2335	2380	2320	2330	2335	2295	2355	2345	2285	2390	2275	2325	2360	2410	2325	2310	2360	2300	2265	2295
Furnace Wall Heat Flux, Btu/ft²/hr	53,430	54,420	47,120	45,810	51,830	52,190	52,610	51,110	45,850	48,820	48,600	50,550	48,430	48,360	52,630	51,120	52,400	59,000	60,000	57,500	68,000	69,000	69,000
Primary Air Flow, scfm	17.13	17.01	17.1	17.3	16.81	16.95	17.04	17.04	16.15	16.36	16.27	16.38	16.86	16.98	15.95	16.33	16.51	15.92	15.94	15.99	16.51	16.59	16.63
Secondary Air Flow, scfm	118.39	120.33	116.97	118.38	112.3	105.52	105.16	105.3	114.95	112.34	113.95	114.01	112.21	110.79	113.12	116.45	111.83	106.46	108.47	105.52	109.24	110.11	105.43
Flue Gas Composition																							
O_2, %, dry	3.61	4.02	3.67	4.25	4.01	3.52	3.57	3.92	3.97	3.92	3.96	3.67	4.12	3.97	3.11	3.75	3.76	3.56	3.95	3.58	2.89	3.17	3.04
CO_2, %, dry	15.45	14.94	15.52	14.83	15.39	14.95	14.98	14.48	15.12	15.35	15.24	14.75	14.53	14.74	15.84	15.28	15.31	15.39	15.02	15.33	15.28	15.49	15.79
SO_2, ppm	275	303	300	221	289	1211	1207	1183	658	750	712	799	977	987	373	365	346	730	719	721	1018	984	1010
Corrected to 3.55% O_2	276	311	302	230	297	1209	1208	1208	669	762	727	803	1010	1011	363	369	350	730	737	722	981	963	981
NO_x, ppm	565	359	616	429	331	367	320	333	537	456	472	488	402	380	426	238	357	216	142	85	327	279	268
Corrected to 3.55% O_2	567	368	620	447	340	367	320	341	550	465	483	491	416	389	416	241	362	216	145	85	316	274	260
Excess Air, %	20.6	23.5	21.01	25.18	23.42	19.7	20.04	22.46	22.96	22.61	22.89	20.81	23.99	22.91	17.14	21.44	21.51	20.02	22.72	20.15	15.63	17.41	16.58
Turndown																							
Time	1235	1305	1335	1400		1221	1302	1337	1258	1330	1403	922	945	1004	1621	1653	1718	1121	1147	1211	1133	1201	1228
Swirl Setting	0.75	0.365	0.62	0.5		0.75	0.29	0.55	0.75	0.33	0.6	0.75	0.35	0.9	0.75	0.36	0.67	0.75	0.48	0.81	0.75	0.32	0.67
Sample Number	93-1072	93-1073	93-1074	93-1075		94-0194	94-0195	94-0196	93-1089	93-1090	93-1091	93-1082	93-1083	93-1084	94-0205	94-0206	94-0207	94-0187	94-0188	94-0189	94-0212	94-0213	94-0214
Carbon in Ash, %	0.2	0.23	0.34	0.14		0.14	6.5	9.9	1.06	2.36	2.5	12.02	3.28	6.54	0.14	0.24	0.11	1.38	1.72	1.7	5.82	4.91	4.76
Fuel Feed Rate, lb/hr	50	50	50	50		32.99	32.87	32.82	41.83	41.83	41.83	36.9	36.9	36.9	50.69	50.53	50.58	42.12	42.14	42.06	36.3	36.97	36.23
Heat Input, Btu/hr	540,750	450,750	450,750	450,750		451,633	449,990	449,306	498,697	498,697	498,697	446,859	446,859	446,859	455,095	453,658	454,107	447,736	447,948	447,098	436,326	444,379	435,485
FEGT, °F	2132	2055	1996	2000		2078	2059	2005	2100	2096	2022	2022	2034	2005	2084	2085	2026	2098	2106	2048	2062	2040	2002
Furnace HVT Temp., °F	2135	2190	2110	2090		2115	2135	2100	2190	2390	2105	2095	2230	2124	2252	2230	2190	2280	2250	2180	2110	2130	2080
Furnace Wall Heat Flux, Btu/ft²/hr	34,770	41,210	36,340	38,040		38,360	36,420	34,110	41,410	38,440	35,260	33,430	36,280	35,360	41,300	38,770	36,820	56,000	56,000	55,000	70,000	55,000	56,000
Primary Air Flow, scfm	16.74	17.19	17.23	16.76		17.08	16.77	16.68	16.89	16.93	16.85	16.88	16.94	16.9	15.8	15.8	15.74	15.98	15.99	15.96	17.24	16.86	16.96
Secondary Air Flow, scfm	68	67.51	67.35	67.9		50.76	51.82	51.23	57.79	52.82	57.29	60.78	61.18	59.03	63.27	64.5	61.24	51.32	51.46	52.24	51.14	53.4	51.37
Flue Gas Composition																							
O_2, %, dry	3.83	3.45	3.65	3.84		2.95	3.62	3.44	4.07	3.3	3.58	3.49	3.89	2.86	3.14	3.65	3.82	3.42	3.52	3.51	3.4	3.8	3.59
CO_2, %, dry	15.08	14.93	15.11	15.04		15.21	14.73	14.85	15.31	16.12	15.89	14.99	14.67	15.73	15.89	15.43	14.97	15.22	15.03	15.19	15.37	15.4	15.83
SO_2, ppm	264	226	209	185		1224	1180	1185	737	781	741	980	970	1031	300	311	258	695	715	701	942	906	939
Corrected to 3.55% O_2	268	225	211	188		1183	1185	1178	760	770	742	976	989	992	293	313	262	690	714	699	934	919	942
NO_x, ppm	411	269	278	358		403	269	184	535	472	461	380	485	327	276	188	236	—	—	—	321	246	246
Corrected to 3.55% O_2	418	268	280	364		389	271	183	552	465	462	379	495	315	241	190	239	—	—	—	319	250	247
Excess Air, %	22.13	19.5	20.87	22.21		15.98	20.38	19.16	23.68	18.36	20.24	19.59	22.35	15.49	17.33	20.75	21.93	19.08	19.75	19.68	18.92	21.65	20.2

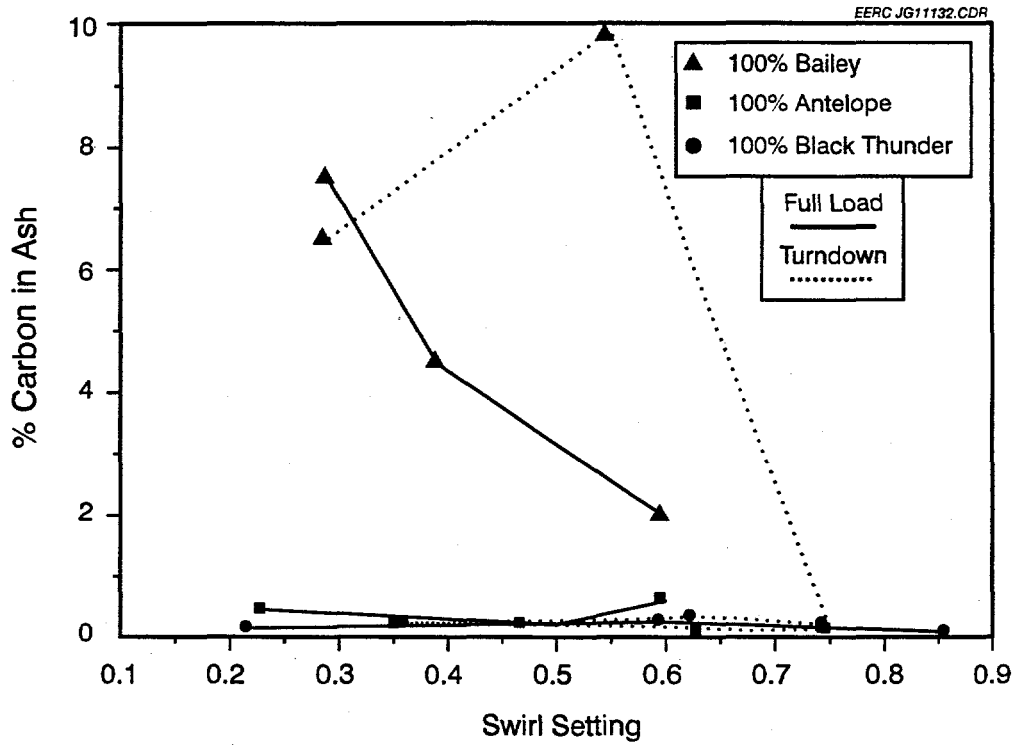

Figure 46. Burner swirl versus % carbon in ash for each parent fuel at full-load and turndown conditions.

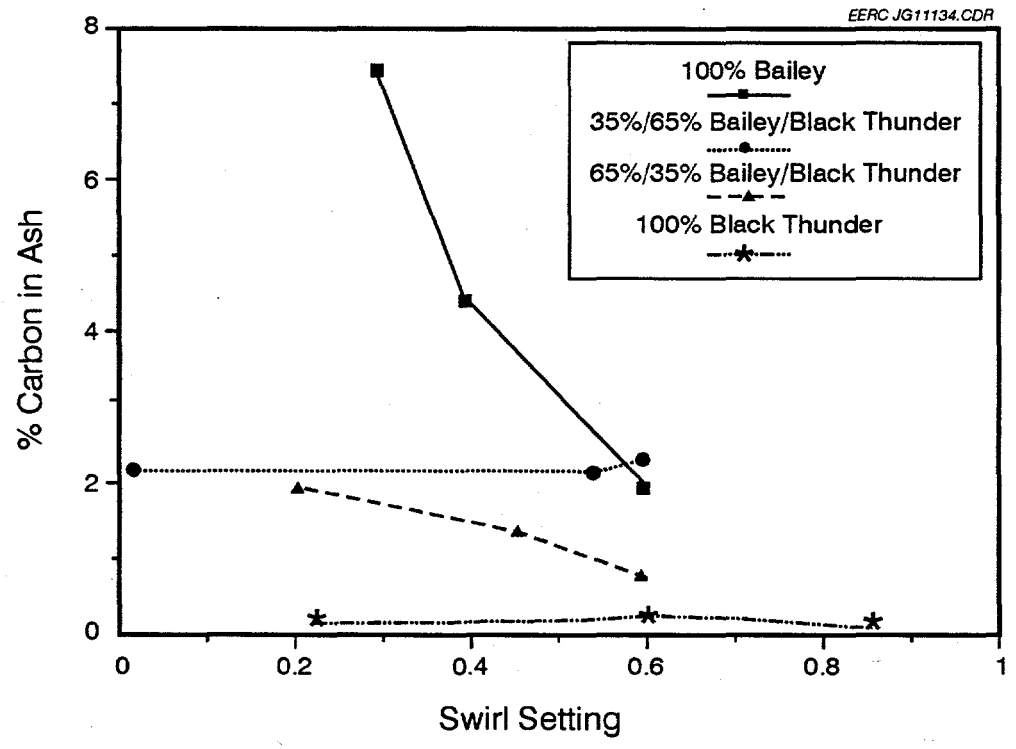

Figure 47. Burner swirl versus % carbon in ash for the Bailey/Black Thunder fuel blends at full-load conditions.

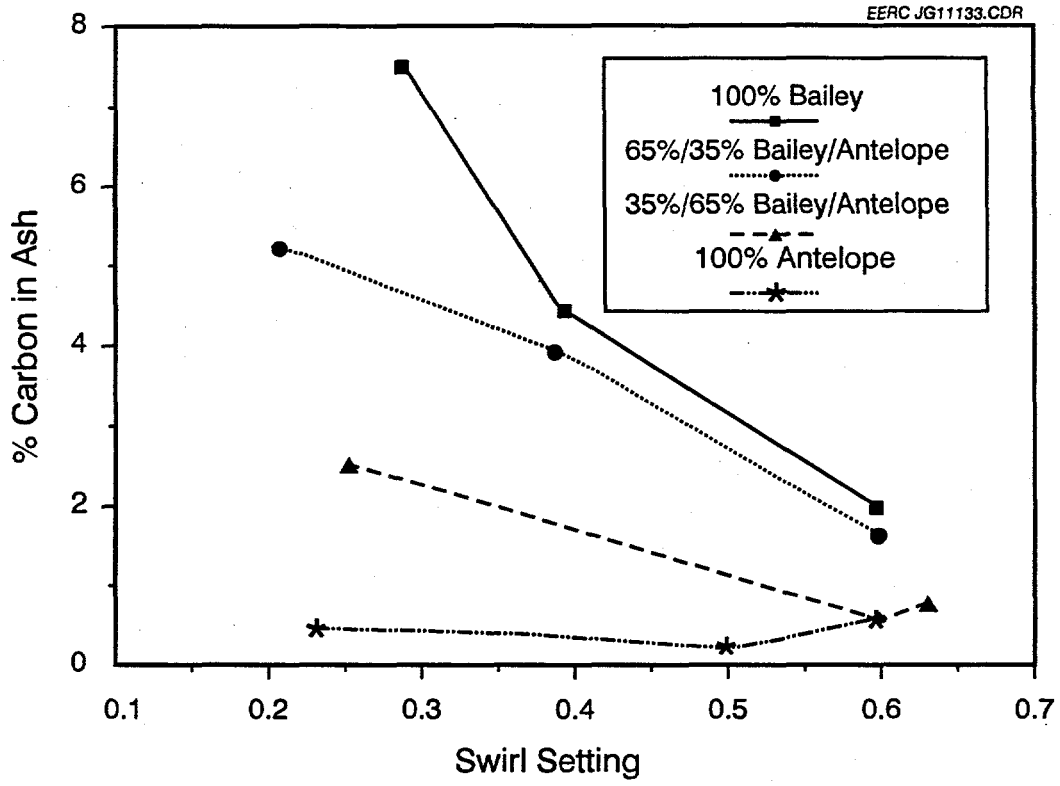

Figure 48. Burner swirl versus % carbon in ash for the Bailey/Antelope fuel blends at full-load conditions.

as AF-CTS-703. Comparable pilot ESP performance was reported for the majority of the fuels tested. The lowest collection efficiencies were reported for the parent Black Thunder subbituminous coal and the parent Bailey bituminous coal. However, these tests also indicated the lowest average power input (56 kV for Black Thunder and 55 kV for Bailey). These restrictions on power input were not imposed by fly ash or flue gas properties, but most likely resulted from operational or equipment limitations during these tests. The ESP operating voltage was maintained near 60 kV for all other tests. Testing of the Antelope subbituminous and the Bailey/Antelope blends indicated a trend toward slightly decreased collection efficiency as the proportion of subbituminous coal in the blend was increased.

Fly ash resistivities for each of the parent fuels and blends were determined by laboratory techniques. The equipment utilized is shown schematically in Figure 51. As configured here, the system can provide a measurement atmosphere in the resistivity oven containing levels of O_2, CO_2 and moisture equivalent to those found in the actual flue gas. However, since this apparatus was originally designed to study resistivity of fly ash from low-sulfur subbituminous coals and lignites from the western United States, no provision has been made to provide low levels of SO_3 to simulate flue gas from higher-sulfur, low-alkali-content bituminous coals from midwestern and eastern United States mines. Fly ash resistivities were also calculated using the Bickelhaupt resistivity model (6), which takes into account expected concentrations of SO_3 in the flue gas.

TABLE 33

Gaseous and Particulate Emissions

Run Number	AF-CTS-700		AF-CTS-701		AF-CTS-702		AF-CTS-703		AF-CTS-706		AF-CTS-707		AF-CTS-708	
Fuel Description	Black Thunder		Bailey		Bailey/Black Thunder		Bailey/Black Thunder		Antelope		Bailey/Antelope		Bailey/Antelope	
Blend Ratio, wt%	100		100		35/65		65/35		100		35/65		65/35	
Date	11/9/93		11/11/93		11/15/93		11/15/93		12/16/93		12/20/93		12/22/93	
Test Designation	A	B	A	B	A	B	A	B	A	B	A	B	A	B
FEGT, °F	2209	2015	2214	2007	2215	2017	2216	2013	2192	2006	2190	2009	2204	2004
Heat Input, Btu/hr	672,165	493,923	627,655	458,982	665,587	449,062	627,047	440,817	696,404	509,010	690,792	472,104	661,045	471,122
Excess Air, %	19.85	23006	19.76	20.30	21.03	20.61	22.59	21.41	19.43	21.14	19.88	21.32	20.38	21.41
SO_2 Input, lb/MMBtu	0.80		2.52		1.52		2.09		0.73		1.47		1.98	
Flue Gas Analysis, System Exit														
O_2, dry %	5.25	5.13	4.65	4.81	5.30	5.27	5.08	4.96	4.65	5.72	5.06	5.72	4.95	4.97
CO_2, dry %	13.16	14.50	14.94	15.04	14.67	14.89	15.08	14.38	14.84	14.00	15.23	14.01	14.90	14.64
SO_2 Emissions														
SO_2, dry ppm	209	219	1022	1059	638	595	812	826	260	171	586	517	862	824
Calc. @ 3.55% O_2	232	241	1091	1198	710	660	891	899	277	195	641	590	937	897
SO_2, lb/MMBtu	0.450	0.467	2.133	2.342	1.435	1.334	1.747	1.763	0.538	0.379	1.235	1.137	1.838	1.760
Apparent SO_2 Retention, %	43.48	41.28	15.26	6.95	5.68	12.32	16.43	15.68	26.55	48.29	16.15	22.82	7.18	11.14
NO_x Emissions, Furnace Exit														
NO_x, dry ppm	110	101	248	126	215	193	218	155	125	155	174	192	235	129
Calc. @ 3.55% O_2	109	104	248	127	200	194	222	156	125	156	173	194	236	130
NO_x lb/MMBtu	0.152	0.145	0.348	0.177	0.291	0.282	0.313	0.220	0.174	0.218	0.240	0.269	0.333	0.183
Particulate Emissions														
Grains/scf	0.0101		0.0065		0.0058		---		0.0042		0.0082		0.0048	
lb/MMBtu	0.0366		0.0327		0.0218		---		0.0106		0.0179		0.0140	

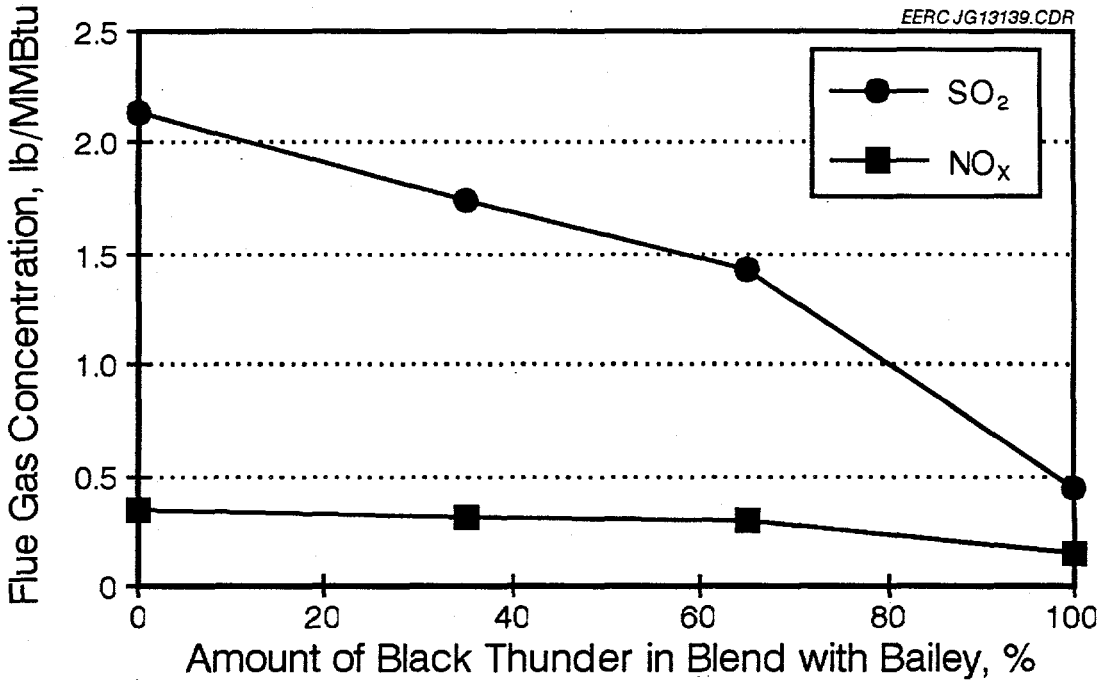

Figure 49. Flue gas emissions of sulfur dioxide and nitrogen oxides, Bailey/Black Thunder system, 2200°F FEGT.

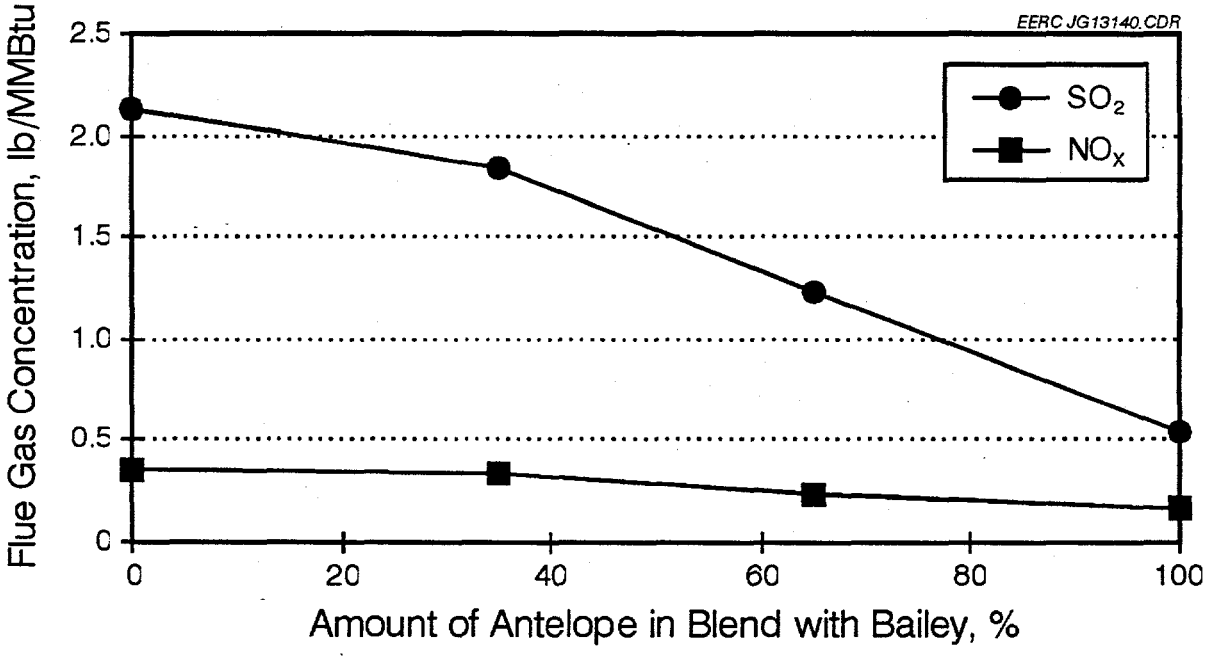

Figure 50. Flue gas emissions of sulfur dioxide and nitrogen oxides, Bailey/Antelope system, 2200°F FEGT.

TABLE 34

ESP Performance Testing

Run Number	AF-CTS-700	AF-CTS-701	AF-CTS-702	AF-CTS-706	AF-CTS-707	AF-CTS-708
Fuel Description	Black Thunder	Bailey	Bailey/Black Thunder	Antelope	Bailey/Antelope	Bailey/Antelope
Blend Ratio, wt%	100	100	35/65	100	35/65	65/35
Date	11/9/93	11/11/93	11/15/93	12/16/93	12/20/93	12/22/93
ESP Inlet						
Temperature, °F	315	371	349	383	319	333
Flue Gas Moisture, vol%	10.20	6.50	8.70	9.50	7.70	7.40
Dust Loading, grains/scf	1.007	0.5712	1.0142	0.7811	1.7279	1.2122
ESP Outlet						
Temperature, °F	291	272	299	306	284	284
Flue Gas Moisture, vol%	10.00	6.90	8.40	10.20	8.10	7.40
Dust Loading, grains/scf	0.0101	0.0065	0.0058	0.0042	0.0082	0.0048
ESP Voltage, kV	56	55	60	61	60	60
Corona Current, mA	0.21	0.19	0.24	0.28	0.26	0.24
Flue Gas Flow Rate, acfm	113	85	94	87	76	63
Gas Velocity, ft/sec	4.24	3.36	3.48	6.06	5.83	4.35
Collection Efficiency, %	99.00	98.86	99.43	99.46	99.53	99.60

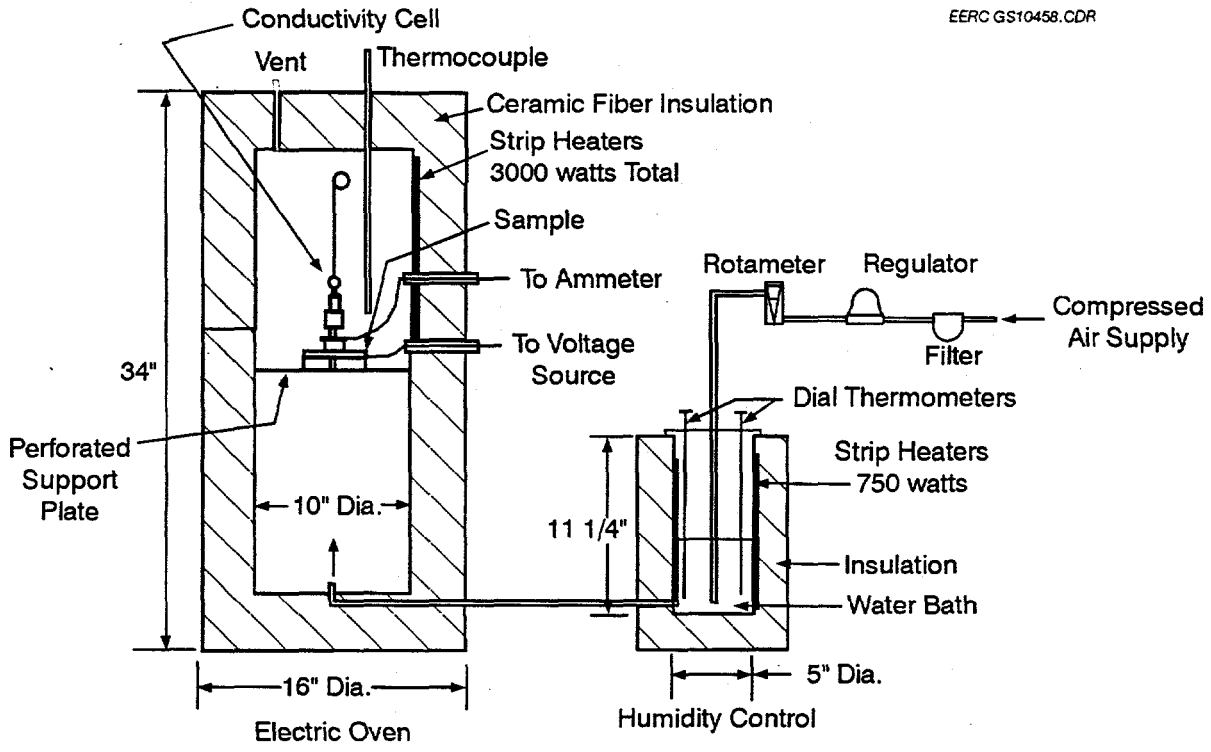

Figure 51. Schematic depicting the equipment utilized for fly ash resistivity testing.

The fly ash resistivities for the three parent coals predicted by the Bickelhaupt model are graphically compared in Figure 52. When flue gas SO_3 contents are taken into consideration, as was the case for the data shown in Figure 52, fly ash resistivity for the higher-sulfur Bailey bituminous coal shows lower resistivity values than the subbituminous coals. The Antelope ash indicates a lower resistivity than that from the Black Thunder, most likely reflecting the higher sodium content of the Antelope hopper ash as show in Table 23. Laboratory resistivity results for pilot ESP hopper ash for the three parent coals are plotted against temperature in Figure 53. While the trend in fly ash resistivity for the subbituminous coals is similar to that in Figure 52, again reflecting the difference in sodium content, the measured resistivity for the Bailey sample is higher than that for either of the subbituminous coals. In this particular instance, the difference in the relationship between predicted and measured fly ash resistivity for these coals likely provides a clue concerning the relative impact of SO_3 conditioning. In Figure 54, the predicted value for the value for the Bailey fly ash with available SO_3 is replaced by the corresponding curve without SO_3 present. This tends to suggest that the trends shown in Figure 53 could be reasonable.

In most respects, the preceding discussion mirrors the phenomena which occur when high-alkali subbituminous coals are blended with higher-sulfur bituminous coals. The presence of very fine and highly reactive alkali particles originating from the subbituminous coals in the furnace results in the effective elimination of the SO_3 contribution from the bituminous coal, leading to fly ash resistivities which are elevated for intermediate blend ratios. This phenomenon was reported in at least one instance involving a marginally sized ESP at a full-scale utility boiler, with acceptable performance on either parent fuel alone, but degraded performance, reflected by opacity values, at

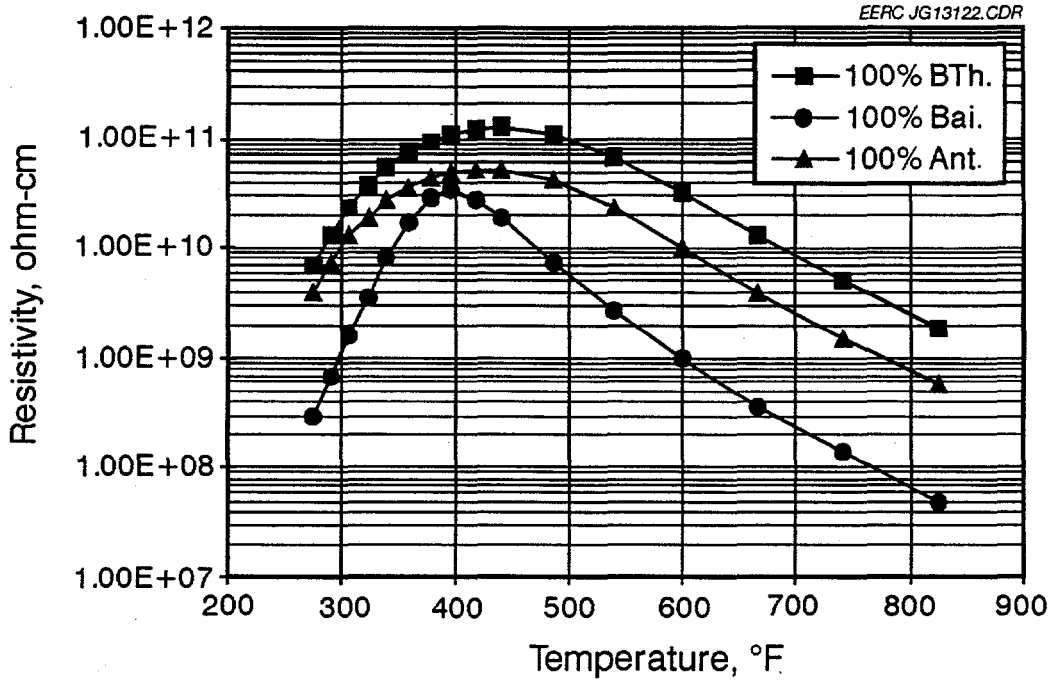

Figure 52. Predicted fly ash resistivities of the parent fuels by the Bickelhaupt model.

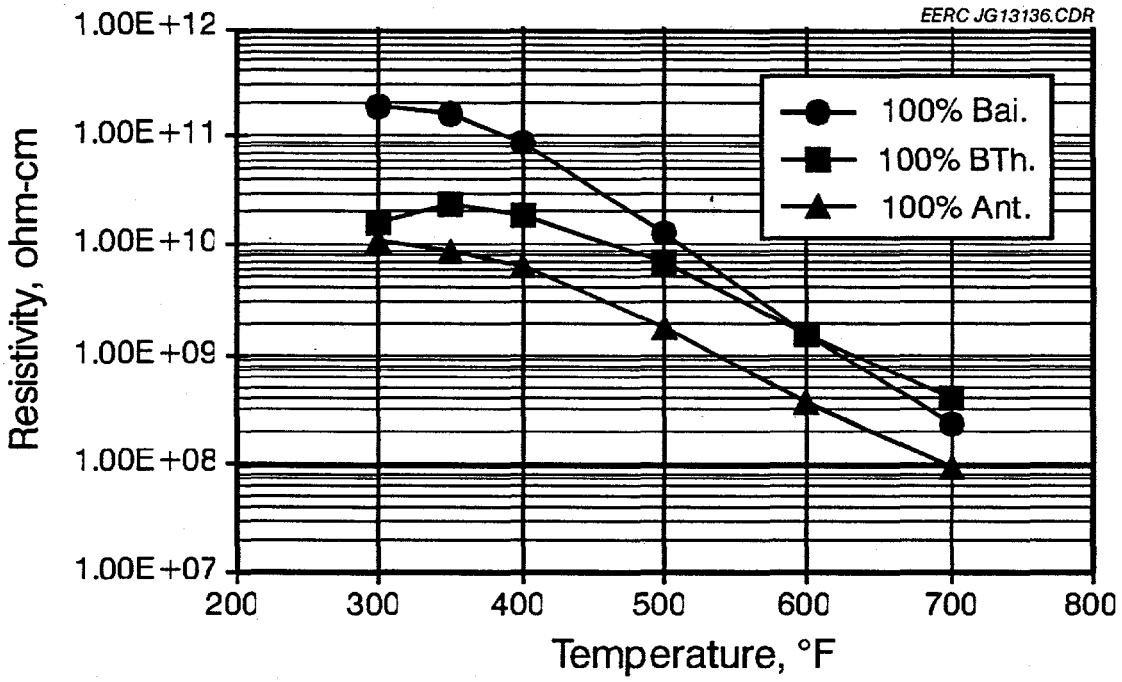

Figure 53. Laboratory resistivity results for EERC pilot plant ESP hopper ash for the three parent fuels.

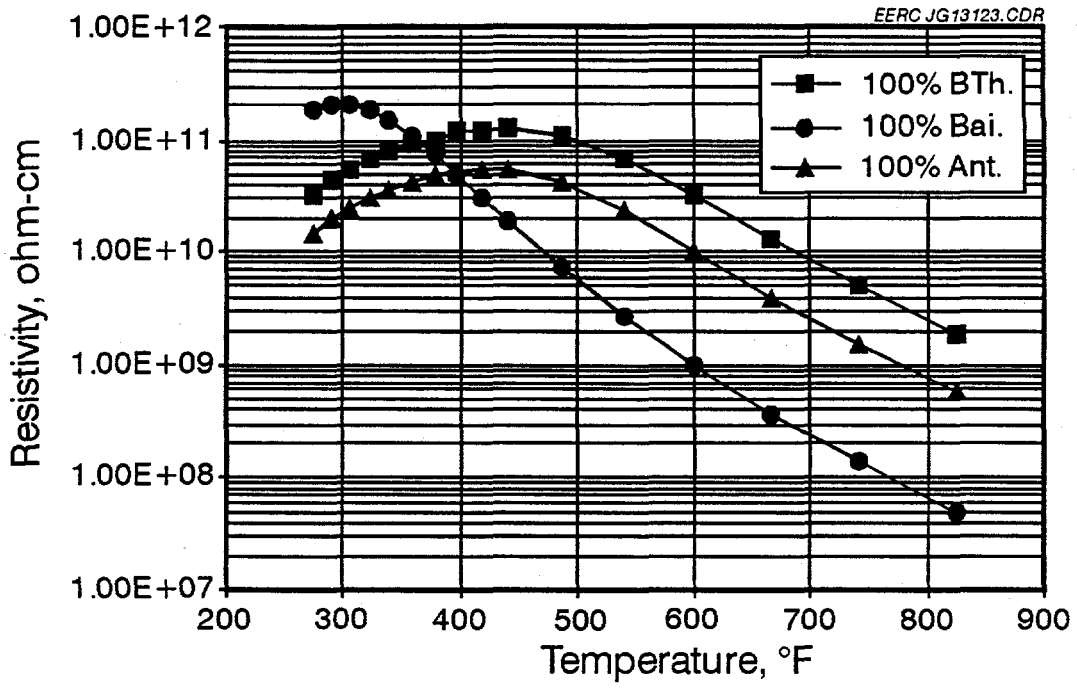

Figure 54. Predicted fly ash resistivities of the parent fuels by the Bickelhaupt model without SO_3 present for the Bailey fly ash.

intermediate blend ratios (7). Most instances reported by those testing blends of western subbituminous coals with midwestern and eastern bituminous coals in utility boilers have indicated results consistent with those suggested by both the pilot ESP and resistivity results reported here (1).

The predicted resistivity values for fly ash from blends of Bailey and Black Thunder coals are presented in Figure 55, with the corresponding results of laboratory measurements plotted in Figure 56. Similar data for blends of Antelope with Bailey are provided in Figures 57 and 58. In both cases, the predicted blend fly ash resistivities at lower temperatures are higher than the Bailey alone. An explanation for these results would take into account the differences in the resistivity-lowering components of the fly ash/flue gas systems involved. The higher sulfur content of the bituminous coal results in a proportional level of SO_3, possibly as high as 12 ppm, which serves as a conditioning agent to reduce fly ash resistivity at lower temperatures (8). On the other hand, research has shown that fly ash resistivity for western subbituminous coals is reduced as the sodium content of the fly ash increases (9). When the two systems are blended, the potential for lowering fly ash resistivity of each of the two mechanisms is counteracted by the other. At intermediate blends, the finely divided high-alkali components of the subbituminous coal combine with the SO_3 from the bituminous coal, thereby making it unavailable to serve as a natural conditioning agent. At the same time, at these intermediate blends, the quantity of sodium contributed by the subbituminous coal may not be sufficient to adequately lower the resistivity of the combined fly ash. Therefore, the laboratory resistivity curves shown in Figures 56 and 58 likely represent the relationship between the blend fly ashes and the parent subbituminous coals.

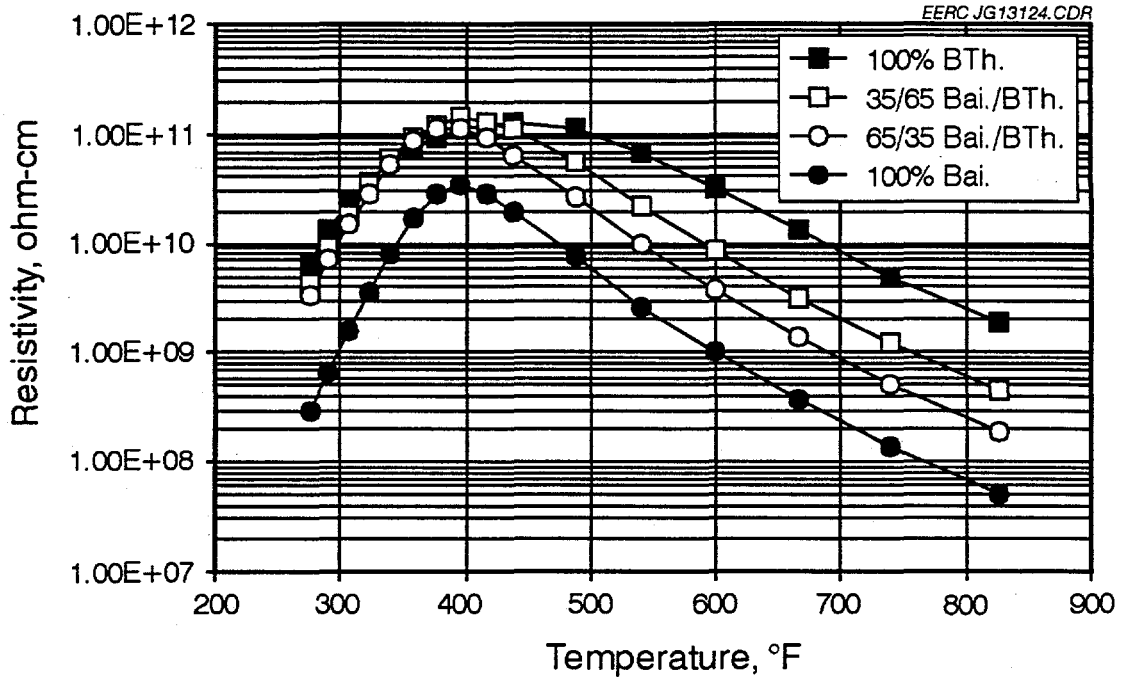

Figure 55. Predicted fly ash resistivities of the Bailey/Black Thunder blend system by the Bickelhaupt model.

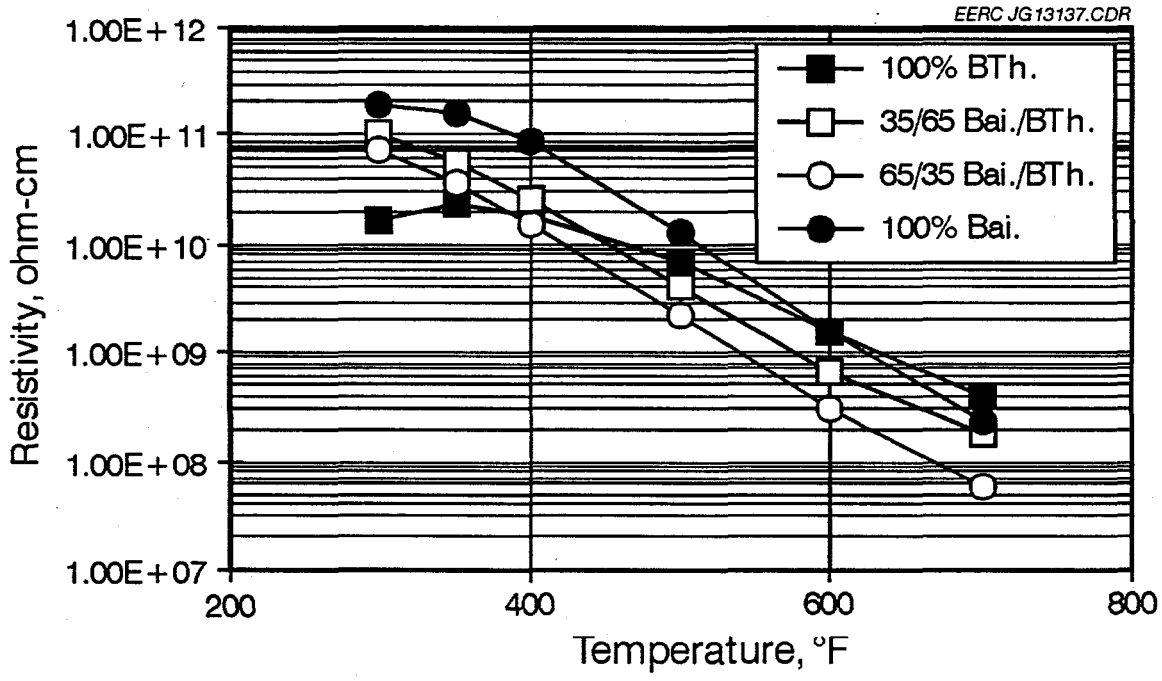

Figure 56. Laboratory resistivity results for EERC pilot plant ESP hopper ash for the Bailey/Black Thunder fuel blend system.

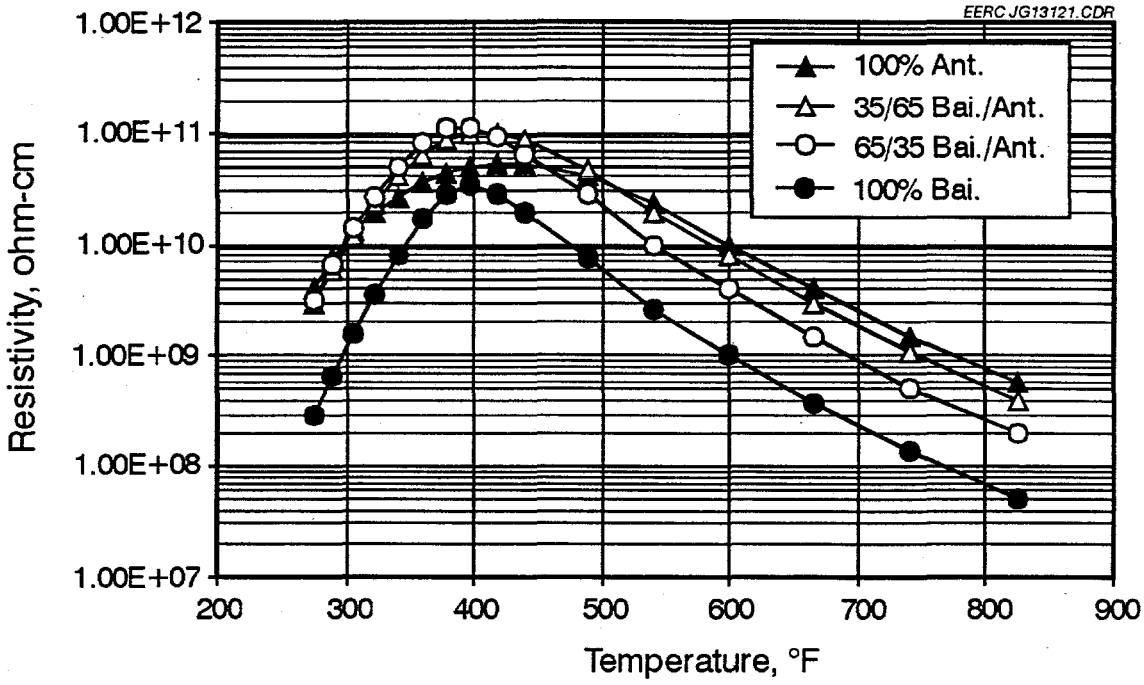

Figure 57. Predicted fly ash resistivities of the Bailey/Antelope blend system by the Bickelhaupt model.

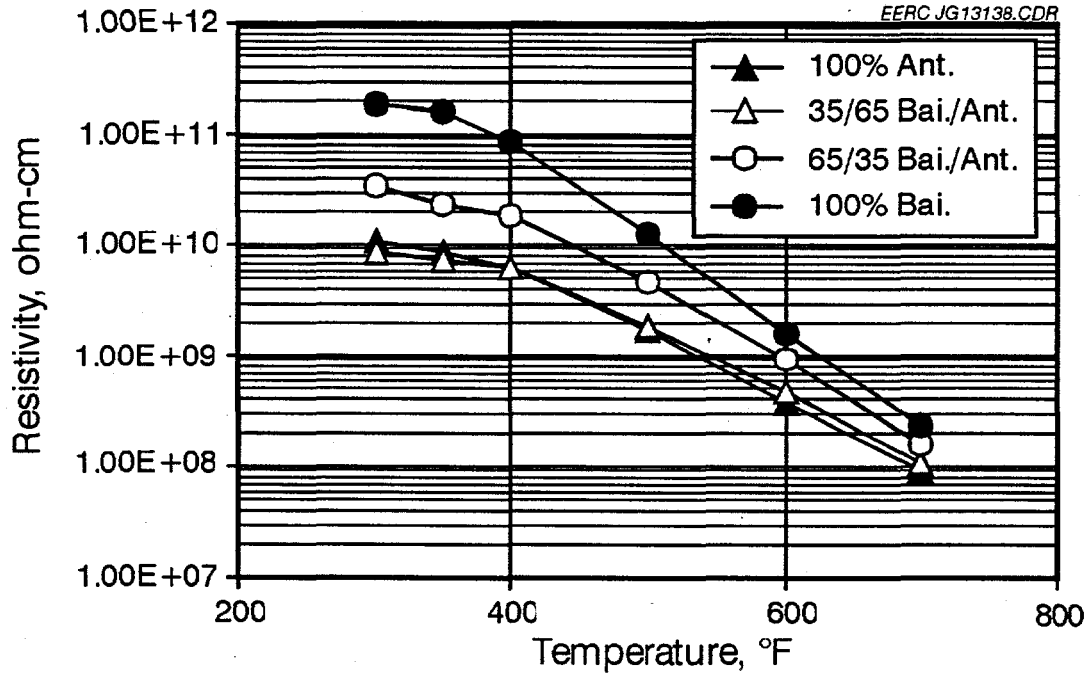

Figure 58. Laboratory resistivity results for EERC pilot-scale ESP hopper ash for the Bailey/Antelope fuel blend system.

5.0 SUMMARY AND CONCLUSIONS

Blending of low-sulfur subbituminous coals with higher-sulfur bituminous coals is becoming increasingly popular as utilities search for cost-effective means for reducing SO_2 emissions. While blending low-sulfur fuels in most cases will lower fuel costs, often additional costs are associated with operational changes required to fire the new fuel. For those units designed to fire bituminous coals, the addition of subbituminous coals to their fuel diet may impact a number of areas, from coal handling to pulverizer performance, furnace and convective pass fouling, and ESP performance. With these potential impacts in mind, a pilot-scale test program was established to quantify some of these changes. Effects of blend characteristics on pulverizer performance were studied by CONSOL, Inc., at its research facility in Library, PA, while effects on combustion performance were studied at the pilot facilities at UND's EERC in Grand Forks, ND.

A series of tests were performed to determine the effects of blending eastern bituminous coals with western subbituminous coals on utility boiler operation. Relative to the baseline bituminous coal, testing reports significant impacts to boiler performance due to the blending of the eastern and western coals. Results indicated that fuel blending can be used to adequately control flue gas emissions of both SO_2 and NO_x at the expense of reduced milling efficiency, increased sootblowing in the high- and low-temperature regions of the boiler and, to a lesser extent, decreased collection efficiency for an ESP. The higher reactivity of the subbituminous coal increased the overall combustion efficiency, which may tend to decrease the impact of the milling efficiency loss. The extent of these impacts was directly related to the percentage of subbituminous coal in the blend. At the lowest blend ratios of subbituminous coal, the impacts were greatly reduced.

Mill performance tests indicated that at design pulverizer conditions (relative to pulverization of bituminous coal), the decreased thermal input of the subbituminous coals resulted in derates on the mill of up to 55% of the maximum thermal input of the bituminous coals. One Pittsburgh seam bituminous coal, one Illinois No. 6 seam bituminous coal, and two PRB subbituminous coals were tested. By raising the mill outlet temperature between 5° and 25°F, thermal throughput for the subbituminous coals increased by 10% to 20%. Increasing the air/fuel ratio also tended to increase thermal throughput, although at the expense of a coarser product. At the maximum thermal throughput for the subbituminous coals at the highest air/fuel ratio, product fineness decreased up to 15 percentage points (less than 200 mesh). Interestingly, the lowest-heat-content subbituminous coal indicated the lowest thermal derate of the two PRB coals tested, but required much higher mill energy input.

Testing performed at the EERC determined the effects of blending one Pittsburgh seam bituminous coal with two PRB subbituminous coals. High-temperature fouling tests were performed at both 2000° and 2200°F, while low-temperature fouling deposits were collected at temperatures between 1500° and 1600°F. High-temperature fouling tests indicated comparable fouling rates for each of the parent coals, with the blends exhibiting a lower ash-fouling rate. The lower fouling rate of the blends was attributed to interactions between the two ash types. However, in each case, deposit strength increased as the percentage of subbituminous coal in the blend increased. The highest-sodium-content subbituminous coal produced consistently stronger deposits than its lower-sodium-content counterpart.

Low-temperature fouling tests indicated similar deposition rates for each of the coals tested, with a slight increase in rate noted as the percentage of subbituminous coal in the blend was increased. Higher-strength deposits were expected as the percentage of subbituminous coal was increased because of the sintering behavior of the high-calcium-content ash from the subbituminous coal. Results were inconclusive to support this theory, as the parent coals exhibited much lower strengths than either of the blends tested. There would appear to be some interaction between ash types to create these stronger deposits, although the mechanism was not easily discernible from the data generated.

Flame stability testing indicated that each of the parent coals and coal blends would exhibit excellent fuel ignitability and flame stability characteristics over a wide range of burner settings. The general trend was toward lower carbon-in-ash values as the percentage of subbituminous coal in blend with the bituminous coal was increased. Based on the results obtained here, the addition of subbituminous coal in blend with the bituminous coal should increase overall carbon conversion and provide adequate or improved flame stability, which may tend to offset some of the limits to grinding efficiency noted above in the mill performance tests performed by CONSOL.

Flue gas emissions of SO_2 were dramatically reduced as the percentage of subbituminous coal was increased in blend with the bituminous coal tested here. In general, the emission reductions followed the decrease noted in the input sulfur concentrations. However, increased sulfur capture in the ash was evident as the percentage of subbituminous coal in the blend was increased. This trend was even more pronounced for those tests performed at the lowest furnace exit gas temperature, indicating a temperature dependence on the level of sulfur capture in ash. Emissions of nitrogen oxides (NO_x) were also decreased as the percentage of subbituminous coal in the blend was increased. Levels noted during testing of the parent subbituminous coals were roughly one-half that of the parent bituminous coal. Particulate emission testing indicated similar results for all fuels tested under similar conditions. There was no apparent trend toward decreased collection efficiency for either of the sets of bituminous/subbituminous coal blends, although one of the bituminous/ subbituminous coal blend sets indicated a slight reduction in collection efficiency as the percentage of subbituminous coal in the blend was increased.

6.0 REFERENCES

1. Gunderson, J.R.; Moe, T.A.; Selle, S.J.; Harding, N.S. "Technology Assessment for Blending Western and Eastern Coals for SO_2 Compliance," final report prepared for U.S. DOE DE-FC21-93MC30098 and Electric Power Research Institute RP1891-07; EERC publication, July 1994.

2. Tufte, P.H.; Gronhovd, G.H.; Sondreal, E.A.; Selle, S.J. "Ash Fouling Potentials of Western Subbituminous Coals as Determined in a Pilot Plant Test Furnace," *In* Proceedings of the American Power Conference; 1976; Vol. 38, pp 661–671.

3. Hurley, J.P.; Benson, S.A.; Erickson, T.A.; Allan, S.E.; Bieber, J. "Project Calcium - Final Report," DOE/MC/10637-3292, 1995.

4. Steadman, E.N.; Erickson, T.A.; Zygarlicke, C.J. "Inorganic Transformations During Combustion: Mineral and Ash Particle Sizing and Typing," *In* Proceedings of the Advanced Research and Technology Development Direct Utilization, Instrumentation, and Diagnostics Contractors' Review Meeting; Pittsburg, PA, Sept. 16–18, 1990; pp 335–344.

5. Hurley, J.P.; Benson, S.A.; Erickson, T.A.; Allan, S.E.; Bieber, J. "Project Calcium - Final Report," EERC publication, Sept. 1992, p 38.

6. Bucher, W.E. "A Study of the Bulk Electrical Resistivity Characteristics of Fly Ash from Lignite and other Western Coals," M.S. Thesis, University of North Dakota, Dec. 1970.

7. Selle, S.J.; Dorris, H.L.; Sobule, J.A. "Blending of Eastern and Western Coal: Results of a Test Burn at Joppa Station," *In* Proceedings of the 16th Biennial Low-Rank Fuels Symposium; Billings, MT, May 1991; LRF 16–91, pp 113–124.

8. White, H.J. "Electrostatic Precipitation of Fly Ash," *Journal of the Air Pollution Control Association* **1977**, *27* (3), 206–217.

9. Selle, S.J.; Hess, L.L.; Sondreal, E.A. "Western Fly Ash Composition as an Indicator of Resistivity and Pilot ESP Removal Efficiency," Presented at the APCA Annual Meeting, Boston, June 1975; 16 pp.

APPENDIX A

DESCRIPTION OF TEST FACILITIES AND PROCEDURES

DESCRIPTION OF FACILITIES AND PROCEDURES

Research programs have been under way at the Energy & Environmental Research Center (EERC) for more than 25 years to study ash fouling of boiler heat-transfer surfaces in coal-fired utility boilers. A 550,000-Btu/hr pulverized-coal pilot plant test furnace was constructed in 1967 to evaluate the influence of variables, including ash composition, excess air, gas temperature, and tube wall temperatures on ash fouling. Results from this work have shown a strong correlation between ash characteristics and degree of fouling.

The research capabilities of the combustion test facility (CTF) have been enhanced and expanded to provide information on a wide range of combustion-related issues. The many research applications of this pilot-scale combustion equipment over the years have included the following:

- Determining ash-fouling rates and the strength, composition, and structure of fouling deposits.
- Applying sophisticated analytical methods to characterize input coal, ash, and deposits and to correlate coal and ash properties with deposit growth rates and strength development.
- Evaluating the effectiveness of ash-fouling additives.
- Studying particle-size distribution and velocity prior to deposition on convective section heat-transfer surfaces.
- Evaluating combustion characteristics of coal–water fuels.
- Studying high-temperature baghouse operation and performance.
- Evaluating sorbent injection for SO_x control.
- Assessing integrated particulate and SO_x–NO_x control.
- Studying NO_x control using selective catalytic reduction and disposable catalysts.
- Evaluating slagging potential in a simulated wet-bottom firing mode.
- Performing flame stability tests for comparing a particular fuel at full load and under turndown conditions.

COMBUSTION TEST FACILITY

An isometric drawing of the EERC CTF is shown in Figure A-1. The furnace capacity is approximately 75 lb/hr (550,000 Btu/hr) of pulverized lignite. The combustion chamber is 30 inches in diameter, 8 feet high, and refractory-lined for combustion testing of low-rank coals.

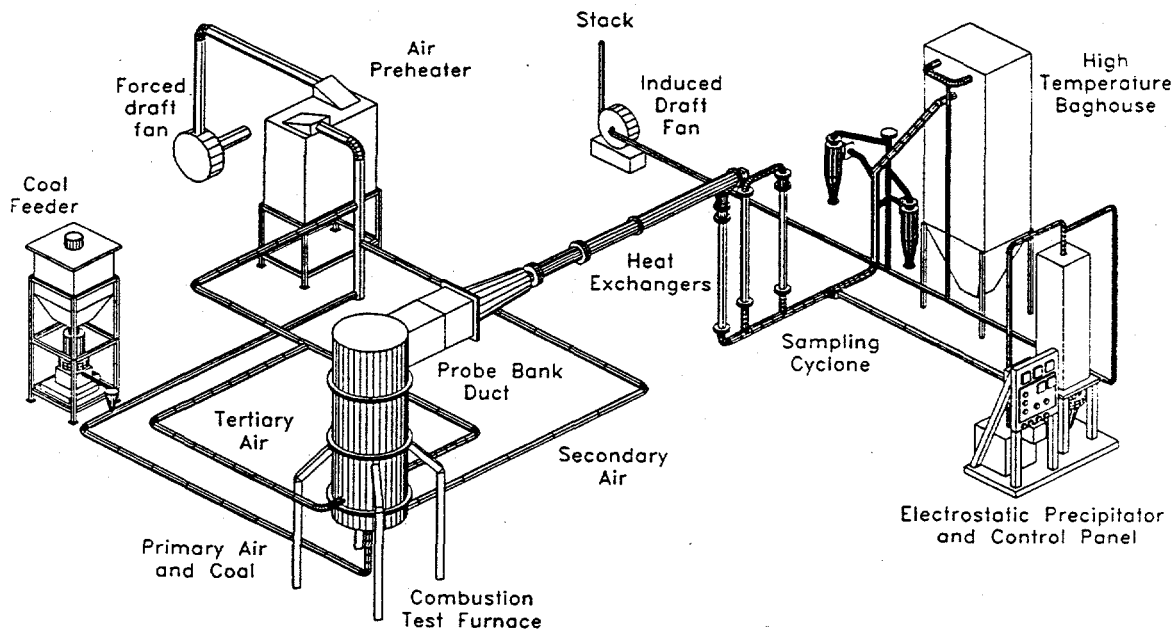

Figure A-1. Combustion test facility and auxiliary systems.

The furnace diameter may be reduced to 26 inches to elevate the temperature entering the convective pass. Furnace exit gas temperatures as high as 2400°F have been achieved during combustion testing in this mode. Most tests are performed using the standard configuration (30-inch inside diameter), with the furnace exit gas temperature maintained at approximately 2000°F for each combustion test.

Coal is pulverized remotely in a hammer mill pulverizer, targeted to a size of 70% less than 200 mesh. The coal is then charged to a microprocessor-controlled weight loss feeder from a transport hopper. Combustion air is preheated by an electric air heater. The pulverized coal is screw-fed by the gravimetric feeder into the throat of a venturi section in the primary air line to the burner. Heated secondary air is introduced through an annular section surrounding the burner. Heated tertiary air is added through two tangential ports located in the furnace wall about 1 foot above the burner cone. The percentages of the total air used as primary, secondary, and tertiary air are usually 10%, 30%, and 60%, respectively. (An adjustable swirl burner, which uses only primary and secondary air with a distribution of approximately 15% and 85%, respectively, was used during flame stability testing). Flue gas passes out of the furnace into a 10-inch-square duct that is also refractory lined. Located in the duct is a vertical probe bank designed to simulate superheater surfaces in a commercial boiler.

Figure A-2 shows the construction of the ash-fouling test probe bank, which is located in a hinged door to facilitate inspection and cleaning. The three fouling probes used during this combustion test were constructed of 1.66-inch-outside-diameter Type 304 stainless steel pipe and were cooled with compressed air. Each probe has two thermocouples embedded in its upstream edge to measure metal temperature. One of the

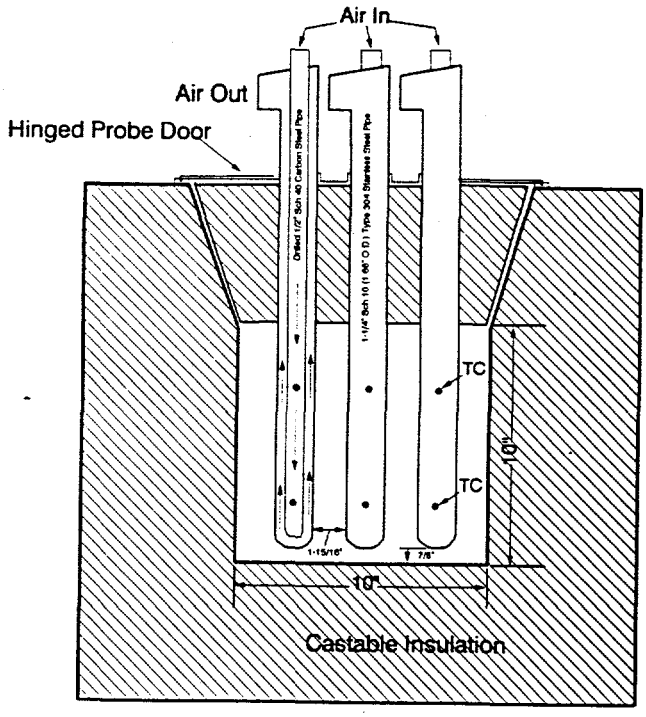

Figure A-2. Detail of probe bank construction.

thermocouples on each probe is attached to a temperature recorder–controller that regulates the cooling air to the probe. The surface temperature of each probe was maintained at 1000°F. The gas velocity between the tubes is normally about 25 ft/s when low-rank coals are fired. The gas temperature entering the probe bank is normally maintained at 2000°F.

After leaving the probe duct, the flue gas passes through a series of water-cooled heat exchangers before being discharged through either an electrostatic precipitator (ESP) or a baghouse.

General Test Method

The relative fouling or other tendencies of test coals are determined by burning coal samples under specified conditions. When starting with a cold furnace, the following 13.25-hour test program is normally used:

	Hours
Preheat on gas	8.00
100% coal firing	5.25
Total	13.25

The coal feed rate is commonly adjusted to keep the flue gas temperature entering the upper duct to the probe bank at 2000°F, with 25% excess air. Coal samples are taken periodically to form a composite sample. Oxygen, carbon dioxide, nitrous oxides, carbon

monoxide, and sulfur dioxide in the flue gas are continuously monitored by recording analyzers. The operating conditions and procedures described above are those normally used when the ash-fouling tendencies of low-rank western coals are studied.

The test furnace has numerous ports that permit observation of the probes and the furnace burner zone during the test run. These ports can also be used for installation of additional test probes, auxiliary measurements, photography, or injection of additives.

At the completion of the test period, the probe door is carefully opened and photographs are taken of the deposit. The deposit is then removed from the probes in two fractions, an inner and an outer layer, and each is weighed and analyzed separately. Normally, the inner white layer weighs less than 10 grams, as compared to 100 to 500 grams for the outer sintered deposit.

The weight of ash deposited on the probe bank during a standard test is used to rank the coal for its relative fouling potential. To ensure that the pilot-scale test results are meaningful for evaluation of ash-fouling potential in full-scale utility boilers, calibration tests were previously conducted with low-rank coals known to produce low and high fouling when used in utility boilers. Comparisons of ash fouling have been made from tests conducted at a number of power stations throughout the western United States: Monticello (Texas Utilities), Big Brown (Texas Utilities), Four Corners (Arizona Public Service Company), St. Clair (Detroit Edison Company), Jim Bridger (Pacific Power and Light), Big Stone (Otter Tail Power Company), Leland Olds (Basin Electric Power Cooperative), and San Miguel (San Miguel Electric Cooperative). Based on these tests, the ash deposit buildup rate on the probe bank was found to be a good indicator of fouling potential. The relationship between deposit weight and a fuel's fouling potential is generally categorized as indicated below:

Deposit Weight, grams	Relative Fouling Potential
0–150	Low
150–300	Medium
Above 300	High

Deposit Strength Tests

The weight of the ash deposit from the probe bank has proven to be a good indicator of the fouling potential for most coals tested in the EERC CTF. Heavy deposits in the 5.25-hour test indicate high deposition rates, which can usually be related to potential ash-fouling problems in utility boilers. However, the deposition rate does not provide an indication of the ease of removal of deposits by sootblowing. Methods to measure deposit tenacity and strength have been reviewed at the EERC, and strength test methods have been developed that appear to provide reliable, reproducible results (1).

Deposit strength is initially assessed by means of the strength rating factor (SRF). This factor is determined from observations made by a pilot plant operator during removal of ash deposits from the probe bank. Deposit hardness and breakability is rated from 1 to 10, with "1" indicating "soft and crumbly" and "10" meaning "hard and unfragmented."

The probe deposit can also be subjected to a laboratory deposit strength evaluation procedure developed at the EERC, which utilizes a drop impactor technique. A known weight is dropped with a measured impact on the sliced face of a 1-inch-long deposit sample. After the drop test, the sample is sieved in a sonic sifter through a series of six screens ranging in size from 5.66 to 0.21 mm. The percentage of each size is determined and, using the procedure from the ASTM Tumbler Test (ASTM Method D441-45), the dust index, friability, and mass mean diameter of the crushed deposit sample are determined. The dust index is indicative of the tendency of the deposit to form dust on impaction. The mass mean diameter is the average size of the fragmented particles after the drop test. An impact resistance value (IRV) is calculated, which adjusts the results of the impactor tests for the test parameters under which they were obtained. The calculation was developed by analysis of a large body of data obtained by this procedure.

Furnace Wall Slag Probes

The combustion test facility at the EERC was originally designed for tests of fouling potential of low-rank coals. As a result, the nominal design values of heat input (550,000 Btu/hr), FEGT (2000°F), and excess air levels (25%) reflect utility industry experience on such fuels. More recently, efforts were made to evaluate slagging potential in the CTF. A slag probe was designed, constructed, and positioned close to the flame region of the furnace, just above the flame. The slagging test probe was water-cooled, to enable monitoring and maintaining surface metal temperatures between 500° and 800°F.

FLAME STABILITY TESTING

Flame stability is assessed by observation of the flame and its relation to the burner quarl as a function of secondary air swirl and operating conditions at full load and under turndown conditions. An International Flame Research Foundation (IFRF)-type adjustable secondary air swirl generator (shown in Figure A-3) uses primary and secondary air at approximately 15% and 85% of the total air, respectively, to adjust swirl between 0 and a maximum of 1.9. Swirl is defined as the ratio of the radial (tangential) momentum to axial momentum imparted to the secondary air by movable blocks internal to the burner and is used to set up an internal recirculation zone (IRZ) within the flame that allows greater mixing of combustion air and coal. Swirl is imparted by moving blocks to set up alternate paths of radial flow and tangential flow, creating a spin on the secondary air stream that increases the turbulence in the near-burner zone. At the fully open position of the swirl block, the secondary air passes through the swirl burner unaffected, and the momentum of this stream has only an axial component (the air enters the combustion chamber as a jet). As the angle of the blocks changes, the air begins to spin or "swirl" and the radial component to the momentum is established, creating the IRZ in the near-burner region. It is the ratio of this radial component of the momentum to the axial component that establishes the quantity defined as "swirl."

The adjustable swirl burner used by the EERC during flame stability testing consists of two annular plates and two series of interlocking wedge-shaped blocks, each attached to one of the plates. The two sets of blocks can form alternate radial and tangential flow channels, such that the air flow splits into an equal number of radial and tangential streams which combine further downstream into one swirling flow as shown in Figure A-4. By a simple rotation of the movable plate, radial channels are progressively

closed and tangential channels opened so that the resulting flux of angular momentum increases continuously, between zero and a maximum value. This maximum swirl depends on the total air flow rate and the geometry of the swirl generator. Swirl can be calculated from the dimensions of the movable blocks (the ratio of the tangential and radial openings of the blocks) or from the measurement of the velocity of the air stream (obtaining both radial and axial components). The following description of that calculation is provided by Beer and Chigier (2):

> When rotating motion is imparted to a fluid upstream of an orifice, the fluid flow emerging from the orifice has a tangential velocity component in addition to the axial and radial components of velocity encountered in nonswirling jets. The presence of the swirl results in the setting up of radial and axial pressure gradients which, in turn, influence the flow field. In the case of strong swirl, the adverse axial pressure gradient is sufficiently large to result in reverse flow along the axis, setting up the internal recirculation zone.

In swirling free jets or flames, both axial flux of the angular momentum (G_φ) and the axial thrust (G_x) are conserved. These can be written as

$$G_\varphi = {}_0\int^R [(Wr)\,\rho U 2\pi r]\,dr = \text{const}$$

$$G_x = {}_0\int^R [U\rho U 2\pi r]\,dr + {}_0\int^R [p 2\pi r]\,dr = \text{const}$$

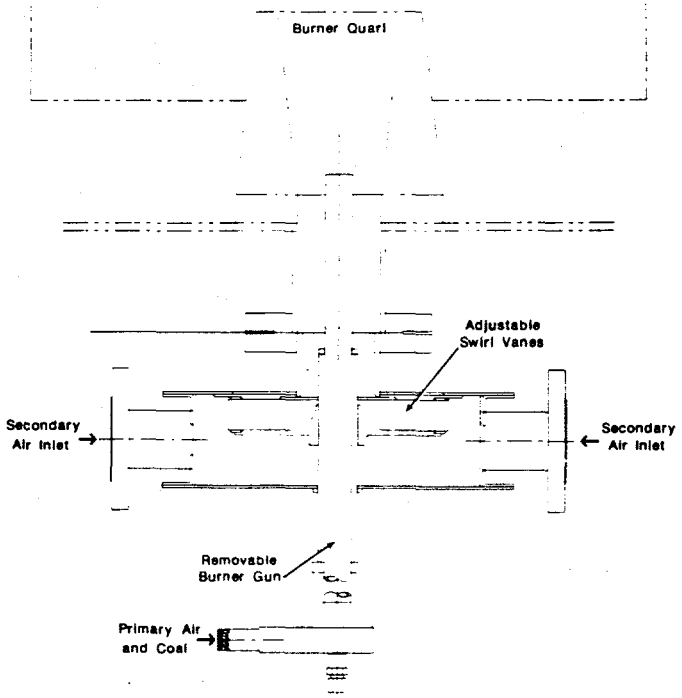

Figure A-3. IFRF adjustable swirl burner.

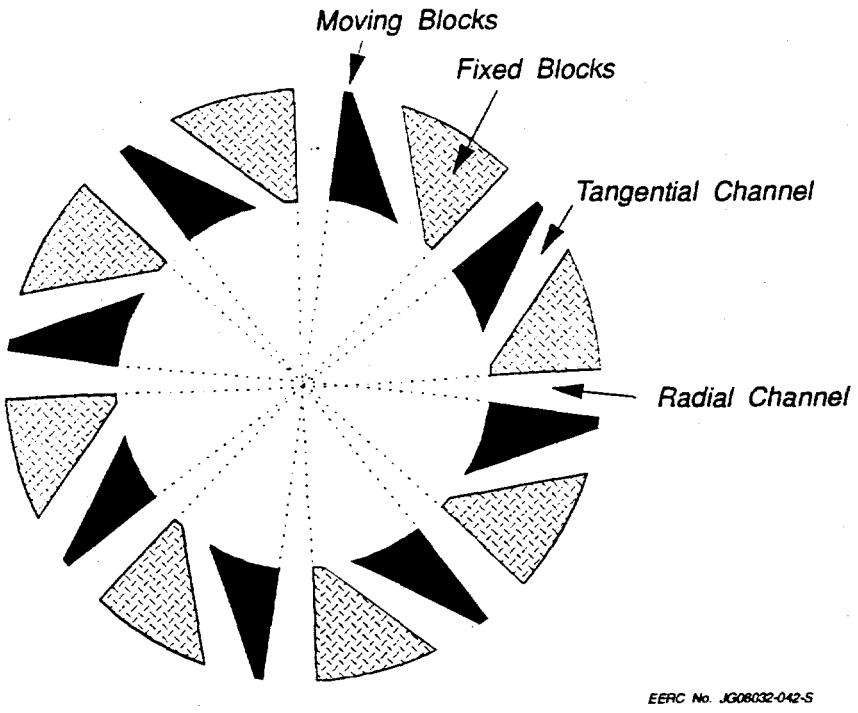

Figure A-4. Cross section of movable block assembly.

where, U, W and p are the axial and tangential components of the velocity and static pressure, respectively, in any cross section of the jet. Since both these momentum fluxes can be considered to be characteristic of the aerodynamic behavior of the flame, a nondimensional criterion based on these quantities can describe the swirl intensity as

$$S = G_\varphi/G_x R \quad (R = \text{exit radius of the burner nozzle}).$$

Experiments have shown that the swirl number S was the significant similarity criterion of swirling jets produced by geometrically similar swirl generators. Other similarity criteria which take account of nonisothermal conditions and of confinement of jet flow by walls can also be applied in conjunction with the swirl number. The calculation of swirl in other types of swirl generators, such as the air registers on a utility boiler, are also described by Beer and Chigier (2), though not mentioned here.

Secondary air swirl is used to stabilize the flame. In the absence of swirl, loss of flame may result, increasing the risk of dust explosion. As swirl is applied to the combustion air, coal particles are entrained in the IRZ, increasing the heating rate of the particles, leading to increased release of volatiles and char combustion. The flame becomes more compact and intense as swirl is increased to an optimum level, which is characterized in the EERC test facility as the point at which the flame makes contact with the burner quarl. Increasing swirl beyond this level can pull the flame into the burner region, unnecessarily exposing metal burner components to the intense heat of the flame and possible combustion in the coal pipe.

Increasing swirl to provide flame stability and increased carbon conversion can also affect the formation of NO_x. The high flame temperatures and increased coal–air mixing associated with increased swirl create an ideal situation under which NO_x may form. In full-scale burners with adjustable vanes, swirl is often increased to reach the optimum condition and then decreased slightly to reduce the production of NO_x.

General Test Method

The general test method sets the burner at its maximum level of swirl and monitors system parameters such as fuel feed rate, excess air, gaseous emissions (CO_2, CO, SO_x, and NO_x), combustor static, and air flow rates. Photographs of the flame and burner zone are then taken through a sight port in the furnace proper just above the burner cone using standard 35-mm film. Flame temperature is also measured using a high-velocity thermocouple (HVT) at a set location in the furnace, and heat flux is monitored using a baseline heat flux probe at the same location. An ash sample is collected at each swirl setting to establish carbon burnout. The swirl setting is then reduced until the flame is visually observed to lift off the burner quarl. At this point, the flame is characterized as unstable under full load conditions (between 600,000 and 650,000 Btu/hr firing rate). Photographs are again taken to record the flame at this setting, temperature and heat flux measurements are taken, and an ash sample is taken once again. Once flame liftoff is established, the optimum swirl setting is located by visual observation of the flame, and measurements are recorded once again.

Flame stability under turndown conditions is characterized by firing the test fuel at reduced load (typically one-half to three-quarters of the full load rate), maintaining the same primary air flow, and adjusting the secondary air flow to meet excess air requirements. The procedure described above is then used to establish flame stability at reduced load.

FLY ASH PARTICULATE CHARACTERIZATION

Fly ash samples are obtained by various means at the inlet and outlet of the pilot plant ESP or baghouse, as shown in Figure A-1. EPA Method 5 is used to establish particulate concentrations in the flue gas. High-volume sample extraction and the pilot plant control device collection hoppers can provide large samples for study. Particulate sizing and laboratory ash resistivity techniques, used to characterize the fly ash from each test, are described below.

Five-Stage Cyclone System

A five-stage cyclone system, shown in Figure A-5, was used to determine the size distribution of particulate entering the ESP. The system consists of five cyclones and a backup filter connected in series to provide five equally spaced particle-size cuts on a logarithmic scale from 0.1 to 10 μm. The nominal flow rate for the system is 1.0 acfm. The five-stage cyclone system was designed to operate in-stack, but is operated out-of-stack (particulate-laden flue gas is isokinetically extracted from the stack using a sampling probe) at the EERC due to the small pipe diameters associated with the pilot-scale combustion equipment.

Laboratory Resistivity Unit

Bulk electrical resistivity measurements are made with an apparatus designed and built according to the American Society of Mechanical Engineers Power Test Code 28 that provides control of temperature and flue gas environment for the ash samples being tested. Temperature control is maintained by an electrically heated oven (Figure A-6). The oven can be heated to a maximum of 800°F in approximately one-half hour and can maintain any temperature between room temperature and 800°F. Flue gas components (O_2, CO_2, SO_2, and N_2 from compressed gas cylinders) are metered with rotameters to match the flue gas concentrations in which the fly ash was collected. Humidity is provided by bubbling gas through a humidity bath maintained at a precisely controlled temperature. The outlet gas is saturated with water vapor at the given temperature. Sulfur dioxide and CO_2 do not go through the humidity bath, but enter the simulated flue gas stream just prior to the oven.

Fly ash resistivity measurements are made using a movable disk electrode, as shown in Figure A-7. This electrode was designed to put a pressure of 10 g/cm^2 on a layer of ash 5 mm thick. The ash sample container and the electrode are made of sintered stainless steel of 25-μm porosity to allow contact between the ash and the flue gas.

A high-voltage supply with a range of 0 to 1200 volts is wired to the sample pan electrode. Current passing through the sample layer from the sample pan to the measuring electrode is measured by an electrometer capable of reading currents from 10^{-14} to 10^{-1} amperes.

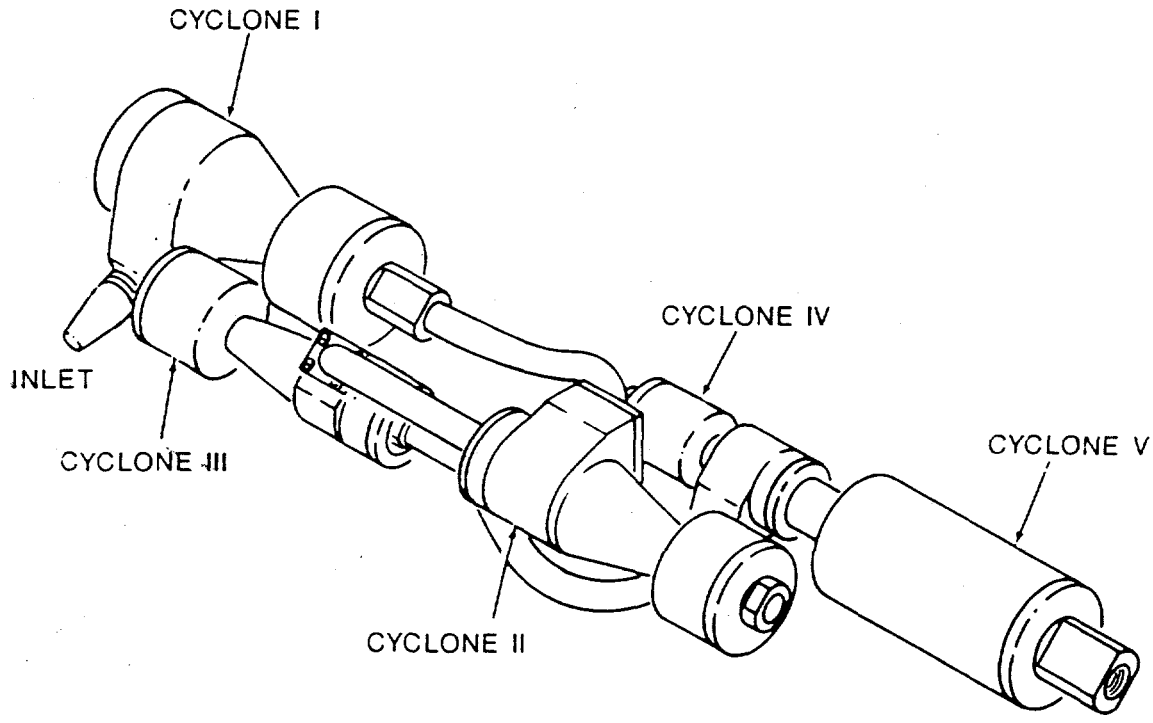

Figure A-5. Five-stage cyclone sampling system.

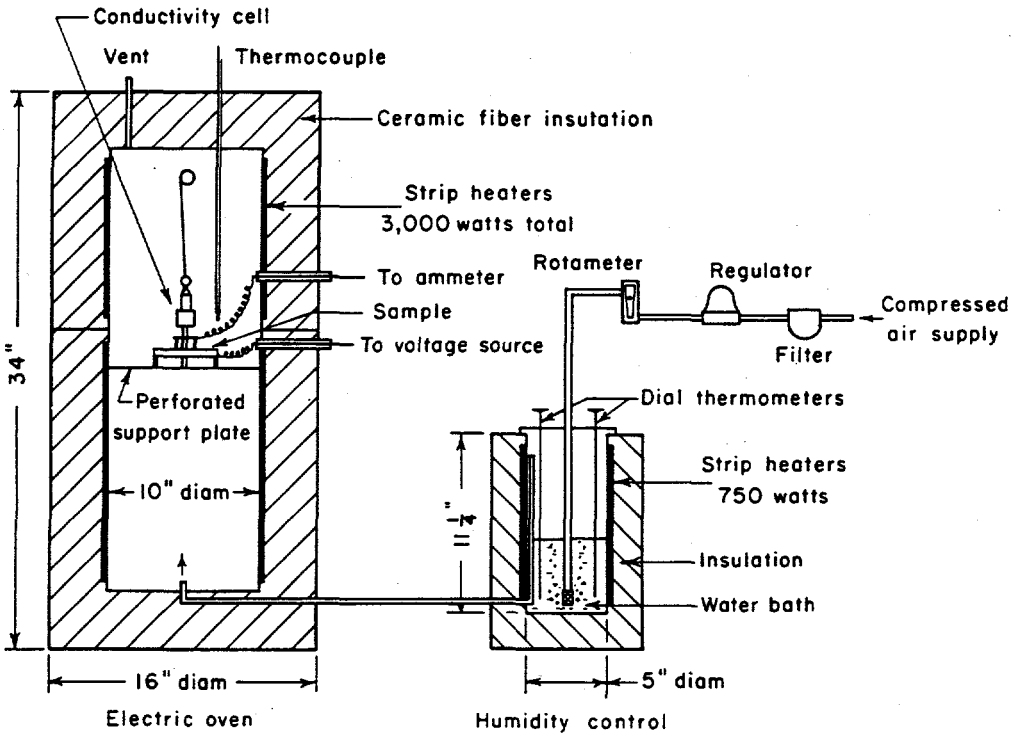

Figure A-6. Schematic of laboratory resistivity apparatus.

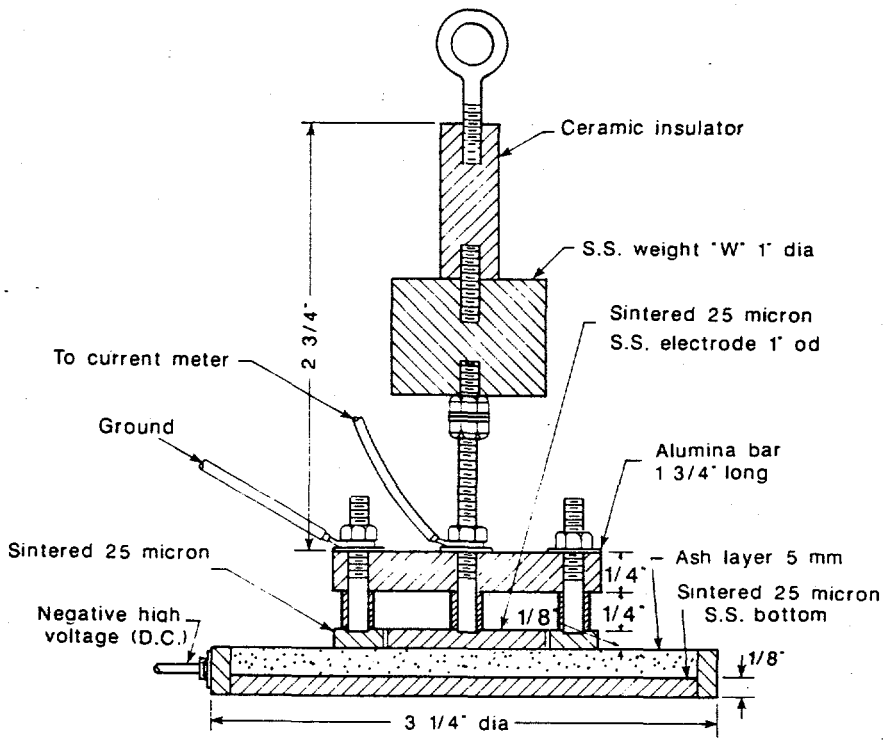

Figure A-7. Resistivity-measuring electrode.

A uniform ash layer is introduced to the conductivity cell, and the electrode is carefully lowered onto the ash layer. The oven door is then closed, and the temperature is set to 200°F. After the oven has maintained the designated temperature for at least 40 minutes, a 750-volt source is applied to the 0.5-cm ash layer. This produces a field strength of 1.5 kV/cm, which is used for all measurements. The current through the ash layer is measured with a high-sensitivity electrometer. The temperature of the oven is increased to the next higher temperature, after which there is a 40-minute waiting period to ensure that the ash layer has a uniform temperature. The test voltage is then applied, the current reading is recorded, and the temperature is increased to the next setting. Analysis duration is normally 8 to 10 hours to complete one set of readings from 200° to 750°F.

The fly ash resistivity is then calculated using the equation:

$$\rho = \frac{VA}{IL}$$

In this expression, V is the applied voltage, which is held constant at 750 volts. A is the area of the one-inch-diameter inner electrode, which is also constant at 5.07 cm^2. L is the thickness of the ash layer, which is 0.5 cm, and I is the measured current in amperes. For a given test, the data are presented as a plot of fly ash resistivity versus temperature.

ANALYTICAL PROCEDURES

Coal Analysis

The coal is analyzed to determine the proximate, ultimate, and heating value analyses. The particle-size distribution is also determined for each combustion test sample. Descriptions of these analyses are as follows:

- Proximate analysis to determine moisture, ash, and volatile matter content is performed with a Fisher 490 coal analyzer. Fixed carbon is calculated by difference as the final remaining constituent.

- Ultimate analysis is performed using a Perkin-Elmer Model 240 elemental analyzer to determine CHN concentrations and a Leco sulfur analyzer for sulfur content. The level of chlorine in the coal is determined by ASTM Method D2361. Ash content is determined by ASTM Method D3174. Oxygen in the coal is calculated by difference as the final remaining constituent.

- Gross caloric value is measured by ASTM Method D2015 using a Parr adiabatic calorimeter and master controller.

- Particle-size distributions are determined by sieve analysis according to ASTM Method D410.

Inorganic and Mineral Component Analysis

Concentrations of major mineral oxides in the coal ash (Al_2O_3, SiO_2, Na_2O, MgO, CaO, P_2O_5, K_2O, Fe_2O_3, TiO_2, and SO_3) are determined by x-ray fluorescence (XRF). The ash samples are prepared using the ASTM D3174 procedure in which the sample is heated to 1382°F in air for 15 hours (a larger sample analyzed by the EERC lab requires additional drying time). Analysis is performed using a Kevex x-ray spectrometer.

Fusion temperatures of the ash are determined under oxidizing and reducing conditions, in accordance with ASTM Method D1857, using a Preier–Mineco electric tube furnace.

Advanced Coal Analyses

A sample of the test coal is also analyzed by chemical fractionation and computer-controlled scanning electron microscopy (CCSEM) to aid in understanding ash behavior. The characteristics of fly ash or ash deposits are dependent on two basic factors: 1) the types, abundance, and associations of the inorganic constituents in the original fuel; and 2) combustion conditions. In order to understand the mechanisms and processes occurring among inorganic components during combustion, a precise and accurate knowledge of the inorganic materials entering the combustion system must be obtained.

Conventional ASTM ash analysis was developed for high-rank coals in which the primary inorganic constituents are minerals. Low-rank coals contain a complex mixture of inorganic components, including cations bound to the organic acid groups and clays, organically coordinated inorganic elements, and discrete mineral phases. The EERC advanced method of coal analysis is a two-part analysis designed to quantitatively determine not only what inorganic elements are present but also their mode of occurrence. The first part of the EERC advanced coal analysis uses the chemical fractionation technique to quantitatively determine the modes of occurrence of inorganics. The second part of the method uses CCSEM to quantify the amounts and sizes of minerals present.

Chemical Fractionation

Chemical fractionation is used to quantitatively determine the modes of occurrence of the inorganic elements in coal, based on the extractability of the elements in solutions of water, 1 molar ammonium acetate, and 1 molar hydrochloric acid. The flow diagram shown in Figure A-8 illustrates the technique. A 75-gram sample of −325-mesh vacuum-dried coal is stirred with 160 mL of deionized water to extract water-soluble minerals such as sodium chloride. After being stirred for 24 hours at room temperature, the water–coal mixture is filtered. The filtered coal is dried, and a portion is removed to be tested by XRF to determine the percent of each element remaining. The residues are then mixed with 160 mL of 1 molar ammonium acetate (NH_4OAc) and stirred at 70°C for 24 hours to extract the elements associated with the coal as ion-exchangeable cations present primarily as the salts of organic acids. The ammonium acetate extractions are performed two more times to effect complete removal of the ion-exchangeable cations. After the third ammonium acetate extraction, a sample of the dried residue is analyzed by XRF. The remaining residue of the ammonium acetate extractions is then stirred with 1 molar hydrochloric acid (HCl) at 70°C for 24 hours to remove the elements held in coordination complexes within the organic structure of the coal, as well as acid-soluble minerals such

as carbonates, oxides, and sulfates. The residue is then analyzed by XRF. The hydrochloric acid extraction is repeated once. The elements remaining in the coal after the chemical fractionation extractions are determined by difference. The nonextractable elements are associated in the coal as silicates, aluminosilicates, sulfides, and insoluble oxides.

CCSEM Analysis

Size and composition of mineral grains in the coal were determined by computer-controlled scanning electron microscopy (CCSEM), a program used in conjunction with the EERC JEOL scanning electron microscope (SEM) and microprobe system. The program is used to characterize inorganic components in samples of coal, char, and inorganic combustion products. The CCSEM system uses a computer to control the operation of the SEM in order to determine the size, quantity, distribution, and association of mineral grains and other particulate matter. The CCSEM analysis system uses an annular backscattered electron detector to locate and size the particles. The backscattered electron detector distinguishes compounds based on the atomic number of their elements. Therefore, particles such as mineral grains appear brighter than the coal or epoxy matrix in which they are mounted. This allows the electron beam to detect the particles by noting contrast differences.

When a particle is detected, the particle center is automatically located, a series of eight diameters about the center of the particle are measured, and the perimeter, area, and shape factor of the particle are calculated. The CCSEM analysis for the coal samples is performed using a magnification of 240x. Particles less than 1 micron in average diameter are not included in the analysis, since 1 micron is the lower limit for the energy-dispersive spectra (EDS) analysis.

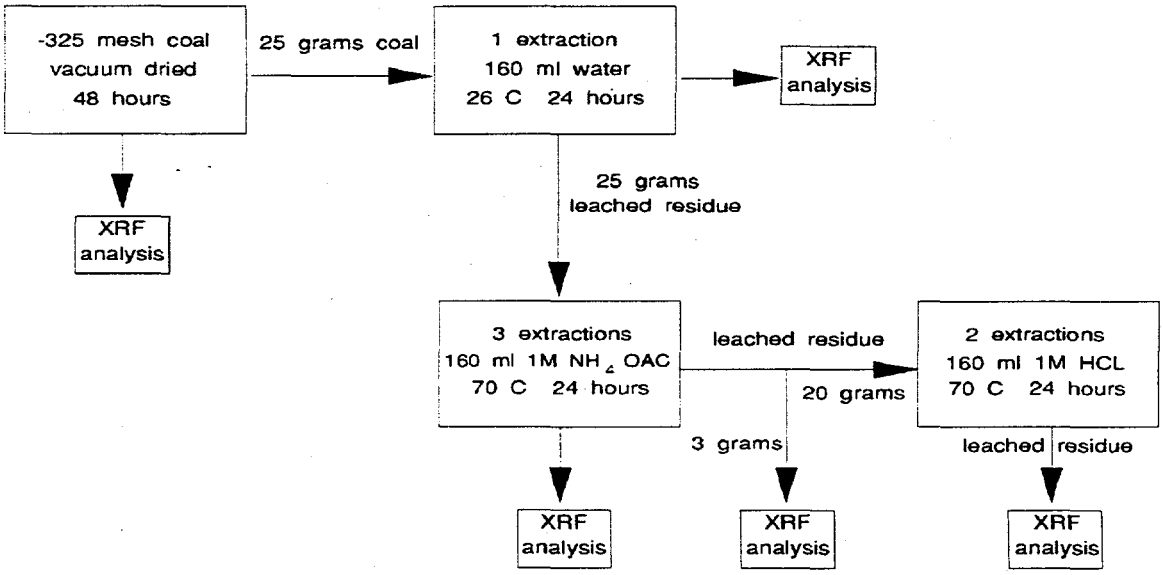

Figure A-8. Flow chart of the EERC chemical fractionation procedure.

The electron beam is then relocated to the center of the particle, and an EDS is taken for 2 seconds. Energy photon counts are accumulated for each element present and normalized to 100%. The CCSEM system can analyze for Na, Mg, Al, Si, P, S, Cl, K, Ca, Fe, Ba, and Ti. All information obtained by the CCSEM program is automatically stored in a microcomputer print file. These data are imported into a spreadsheet where phases are identified by the relative proportions of elements in each sized particle. Size distributions are also tabulated.

Ash Deposit Characterization

Chemical compositions of probe deposit and fly ash samples are determined by means of XRF. X-ray diffraction (XRD), which allows the identification of major crystalline forms, is used to support more quantitative SEM techniques in evaluating ash deposition phenomena. Identification, selection, and analysis of critical regions of the deposits are accomplished using SEM techniques.

SEMPC Analysis

A scanning electron microscopy point count technique (SEMPC) is used to quantify the phases present in the deposit. The SEM microprobe system is a powerful tool that can be used to examine the microscopic features of deposits and fly ash and provide chemical analysis of points as small as 1 micron in size. The system is automated and computer controlled, which increases data manipulation and data storage capabilities. The SEMPC technique was developed at the EERC to systematically and quantitatively determine the distribution of phases in ash deposits and fly ash. The SEMPC technique provides information on the degree of interaction and melting of the deposited ash components and the abundance of crystalline, amorphous, and unreacted ash particles. The data obtained from the technique are critical in identifying the components in ash deposits that are responsible for deposit growth and strength development. In addition, viscosity distribution profiles can be calculated for the amorphous or liquid phases using SEMPC data. This information provides insight into the propensity of a particular ash to form a strong deposit.

The procedure for SEMPC analysis involves preparing a cross section of the sample by mounting the ash deposit sections in epoxy. The epoxy block is sectioned to expose the ash deposit material. The exposed section is then polished to provide a very smooth surface for examination with the SEMPC technique.

The polished sample is placed in the SEM, and a compositional analysis is obtained from a series of 250 grid points across approximately 35 mm^2 of the sample. The Tracor Northern 5500 computer system differentiates between epoxy and deposit material and stores the chemical information. The stored chemical information is transferred to a microcomputer that identifies and quantifies the amorphous and crystalline components in the deposit. The crystalline components are readily identified as minerals based on chemical composition and molar ratios. The amorphous component is classified as either derived phases or unclassified material. Derived phases resemble their coal mineral precursor. Unclassified material has no crystalline structure and shows no molar ratios that conform to mineral formulas stored in the SEMPC program.

REFERENCES

1. Honea, F.I. "Studies of Ash Fouling Potential and Deposit Strength in the GFETC Pilot Plant Test Furnace," In *Fouling and Slagging from Impurities in Combustion Gases;* Bryers, R.W., Ed.; Engineering Foundation: New York, 1983; pp 117–141.

2. Beer, J.M.; Chigier, N.A. *Combustion Aerodynamics;* John Wiley & Sons: New York, 1972; pp 100–146.

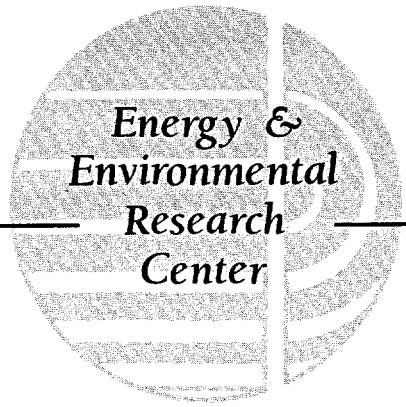

APPENDIX B

PLOTS OF ADDITIONAL DATA

MALVERN Instruments M6.10 Date 12-08-1994 Time 02:00

SAMPLE ID: 94-528 L# 3287
LENSE TYPE: 63MM LENSE SMALL CELL / SONICATED
DATE: 08-12-94
OPERATOR: Jan Lucht for B. Docktor
100% Bailey

System number 2362 Diode at1301

Malvern Instruments EASY Particle Sizer M6.10 Date 12-08-94 Time 02-00

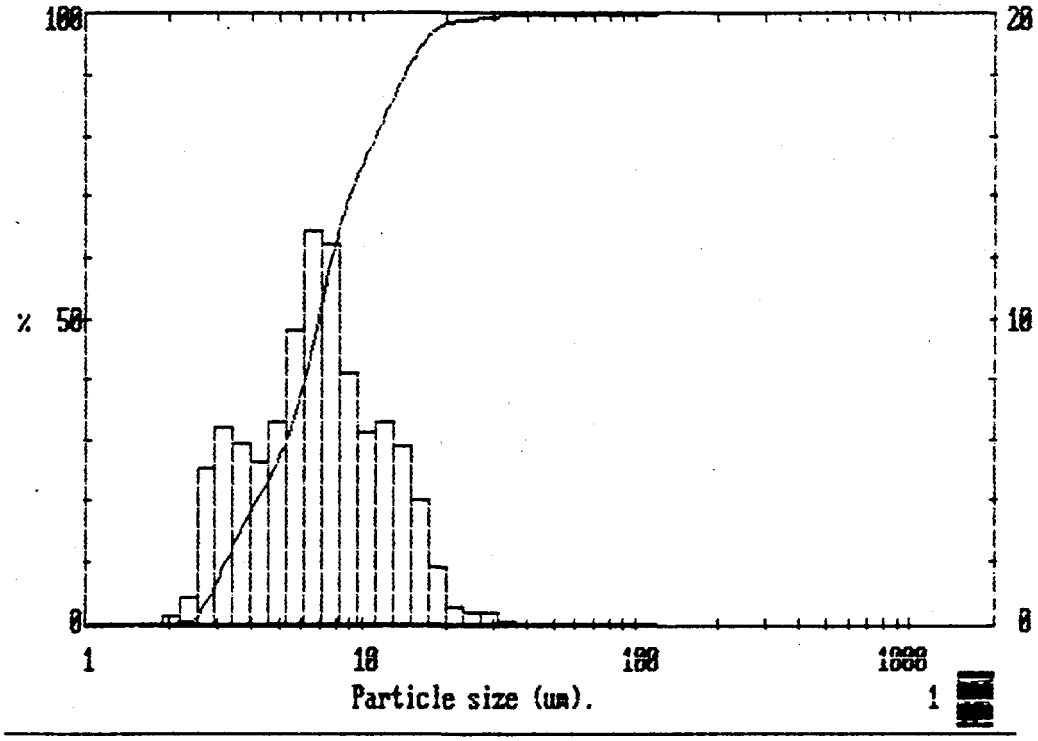

Size microns	under	% in band	Size microns	under	% in band
118.4	100.0	0.0	11.1	80.2	6.3
102.1	100.0	0.0	9.6	74.0	8.2
88.1	100.0	0.0	8.3	65.7	12.5
76.0	100.0	0.0	7.2	53.3	13.0
65.6	100.0	0.0	6.2	40.3	9.7
56.6	100.0	0.0	5.3	30.6	6.7
48.8	100.0	0.0	4.6	23.9	5.3
42.1	100.0	0.0	4.0	18.6	5.9
36.3	100.0	0.1	3.4	12.7	6.5
31.3	99.9	0.3	3.0	6.3	5.1
27.0	99.5	0.4	2.6	1.1	0.9
23.3	99.2	0.6	2.2	0.2	0.2
20.1	98.6	1.9	1.9	0.0	0.0
17.4	96.7	4.1	1.6	0.0	0.0
15.0	92.7	5.8	1.4	0.0	0.0

Result source= Sample
Record No. = 0
Focal length = 63 mm.
Experiment type pil
Volume distribution
Beam length = 14.3 mm.
Obscuration =0.1363
Volume Conc. = 0.0021 %
Log. Diff. =3.97
Model indp

D(v,0.5) = 6.9 um
D(v,0.9) = 13.9 um
D(v,0.1) = 3.2 um
D(4,3) = 7.7 um
D(3,2) = 6.1 um
Span = 1.6

MALVERN Instruments M6.10 Date 12-08-1994 Time 02:20 *

SAMPLE ID: 94-629 L# 3288
LENSE TYPE: 63MM LENSE SMALL CELL / SONICATED
DATE: 08-12-94
OPERATOR: Jan Lucht for B. Docktor
100% Antelope

System number 2362 Diode at1301

Malvern Instruments EASY Particle Sizer M6.10 Date 12-08-94 Time 02-21

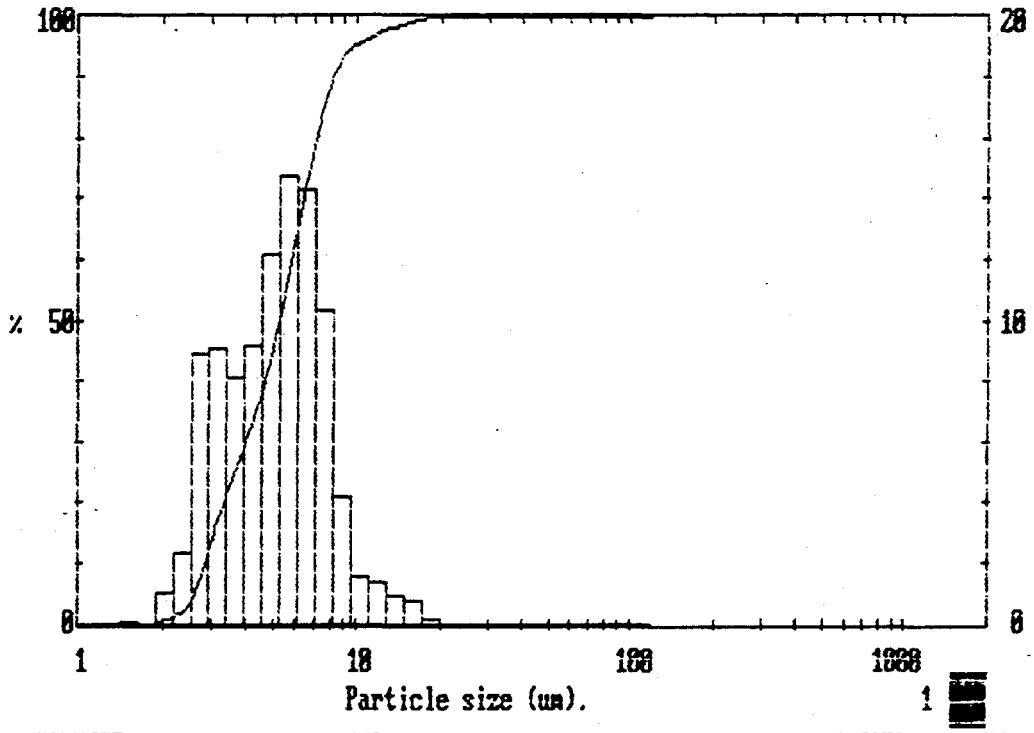

Size : microns	: under	% in band:	Size : microns	: under	% in band:
118.4	100.0	0.0	11.1	96.7	1.6
102.1	100.0	0.0	9.6	95.1	4.2
88.1	100.0	0.0	8.3	90.9	10.3
76.0	100.0	0.0	7.2	80.6	14.3
65.6	100.0	0.0	6.2	66.2	14.8
56.6	100.0	0.0	5.3	51.4	12.2
48.8	100.0	0.0	4.6	39.1	9.2
42.1	100.0	0.0	4.0	29.9	8.1
36.3	100.0	0.0	3.4	21.8	9.1
31.3	100.0	0.0	3.0	12.6	8.9
27.0	100.0	0.0	2.6	3.7	2.4
23.3	100.0	0.0	2.2	1.3	1.1
20.1	100.0	0.2	1.9	0.2	0.0
17.4	99.8	0.8	1.6	0.2	0.1
15.0	99.0	0.9	1.4	0.0	0.0

Result source= Sample
Record No. = 0
Focal length = 63 mm.
Experiment type pil
Volume distribution
Beam length = 14.3 mm.
Obscuration =0.1938
Volume Conc. = 0.0023 %
Log. Diff. =3.63
Model indp

D(v,0.5) = 5.3 um
D(v,0.9) = 8.2 um
D(v,0.1) = 2.8 um
D(4,3) = 5.4 um
D(3,2) = 4.7 um
Span = 1.0
Spec. surf. area

MALVERN Instruments M6.10 Date 12-08-1994 Time 02:53 *

SAMPLE ID: 94-630 L# 9289
LENSE TYPE: 63MM LENSE SMALL CELL / SONICATED
DATE: 08-12-94
OPERATOR: Jan Lucnt for B. Docktor
35%/65% Bailey/Antelope

System number 2362 Diode at1301

Malvern Instruments EASY Particle Sizer M6.10 Date 12-08-94 Time 02-53

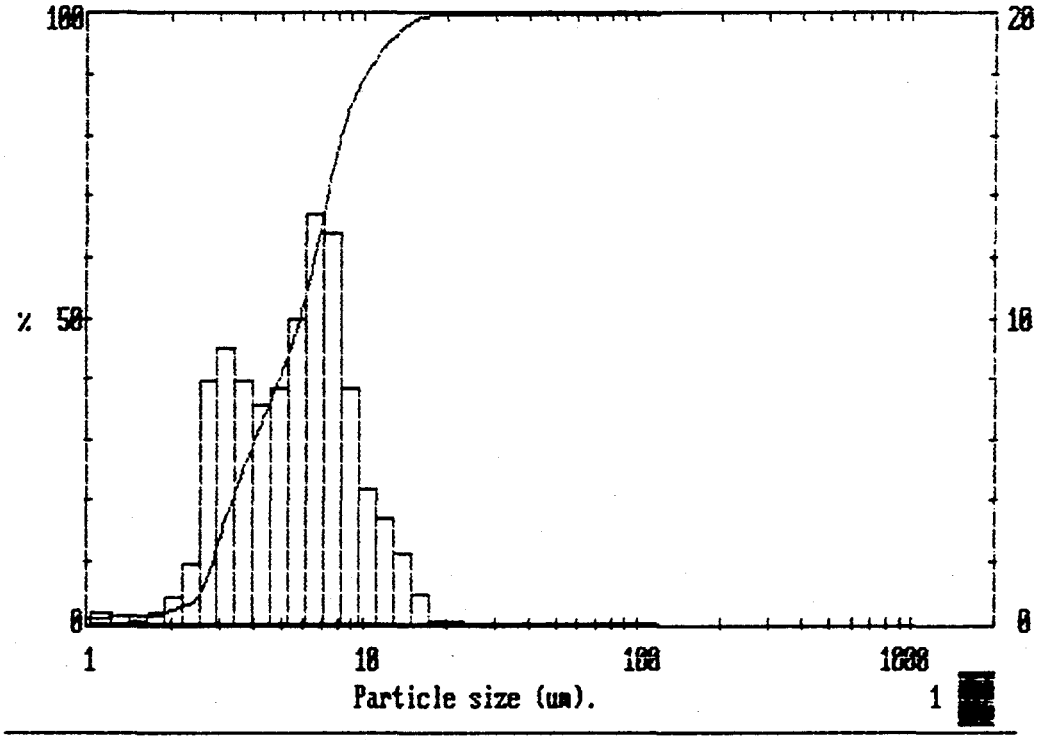

Size microns	under	% in band	Size microns	under	% in band
118.4	100.0	0.0	11.1	93.1	4.5
102.1	100.0	0.0	9.6	88.6	7.7
88.1	100.0	0.0	8.3	80.9	12.8
76.0	100.0	0.0	7.2	68.1	13.4
65.6	100.0	0.0	6.2	54.7	10.0
56.6	100.0	0.0	5.3	44.7	7.7
48.8	100.0	0.0	4.6	36.9	7.2
42.1	100.0	0.0	4.0	29.8	8.0
36.3	100.0	0.0	3.4	21.8	9.1
31.3	100.0	0.0	3.0	12.7	8.0
27.0	100.0	0.0	2.6	4.7	2.0
23.3	100.0	0.1	2.2	2.7	0.9
20.1	99.9	0.1	1.9	1.8	0.3
17.4	99.9	1.0	1.6	1.5	0.1
15.0	98.9	2.3	1.4	1.4	0.3
12.9	96.5	3.5	1.2	1.1	

Result source= Sample
Record No. = 0
Focal length = 63 mm.
Experiment type pil
Volume distribution
Beam length = 14.3 mm.
Obscuration =0.2835
Volume Conc. = 0.0036 %
Log. Diff. =3.29
Model indp

D(v,0.5) = 5.8 um
D(v,0.9) = 10.0 um
D(v,0.1) = 2.8 um
D(4,3) = 6.0 um
D(3,2) = 4.9 um
Span = 1.2
Spec. surf. area
1.3203 sq.m./cc.

MALVERN Instruments M6.10 Date 12-08-1994 Time 03:05

SAMPLE ID: 94-631 L# 3250
LENSE TYPE: 63MM LENSE SMALL CELL / SONICATED
DATE: 08-12-94
OPERATOR: Jan Lucht for B. Docktor
65%/35% Bailey/Antelope

System number 2362 Diode at1301

Malvern Instruments EASY Particle Sizer M6.10 Date 12-08-94 Time 03-05

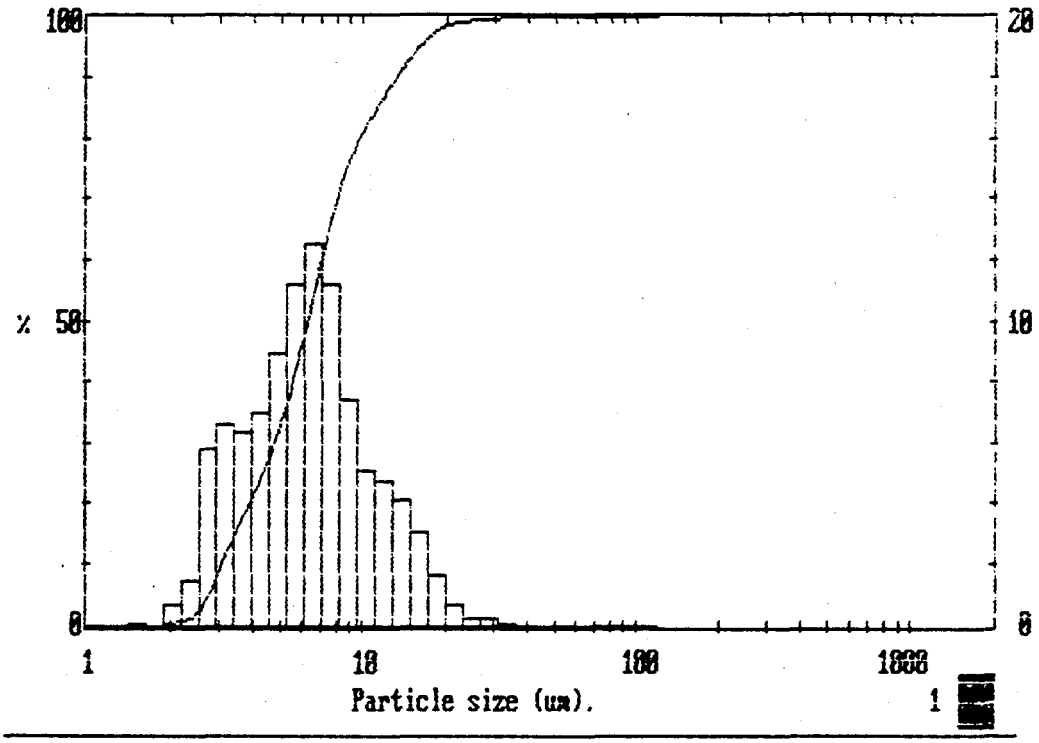

Size microns	under	% in band	Size microns	under	% in band
118.4	100.0	0.0	11.1	84.9	5.2
102.1	100.0	0.0	9.6	79.7	7.4
88.1	100.0	0.0	8.3	72.3	11.2
76.0	100.0	0.0	7.2	61.0	12.6
65.6	100.0	0.0	6.2	48.4	11.3
56.6	100.0	0.0	5.3	37.1	8.9
48.8	100.0	0.0	4.6	28.2	7.0
42.1	100.0	0.0	4.0	21.3	6.4
36.3	100.0	0.1	3.4	14.9	6.7
31.3	99.9	0.3	3.0	8.2	5.9
27.0	99.6	0.3	2.6	2.3	1.5
23.3	99.4	0.7	2.2	0.8	0.7
20.1	98.7	1.7	1.9	0.1	0.0
17.4	96.9	3.1	1.6	0.1	0.1
15.0	93.8	4.2	1.4	0.0	0.0
12.9	89.6	4.8	1.2	0.0	

Result source= Sample
Record No. = 0
Focal length = 63 mm.
Experiment type pll
Volume distribution
Beam length = 14.3 mm.
Obscuration =0.3155
Volume Conc. = 0.0049 %
Log. Diff. =3.17
Model indp

D(v,0.5) = 6.3 um
D(v,0.9) = 13.1 um
D(v,0.1) = 3.1 um
D(4,3) = 7.0 um
D(3,2) = 5.6 um
Span = 1.6
Spec. surf. area
1.0922 sq.m./cc.

MALVERN Instruments M6.10 Date 12-08-1994 Time 01:44

SAMPLE ID: 94-673 L# 9335
LENSE TYPE: 63MM LENSE SMALL CELL / SONICATED
DATE: 08-12-94
OPERATOR: Jan Lucht for B. Docktor
100% Black Thunder

System number 2362 Diode at1301

Malvern Instruments EASY Particle Sizer M6.10 Date 12-08-94 Time 01-44

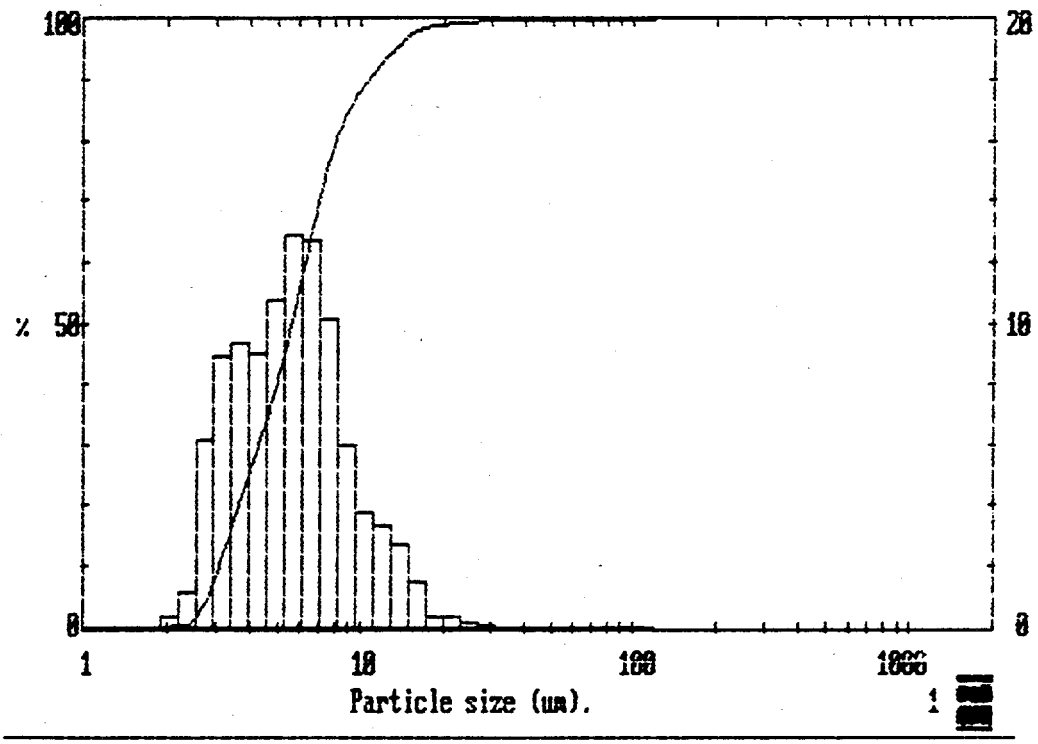

Size microns	under	% in band	Size microns	under	% in band
118.4	100.0	0.0	11.1	91.4	3.8
102.1	100.0	0.0	9.6	87.6	6.0
88.1	100.0	0.0	8.3	81.6	10.2
76.0	100.0	0.0	7.2	71.5	12.7
65.6	100.0	0.0	6.2	58.7	12.9
56.6	100.0	0.0	5.3	45.8	10.8
48.8	100.0	0.0	4.6	35.0	9.0
42.1	100.0	0.0	4.0	26.0	9.4
36.3	100.0	0.0	3.4	16.6	8.9
31.3	100.0	0.1	3.0	7.7	6.2
27.0	99.9	0.2	2.6	1.5	1.1
23.3	99.7	0.3	2.2	0.4	0.3
20.1	99.3	0.4	1.9	0.0	0.0
17.4	99.0	1.5	1.6	0.0	0.0
15.0	97.5	2.7	1.4	0.0	0.0

Result source= Sample
Record No. = 0
Focal length = 63 mm.
Experiment type pil
Volume distribution
Beam length = 14.3 mm.
Obscuration =0.1675
Volume Conc. = 0.0022 %
Log. Diff. =3.91
Model indp

D(v,0.5) = 5.6 um
D(v,0.9) = 10.5 um
D(v,0.1) = 3.1 um
D(4,3) = 6.1 um
D(3,2) = 5.1 um
Span = 1.3
Spec. surf. area

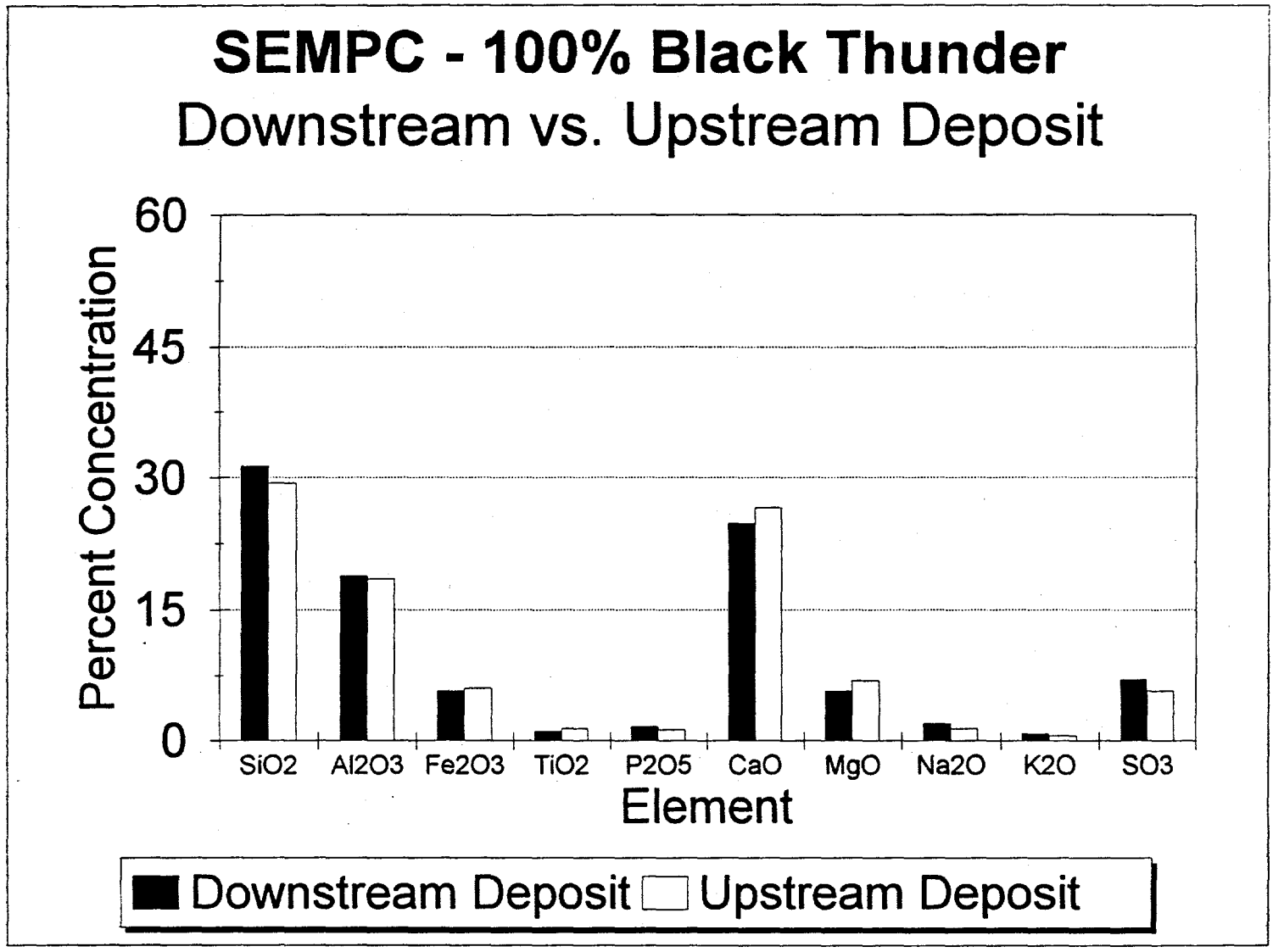
SEMPC - 100% Black Thunder
Downstream vs. Upstream Deposit
Percent Concentration
60
45
30
15
0
SiO2
Al2O3
Fe2O3
TiO2
P2O5
CaO
MgO
Na2O
K2O
SO3
Element
Downstream Deposit
Upstream Deposit

SEMPC - 100% Black Thunder, SO3 free

Downstream vs. Upstream Deposit

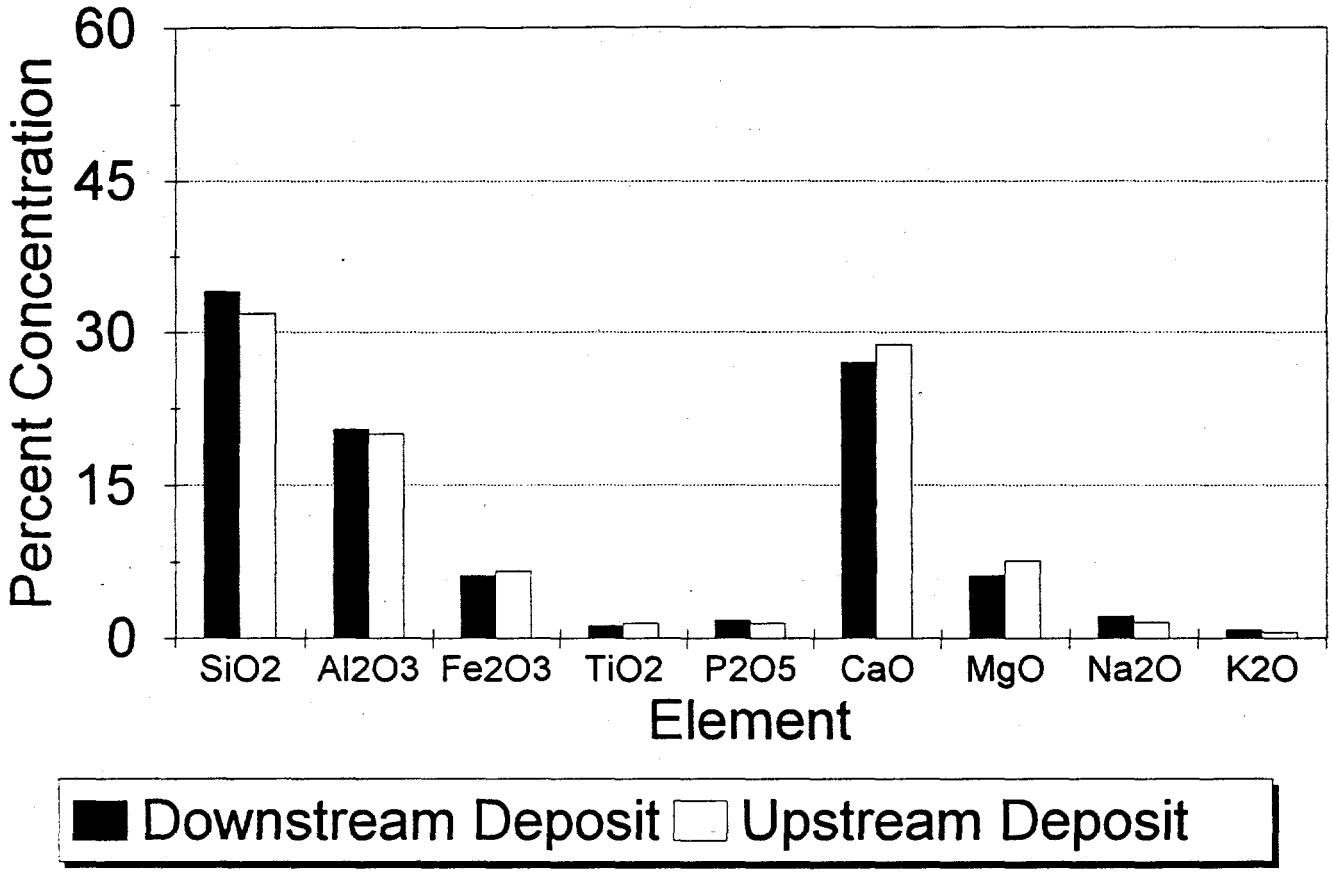

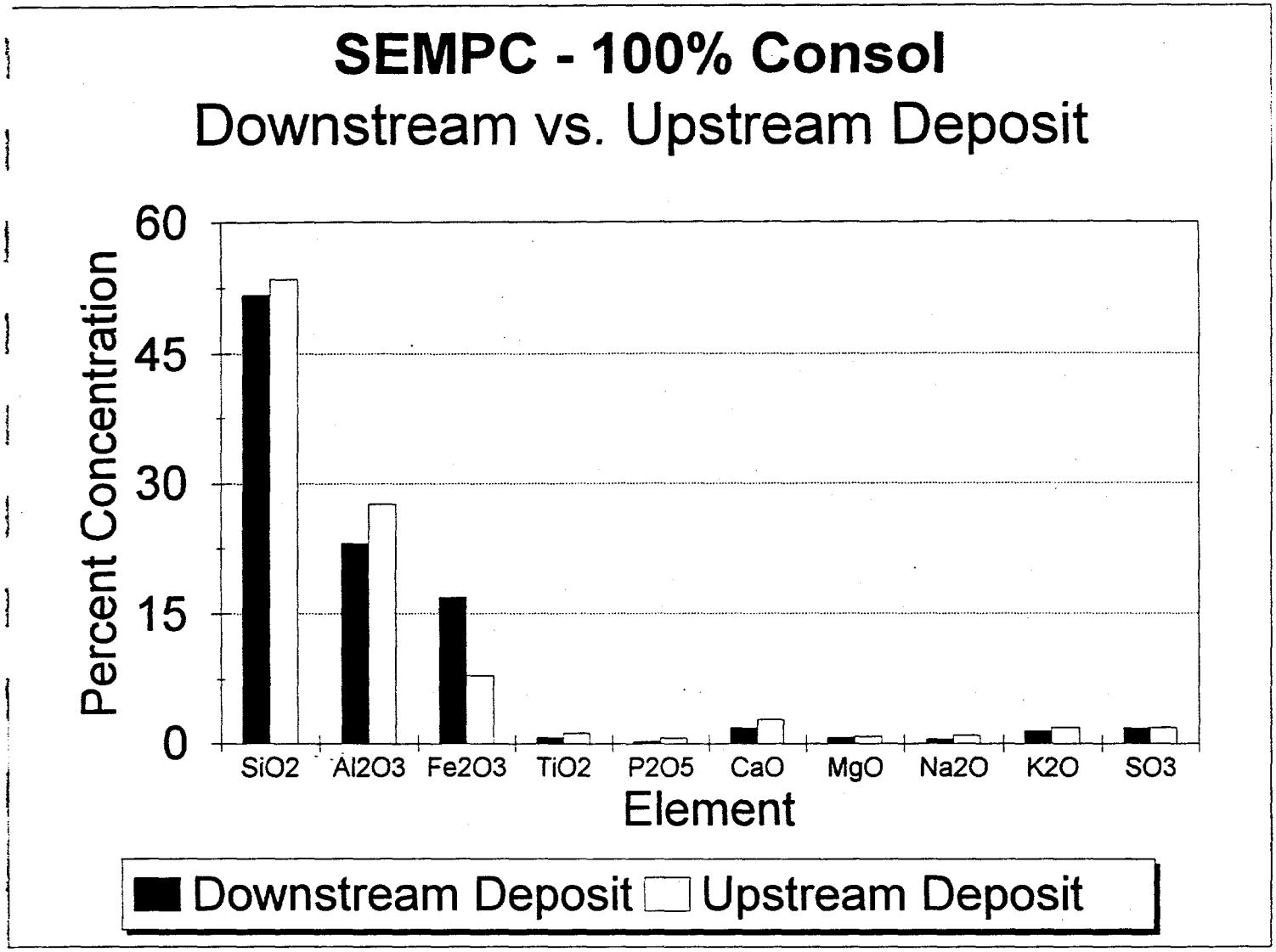
SEMPC - 100% Consol
Downstream vs. Upstream Deposit
Percent Concentration
60
45
30
15
0
SiO2
Al2O3
Fe2O3
TiO2
P2O5
CaO
MgO
Na2O
K2O
SO3
Element
Downstream Deposit
Upstream Deposit

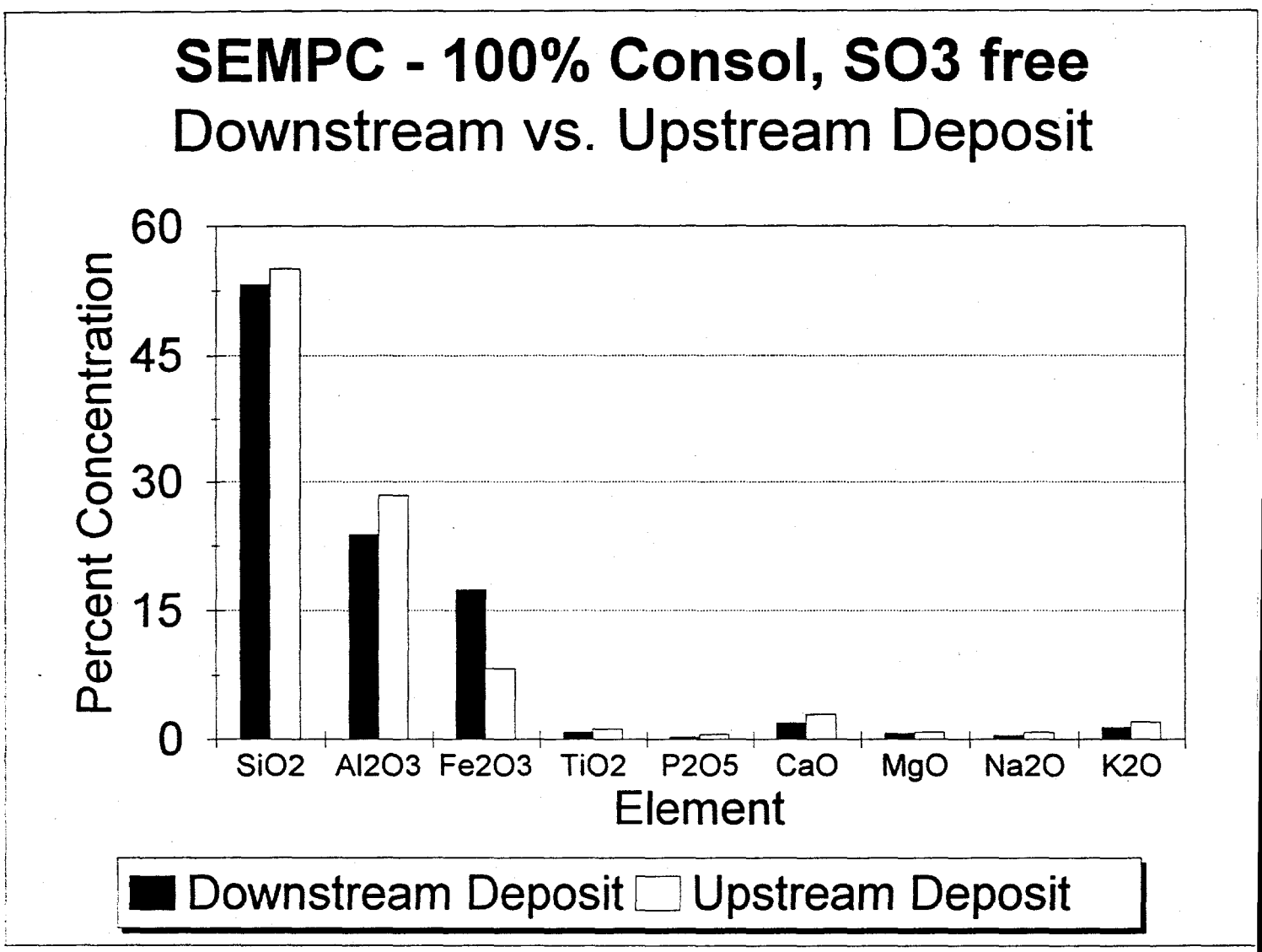
SEMPC - 100% Consol, SO3 free
Downstream vs. Upstream Deposit
Percent Concentration
60
45
30
15
0
SiO2
Al2O3
Fe2O3
TiO2
P2O5
CaO
MgO
Na2O
K2O
Element
Downstream Deposit
Upstream Deposit

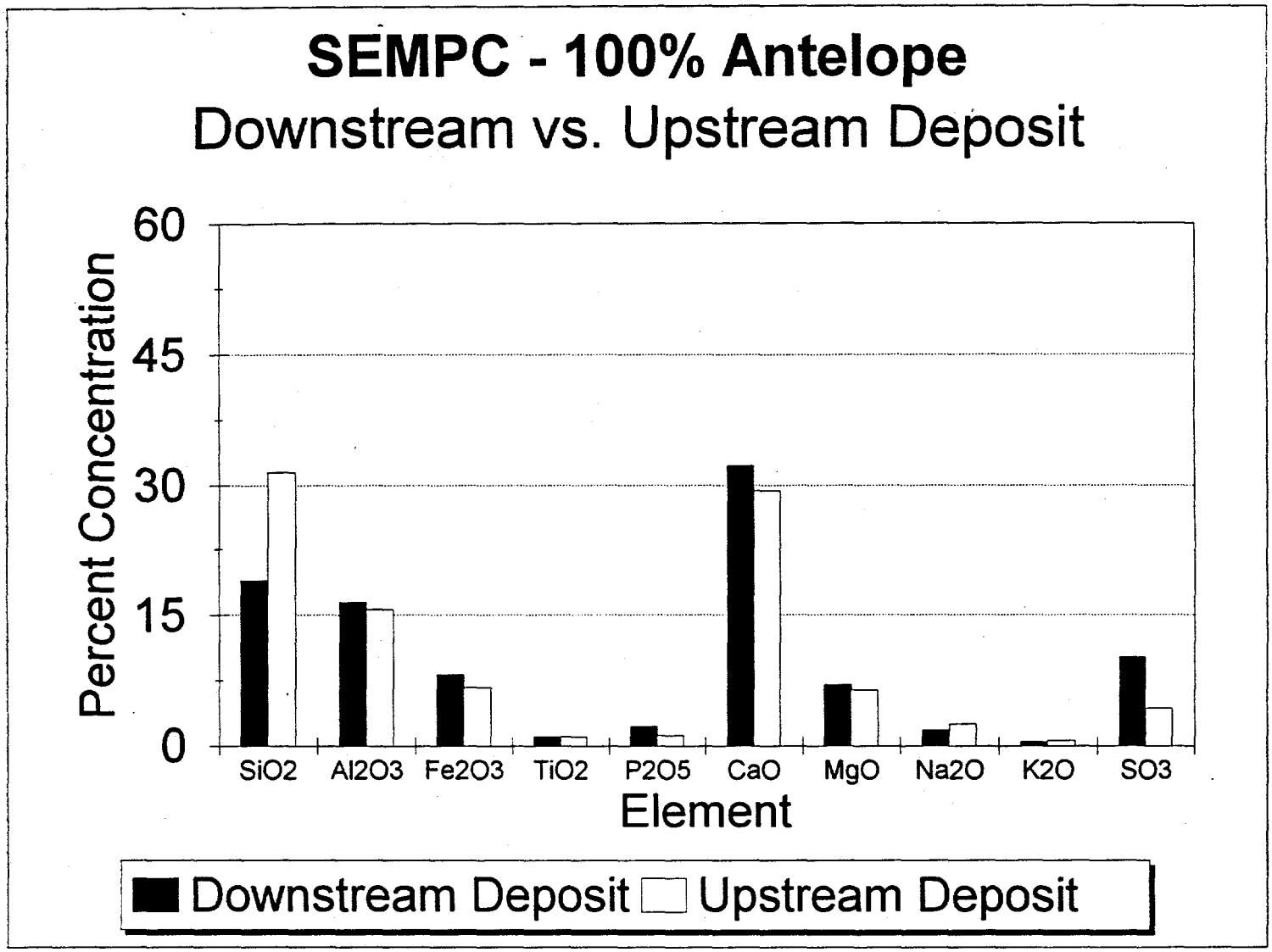
SEMPC - 100% Antelope
Downstream vs. Upstream Deposit
Percent Concentration
60
45
30
15
0
SiO2
Al2O3
Fe2O3
TiO2
P2O5
CaO
MgO
Na2O
K2O
SO3
Element
Downstream Deposit
Upstream Deposit

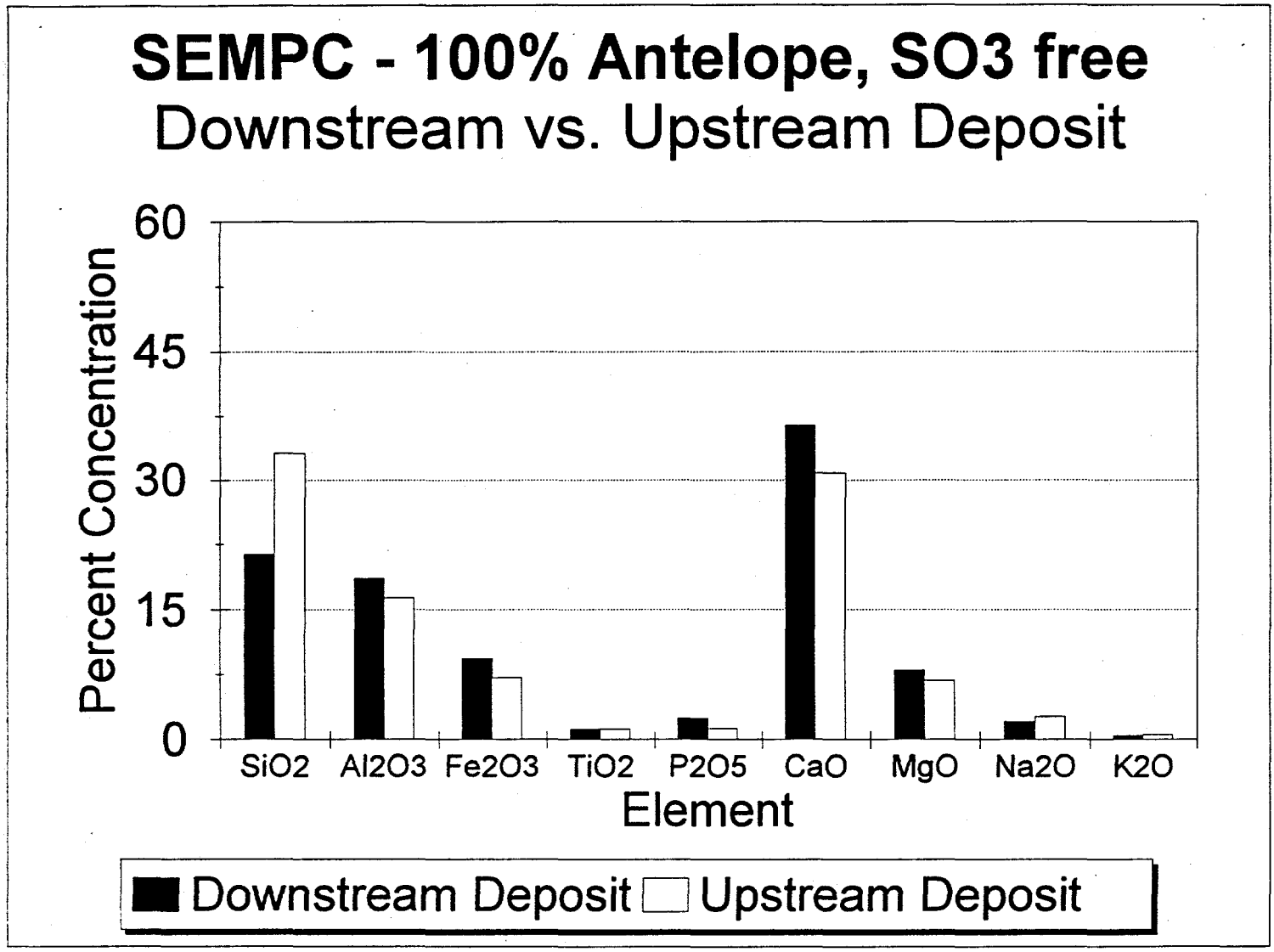
SEMPC - 100% Antelope, SO3 free
Downstream vs. Upstream Deposit
Percent Concentration
60
45
30
15
0
SiO2
Al2O3
Fe2O3
TiO2
P2O5
CaO
MgO
Na2O
K2O
Element
Downstream Deposit
Upstream Deposit

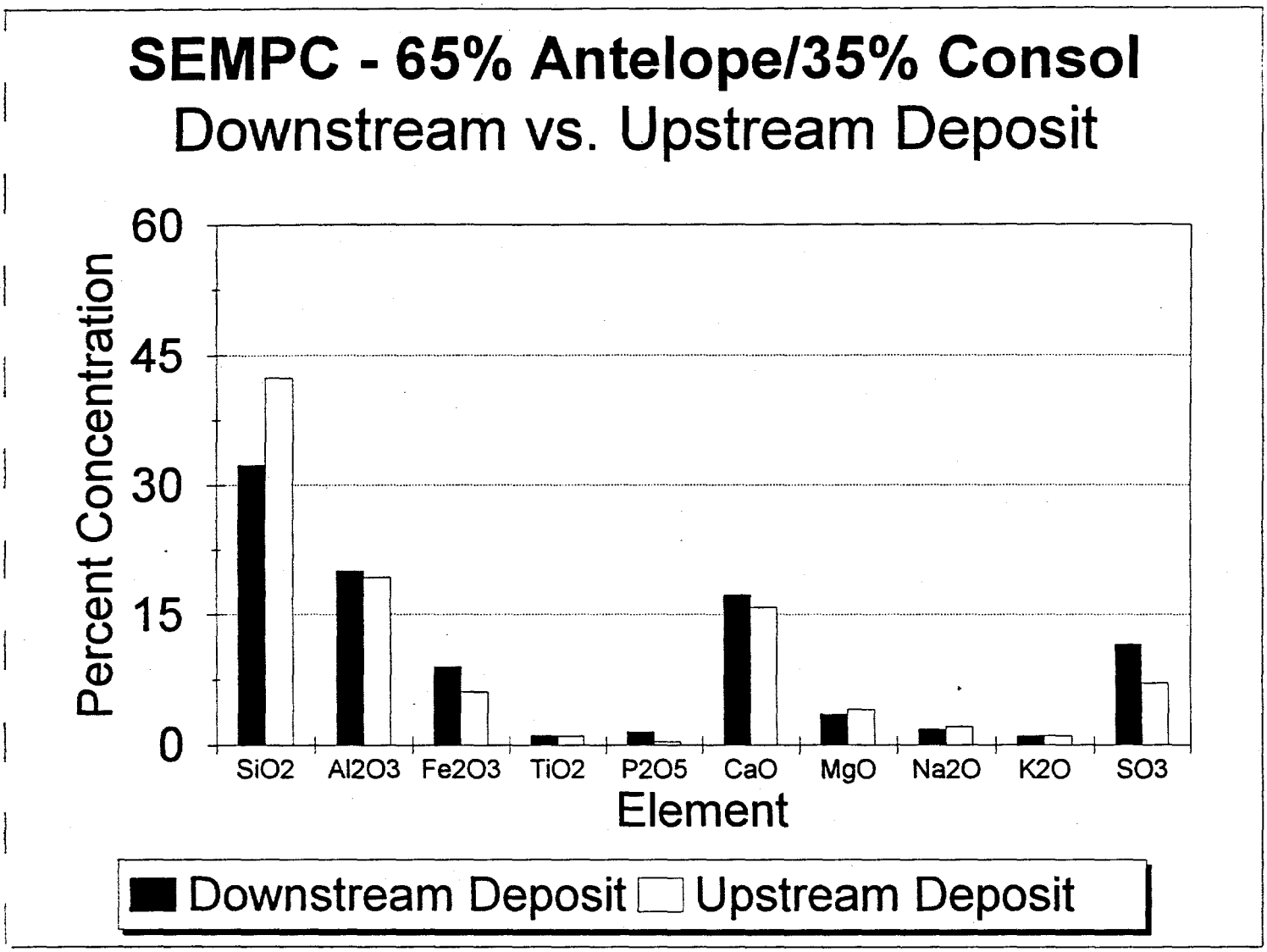
SEMPC - 65% Antelope/35% Consol
Downstream vs. Upstream Deposit
Percent Concentration
60
45
30
15
0
SiO2
Al2O3
Fe2O3
TiO2
P2O5
CaO
MgO
Na2O
K2O
SO3
Element
Downstream Deposit
Upstream Deposit

SEMPC - 65% Ant./35% Consol, SO3 free

Downstream vs. Upstream Deposit

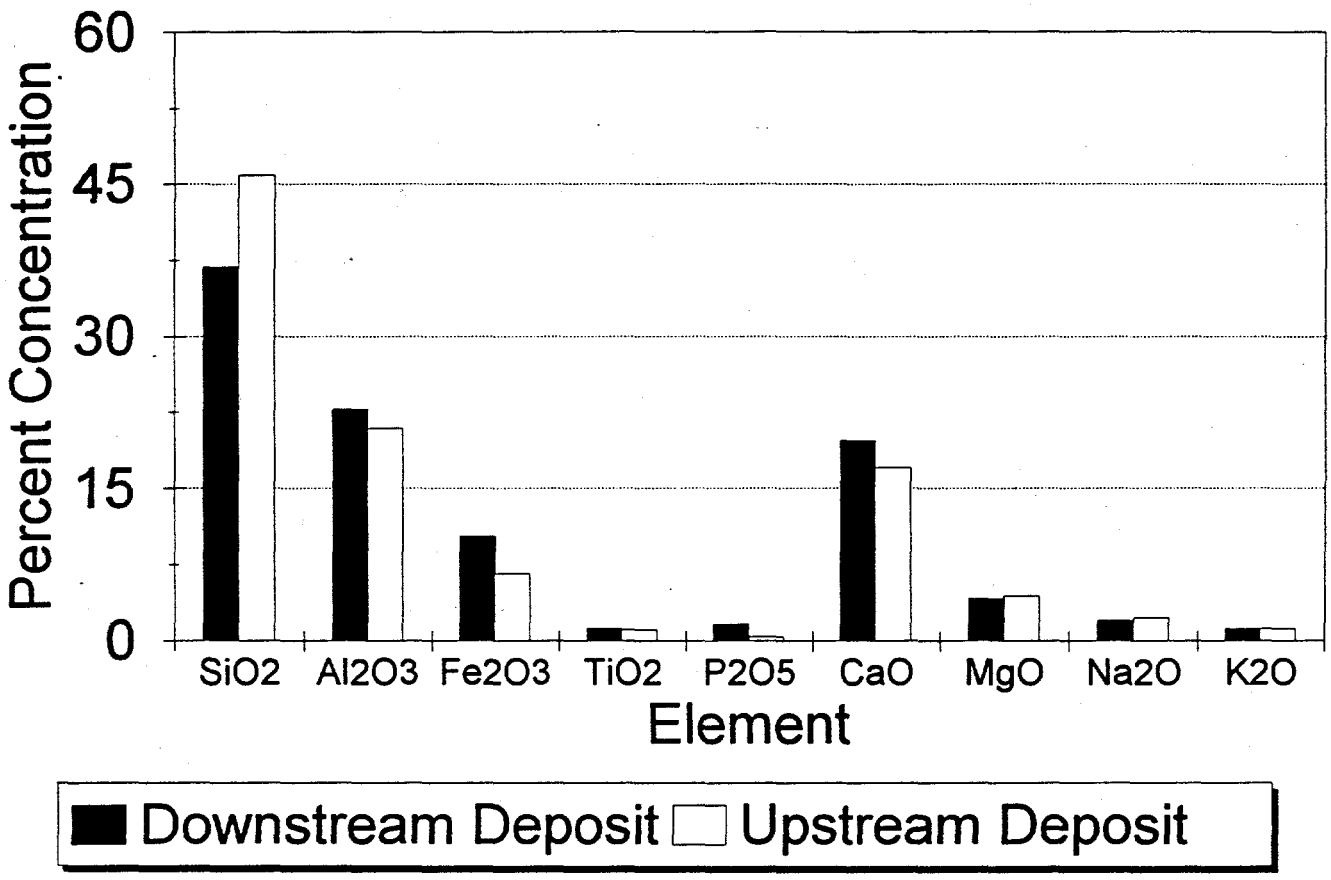

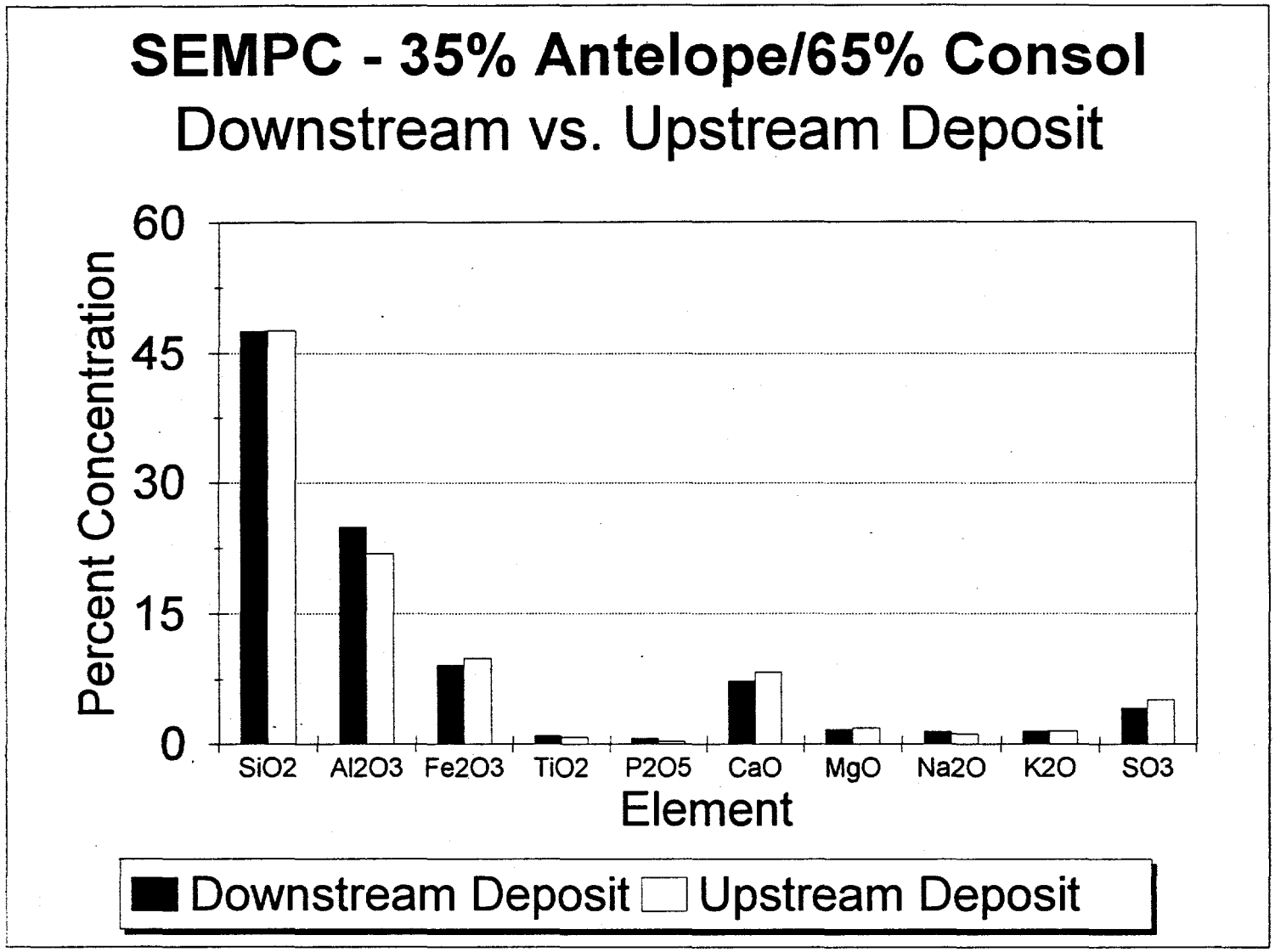
SEMPC - 35% Antelope/65% Consol
Downstream vs. Upstream Deposit
Percent Concentration
60
45
30
15
0
SiO2
Al2O3
Fe2O3
TiO2
P2O5
CaO
MgO
Na2O
K2O
SO3
Element
Downstream Deposit
Upstream Deposit

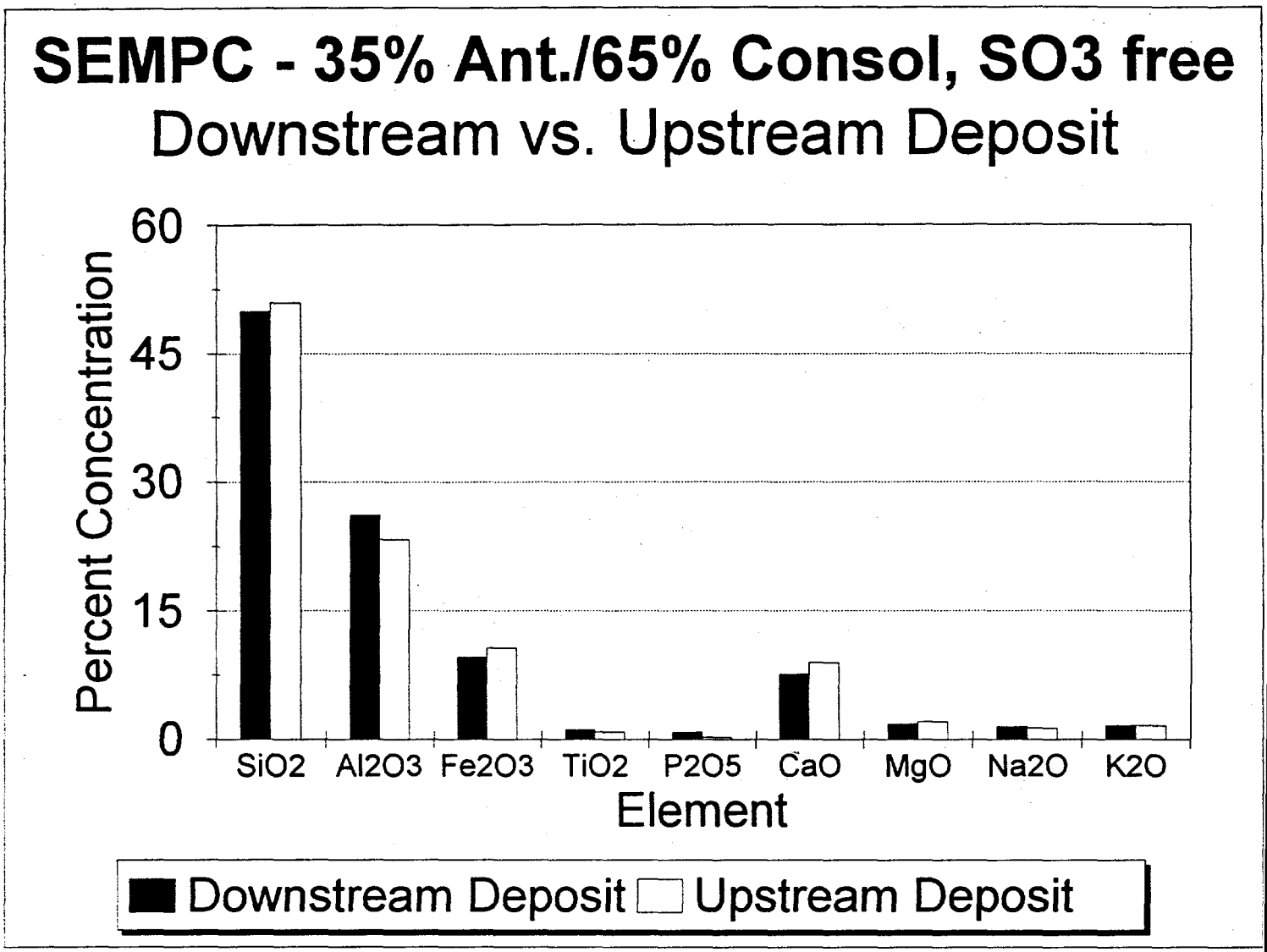
SEMPC - 35% Ant./65% Consol, SO3 free
Downstream vs. Upstream Deposit
Percent Concentration
60
45
30
15
0
SiO2
Al2O3
Fe2O3
TiO2
P2O5
CaO
MgO
Na2O
K2O
Element
Downstream Deposit
Upstream Deposit

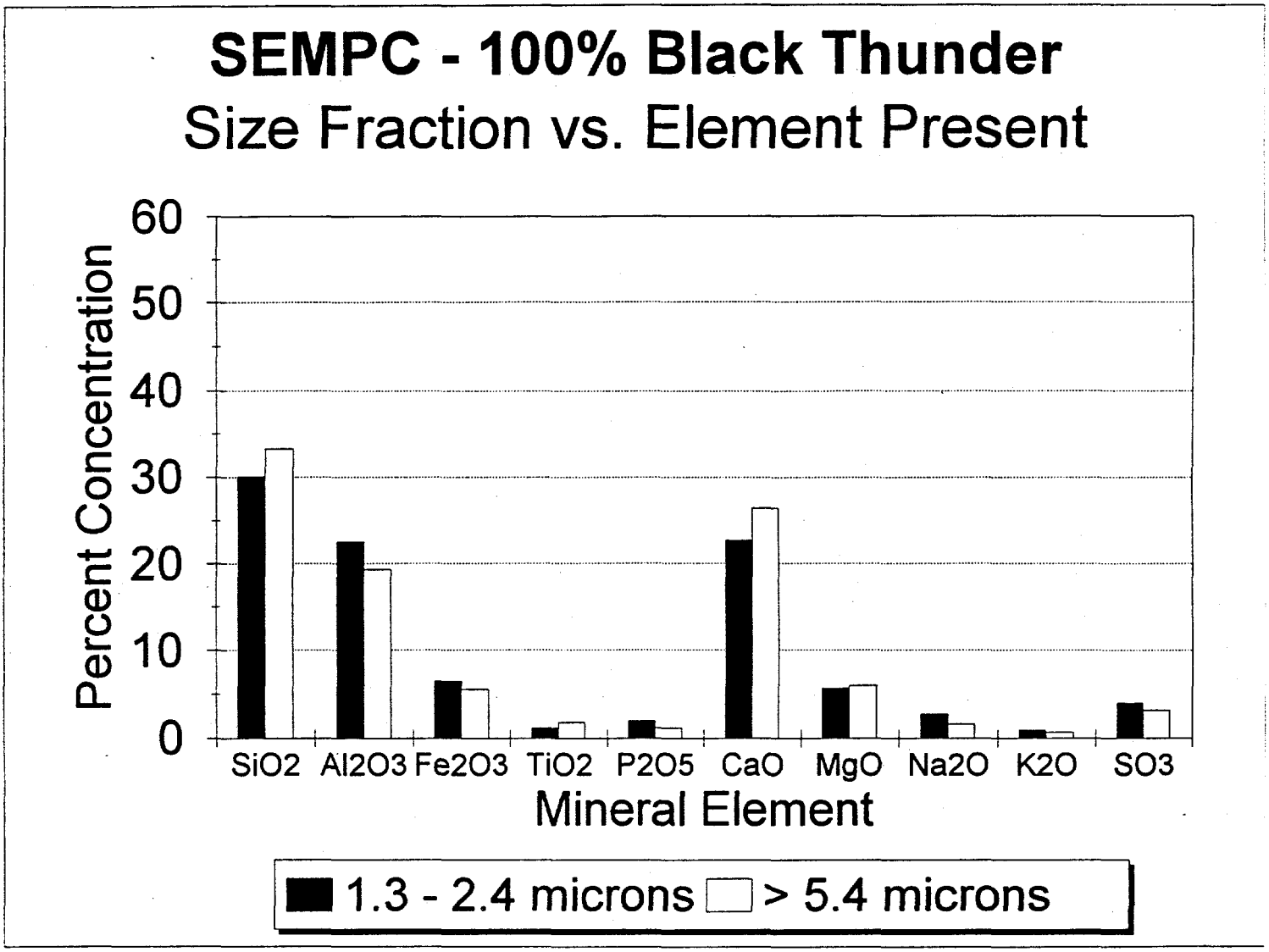
SEMPC - 100% Black Thunder
Size Fraction vs. Element Present
Percent Concentration
60
50
40
30
20
10
0
SiO2
Al2O3
Fe2O3
TiO2
P2O5
CaO
MgO
Na2O
K2O
SO3
Mineral Element
1.3 - 2.4 microns
> 5.4 microns

SEMPC - 100% Black Thunder (SO3 free)

Size Fraction vs. Element Present

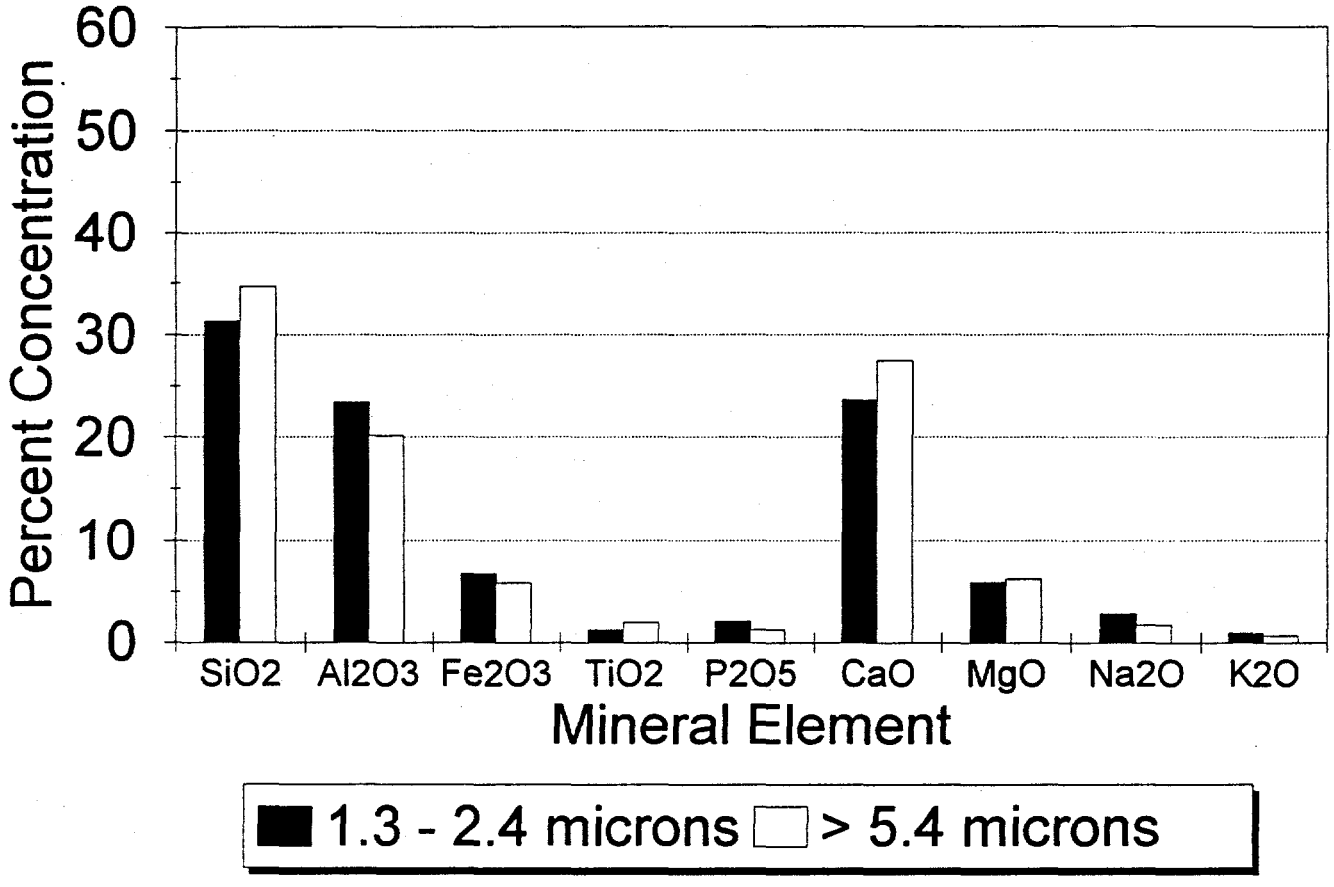

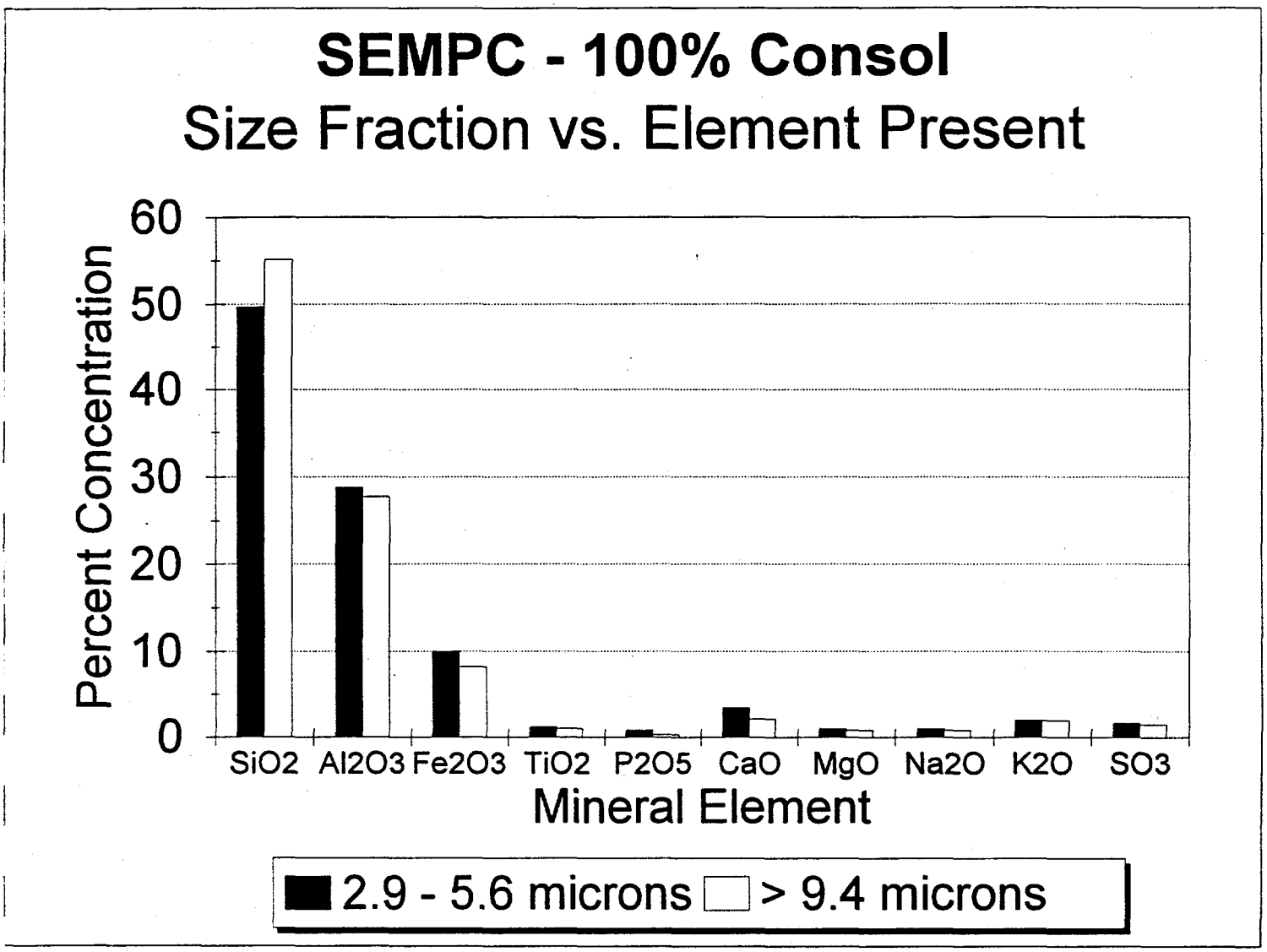
SEMPC - 100% Consol
Size Fraction vs. Element Present
Percent Concentration
60
50
40
30
20
10
0
SiO2
Al2O3
Fe2O3
TiO2
P2O5
CaO
MgO
Na2O
K2O
SO3
Mineral Element
2.9 - 5.6 microns
> 9.4 microns

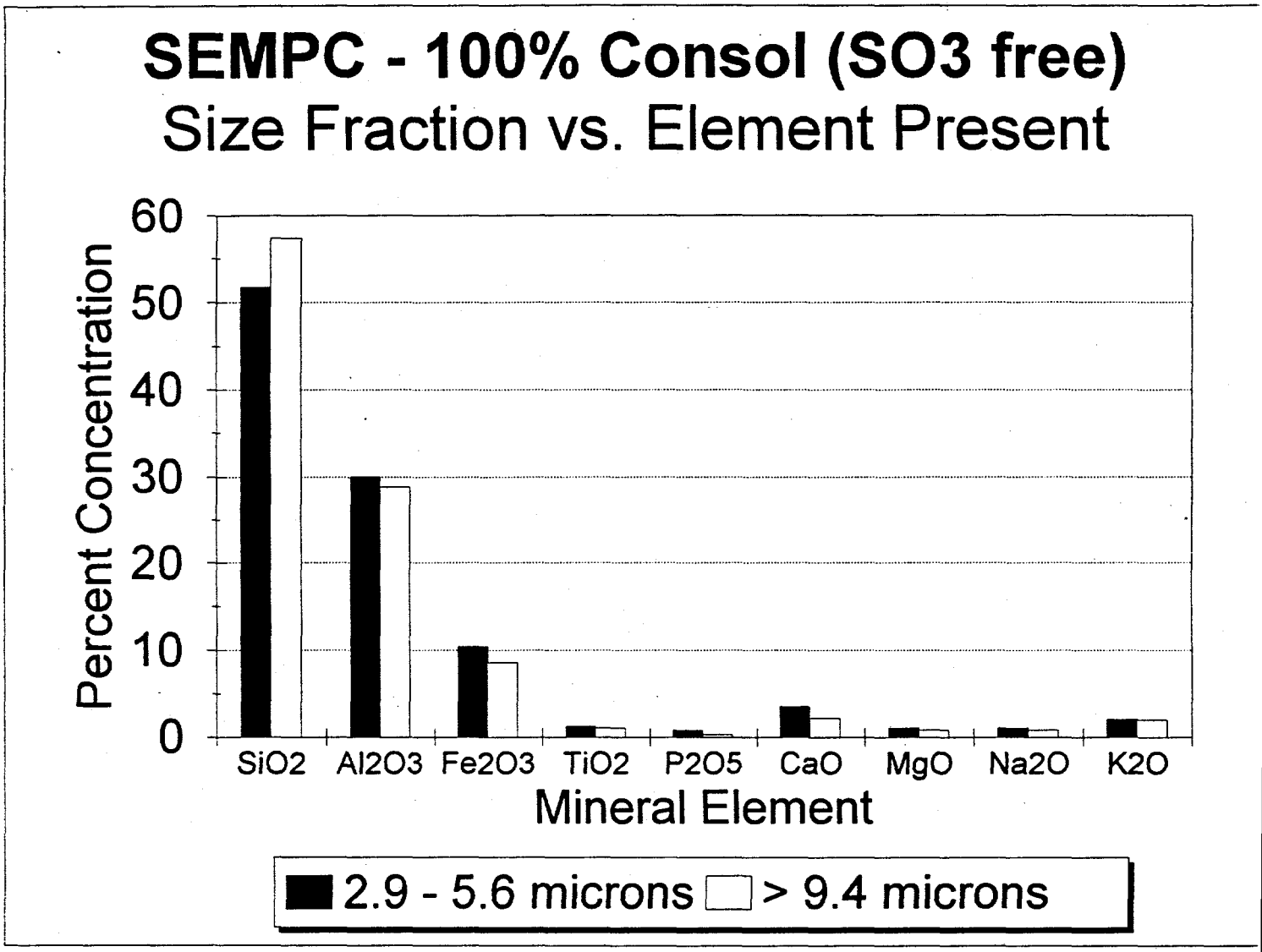
SEMPC - 100% Consol (SO3 free)
Size Fraction vs. Element Present
Percent Concentration
60
50
40
30
20
10
0
SiO2
Al2O3
Fe2O3
TiO2
P2O5
CaO
MgO
Na2O
K2O
Mineral Element
2.9 - 5.6 microns
> 9.4 microns

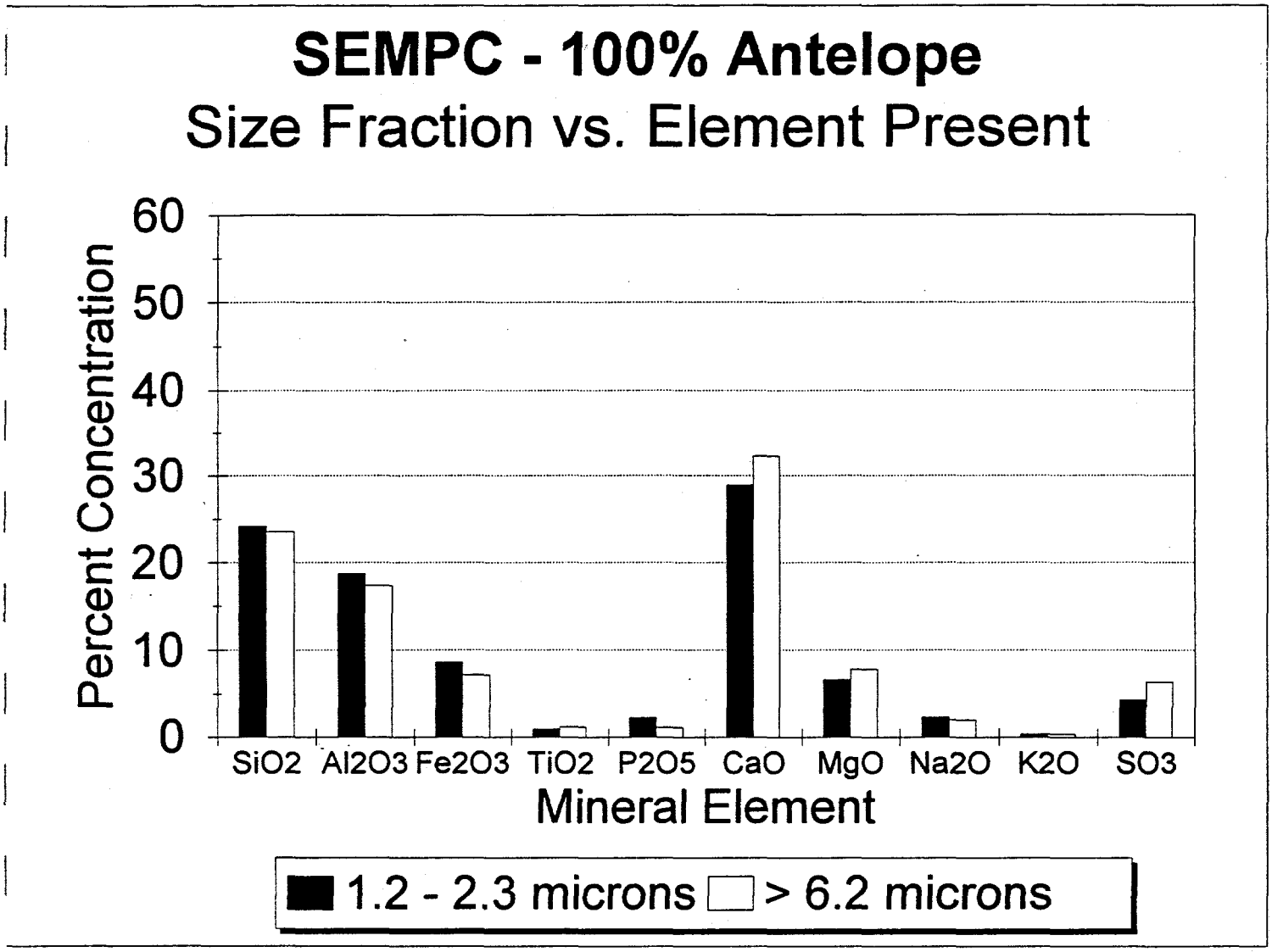
SEMPC - 100% Antelope
Size Fraction vs. Element Present
Percent Concentration
60
50
40
30
20
10
0
SiO2
Al2O3
Fe2O3
TiO2
P2O5
CaO
MgO
Na2O
K2O
SO3
Mineral Element
1.2 - 2.3 microns
> 6.2 microns

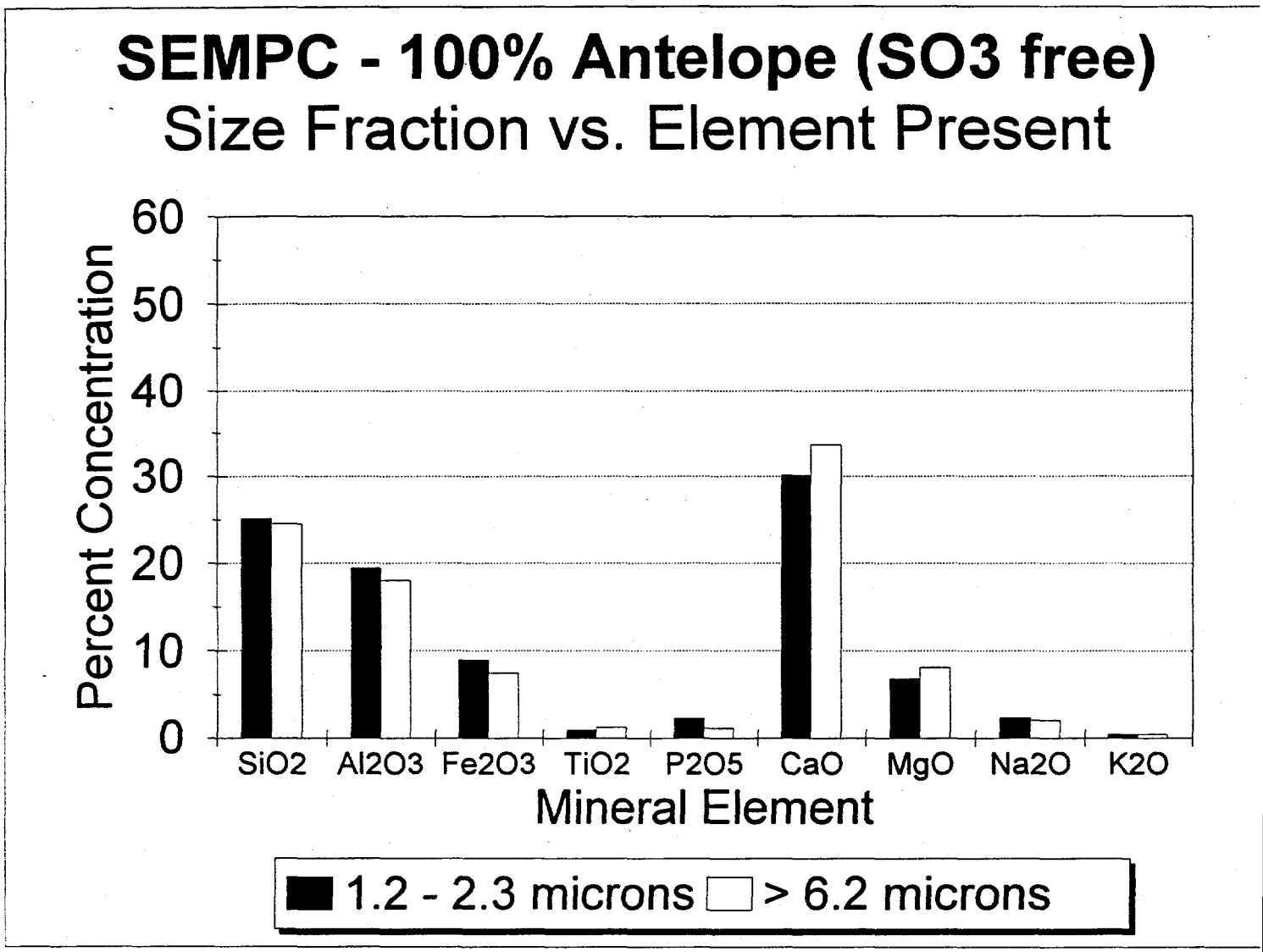
SEMPC - 100% Antelope (SO3 free)
Size Fraction vs. Element Present
Percent Concentration
60
50
40
30
20
10
0
SiO2
Al2O3
Fe2O3
TiO2
P2O5
CaO
MgO
Na2O
K2O
Mineral Element
1.2 - 2.3 microns
> 6.2 microns

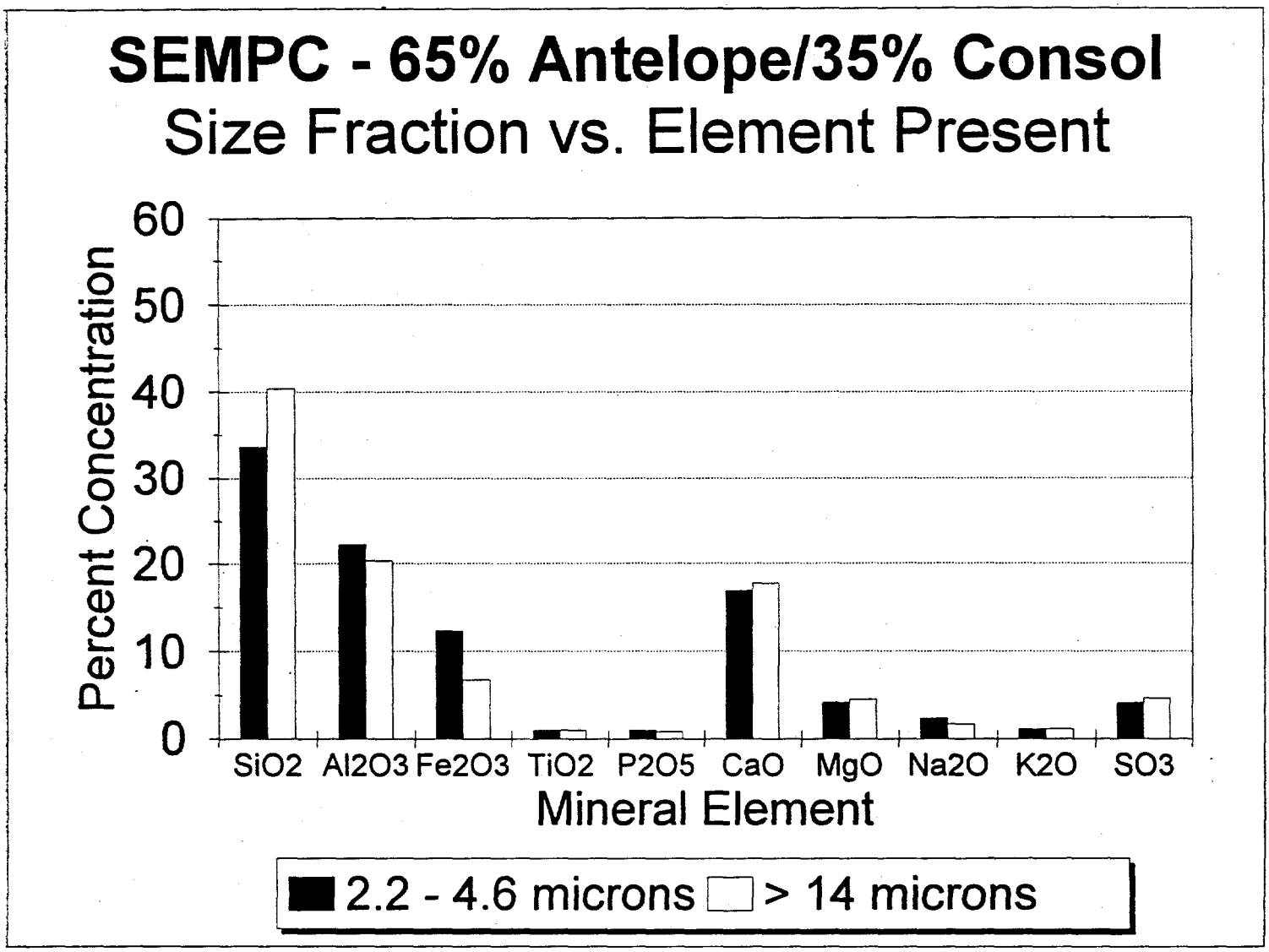
SEMPC - 65% Antelope/35% Consol
Size Fraction vs. Element Present
Percent Concentration
60
50
40
30
20
10
0
SiO2
Al2O3
Fe2O3
TiO2
P2O5
CaO
MgO
Na2O
K2O
SO3
Mineral Element
2.2 - 4.6 microns
> 14 microns

SEMPC - 65% Ant./35% Consol (SO3 free)

Size Fraction vs. Element Present

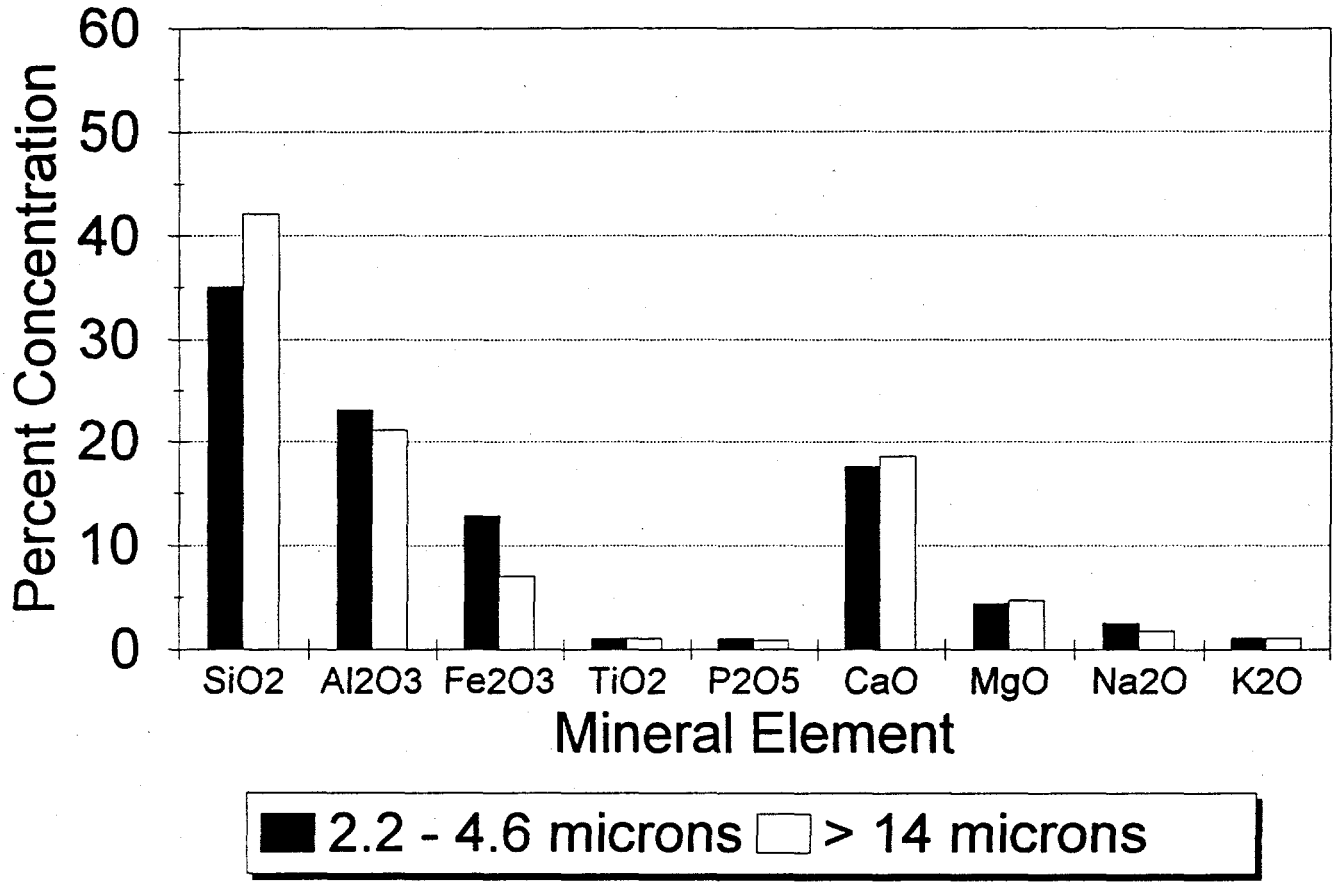

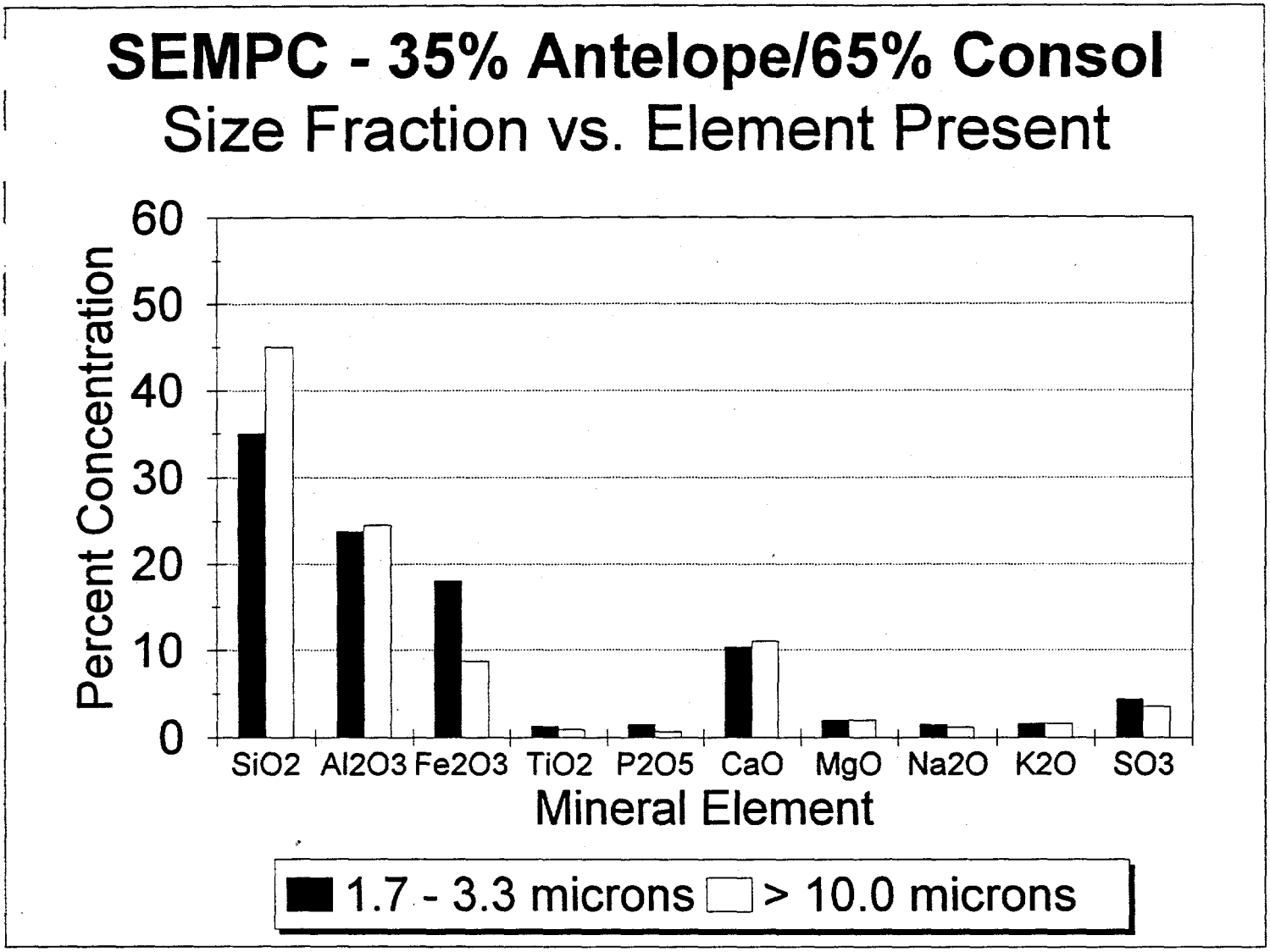
SEMPC - 35% Antelope/65% Consol
Size Fraction vs. Element Present
Percent Concentration
60
50
40
30
20
10
0
SiO2
Al2O3
Fe2O3
TiO2
P2O5
CaO
MgO
Na2O
K2O
SO3
Mineral Element
1.7 - 3.3 microns
> 10.0 microns

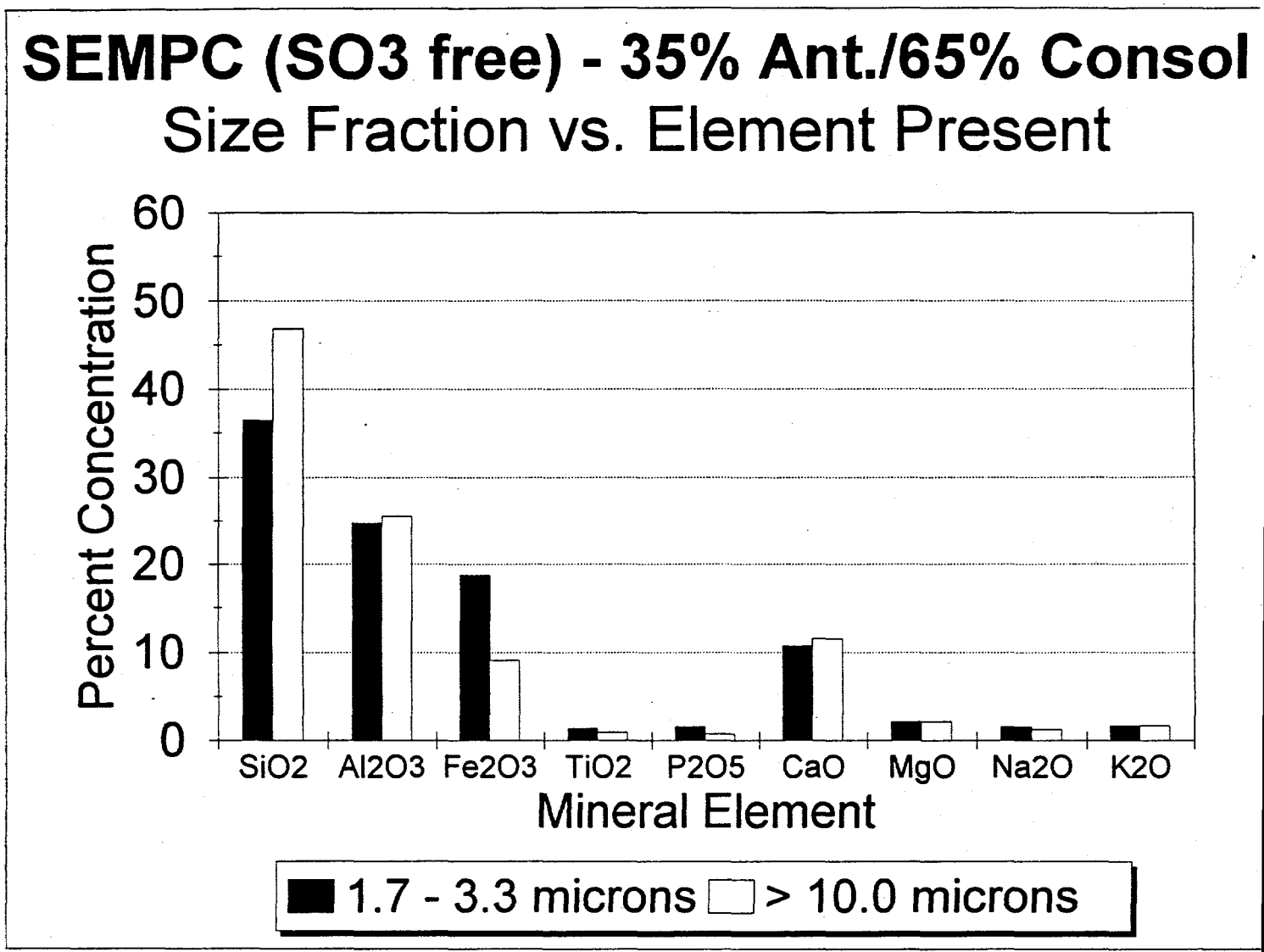
SEMPC (SO3 free) - 35% Ant./65% Consol
Size Fraction vs. Element Present
Percent Concentration
60
50
40
30
20
10
0
SiO2
Al2O3
Fe2O3
TiO2
P2O5
CaO
MgO
Na2O
K2O
Mineral Element
1.7 - 3.3 microns
> 10.0 microns